

## Aqueous two-phase systems applied to the enzymatic hydrolysis of sugarcane bagasse Screening methodology, thermodynamic modelling and process design

Consorti Bussamra, B.

### DOI

[10.4233/uuid:d07534b8-d3bf-404e-ae6e-ccf1acc7bc1d](https://doi.org/10.4233/uuid:d07534b8-d3bf-404e-ae6e-ccf1acc7bc1d)

### Publication date

2021

### Document Version

Final published version

### Citation (APA)

Consorti Bussamra, B. (2021). *Aqueous two-phase systems applied to the enzymatic hydrolysis of sugarcane bagasse: Screening methodology, thermodynamic modelling and process design*. [Dissertation (TU Delft), Delft University of Technology, Unicamp, Campinas]. <https://doi.org/10.4233/uuid:d07534b8-d3bf-404e-ae6e-ccf1acc7bc1d>

### Important note

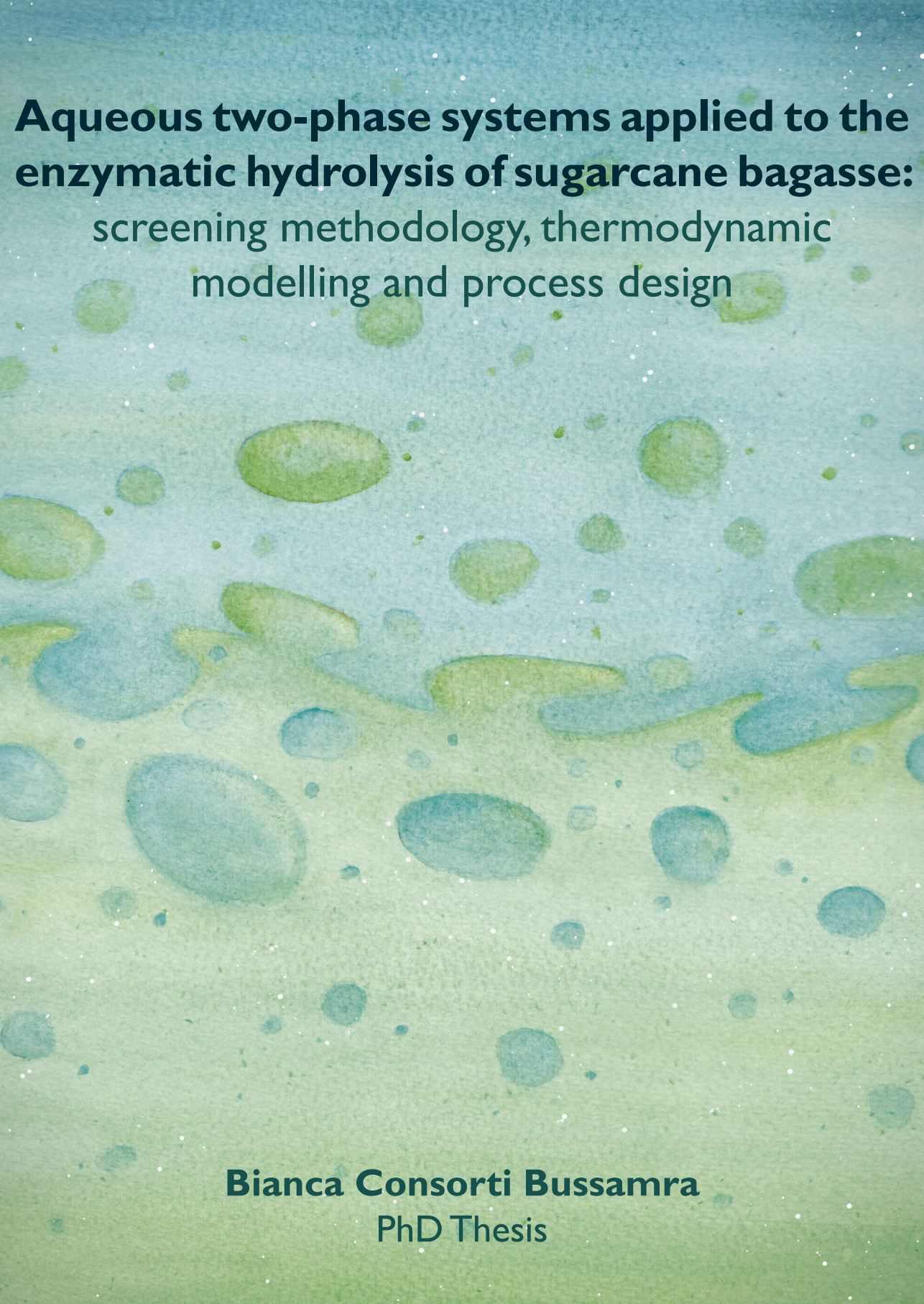
To cite this publication, please use the final published version (if applicable).  
Please check the document version above.

### Copyright

Other than for strictly personal use, it is not permitted to download, forward or distribute the text or part of it, without the consent of the author(s) and/or copyright holder(s), unless the work is under an open content license such as Creative Commons.

### Takedown policy

Please contact us and provide details if you believe this document breaches copyrights.  
We will remove access to the work immediately and investigate your claim.



# **Aqueous two-phase systems applied to the enzymatic hydrolysis of sugarcane bagasse:** screening methodology, thermodynamic modelling and process design

**Bianca Consorti Bussamra**  
PhD Thesis

**Aqueous two-phase systems applied to the enzymatic hydrolysis of  
sugarcane bagasse: screening methodology, thermodynamic modelling and  
process design**

Dissertation

for the purpose of obtaining the degree of doctor at Delft University of Technology  
by the authority of the Rector Magnificus prof.dr.ir. T.H.J.J. van der Hagen chair of  
the Board for Doctorates to be defended publicly on Monday 26<sup>th</sup>, April 2021 at  
17:30 o'clock

by

**Bianca CONSORTI BUSSAMRA**

Master in Chemical Engineering, University of Campinas, Brazil  
born in Tietê, Brazil

This dissertation has been approved by the promotor.

Composition of the doctoral committee:

Rector Magnificus	chairperson
Assoc. Prof. dr. ir. M. Ottens	Delft University of Technology, promotor
Prof. dr. ir. L.A.M. van der Wielen	Delft University of Technology, promotor
Prof. dr. A.C. da Costa	University of Campinas, promotor

Independent members:

Prof. dr. T. Teixeira Franco	University of Campinas
Prof. dr. F. Hollmann	Delft University of Technology
Prof. dr. M.H.M Eppink	Wageningen University
Dr. G.N.M. Ferreira	University of Lisbon

Reserve member:

Prof. dr. P. Osseweijer	Delft University of Technology
-------------------------	--------------------------------

Prof. dr. S.I. Mussatto, Technical University of Denmark has, as supervisor, contributed significantly to the preparation of this dissertation.

Dr. P. Verheijen, Delft University of Technology, has provided substantial assistance in the preparation of this doctoral dissertation.

The doctoral research has been carried out in the context of an agreement on joint doctoral supervision between University of Campinas, Brazil and Delft University of Technology, the Netherlands. This work was financially supported by the Foundation for Research of State of Sao Paulo, Brazil [grant numbers 2015/20630-4, 2016/ 04749-4, 2016/06142-0 and BEPE 2016/21951-1]; and the BE-Basic Foundation, The Netherlands.

This is a PhD thesis in the dual degree program as agreed between UNICAMP and TU Delft. Esta é uma tese de doutorado de co-tutela conforme acordado entre UNICAMP e TU Delft.

Cover: Alessandra B Consorti

Printed by: Rijnja – The Netherlands

Keywords: aqueous two-phase systems (ATPS); thermodynamic analysis; enzymatic hydrolysis; sugarcane bagasse; process design.

ISBN number: 978-94-6366-411-0

Copyright © 2021 Bianca Consorti Bussamra, The Netherlands

All rights reserved. No part of the material protected by this copyright notice may be reproduced or utilized in any form or by any means, electronic or mechanical, including photocopying, recording or by any information storage or retrieval system, without written permission by the author.

An electronic version of this dissertation is available at <http://repository.tudelft.nl/>



*Dedico esse trabalho para aqueles que  
abriram caminho para a minha  
existência e me fazem ser quem sou. Aos  
meus avós Enio, Neuza, Narcizo e Maria  
Luiza, aos meus pais Beto e Luzia e ao  
meu filho Ennio.*



## TABLE OF CONTENTS

SUMMARY .....	7
SAMENVATTING .....	9
RESUMO .....	13
CHAPTER 1	
General Introduction .....	15
CHAPTER 2	
A robotic platform to screen aqueous two-phase systems for overcoming inhibition in enzymatic reactions .....	45
CHAPTER 3	
A critical assessment of the Flory-Huggins (FH) theory to predict aqueous two-phase behaviour .....	93
CHAPTER 4	
A Enzymatic hydrolysis of sugarcane bagasse in aqueous two-phase systems (ATPS): exploration and conceptual process design .....	141
CHAPTER 5	
Model-based evaluation and techno-economic analysis of aqueous two-phase systems (ATPS) for enzymatic hydrolysis of sugarcane bagasse .....	187
CHAPTER 6	
Conclusion and outlook .....	237
SUPPLEMENTARY MATERIAL .....	241
ACKNOWLEDGEMENT .....	259
PUBLICATION RECORD .....	263
ABOUT THE AUTHOR .....	265





## SUMMARY

Targeting to improve the utilization of lignocellulosic residues in the ethanol processing industry, this work aimed to test if the product inhibition of the enzymatic hydrolysis could be relieved by extractive reaction using aqueous two-phase systems (ATPS). The performance of enzymatic hydrolysis in ATPS is not well defined in literature. In this thesis, this extractive reaction was tested in terms of experimental conversion of sugarcane bagasse, simulations through conceptual process design and economic feasibility. A thermodynamic framework was developed in order to predict ATPS formation.

The screening of ATPS and partition coefficient of the solutes were performed in a high throughput station. The ATPS were composed by polymer and salt. The enzymes were represented by the enzymatic cocktail Cellic CTec (Novozymes). The development of this platform consisted of two main parts: determination of phase diagrams (binodal curves and tie lines) and quantification of the solutes (sugar and proteins) in both top and bottom phases. The most promising ATPS were experimentally explored for enzymatic hydrolysis of sugarcane bagasse. Process design simulated two scenarios: hydrolysis occurring in the bottom phase and in the top phase. Topics such as the adsorption of phase forming components to the bagasse fibers and the influence of enzyme load on the hydrolysis were explored. The sugarcane bagasse hydrolysis in ATPS was conceptually assessed through the implementation of a model composed by two parts: hydrolysis and ATPS multi-batch separation. The designed case characterized by the ATPS hydrolysis was compared to the base case defined as conventional hydrolysis. Regarding the thermodynamic modelling of ATPS, the application of Flory-Huggins (FH) model to predict phase separation in polymer-salt systems was assessed. The implementation and analysis of FH theory involved the estimation of interchange energy ( $w_{ij}$ ) and the calculation of phase diagrams.

There were no statistical differences in determining the phase diagram in HTP platforms and bench-scale, verifying the reliability of methods and equipment suggested in this work. Moreover, tailored approaches to quantify the solutes were

presented, taking into account the limitations of techniques that can be applied with ATPS due to the interference of phase forming components with the analytics. This fast methodology proposes to screen up to six different polymer-salt systems in eight days and supplies the results to understand the influence of sugar and protein concentrations on their partition coefficients. Exploring experimentally the ATPS hydrolysis provided strategies on how to conduct extractive enzymatic hydrolysis in ATPS and how to explore the experimental results in order to design a feasible process. In the conceptual design of extractive enzymatic hydrolysis, one of the major bottlenecks identified was the partitioning of glucose to both phases. The resultant conceptual process design operates as a tool to evaluate ATPS hydrolysis and compare it to conventional one. On the other hand, the thermodynamic model could not quantitatively describe the data. This occurs mainly because of the strong influence of random experimental errors on the estimation of interchange energy, systematic errors when translating the observed data to calculated partition concentrations, and FH not being an exact description of phase separation in salt based ATPS.

The high throughput screening methodology indicated ATPS able to partition sugar and enzymes. The selected ATPS presented no significant improvements to perform the enzymatic conversion of sugarcane bagasse compared to the conventional hydrolysis. The main reasons were the influence of phase forming components on the enzymatic activity and the low selectivity of sugars in the ATPS. To disclose the application of ATPS in the ethanol processing industry, the recovery and reuse of the phase forming components are imperative for economic feasibility. Moreover, the developed high throughput platform could be further employed to exhaustively screen systems to design effective ATPS for the partition of sugars and proteins in polymer-salt systems.

## SAMENVATTING

(Translated by Peter Verheijen)

Om het gebruik van lignocellulose restafval in de ethanolverwerkende industrie te verbeteren, was dit werk erop gericht om te testen of de productinhibitie van enzymatische hydrolyse kan worden verlicht door een extractieve reactie met behulp van een waterig tweefasensystemen (aqueous two-phase systems, ATPS). De prestaties van enzymatische hydrolyse in ATPS zijn in de literatuur niet goed gedefinieerd. In dit proefschrift is deze extractieve reactie getest in termen van de experimentele omzetting van suikerrietbagasse, van simulaties via een conceptueel procesontwerp en van een economische haalbaarheidsanalyse. Er werd een thermodynamisch raamwerk ontwikkeld om ATPS-vorming te voorspellen.

De screening van ATPS en de verdelingscoëfficiënt van de opgeloste stoffen werden uitgevoerd in een high-throughput station. De ATPS werden samengesteld met een mengsel van polymeer en zout. De enzymen werden vertegenwoordigd door het enzymatische cocktail Cellic CTec (Novozymes). De ontwikkeling van dit platform bestond uit twee hoofdonderdelen: bepaling van de fasediagrammen (binodale curves en bindlijnen) en kwantificering van de opgeloste stoffen (suiker en eiwitten) in zowel de top- als de bodemfase. De meest veelbelovende ATPS-systemen werden experimenteel onderzocht voor enzymatische hydrolyse van suikerrietbagasse. Het procesontwerp simuleerde twee scenario's: hydrolyse in de onderste fase en in de bovenste fase. Onderwerpen zoals de adsorptie van fasevormende componenten aan de bagassevezels en de invloed van enzymlasting op de hydrolyse werden onderzocht. De suikerriet hydrolyse in ATPS werd conceptueel beoordeeld door de implementatie van een model dat bestaat uit twee delen: hydrolyse en ATPS multi-batch scheiding. Het ontworpen geval dat gekenmerkt wordt door de ATPS hydrolyse werd vergeleken met het basisgeval dat gedefinieerd is als conventionele hydrolyse. Met betrekking tot de thermodynamische modellering van ATPS, werd de toepassing van het Flory-Huggins (FH) model voor het voorspellen van fasescheiding in polymeer-zoutsystemen geëvalueerd. De implementatie en analyse van de FH-theorie

omvatte de schatting van de uitwisselingsenergieën ( $w_{ij}$ ) en de berekening van de fasediagrammen.

Er waren geen statistische verschillen in het bepalen van het fasediagram in HTP-platforms en bench-scale, waarbij de betrouwbaarheid van de in dit werk voorgestelde methoden en apparatuur werd geverifieerd. Bovendien werden op maat gemaakte benaderingen voor het kwantificeren van de oplossingen gepresenteerd, rekening houdend met de beperkingen van technieken die kunnen worden toegepast met ATPS als gevolg van de interferentie van de fasevormende componenten met de analyses. Deze snelle methodologie stelt voor om tot zes verschillende polymeer-zoutsystemen te screenen in acht dagen en levert de resultaten om de invloed van suiker- en eiwitconcentraties op hun verdelingscoëfficiënten te begrijpen. Het experimenteel onderzoeken van de ATPS hydrolyse leverde strategieën op voor het uitvoeren van extractieve enzymatische hydrolyse in ATPS en voor het verkennen van de experimentele resultaten om een haalbaar proces te ontwerpen. In het conceptuele ontwerp van extractieve enzymatische hydrolyse, was het een van de belangrijkste knelpunten de verdeling van glucose over beide fasen. Het resulterende conceptuele procesontwerp werkt als een instrument om ATPS-hydrolyse te evalueren en te vergelijken met conventionele hydrolyse. Aan de andere kant kon het thermodynamische model de gegevens niet kwantitatief beschrijven. Dit komt vooral door de sterke invloed van experimentele fouten op de schatting van de uitwisselingsenergie, systematische fouten bij het vertalen van de waargenomen gegevens naar berekende partitieconcentraties en het feit dat FH geen exacte beschrijving is van de fasescheiding in ATPS op basis van zout.

De high-throughput screeningmethode gaf aan, dat ATPS in staat is om suiker en enzymen te scheiden. De geselecteerde ATPS bood echter geen significante verbeteringen voor het uitvoeren van de enzymatische omzetting van suikerrietbagasse in vergelijking met de conventionele hydrolyse. De belangrijkste redenen waren de invloed van fasevormende componenten op de enzymatische activiteit en de lage selectiviteit van de suikers in het ATPS. Om de toepassing van ATPS in de ethanolverwerkende industrie bekender te maken, is de terugwinning en



het hergebruik van de fasevormende componenten noodzakelijk voor de economische haalbaarheid. Bovendien zou het ontwikkelde high-throughput platform verder kunnen worden ingezet voor het uitvoerig screenen van systemen voor het ontwerpen van effectieve ATPS voor de scheiding van suikers en eiwitten in polymeer-zoutsystemen.



## RESUMO

Almejando melhorar a utilização de resíduos lignocelulósicos na indústria de processamento do etanol, este trabalho visa testar se a inibição por produto da hidrólise enzimática pode ser aliviada através de reação extrativa usando sistemas aquosos bifásicos (ATPS). A performance da hidrólise enzimática em ATPS não está bem definida na literatura. Nesta tese, a reação extrativa foi testada em termos de conversão experimental do bagaço de cana-de-açúcar, simulações através de design conceitual de processo e viabilidade econômica. O modelo termodinâmico foi desenvolvido para prever a formação de ATPS.

A triagem de ATPS e coeficiente de partição dos solutos foram conduzidos em uma estação de *high throughput* (HTP). Os ATPS foram compostos por polímero e sal. As enzimas foram representadas pelo coquetel enzimático Cellic CTec (Novozymes). O desenvolvimento desta plataforma consistiu de duas principais partes: determinação do diagrama de fases (curvas binodais e tie lines) e quantificação do soluto (açúcar e proteínas) nas fases de topo e de fundo. O ATPS mais promissor foi experimentalmente explorado para a hidrólise enzimática do bagaço de cana-de-açúcar. O design do processo simulou dois cenários: hidrólise ocorrendo na fase de topo e na fase de fundo. Tópicos como adsorção dos componentes formadores de fase às fibras do bagaço e a influência da carga enzimática na hidrólise foram explorados. A hidrólise do bagaço em ATPS foi conceitualmente avaliada através da implementação de um modelo composto de duas partes: hidrólise e separação multi-batelada em ATPS. O modelo projetado para a hidrólise em ATPS foi comparado com o modelo base definido como hidrólise convencional. Considerando a modelagem termodinâmica do ATPS, foi avaliada a aplicação do modelo de Flory-Huggins (FH) para prever a separação de fases em sistemas polímero-sal. A implementação e análise da teoria de FH envolveu a estimativa da energia de interação ( $w_{ij}$ ) e o cálculo do diagrama de fases.

Não houve diferenças significativas na determinação do diagrama de fases nas plataformas HTP e escala de bancada, verificando a confiabilidade dos métodos e equipamento sugeridos neste trabalho. Além disso, abordagens personalizadas

para quantificar os solutos foram apresentadas, levando em consideração as limitações das técnicas que poderiam ser aplicadas em ATPS devido à interferências dos componentes de fases com os analíticos. Esta metodologia rápida propõe a estudar até seis diferentes sistemas polímero-sal em oito dias e fornecer os resultados para entender a influência das concentrações de açúcar e proteína nos coeficientes de partição. A exploração experimental da hidrólise em ATPS forneceu estratégias de como conduzir a hidrólise enzimática extrativa em ATPS e de como explorar os resultados experimentais a fim de projetar um processo factível. No design conceitual da hidrólise enzimática extrativa, um dos maiores gargalos identificados foi a partição da glicose para ambas as fases. O design do processo resultante deste trabalho opera como uma ferramenta para avaliar hidrólise em ATPS e compará-la com a hidrólise convencional. Por outro lado, o modelo termodinâmico não pode descrever quantitativamente os dados. Isso ocorre principalmente por causa da forte influência dos erros experimentais randômicos na estimação da energia de interação, erros sistemáticos ao converter dados observados para concentrações de partição calculadas, e FH não ser uma descrição exata da separação de fases em ATPS formados por sais.

A metodologia de triagem *high throughput* indicou ATPS capazes de particionar açúcar e enzimas. O ATPS selecionado não apresentou melhorias significativas em conduzir a conversão enzimática do bagaço de cana-de-açúcar em comparação à hidrólise convencional. As principais causas foram a influência dos componentes formadores de fases na atividade enzimática e a baixa seletividade dos açúcares em ATPS. Para revelar a aplicação de ATPS na indústria do processamento do etanol, a recuperação e reuso dos componentes formadores de fases são imperativos para a viabilidade econômica. Além disso, a plataforma HTP desenvolvida pode ser futuramente empregada para filtrar exaustivamente sistemas para projetar ATPS efetivos à partição de açúcares e proteínas em sistemas polímero-sal.



# CHAPTER 1

## General Introduction

### 1. Biofuel and renewable products from biomass

Processing of lignocellulosic materials can generate energy, fuel and value-added chemicals. The versatility of the biomass provides a competitive advance against other renewable sources to produce exclusively energy. Moreover, the lignocellulosic materials are generally abundant residues of commodities plantation, paper and cellulose industry, and forests (Haghighi Mood et al., 2013).

Sugarcane bagasse is the residue of processing sugarcane for the production of sugar and ethanol. In the first ethanol generation industry, after the reception and milling of the sugarcane, the juice is treated and processed to sugar (via crystallization) and/or (first generation) ethanol (via fermentation and distillation). The solid fraction of the milling unit operation is the sugarcane bagasse (Hahn-Hägerdal et al., 2006). Although this residue is non-food related and available without geographical limitations, the low mass and energy densities of lignocellulosic biomass results in logistic challenges. High logistic costs are mainly related to the collection, storage and transportation of the raw material. These features requires a cellulosic ethanol production plant with small processing capacities and located next to the first generation ethanol production plant (feedstock supply) (Liu et al., 2019).

In an integrated first-generation fuel and biorefinery plant, sugarcane bagasse is processed into second generation fuel sharing facilities, equipment and labour with the processing of first generation ethanol. This configuration provides cost reduction through the sharing of the common unit operations: sugar extraction, juice preparation, fermentation, distillation, and biomass combustion (Losordo et al., 2016). Second generation (2G) ethanol product cost is also closely connected to the global location and technology

development. Brazil and Asia are estimated to be the cheapest locations to produce 2G ethanol, mainly because of local feedstock prices, local plant and installation costs, local energy costs and local market prices for the biorefinery products (Larsen et al., 2012).

The diversified range of value-added products that can be derived from the lignocellulosic material processing can increase the diversity of products and improve the financial performance of biorefineries (Yamakawa et al., 2018). In an optimized biorefinery, the sugar stream can be converted to fuels and/or chemicals. This sugar switch enables the production of low market volume and high market price products. Lignin can also be used as a precursor and substrate for value-added components. Part of lignin can still supply the power and heat demand (Yamakawa et al., 2018). At the demonstration plant for 2G ethanol constructed by Inbicon, in Kalundborg, Denmark, lignin was recovered as the bottom product after distillation. Even though that process configuration limited the applications and valorisation of lignin, the lignin cake was dried and pelletized into lignin pellets, which have a high heating value (Larsen et al., 2012). The main by-products of the lignocellulosic biomass processing are fufural, hydroxymethylfurfural, heavy metals, acetic acid and the ones derived from lignin. The products butanediol, propanediol, acetaldehyde, acetic acid, acetic anhydride, acetone, butanol, ethanol, ethyl acetate, ethyl lactate, ethylene, ethylene glycol, furfural, glutamic acid, isobutanol, itaconic acid, lactic acid, lactide, lysine, microfibrillated cellulose, polyethylene glycol (PEG), polylactic acid, sorbitol, succinic acid, xylitol and terpenes appear as potential candidates for a biorefinery, with a Technology Readiness Level (TRL) of at least 8. These products have reached a commercial scale and are ready to be implemented into a cellulosic ethanol process (Rosales-Calderon and Arantes, 2019). The recycle of the process residues and optimized use of the lignocellulosic biomass fractions support the sustainable and environmentally friendly approach of the biorefinery.

In Figure 1, the aspects influencing the lignocellulosic material processing are depicted and classified per unit operation. The work performed in this thesis aimed to overcome the product inhibition of the enzymes during the biomass conversion to sugar. Additionally, issues related to the process operation (e.g. recycle of process

16

residues, recycle of enzymes and operation in continuous mode) were also assessed during the process design and techno-economic analysis. The description of the unit operation related to the 2G ethanol production, their limitations and the readiness of the technique are treated below.

The recalcitrance of the lignocellulosic biomass to release the sugar monomers requires several chemical, thermochemical and/or biological transformations before being processed to sugar and liquid fuels. The main unit operations to deal with this residue are the pre-treatment and enzymatic hydrolysis. However, improvements in lignocellulosic utilization are evident in the fields of pre-treatment of the biomass (Liu et al., 2019), detoxification of the hydrolysate (Cray et al., 2015), (incomplete) conversion during hydrolysis and fermentation (Yamakawa et al., 2018); and development of new biocatalysts (Gupta et al., 2016).

The pre-treatment of the biomass is necessary to loosen the fibres and make the biomass more accessible to enzymatic degradation. However, the main challenges of this unit operation are the high costs associated and the production of toxic by-products (Yamakawa et al., 2018), which can inhibit further unit operations and impair their performance. Physicochemical reactions (e.g. liquid hot water and steam explosion) could have their sugar yield improved by acids and alkalis. Even though the addition of chemicals could conduct the pre-treatment at mild temperatures, the acids and alkalis pose as a risk to the environment and to the stainless steel equipment (Liu et al., 2019). The combination of pre-treatments is a reasonable approach to obtain the advantages of each option. For example, the ammonia fibre explosion (AFEX™, registered trademark of MBI International, Lansing, MI) is a combination of ammonia pre-treatment and steam explosion (Garlock et al., 2012).

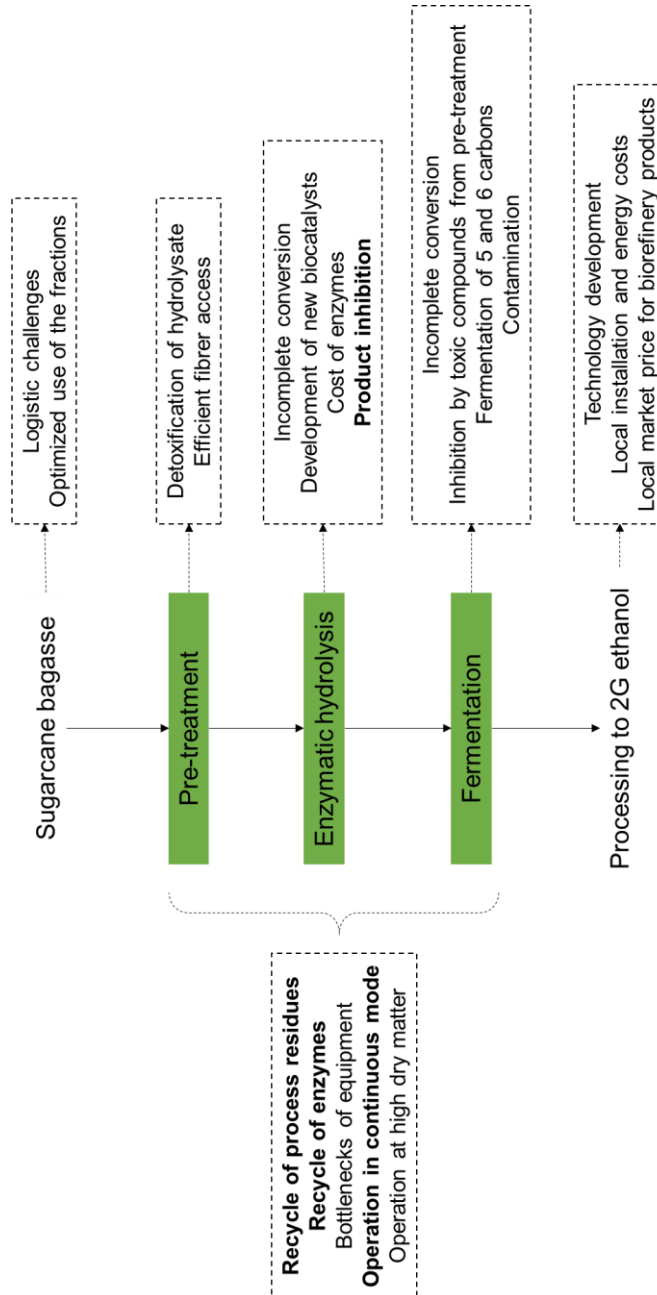


Figure 1: Important aspects influencing the lignocellulosic processing to second generation ethanol. Aspects in bold are treated in this thesis.

The selection of the pre-treatment defines whether lignin will be present in further unit operations. Alkalis react with lignin, and are an option for delignification processes. When lignin is separated from the fibres before the fermentation, more value can be associated to it. Lignin utilization hides a great opportunity of adding competitiveness to the biorefinery through the development of its application (Yamakawa et al., 2018). The presence of lignin in the subsequent unit operations leads to an unproductive space on the reactors and consequently extra mixing, and energy input, are required. Moreover, lignin deposition on the fibres blocks the access of the enzymes, leading to ineffective hydrolysis. Further in the process, the decomposition of lignin produces toxic compound for the microbial growth. However, delignification processes involving alkalis impact negatively the environment, via production of salt, wastewater and the black liquor (Liu et al., 2019).

The challenges involving the enzymatic hydrolysis concerns the cost of enzymes and solids effect (mainly product inhibition) (Gupta et al., 2016; Bezerra and Dias, 2005). In order to overcome the product inhibition, the product removal emerges as an option. This strategy has been reported via centrifugation and removal of supernatant (Yang et al., 2011), design of reactors (Andrić et al., 2010) and continuous hydrolysis (Stickel et al., 2018). Inbicon has patented a hydrolysis process to operate the conversion at high solid load (25% mass fraction) using a horizontal reactor and a gravity mixing system. The strategy to overcome product inhibition at high solid content was the continuous hydrolysis and fermentation. The liquefaction of the substrate (as the authors call the enzymatic hydrolysis) occurred for 6 hours before the liquefied slurry was pumped to fermentation (Larsen et al., 2012). Apart from the product removal, the conventional (batch) process to perform enzymatic hydrolysis offers room for improvement regarding the reaction conditions, enzyme recycling and recovery strategies.

Although the conversion of hexoses to ethanol is a well established process, the sugar provided from lignocellulosic biomass presents challenges to the fermentation process. Because of the unit operations aiming to release the fermentable sugars (pre-treatment), important inhibitors to the fermentation step are present (Mussatto and Roberto, 2004). Also, the hemicellulosic fraction of the biomass is hydrolysed

into pentose sugars, which are not consumed by the yeasts commonly used in the first generation process. A microorganism able to ferment both pentoses and hexoses and an optimized fermentation process are required to overcome the inhibition challenge and improve the fermentation performance. The contamination in the fermentation step is also a hindrance for the establishment of a well-proven and mature 2G industrial production plant. The demonstration plant constructed by Inbicon overcame this challenge by adjusting the concentration of inhibitors from the pre-treatment (mainly hemicellulose and lignin degradation products) (Larsen et al., 2012).

Currently, the production of 2G biofuels have been performed at commercial scale by companies in United States, China, Europe and Brazil. Even though some of them are idle at the moment (e.g. Abengoa, United States; Beta Renewables, Italy; Dupont, United States; Henan Tianguan, China; Ineos Bio, United States; and Longlive Bio-technology, China), some commercial plant have succeeded in the production of cellulosic ethanol: Raízen (Brazil), POET-DSM (United States), GranBio (Brazil), Borregaard Industries (Norway) (Padella et al., 2019).

However, there are still several bottlenecks to improve the lignocellulosic biomass utilization in order to turn the process based on this feedstock as competitive as fossil-based processes and delivering similar products on the market. At the demonstration plant by Inbicon, the optimization of the technology to lower the production costs of ethanol consisted of reducing the energy consumption, improving the water balance, adding a fermentation step for C5 sugars, recycling of enzymes in the process and identifying and improving bottlenecks of equipment (Larsen et al., 2012). The technology developed by the company Clariant, named Sunliquid®technology, is revolutionizing the cellulosic ethanol industry. They claim to have achieved an energy self-efficient process, and economically feasible. Sunliquid®technology integrates the enzyme production to the process, reducing the dependence on suppliers and making the overall process more cost efficient. The tailored production of enzymes specifically to the substrate in use determines a high conversion to sugar during enzymatic hydrolysis. Regarding the fermentation step, both sugars (C5 and C6) are metabolized into ethanol, increasing in around 50% the

20

ethanol yield. The breakthrough innovation in terms of energy efficiency is related to the ethanol recovery. Instead of distillation, Sunliquid® technology applies an adsorption technique to separate ethanol and water (Rarbach and Sötl, 2013). The first commercial scale cellulosic ethanol production plant featured by Clariant started the production in 2020, in Romania. Sunliquid® cellulosic ethanol plant has already been licensed by Enviral, in Slovakia, Anhui Guozhen Group, in China, and Eta Bio, in Bulgaria.

The readiness of the 2G ethanol and bio-based building blocks production is still limited by the efficiency and costs associated with the pre-treatment and enzymatic hydrolysis. In terms of the technology development, the operation in continuous mode and at high dry matter are key factors to reduce costs of the 2G ethanol production (Larsen et al., 2012). The experience of Inbicon in releasing a demonstration plant suggests that partnership with enzyme suppliers, component suppliers, engineering companies, construction companies and suppliers of utility plants are key strategy to build a cost-effective technology. Still, the cellulosic ethanol production has not been competitive enough compared to conventional ethanol.

## **2. Aqueous two-phase systems (ATPS)**

To overcome the challenge of product inhibition during hydrolysis of lignocellulosic materials, sugars should be separated from the reaction phase (containing enzymes). Aqueous two-phase systems (ATPS) appear as a potential technique to partition sugar and enzymes to different phases and, consequently, provide an *in situ* extraction of the product during the conversion of biomass.

### **ATPS fundamentals**

ATPS are liquid solutions composed of immiscible phases above a certain concentration. These systems are formed most of the time by a pair combination of polymers, salts and ionic liquids (Freire et al., 2012). Solutes can partition unevenly among the system, partially because of the different properties of these phases. The mild environment, connected to the ability to separate solutes among the phases, define the ATPS as an interesting liquid-liquid separation technique to recover and/or

purify molecules (Albertsson, 1961). In the application of ATPS for the processing of lignocellulosic material, the mild environment is an important condition for the enzymatic activity during the hydrolysis.

The ATPS can be described by the phase diagram, composed by binodal curve and tie lines (Kaul, 2000). The binodal curve, which refers to the concentration of phase forming components (PFC), defines if the system is homogeneous or biphasic at a certain concentration. For biphasic systems, the tie lines connect the compositions of top phase and the respective bottom phase in equilibrium. Moreover, the longer the tie line, the greater the difference between the composition of the phases in equilibrium (Albertsson, 1961). Systems with different total concentration of PFC, when lying down on the same tie line, present the same concentration of top and bottom phases. These systems differ only in the volume ratio of the phases. The volume of the two liquid phases should be in an intermediate and optimum composition, once equal volumes enable emulsion occurrence in both phases, and volumes of different sizes enables emulsion occurrence in the largest phase (Albertsson, 1958). Another feature of ATPS belonging to the same tie line is the ability to partition the solutes in the same proportion between the phases (the same partition coefficient). The characterization of phase diagrams, as well as the influence of the hydrolysis components on the ATPS, provide decisive information to the definition of process designs suitable for the processing of lignocellulosic materials.

Dextran and polyethylene glycol compose one of the most widely-spread aqueous two-phase systems for recovery of biological compounds (Gustafsson and Tjerneld, 1986). However, the high cost of fractioned dextran makes its application not feasible at large scales. On the other hand, crude dextran presents high viscosity and it is not suitable for systems which depends on efficient mass transfer. Polymer-polymer ATPS have been applied for extractive bioconversions, in order to remove the products from the biocatalysts (Yau et al., 2015).

In order to fulfil the industrial demand for cost-effective and efficient downstream separation technologies, polymer-salt ATPS have been extensively explored (Yau et



al., 2015) as an alternative to chromatography (Yau et al., 2015). Since 2008, salt-based ATPS are the vast majority of the research involving ATPS, due to their lower cost and easier manipulations and availability (Grilo et al., 2016). These biphasic systems have already proved to be economically and environmentally worth for the recovery of antibodies (Rosa et al., 2011). Examples of other biopharmaceutical applications of salt-based ATPS are reviewed by Yau et al. (2015), including the purification of human growth hormone, insulin-like growth factor and interleukin. Although several studies apply phosphate salt as a phase forming constituent (Ventura et al., 2011) (Moreira et al., 2013) (Costa et al., 1998), there is a tendency to study biodegradable and less harmful salts to the environment, such as citrate, tartrate and acetate (Herculano et al., 2012) (Passos et al., 2012). In this thesis, polymer-salt ATPS were explored for the separation of proteins and sugars, the solutes of the enzymatic hydrolysis of lignocellulose materials.

ATPS can also be constituted by ionic liquids (IL), which are asymmetric organics salts in liquid phase in temperatures below 100 °C. Normally, they consist of an organic cation and an inorganic anion. Physicochemical properties of IL, as hydrophobicity, density, viscosity (IL are less viscous than typical polymer-based ATPS) (Ventura et al., 2011), melting point, polarity and solvent miscibility can be controlled through specific cation (specifically its R group) and anion combinations (Hernández-Fernández et al., 2010). The most common cations used in ionic liquids based two-phase systems are imidazolium, phosponium and ammonium with the bromide, chloride and tetrafluoroborate (BF<sub>4</sub>) counterions (Passos et al., 2012). IL based ATPS can be applied for protein extraction (Desai et al., 2014), enzyme purification and stabilization. However, it is reported that high concentration of ionic liquids can cause aggregates of the solute proteins, because of the interaction of exposed hydrophobic regions between proteins. Moreover, Turner et al. (Turner et al., 2003) conducted enzymatic hydrolyses of cellulose in the presence of two ILs: [bmim]Cl (1-butyl-3-methylimidazolium chloride) and [bmim][BF<sub>4</sub>] (1-butyl-3-methylimidazolium tetrafluoroborate). Increasing the concentration of IL lead to a decrease of enzymatic activity, probably because of the denaturing effect of the chloride ion. That work concluded that “salt-like” (strongly basic) IL produces a

dehydrating environment which is not beneficial for enzymes. Additionally, there is evidence that some ionic liquids dissolve cellulose, contribute to lignocellulosic material delignification or present acid catalytic activity (Sakdaronnarong et al., 2016).

Other formulations of ATPS include thermo-separating polymers, alcohol, surfactants, affinity ligands, and carbohydrates. The thermo-separating polymers are commonly suggested to facilitate the recovery of the product, the recycle of the components and to mitigate the environmental impact (Yau et al., 2015) (Grilo et al., 2016). Also, renewable, biodegradable and non-toxic phase forming components, such as the carbohydrates, can generate a more friendly environment to the biomolecules (De Brito Cardoso et al., 2013). In case of the affinity ligands, they are covalently coupled to one or both of the phase forming polymers. Then, the target molecule is attracted by the affinity ligand, partitioning preferentially to that phase. In this case, a rapid enzyme purification can be conducted (Gustafsson and Tjerneld, 1986).

The efficiency of a certain solute to partition among top and bottom phases can be expressed through the partition coefficient, which is the concentration of the referred solute at top phase over the one at bottom phase (Grilo et al., 2016). In order to understand and predict the partition of biomolecules in aqueous two-phase system (ATPS), it is important to consider the parameters governing this behaviour. The main parameters are divided into two groups: structural factors, such as biomaterial size (surface area), surface properties, structure and hydrophobicity, net charge; and environmental factors, such as type, molecular weight and concentration of phase polymers, type and concentration of phase salt, pH, temperature and affinity ligands (Baskir et al., 1989) (Grilo et al., 2016). Interfacial tension and electrical potential difference between the two phases also play an important role in the partitioning of solutes in ATPS (Grilo et al., 2016). Another approach of evaluating the contributions to the overall partition of a solute was developed by Johansson (1986) (Albertsson, 1986). In that model, the partition is governed by the size, electrochemical, hydrophobic, affinity and conformational contributions. Even though several models

can be found in literature to describe the partition of solutes in ATPS, the mechanisms behind are poorly understood (Grilo et al., 2016).

Large proteins (higher molecular weight) tend to partition more unevenly (one-side distributed) and are likely more affected by component concentration than smaller ones. Besides the biomaterial size, surface properties (such as polarity, charge and hydrophobicity) and conformation of the proteins can influence the distribution of them between the phases (Dreyer and Kragl, 2008). The molecular affinity towards a determined phase component can also be governed by the miscibility of the compound and viscosity of the phase. The greater the polymer molecular weight, the greater the viscosity and the greater the difficult of phase separation (Mazzola et al., 2008). Moreover, the protein concentration should be an order of magnitude lower than the phase polymer concentration to not affect the system properties. In the hydrolysis system, when enzymes are adsorbed to the lignocellulosic material (sugarcane bagasse), these factors are less relevant to the partition of the proteins.

The polymer molecular weight can influence the composition of the phases (and alter the phase diagram) and the number of polymer-protein interactions. The higher the molecular weight, the lower the concentration of polymers necessary for the formation of two phases (Albertsson, 1958). Moreover, the increase in molecular weight (chain length) of the polymer phase component where protein should be partitioned in, can lead to protein precipitation due to the increase in hydrophobicity of the phase (Dreyer and Kragl, 2008). Another consequence of high molecular weights of PEG is the partition of enzymes to the bottom phase (Gustafsson and Tjerneld, 1986).

Regarding the charged phase forming components, such as the salt, a potential difference between phases can be created. This influences the partitioning of charged biomolecules, such as proteins. An additional salt, generally sodium chloride, to polymer/polymer ATPS can also alter their equilibrium. The salt concentration can also influence the mixing of two different polymer solutions (Albertsson, 1986). For instance, systems containing two polyelectrolytes with opposite net charges (for example sodium dextran sulphate and chloride salt of

diethylaminoethyl(DEAE)dextran) are collected in the same phase at low NaCl concentrations, due to the coacervation phenomena. If the same system is formed in the presence of high salt concentration, the polymers are collected in different phases. A miscible system can also be formed at intermediate NaCl concentrations (Albertsson, 1986). However, systems containing only nonionic polymers, such as PEG and dextran, separate regardless the salt concentration or pH.

The conditions (pH and temperature) in which the ATPS is formed and separated also play an important role in the systems. pH variation can influence protein partition due to electrostatic interaction between the molecule and the phase component (Desai et al., 2014). In this case, the isoelectric point in combination with the pH of the phase can lead to a positive or negative charge in proteins. The charged protein will present more affinity by the phase with opposite charge. Regarding to the temperature, a variation on this parameters alter the shape of the binodal curve of the phase diagram (Baskir et al., 1989). Moreover, temperature appears to influence the partition behaviour of enzymes in ATPS. Tjerneld et. al (1984) (Tjerneld et al., 1985) showed that enzymes tend to be two-sided partitioned under temperature of 50 Celsius degree. At this temperature, partition coefficients were increased by a factor of two. For the system studied by Dreyer (2007) (Dreyer and Kragl, 2008) (ions of Ammoeng110TM and K<sub>2</sub>HPO<sub>4</sub>/KH<sub>2</sub>PO<sub>4</sub>), the dependence of phase separation on temperature is inversely proportional. A decrease in temperature enables phase separation at lower concentrations of phase forming compounds. ATPS aimed for enzymatic reactions are limited to the optimal pH and temperature operational range of the enzymes.

Predictive models, through thermodynamic analysis or molecular dynamic simulations, can contribute to the understanding of the governing principles in phase diagrams and partitioning behaviour of molecules. These models could reduce experimental work and assist on the perception of the system prior to its lab optimization and/or implementation at industrial-scale. Moreover, predictive models would enable the optimization of a feasible system identified at bench-scale. However, these predictions are qualitative rather than quantitative — applied to the specific conditions in which it was built —, since a large variation in the systems can

be detected when the characteristics are varied (Torres-Acosta et al., 2019). Progress in this field would investigate and develop models with a more universal prediction ability.

### *ATPS trends, applications and industrial perspective*

Conceptual process design and economic analysis assist the scale-up of technologies and process by identifying the production cost and the critical contributors for the cost, by analysing the effect of variations on parameters (e.g. Monte Carlo simulation), by describing the behaviour of the bioprocess under real variation scenarios, and by creating strategies to control the process (Torres-Acosta et al., 2019). This prior evaluation identifies the bottlenecks and assists on the decision-making related to the process implementation of biomolecules at industrial scale.

In order to accelerate the screening and optimization of the ATPS conditions, high-throughput platforms have emerged as a tool/workspace able to miniaturize and automate the phase formation and partition of molecules. High throughput screening can also generate data set to ATPS intensification (optimized combination of volume ratio and sample size) and to the development of predictive models. For instance, the volume ratio and tie line length of a certain system can define which is the continuous phase, impacting the time for the phase separation (Torres-Acosta et al., 2019). High-throughput platforms have been applied to assess biomass digestibility (Chundawat et al., 2008), to perform enzymatic assays for measuring activity of enzymes (cellulases) (Decker et al., 2003) and to conduct an integrated pre-treatment and enzymatic hydrolysis (Selig et al., 2010).

High throughput techniques and developing of reliable predictive models have been identified as novels approaches to facilitate the incorporation of ATPS into large-scale operations (Torres-Acosta et al., 2019). So far, the application of ATPS in large scales are limited to pilot plants. At that scale, the equilibrium of the phases was reported to be achieved by gravitational and centrifugal fields. After phase separation and partition of the solute according to the application, the phase forming

components are considered impurities in the operation. The recycle of the phase forming components is important in order to reduce the operational costs of the implemented technology (50% of the total process cost corresponds to the phase forming components (Rosa et al., 2011)). Currently, ultrafiltration and precipitation techniques have been applied for the recycle of phase forming components at large-scale. Development in this topic would seek for recycle techniques that does not require an extra unit operation, in order to avoid higher production cost (Torres-Acosta et al., 2019). Moreover, the time for a system to achieve phase separation is of paramount importance to preserve the attractiveness of the ATPS optimized at bench-scale (Torres-Acosta et al., 2019).

Although ATPS have been extensively researched at lab scale and also tested at pilot (large) scale, they have not been yet implemented at industrial scale. The research lacks applied case studies, in which the perspective of the industrial reality is taken into account during the research development (Pereira et al., 2020). Even though ATPS is proven to be scalable (Torres-Acosta et al., 2019), the main bottlenecks restricting the implementation of ATPS at industrial plants are thought to be the technologies promoting a continuous and integrative ATPS to the process (González-Valdez et al., 2018).

The integration of the ATPS unit operation with enzymatic reaction processes provides the compartmentalization of the reaction, alongside the all-in-one concept (reaction and separation). This strategy has already been applied in enzymatic reactions in order to immobilize the catalysts in porous support (Hernandez-Justiz et al., 1998). Separating the product and the catalyst is a strategy for water soluble substrates and products. Moreover, the extractive feature offered through ATPS has also been applied to fermentation processes, where the microorganism growth and the fermentation products recovery are polarized, while yet all-in-one (Kulkarni et al., 1999) (Hahn-Hägerdal et al., 1981).

Developing a reliable ATPS continuous process brings competitive advantages towards its implementation at industrial scale, such as: recycle of phase forming components, *in situ* separation (Pereira et al., 2020) and reduction of process time

(Espitia-Saloma et al., 2014). An equipment design platform would enable the selection of the ATPS continuous device according to the application and in order to avoid the main limitations of the operation: high flooding, backmixing, emulsification, and low separation efficiency (Espitia-Saloma et al., 2014). The main equipment used to conduct ATPS in continuous mode can be grouped in column contactor and mixer settler unit, being the later the most broadly used due to its inherent assembling easiness and the lack of versatility and limited margin for mass transfer and separation performance related to the column contactors (Espitia-Saloma et al., 2014).

The main advantages of exploring continuous processes at lab and/or mL-scale are the elucidation of the mechanisms governing the equilibrium and separation, and faster data acquisition (Espitia-Saloma et al., 2014), providing reliable information for accurate models development. The miniaturization of ATPS for micro-scale provides a better use of the resources (Espitia-Saloma et al., 2014) and fast partition, reducing associated costs and time (Soares et al., 2016). Microfluidics emerges as an approach to perform ATPS in which both continuous mode and high throughput operation are placed. In these devices, the systems are formed and partitioned in microfluidic channels, where the samples and phase forming components are injected via inlet streams in a continuous laminar flow. Consequently, the liquid flow rates and channel dimensions stand as the critical variable of the process. Because of the high ratio of interfacial area to total volume, the phase separation in microfluidics channels is governed only by diffusion. Top and bottom phases are differentiated only by the density of the phases. The allowance to dismiss the convective mixing (e.g. centrifugation) reduces one unit operation in the process (phase separation), which can confer advantages of the micro-scale over the mL-scale (Soares et al., 2016).

The versatility of the microfluidic devices confers the capability of operating multi-dimensional separations. The channels can be tailored with more than two conventional inlets designed for the phase forming components. Moreover, the micro channels can present different characteristics along their length, allowing for the micropatterning of cells. Through the micropatterning, the sample preparation and

concentration are integrated. However, the microfluidic approach is limited to scale-up, being mainly destined for analytical and screening purposes (Soares et al., 2016).

Although the above mentioned technological issues can be researched and solutions proposed at lab and pilot scale, other challenges will only be assessed whether ATPS turns into an industrial reality, such as: challenges with real implementation, validation, infrastructure and impurities of the (recycle) streams (Pereira et al., 2020). The technical challenges are not the only hindrance to the industrial implementation of ATPS. The ATPS based processes should present high resolution, let alone reduction in costs and increase efficiency when compared to the established technology. Moreover, the industrial/commercial reluctance of adopting ATPS should also be considered as an hindrance (Pereira et al., 2020).

In current research, the main applications of ATPS involves separation/extraction/purification in downstream bioprocessing, and analytical (concentration) procedures. ATPS have also been applied in hydrometallurgy for the selective extraction of metal ions, and in environmental remediation of industrial aqueous effluents. However, non-conventional applications of ATPS have been overcoming limitations in diagnosis (Pereira et al., 2020). Because of the competence of purifying and concentrating, ATPS can improve the detection of biomarkers related to diseases, let alone reducing the analysis costs and the shortening the assay in time. Moreover, ATPS have also been applied to the cultivation and compartmentalization of cells and microorganisms, microcapsule production, 3-D tissue assembly and synthetic biology (Teixeira et al., 2018). ATPS have been involved not only in novel applications, but they have also prompted the development of new systems based on the ATPS principles. Examples are the aqueous two-phase flotation (ATPF), which applies gas flow in order to achieve higher partition coefficients; and magnetic ATPS, which incorporates magnetic sensible particles and/or magnetic phase components, and allows the separation to occur under a magnetic field (Torres-Acosta et al., 2019).



Although there are some published works regarding the application of ATPS in biomass conversion, they do not use the two-phase system as an extractive environment for relieve product inhibition. Sakdaronnarong et al. (Sakdaronnarong et al., 2016) conducted the hydrolysis of sugarcane bagasse in an aqueous biphasic system. However, the authors applied the aqueous biphasic system for lignin fractionation (delignification), while cellulose hydrolysis was simultaneously occurring in the other phase. Koruda et al. (Kuroda et al., 2016) proposed a liquid-liquid biphasic system composed by water and hydrophobic acid and ionic liquid (hydrophobic cation and acidic anion). The purpose of that research was to hydrolyse the biomass and remove the fermentation inhibitor 5-hydroxymethyl furfural (5-HMF) from the system. Hydrolysis of cellulose occurs in the aqueous phase, and glucose remains in the same water phase (98% distribution ratio). 5-HMF (hydrophobic material) was shifted for the IL phase due to hydrophobicity of these molecules. A very little amount of IL is necessary to hydrolyse the cellulose, although the reaction occurs in the water phase. This can be justified by the fact that sugar yield kept increasing for the longest time when an IL-saturated aqueous solution system was applied. This approach (Kuroda et al., 2016) consists of a purification step development, which does not aim to relieve product inhibition related to the hydrolysis. On the other hand, a inhibition problem in the further unit operation (fermentation) is assessed.

Moreira et al. (2013) (Moreira et al., 2013) studied the recovery of laccase from a complex fermented medium using ATPS composed by ethylene oxide/propylene oxide copolymer (UCON) with potassium phosphate salts. The enzyme interaction with UCON is lower than with PEG, justifying the use of the former. In this case, protein partitioned mainly to the bottom phase (salt-rich phase), where UCON concentration is much lower (0.3–0.6% w/w). The thermo-sensitivity characteristic of UCON facilitates its recovery and reutilization (Silvério et al., 2013). Consequently, UCON-based ATPS presents a relative lower temperature to phase separation than PEG-based ATPS. Ventura et al. (2011) (Ventura et al., 2011) reported an ATPS formation for enzyme recovery, which was composed by hydrophilic IL (salting-in inducing electrolytes), solution of salting-out inorganic salts and water. The driving

force for phase splitting was due to the highest affinity of the used buffer (potassium phosphate) for water. Consequently, there was a migration of water molecules away from the IL, reducing its solubility in water. The IL cation alkyl chain length is the main feature that controls enzyme partition in a system composed by the IL and a salt-rich phase, followed by the anion nature and, at last, by the cation core (Ventura et al., 2011). Regarding the alkyl chain length influence on ATPS formation, the higher the number of carbon atoms (up to 6), the easier the phase separation, due to the increase in the hydrophobic character and lower affinity of the IL for water. Benzyl groups also promote an increase in the ability to form IL-based ATPS. Regarding the anion nature of the ionic liquid, the ability to form aqueous two-phase systems is related to the capability to form hydration complex. Then, anions of the ionic liquid compete with salt ions to interact with water. The stronger the interaction between ionic liquids anion with water or the lower their hydrogen bond accepting strength, the more able they will be to form ATPS. This means that less amount of salt is needed. This behaviour is independent on the salt nature or pH of the aqueous salt solution employed in the system (Passos et al., 2012). Considering the recovery of the product from the reaction system, Liu et al. (2017) developed an aqueous two-phase system based on ionic liquids and salt ( $K_3PO_4$ ). The sugar partitioned to the bottom salt-rich phase. Because the hydrolysis occurred in the presence of acid instead of enzymes, the aim of that research was to promote an extraction step to further fermentation of the sugars.

Adsorption of the enzymes to the substrate should be an alternative to enhance the one-sided partition, since cellulolytic enzymes have a strong affinity for particulate cellulose (Tjerneld et al., 1985). Tjerneld et. al (1984) (Tjerneld et al., 1985) studied the partitioning of *Trichoderma reesei* enzymes in ATPS composed by PEG-dextran. The aim was to extract the glucose (low-molecular-weight product) with the top phase. The partition coefficient of exo-beta-glucanase was essentially the same as for endo-beta-glucanase. Comparing endo-beta-glucanase with  $\beta$ -glucosidase, the former tends to be more evenly distributed between the phases, due to the presence of several components with different properties composing its molecule. On the other hand,  $\beta$ -glucosidase seems to partition to the bottom salt-rich phase in PEG-salt

systems. Both endo-glucanase and  $\beta$ -glucosidase are partitioned more to the bottom phase (dextran-rich phase) when dextran of low molecular weight and PEG of high molecular weight are used. Additionally, the higher the ratio substrate/enzymes, the lower the partition coefficient of endo-glucanase, once this enzyme is strongly adsorbed to the cellulose particles. The beta-glucosidase doesn't specifically bind to the cellulose particles. However, the enzymes were all partitioned in the bottom phase in an appropriated phase system (Dextran 40-PEG 40000) and under the influence of cellulose adsorption. Herculano et. al (2012) (Herculano et al., 2012) studied the partition and purification of a cellulolytic enzymatic cocktail in PEG/citrate ATPS. The four parameters studied (PEG molar mass, PEG concentration, sodium citrate concentration and pH) showed a positive effect on the partition coefficient of  $\beta$ -glucosidase (Herculano et al., 2012) (higher the partition of this enzyme to the PEG-rich top phase) as the the values of the parameters were increased. However, the partition of enzymes in ATPS presented by Herculano et. al (2012) was not evaluated under the influence of a substrate in the system.

The potential for an industrial application of ATPS aiming the partitioning of biomolecules are supported by the mild physicochemical environment (González-Valdez et al., 2018), scalability, biocompatibility, selectivity and continuous operation possibility of the technique. However, the lack of know-how on dealing with ATPS based process remains as an important weaknesses (Soares et al., 2015). Through research focused on generating knowledge and advances in high throughput screenings, predictive models and process design on continuous and integrative ATPS, the implementation of this technique to an industrial reality can be shortened.

The scientific findings of this thesis and the potential of defining a novel and competitive process to the hydrolysis of sugarcane bagasse can stimulate research groups to expand the work developed and presented here. The outcomes of the biomass utilization, especially regarding the opportunities for the value-added chemicals, have the potential to create new value chains based on renewable products. Increasing the utilization of the lignocellulosic biomass would stimulate rural development, and develop the industrial sector. The society directly benefits

from these outcomes, with sustainable options and healthier alternatives than fossil-based products.

Concerning the environmental benefits, the utilization of biomass for energy, fuels and chemicals would reduce the amount of waste and cooperate to sustainable processes. The use of biomass promotes a balanced life cycle of carbon dioxide and a reduction on the greenhouse gases emissions, both issues contributing to mitigate climate change. However, a life cycle analysis of the suggested extractive process would be necessary to evaluate the extension of the environmental impact, mainly due to the use of polymer and salts. In the economic aspect, the establishment of a bio-based industry for fuels and chemicals would reduce the dependency on fossil fuels and stimulate the competitiveness between these sectors.

### **3. Statement of purpose**

This work aimed to test if the product inhibition of the enzymatic hydrolysis could be relieved by extractive reaction using aqueous two-phase system.

### **4. Scope of the thesis**

The current development of the use of lignocellulosic materials urges for efficient processes to access the fibre components. The product inhibition of the enzymes during the batch process on conventional hydrolysis could be reduced by removal of the product (sugar) (Yang et al., 2011). Applying ATPS to enzymatic hydrolysis of lignocellulosic materials would provide an *in situ* removal of the products, through the uneven partition of the solutes (sugar and enzymes).

The composition of the ATPS can modulate the partition of the solutes and characterize the system in terms of phase separation, volume ratio of the phases, viscosity, etc. On face of it, an appropriate selection of phase forming components (polymer and salt) is of paramount importance to identify suitable systems to perform extractive enzymatic reactions. In **Chapter 2**, we present a high-throughput platform developed for the screening of phase forming components. After a pre-selection of phase forming components according to maintenance of enzymatic activity of the

cellulolytic enzymes, the platform determines phase diagrams and partition coefficients of the solutes (sugar and proteins). Moreover, this chapter discusses the limitation of techniques to quantify the solutes in ATPS due to the interference of phase forming components with the analytics, and suggest a novel way for protein quantification under polymer and salt influence. This automated and miniaturized platform can screen six different polymer-salt systems in eight days.

Phase separation in ATPS can be described by thermodynamic models. This approach enables the prediction of phase diagrams and provides a useful framework to conduct sensitivity analysis on parameters (e.g. salt type, polymer molecular mass, ionic strength) without the necessity of experimental assays. When trying to apply the Flory-Huggins (FH) theory to the high-throughput data collected in Chapter 2, the fit of the experimental data to the model was poor. To elucidate the application and limitations of FH theory to polymer-salt based ATPS, **Chapter 3** brings an analysis on FH-based models used to calculate phase separation in ATPS, in terms of problem formulation and mathematical solving algorithm. To test if the FH thermodynamic model could describe and predict our data, an algorithm was developed to estimate the pair-wise interchange energy and calculate the phase composition. The suggested mathematical approach to determine the FH interaction parameters, derived from the interchange energy, is a step forward to boost the FH mean-field model for predicting phase separation.

In **Chapter 4**, strategies to perform the enzymatic hydrolysis of sugarcane bagasse in ATPS were explored. The composition for the model systems were defined based on results in Chapter 2, considering the relative partitioning of the solutes. The experimental results provided the background (technical conditions) to the definition of the parameters in the conceptual process design, for hydrolysis occurring in the bottom phase and in the top phase. This study provided clarity in certain topics of the ATPS enzymatic hydrolysis, such as adsorption of phase forming components to the bagasse fibres, substrate partitioning and influence of solute partition on conversion. Moreover, advances on the conventional batch hydrolysis were also acquired, regarding the adsorption of proteins to the fibres.

The insights on how feasible the extractive conversion could be, initiated in Chapter 4, were quantitatively assessed in **Chapter 5**. The ATPS enzymatic hydrolysis of sugarcane bagasse was simulated by integrating hydrolysis and ATPS models. The integrated developed model enables the analysis of the ATPS hydrolysis (for batch and continuous mode) in terms of recycle of components and identification of the major influencers for the process, both technically and economically.

The concluding **Chapter 6** indicates the main conclusion of the work findings and how they contribute to the advances on enzymatic conversion of biomass and ATPS fields. Moreover, it presents an explanation of the scientific and technical implications of the research findings for society.

## References

Albertsson, P.-Å., 1986. Aqueous Polymer-Phase Systems, in: Partition of Cell Particles and Macromolecules. John Wiley & Sons, p. 346.

Albertsson, P.-Å., 1958. Particle fractionation in liquid two-phase systems. The composition of some phase systems and the behaviour of some model particles in them. Application to the isolation of cell walls from microorganisms. *Biochim. Biophys. Acta* 27, 378–395. [https://doi.org/10.1016/0006-3002\(58\)90345-7](https://doi.org/10.1016/0006-3002(58)90345-7)

Albertsson, P.Å., 1961. Fractionation of particles and macromolecules in aqueous two-phase systems. *Biochem. Pharmacol.* 5, 351–358. [https://doi.org/10.1016/0006-2952\(61\)90028-4](https://doi.org/10.1016/0006-2952(61)90028-4)

Andrić, P., Meyer, A.S., Jensen, P. a., Dam-Johansen, K., 2010. Reactor design for minimizing product inhibition during enzymatic lignocellulose hydrolysis: I. Significance and mechanism of cellobiose and glucose inhibition on cellulolytic enzymes. *Biotechnol. Adv.* 28, 308–324. <https://doi.org/10.1016/j.biotechadv.2010.01.003>

Baskir, J.N., Hatton, T.A., Suter, U.W., 1989. Protein partitioning in two-phase aqueous polymer systems. *Biotechnol. Bioeng.* 34, 541–558. <https://doi.org/10.1002/bit.260340414>

Bezerra, R.M.F., Dias, A.A., 2005. Enzymatic kinetic of cellulose hydrolysis: Inhibition by ethanol and cellobiose. *Appl. Biochem. Biotechnol.* 126, 49–59. <https://doi.org/10.1007/s12010-005-0005-5>

Chundawat, S.P.S., Balan, V., Dale, B.E., 2008. High-throughput microplate technique for enzymatic hydrolysis of lignocellulosic biomass. *Biotechnol. Bioeng.* 99, 1281–1294. <https://doi.org/10.1002/bit.21805>

Costa, S.A., Pessoa Jr, A., Roberto, I.C., 1998. Xylanase Recovery: Effect of extraction conditions on the aqueous two-phase system using experimental design. *Appl Biochem biotechnol* 70, 629–639.

Cray, J.A., Stevenson, A., Ball, P., Bankar, S.B., Eleutherio, E.C.A., Ezeji, T.C., Singhal, R.S., Thevelein, J.M., Timson, D.J., Hallsworth, J.E., 2015. Chaotropicity: A key factor in product tolerance of biofuel-producing microorganisms. *Curr. Opin. Biotechnol.* 33, 228–259. <https://doi.org/10.1016/j.copbio.2015.02.010>

De Brito Cardoso, G., Mourão, T., Pereira, F.M., Freire, M.G., Fricks, A.T., Soares, C.M.F., Lima, Á.S., 2013. Aqueous two-phase systems based on acetonitrile and carbohydrates and their application to the extraction of vanillin. *Sep. Purif. Technol.* 104, 106–113. <https://doi.org/10.1016/j.seppur.2012.11.001>

Decker, S.R., Adney, W.S., Jennings, E., Vinzant, T.B., Himmel, M.E., 2003. Automated Filter Paper Assay for Determination of Cellulase Activity. *Appl. Biochem. Biotechnol.* 105–108, 689–703.

Desai, R.K., Streefland, M., Wijffels, R.H., H. M. Eppink, M., 2014. Extraction and stability of selected proteins in ionic liquid based aqueous two phase systems. *Green Chem.* 16, 2670. <https://doi.org/10.1039/C3GC42631A>

Dreyer, S., Kragl, U., 2008. Ionic liquids for aqueous two-phase extraction and stabilization of enzymes. *Biotechnol. Bioeng.* 99, 1416–1424. <https://doi.org/10.1002/bit.21720>

Espitia-Saloma, E., Vázquez-Villegas, P., Aguilar, O., Rito-Palomares, M., 2014. Continuous aqueous two-phase systems devices for the recovery of biological products. *Food Bioprod. Process.* 92, 101–112. <https://doi.org/10.1016/j.fbp.2013.05.006>

Freire, M.G., Cláudio, A.F.M., Araújo, J.M.M., Coutinho, J. a. P., Marrucho, I.M., Lopes, J.N.C., Rebelo, L.P.N., 2012. Aqueous biphasic systems: a boost brought about by using ionic liquids. *Chem. Soc. Rev.* 41, 4966. <https://doi.org/10.1039/c2cs35151j>

Garlock, R.J., Balan, V., Dale, B.E., 2012. Optimization of AFEX™ pretreatment conditions and enzyme mixtures to maximize sugar release from upland and lowland switchgrass. *Bioresour. Technol.* 104, 757–768. <https://doi.org/10.1016/j.biortech.2011.11.034>

González-Valdez, J., Mayolo-Deloya, K., Rito-Palomares, M., 2018. Novel aspects and future trends in the use of aqueous two-phase systems as a bioengineering tool. *J. Chem. Technol. Biotechnol.* 93, 1836–1844. <https://doi.org/10.1002/jctb.5434>

Grilo, A.L., Raquel Aires-Barros, M., Azevedo, A.M., 2016. Partitioning in Aqueous Two-Phase Systems: Fundamentals, Applications and Trends. *Sep. Purif. Rev.* 45, 68–80. <https://doi.org/10.1080/15422119.2014.983128>

Gupta, V.K., Kubicek, C.P., Berrin, J.G., Wilson, D.W., Couturier, M., Berlin, A., Filho, E.X.F., Ezeji, T., 2016. Fungal Enzymes for Bio-Products from Sustainable and Waste Biomass. *Trends Biochem. Sci.* 41, 633–645. <https://doi.org/10.1016/j.tibs.2016.04.006>

Gustafsson, A., Tjerneld, F., 1986. Aqueous Polymer two-phase systems in Biotechnology. *Fluid Phase Equilib.* 29, 457–474.

Haghighi Mood, S., Hossein Golfeshan, A., Tabatabaei, M., Salehi Jouzani, G., Najafi, G.H., Gholami, M., Ardjmand, M., 2013. Lignocellulosic biomass to bioethanol, a comprehensive review with a focus on pretreatment. *Renew. Sustain. Energy Rev.* 27, 77–93. <https://doi.org/10.1016/j.rser.2013.06.033>



Hahn-Hägerdal, B., Galbe, M., Gorwa-Grauslund, M.F., Lidén, G., Zacchi, G., 2006. Bio-ethanol – the fuel of tomorrow from the residues of today. *Trends Biotechnol.* 24, 549–556. <https://doi.org/10.1016/j.tibtech.2006.10.004>

Hahn-Hägerdal, B., Mattiasson, B., Albertsson, P.-A., 1981. Extractive bioconversion in aqueous two-phase systems. A model study on the conversion of cellulose to ethanol. *Biotechnol. Lett.* 3, 53–58. <https://doi.org/10.1007/BF00145110>

Herculano, P.N., Porto, T.S., Maciel, M.H.C., Moreira, K.A., Souza-Motta, C.M., Porto, A.L.F., 2012. Partitioning and purification of the cellulolytic complex produced by *Aspergillus japonicus* URM5620 using PEG-citrate in an aqueous two-phase system. *Fluid Phase Equilib.* 335, 8–13. <https://doi.org/10.1016/j.fluid.2012.08.008>

Hernández-Fernández, F.J., de los Ríos, A.P., Lozano-Blanco, L.J., Godínez, C., 2010. Biocatalytic ester synthesis in ionic liquid media. *J. Chem. Technol. Biotechnol.* 85, 1423–1435. <https://doi.org/10.1002/jctb.2453>

Hernandez-Justiz, O., Fernandez-Lafuente, R., Terreni, M., Guisan, J.M., 1998. Use of aqueous two-phase systems for in situ extraction of water soluble antibiotics during their synthesis by enzymes immobilized on porous supports. *Biotechnol. Bioeng.* 59, 73–79. [https://doi.org/10.1002/\(SICI\)1097-0290\(19980705\)59:1<73::AID-BIT10>3.0.CO;2-3](https://doi.org/10.1002/(SICI)1097-0290(19980705)59:1<73::AID-BIT10>3.0.CO;2-3)

Kaul, A., 2000. The Phase Diagram, in: Hatti-Kaul, R. (Ed.), *Methods in Biotechnology. Aqueous Two-Phase Systems*. Human Press, Totowa, New Jersey, pp. 11–21. <https://doi.org/10.1385/1-59259-028-4:11>

Kulkarni, N., Vaidya, A., Rao, M., 1999. Extractive Cultivation of Recombinant *Escherichia coli* Using Aqueous Two Phase Systems for Production and Separation of Extracellular Xylanase. *Biochem. Biophys. Res. Commun.* 255, 274–278.

Kuroda, K., Miyamura, K., Satria, H., Takada, K., Ninomiya, K., Takahashi, K., 2016. Hydrolysis of Cellulose Using an Acidic and Hydrophobic Ionic Liquid and Subsequent Separation of Glucose Aqueous Solution from the Ionic Liquid and 5-

(Hydroxymethyl)furfural. *ACS Sustain. Chem. Eng.* 4, 3352–3356. <https://doi.org/10.1021/acssuschemeng.6b00420>

Larsen, J., Haven, M.Ø., Thirup, L., 2012. Inbicon makes lignocellulosic ethanol a commercial reality. *Biomass and Bioenergy* 46, 36–45. <https://doi.org/10.1016/j.biombioe.2012.03.033>

Liu, C.G., Xiao, Y., Xia, X.X., Zhao, X.Q., Peng, L., Srinophakun, P., Bai, F.W., 2019. Cellulosic ethanol production: Progress, challenges and strategies for solutions. *Biotechnol. Adv.* 37, 491–504. <https://doi.org/10.1016/j.biotechadv.2019.03.002>

Liu, Z., Li, L., Liu, C., Xu, A., 2017. Saccharification of cellulose in the ionic liquids and glucose recovery. *Renew. Energy* 106, 99–102. <https://doi.org/10.1016/j.renene.2017.01.023>

Losordo, Z., McBride, J., Rooyen, J. Van, Wenger, K., Willies, D., Froehlich, A., Macedo, I., Lynd, L., 2016. Cost competitive second-generation ethanol production from hemicellulose in a Brazilian sugarcane biorefinery. *Biofuels, Bioprod. Biorefining* 10, 589–602. <https://doi.org/10.1002/bbb.1663>

Mazzola, P.G., Lopes, A.M., Hasmann, F.A., Jozala, A.F., Penna, T.C., Magalhaes, P.O., Rangel-Yagui, C.O., Pessoa Jr, A., 2008. Liquid-liquid extraction of biomolecules: an overview and update of the main techniques. *J. Chem. Technol. Biotechnol.* 83, 143–157. <https://doi.org/10.1002/jctb>

Moreira, S., Silvério, S.C., Macedo, E.A., Milagres, A.M.F., Teixeira, J.A., Mussatto, S.I., 2013. Recovery of *Peniophora cinerea* laccase using aqueous two-phase systems composed by ethylene oxide / propylene oxide copolymer and potassium phosphate salts. *J. Chromatogr. A* 1321, 14–20. <https://doi.org/10.1016/j.chroma.2013.10.056>

Mussatto, S.I., Roberto, I.C., 2004. Alternatives for detoxification of diluted-acid lignocellulosic hydrolyzates for use in fermentative processes: A review. *Bioresour. Technol.* 93, 1–10. <https://doi.org/10.1016/j.biortech.2003.10.005>

Padella, M., O'Connell, A., Prussi, M., 2019. What is still limiting the deployment of cellulosic ethanol? Analysis of the current status of the sector. *Appl. Sci.* 9. <https://doi.org/10.3390/app9214523>

Passos, H., Ferreira, A.R., Cláudio, A.F.M., Coutinho, J. a P., Freire, M.G., 2012. Characterization of aqueous biphasic systems composed of ionic liquids and a citrate-based biodegradable salt. *Biochem. Eng. J.* 67, 68–76. <https://doi.org/10.1016/j.bej.2012.05.004>

Pereira, J.F.B., Freire, M.G., Coutinho, J.A.P., 2020. Aqueous two-phase systems: Towards novel and more disruptive applications. *Fluid Phase Equilib.* 505, 112341. <https://doi.org/10.1016/j.fluid.2019.112341>

Rarbach, M., Sötl, Y., 2013. sunliquid<sup>®</sup>: Sustainable and Competitive Cellulosic Ethanol from Agricultural Residues. *Chim. Int. J. Chem.* 67, 732–734. <https://doi.org/10.2533/chimia.2013.732>

Rosa, P.A.J., Azevedo, A.M., Sommerfeld, S., Bäcker, W., Aires-Barros, M.R., 2011. Aqueous two-phase extraction as a platform in the biomanufacturing industry: Economical and environmental sustainability. *Biotechnol. Adv.* 29, 559–567. <https://doi.org/10.1016/j.biotechadv.2011.03.006>

Rosales-Calderon, O., Arantes, V., 2019. A review on commercial-scale high-value products that can be produced alongside cellulosic ethanol, *Biotechnology for Biofuels*. BioMed Central. <https://doi.org/10.1186/s13068-019-1529-1>

Sakdaronnarong, C., Saengsawang, A., Siriyutta, A., Jonglertjunya, W., Nasongkla, N., Laosiripojana, N., 2016. An integrated system for fractionation and hydrolysis of sugarcane bagasse using heterogeneous catalysts in aqueous biphasic system. *Chem. Eng. J.* 285, 144–156. <https://doi.org/10.1016/j.cej.2015.09.098>

Selig, M.J., Tucker, M.P., Sykes, R.W., Reichel, K.L., Brunecky, R., Himmel, M.E., Davis, M.F., Decker, S.R., 2010. Lignocellulose recalcitrance screening by integrated high-throughput hydrothermal pretreatment and enzymatic saccharification. *Ind. Biotechnol.* 6, 104–111. <https://doi.org/10.1089/ind.2010.0009>

Silvério, S.C., Rodríguez, O., Tavares, A.P.M., Teixeira, J.A., Macedo, E.A., 2013. Laccase recovery with aqueous two-phase systems: Enzyme partitioning and stability. *J. Mol. Catal. B Enzym.* 87, 37–43. <https://doi.org/10.1016/j.molcatb.2012.10.010>

Soares, R.R.G., Azevedo, A.M., Van Alstine, J.M., Raquel Aires-Barros, M., 2015. Partitioning in aqueous two-phase systems: Analysis of strengths, weaknesses, opportunities and threats. *Biotechnol. J.* 10, 1158–1169. <https://doi.org/10.1002/biot.201400532>

Soares, R.R.G., Silva, D.F.C., Fernandes, P., Azevedo, A.M., Chu, V., Conde, J.P., Aires-Barros, M.R., 2016. Miniaturization of aqueous two-phase extraction for biological applications: From micro-tubes to microchannels. *Biotechnol. J.* 11, 1498–1512. <https://doi.org/10.1002/biot.201600356>

Stickel, J.J., Adhikari, B., Sievers, D.A., Pellegrino, J., 2018. Continuous enzymatic hydrolysis of lignocellulosic biomass in a membrane-reactor system. *J. Chem. Technol. Biotechnol.* 93, 2181–2190. <https://doi.org/10.1002/jctb.5559>

Teixeira, A.G., Agarwal, R., Ko, K.R., Grant-Burt, J., Leung, B.M., Frampton, J.P., 2018. Emerging Biotechnology Applications of Aqueous Two-Phase Systems. *Adv. Healthc. Mater.* <https://doi.org/10.1002/adhm.201701036>

Tjerneld, F., Persson, I., Albertsson, P.-Å., Hahn-Hägerdal, B., 1985. Enzymatic hydrolysis of cellulose in aqueous two-phase systems. I. partition of cellulases from *Trichoderma reesei*. *Biotechnol. Bioeng.* 27, 1036–1043. <https://doi.org/10.1002/bit.260270715>

Torres-Acosta, M.A., Mayolo-Deloya, K., González-Valdez, J., Rito-Palomares, M., 2019. Aqueous Two-Phase Systems at Large Scale: Challenges and Opportunities. *Biotechnol. J.* <https://doi.org/10.1002/biot.201800117>

Turner, M.B., Spear, S.K., Huddleston, J.G., Holbrey, J.D., Rogers, R.D., 2003. Ionic liquid salt-induced inactivation and unfolding of cellulase from *Trichoderma reesei*. *Green Chem.* 5, 443–447. <https://doi.org/10.1039/b302570e>

Ventura, S.P.M., Sousa, S.G., Freire, M.G., Serafim, L.S., Lima, Á.S., Coutinho A.P., J. a P., 2011. Design of ionic liquids for lipase purification. *J. Chromatogr. B Anal. Technol. Biomed. Life Sci.* 879, 2679–2687. <https://doi.org/10.1016/j.jchromb.2011.07.022>

Yamakawa, C.K., Qin, F., Mussatto, S.I., 2018. Advances and opportunities in biomass conversion technologies and biorefineries for the development of a bio-based economy. *Biomass and Bioenergy* 119, 54–60. <https://doi.org/10.1016/j.biombioe.2018.09.007>

Yang, J., Zhang, X., Yong, Q., Yu, S., 2011. Three-stage enzymatic hydrolysis of steam-exploded corn stover at high substrate concentration. *Bioresour. Technol.* 102, 4905–4908. <https://doi.org/10.1016/j.biortech.2010.12.047>

Yau, Y.K., Ooi, C.W., Ng, E.-P., Lan, J.C.-W., Ling, T.C., Show, P.L., 2015. Current applications of different type of aqueous two-phase systems. *Bioresour. Bioprocess.* 2, 49. <https://doi.org/10.1186/s40643-015-0078-0>



## CHAPTER 2

### **A robotic platform to screen aqueous two-phase systems for overcoming inhibition in enzymatic reactions\***

Bianca Consorti Bussamra<sup>1,2</sup>, Joana Castro Gomes<sup>1</sup>, Sindelia Freitas<sup>2</sup>, Solange I. Mussatto<sup>3</sup>, Aline Carvalho da Costa<sup>2</sup>, Luuk van der Wielen<sup>1,4</sup>, Marcel Ottens<sup>1</sup>

<sup>1</sup>Department of Biotechnology, Delft University of Technology. Van der Maasweg 9, 2629HZ. Delft, The Netherlands.

<sup>2</sup>Development of Processes and Products (DDPP), University of Campinas. Av. Albert Einstein, 500. Post Code: 6066. Campinas, Brazil.

<sup>3</sup>Novo Nordisk Foundation Center for Biosustainability, Technical University of Denmark. Kemitorvet, Building 220. 2800, Kongens Lyngby, Denmark.

<sup>4</sup>Bernal Institute, University of Limerick. Castletroy. Limerick, Ireland.

---

\*This Chapter has been published as: Bussamra, B.C., Castro Gomes, J., Freitas, S., Mussatto, S.I., Carvalho da Costa, A., van der Wielen, L., Ottens, M., 2019. *Bioresourcetechnology* 280, 37–50.  
<https://doi.org/10.1016/j.biortech.2019.01.136>

### **Abstract**

Aqueous two-phase systems (ATPS) can be applied to enzymatic reactions that are affected by product inhibition. In the biorefinery context, sugars inhibit the cellulolytic enzymes in charge of converting the biomass. Here, we present a strategy to select an ATPS (formed by polymer and salt) that can separate sugar and enzymes. This automated and miniaturized method is able to determine phase diagrams and partition coefficients of solutes in these. Tailored approaches to quantify the solutes are presented, taking into account the limitations of techniques that can be applied with ATPS due to the interference of phase forming components with the analytics. The developed high-throughput (HT) platform identifies suitable phase forming components and the tie line of operation. This fast methodology proposes to screen up to six different polymer-salt systems in eight days and supplies the results to understand the influence of sugar and protein concentrations on their partition coefficients.

**Keywords:** aqueous two-phase system (ATPS); high-throughput screening; glucose partitioning; protein partitioning; product inhibition.



## 1. Introduction

The use of enzymes for a variety of processes has a significant role in industries. Generally, enzymes are applied to catalyse different type of reactions in food, animal feed, pharmaceutical, textile, pulp and paper and biofuel industries (Ogawa and Shimizu, 1999). Enzymatic reactions are also used to replace chemical routes, making processes more environmentally friendly (Margeot et al., 2009). For example, lignocellulosic materials, which are residues of agro-industries, can be converted into sugars by hydrolytic enzymes. In a biorefinery context, the efficiency of this reaction would contribute to the generation of renewable energy, which could reduce the usage of fossil fuels. Because more products can be generated from the same amount of (renewable) raw material, the productivity and possibilities to vary the portfolio of products in a biorefinery would be enhanced. Some studies claim that the enzymatic hydrolysis is the bottleneck in the conversion of lignocellulose to second generation ethanol and renewable sugars (Mesa et al., 2016). Thus, technologies to make enzymatic hydrolysis economically attractive have been a topic of much discussion in terms of operation mode, and load of solids and enzymes.

Product inhibition plays a significant role among the many obstacles that prevent enzymes to perform at their maximum activity (Modenbach and Nokes, 2013). Yang et al. (2011) demonstrated how the removal of end products was crucial to enhance the productivity of enzymatic hydrolysis. Thus, the inhibition by products can be overcome through an *in situ* removal of products during the reaction. In this work, we suggest aqueous two-phase systems (ATPS) as a strategy to separate sugars (product) and enzymes. Consequently, high sugar production could be achieved during hydrolysis of lignocellulosic material.

A wide range of studies have identified ATPS as an interesting technique to extract, separate, purify and concentrate substances (Iqbal et al., 2016). This type of system was first described by Albertsson (1961). Being formed by two immiscible components, named phase forming components, these systems constitute two aqueous phases that can unevenly partition molecules, also called solutes, based on properties of both system and solutes (Baskir et al., 1989). A range of

components can be used to form the different phases, such as two polymers, a polymer and a salt (Van Sonsbeek et al., 1993), or ionic liquids (Freire et al., 2012). Hence, both phases are mainly composed by water (79-90%), but each of them is enriched in a different component, which contributes to some advantages of ATPS, such as biocompatibility, simplicity and easy scale up (Phong et al., 2018). Moreover, ATPS presents a suitable environment to maintain enzymatic activity, as proved by Tjerneld et al. (1991), and has been already applied to biological processes involving laccase and further extraction of products and recovery of enzymes (Ferreira et al., 2018). Hence, an ATPS that can separate enzymes and sugar (reaction product) to opposite phases presents two main advantages: a friendly environment for enzymatic reaction and the *in situ* removal of products while they are released.

High-throughput (HT) platforms have gained attention in recent years in order to enable an automated and miniaturized experimental setup. Oelmeier et al. (2011), Diederich et al. (2013), Zimmermann et al. (2016) and Pirrung et al. (2018) demonstrated the improvements that a HT platform brings to the pharmaceutical field. In line with these authors, Bensch et al. (2007) also called the attention to the advantage of designing processes meanwhile screening a variety of parameters, which is offered by HT platforms. In the field of lignocellulose-to-biofuels, there are reported advances of HT techniques focused on pre-treatment, hydrolysis (Chundawat et al., 2008) and enzymatic assays (Goddard and Reymond, 2004). Selig et al. (2010) described a HT assay to perform hydrothermal pre-treatment of lignocellulosic material followed by enzymatic hydrolysis. The main outcomes of the automated and miniaturized technique of their research included the 96-well pre-treatment reactor, the direct use of the pre-treated slurry to enzyme saccharification and the solids handling system (Selig et al., 2010). Aiming to optimize biomass conversion, Chundawat et al. (2008) developed a HT platform to assess lignocellulosic digestibility. When conducting hydrolysis in a miniaturized scale, some parameters such as particle size, solid load, mass transfers and reaction time should be appropriately defined. However, delivering reproducible quantities of solids into micro-wells is an inherent problem of HT platforms. Other researches focused on the enzymatic assay developments — for example, the traditional filter

paper assay to measure activity of cellulase was applied to an automated robotic platform (Decker et al., 2003). However, to the best of our knowledge, there is no literature reporting the use of an automated and miniaturized robotic platform to determine phase diagrams and concentration of solutes in the phases (top and bottom), as well as solutions for the interference of system components on the analytics (e.g. in protein measurements), focusing to overcome inhibition of enzymatic reactions through ATPS.

This work aimed to develop a strategic methodology to screen and select ATPS able to separate sugar and hydrolytic enzymes. We found that both solutes (sugar and enzymes) could be quantified taking into account the interference of the phase forming components in the measurements. Then, this paper indicates a reliable manner to HT determine phase diagrams and partition coefficients in ATPS. Step by step the developed strategy is presented, which was tested with different system components. Therefore, this platform provides the tools to overcome enzymatic inhibition, attributed to the reasonable selection of systems which are able to extract the product (inhibitors) from reaction medium. Integrating our novel technique with the available HT advances in the field of lignocellulose-to-biofuels, we provide tools to accelerate the development of feasible lignocellulose conversions.

## **2. Materials and Methods**

### **2.1. Research Design**

In this research, we developed a HT platform to screen ATPS formed by polymer and salt. The ATPS can be applied to conduct enzymatic reactions that are inhibited by products. Here, enzymatic hydrolysis of biomass was the reaction in focus. This reaction is catalyzed by hydrolytic enzymes that convert lignocellulosic biomass into sugars. The enzymes were represented by the enzymatic cocktail Cellic CTec (Novozymes). For simplification purpose, the addition of glucose simulated the degradation of the sugarcane bagasse by enzymes, since the substrate (bagasse) was not included in the screening experiments.

The development of this platform consisted of two main parts: determination of phase diagrams (binodal curves and tie lines) and quantification of the solutes (sugar and proteins) in both top and bottom phases. We chose the well-reported system composed of potassium phosphate buffer and polyethylene glycol 2000 g/mol to establish the methodology for phase diagrams determination. In this part, the robotic platform generated a large number of points — consisted of different concentrations of phase forming components —, in order to detect the minimum number necessary to determine a precise binodal curve and tie lines. The definition of liquid handling parameters (e. g. aspiration speed and delay, retract speed of the tips, dispense and breakoff speed, air gap sizes, aspiration and dispense positions) requires an extensive theoretical knowledge as well as trial and error tests. The parameters of aspiration and dispense applied to this work for each solution handled in the robotic platform facilitates its immediate application.

In the second part of the platform development, we evaluated analytical methods for quantification of the solutes. The platform presents an approach that takes into account the interference of the phase forming components in the analytics and is able to predict the protein quantification in a HT way. Six ATPS formed by the combination of different molecular weights of PEG (2000 g/mol, 4000 g/mol and 6000 g/mol) and different salt types (potassium citrate and magnesium sulphate) illustrated the performance of the robotic platform. Hence, in a practical approach, we validated the feasibility of the platform.

### **2.2. Materials and stock solutions**

Table 1 presents the reagents and components used with their supplier and purity, when applied. Polyethylene glycol with molar mass 2000 g/mol (PEG 2000), 4000 g/mol (PEG 4000), 6000 g/mol (PEG 6000) were dissolved in double distilled deionized water (Milli-Q water) to prepare the following stock solutions: 41 and 38% (w/w) PEG 2000, 41% (w/w) PEG 4000 and 31 and 39% (w/w) PEG 6000. The volumetric concentrations of stock solutions (grams of polymer per 100 mL of solution) were verified by a linear relation between density and concentration.

**Table 1.** List of reagents and components used in the development of the HT platform, as well as their supplier and respective purities.

Reagents and components	Supplier	Purity
Polyethylene glycol 2000 g/mol	Merck (Darmstad, Germany)	-
Polyethylene glycol 4000 g/mol	Merck (Darmstad, Germany)	-
Polyethylene glycol 6000 g/mol	J.T. Baker (Fisher, New Jersey, USA)	-
Potassium citrate tribasic monohydrate ( $\text{K}_3\text{C}_6\text{H}_5\text{O}_7 \cdot \text{H}_2\text{O}$ )	Sigma Aldrich (Taufkirchen, Germany)	≥ 99 %
Potassium sodium tartrate tetrahydrate ( $\text{KNaC}_4\text{H}_4\text{O}_6 \cdot 4\text{H}_2\text{O}$ )	Sigma Aldrich (Taufkirchen, Germany)	≥ 99 %
Sodium phosphate monobasic dehydrate ( $\text{NaH}_2\text{PO}_4 \cdot 2\text{H}_2\text{O}$ )	Sigma Aldrich (Taufkirchen, Germany)	≥ 95 %
Ammonium citrate dibasic ( $(\text{NH}_4)_3\text{C}_6\text{H}_5\text{O}_7$ )	Honeywell Fluka (Buchs, Switzerland)	≥ 99 %
Sodium tartrate dehydrate ( $\text{Na}_2\text{C}_4\text{H}_4\text{O}_6 \cdot 2\text{H}_2\text{O}$ )	Sigma Aldrich (Taufkirchen, Germany)	≥ 99 %
Magnesium sulphate heptahydrate ( $\text{MgSO}_4 \cdot 7\text{H}_2\text{O}$ )	J.T. Baker (Fisher, New Jersey, USA)	-
Potassium dihydrogen phosphate ( $\text{KH}_2\text{PO}_4$ )	Merck (Darmstad, Germany)	≥ 99 %

## Robotic platform to screen aqueous two-phase systems

Sodium sulphate ( $\text{Na}_2\text{SO}_4$ )	Merck (Darmstad, Germany)	$\geq 99 \%$
Potassium phosphate dibasic ( $\text{K}_2\text{HPO}_4$ )	Honeywell Fluka (Buchs, Switzerland)	$\geq 99 \%$
Sodium succinate dibasic hexahydrate ( $\text{Na}_2\text{C}_4\text{H}_6\text{O}_4 \cdot 6\text{H}_2\text{O}$ )	Sigma Aldrich (Taufkirchen, Germany)	$\geq 99 \%$
Potassium oxalate monohydrate ( $\text{K}_2\text{C}_2\text{O}_4 \cdot \text{H}_2\text{O}$ )	Honeywell Fluka (Buchs, Switzerland)	$\geq 99 \%$
Tri-Sodium citrate dihydrate ( $\text{Na}_3\text{C}_6\text{H}_5\text{O}_7 \cdot 2\text{H}_2\text{O}$ )	Merck (Darmstad, Germany)	$\geq 99 \%$
Anhydrous glucose	Sigma Aldrich (Taufkirchen, Germany)	-
Sodium carbonate ( $\text{Na}_2\text{CO}_3$ )	Sigma Aldrich (Taufkirchen, Germany)	$\geq 99 \%$
3,5-Dinitrosalicylic acid (DNS)	Sigma Aldrich (Taufkirchen, Germany)	$\geq 98 \%$
Methyl violet	Merck (Darmstad, Germany)	-

Stock solutions presented the final concentration of 40% (w/w) in Milli-Q water [buffer solutions were prepared at a final concentration of salts of 40% (w/w) in Milli-Q water], except for the salt solutions of sodium sulphate [25% (w/w)] and potassium citrate tribasic [50% (w/w)]. The pH was adjusted by adding sodium hydroxide (4 M) or hydrogen chloride, both purchased from Merck. Citrate buffer 50 mM was prepared by adding 10.505 g of citric acid monohydrate to a final volume of 1L Milli-Q water, already considering the volume of NaOH (4 M) used to correct the pH to 4.8.

The commercial enzyme Cellic CTec2 (Novozymes, Bagsværd, Denmark) presented an activity of 146 FPU/mL, measured according to the NREL protocol (Adney and Baker, 2008). Sugar solutions of different concentrations were prepared in Milli-Q water with anhydrous glucose. Sodium carbonate ( $\text{Na}_2\text{CO}_3$ ) and 3,5-Dinitrosalicylic acid (DNS) were used for enzymatic activities assays; and methyl violet, a hydrophobic dye, was used in the determination of phase diagrams in the HT platform.

### **2.3. Formation of ATPS**

The automated determination of phase diagrams and partition coefficient of solutes was conducted at a Tecan Freedom Evo 200 platform equipped with one Liquid Handling Arm (LiHa), one Multi-Channel Arm™ (MCA), a robotic manipulator (RoMa) arm and an Infinite 200 PRO spectrophotometer (Tecan, Crailsheim, Germany). The systems were prepared by adding the required amounts of phase forming components in the 2 mL ninety-six deep well plates (Eppendorf, Hamburg, Germany). PEG solution was added first to each well (in a dry contact mode — tips in contact with the empty bottom of the recipient during liquid dispense), followed by Milli-Q water (in a free dispense mode — no contact of the tips with the recipient or another liquid during liquid dispense), and later the salt solution, which were dispensed through a wet contact mode (tips in contact with the liquids already present in the recipient during liquid dispense). The total working volume was established as 1 mL. Sugar and protein solutions (required in the partition coefficient experiments) were also added to the system by the liquid handling station.

Information on source labware position, destination position, volume of pipetting and dispense and applied liquid class was defined per each solution and accessed by the EVOware system through worklists. The 96 systems formed into the deep well plate reached equilibrium by mixing on Eppendorf Thermomixer® C (plate adaptor SmartBlock) at 1300 rpm for 1 h at 21 °C for potassium phosphate and PEG 2000 systems (for the development of the binodal curve determination methodology) and 40 °C for all other systems. The target of the equilibrium tests (not shown) was to achieve constant partition coefficient of methyl violet in different ATPS. Even though literature evidences that 5 – 8 min is sufficient to mix ATPS containing methyl violet (Zimmermann et al., 2016; Oelmeier et al., 2011), we opted for a longer time (1 h), since the equilibrium tests were not performed for all the phase forming components screened. The plate was centrifuged for 30 min at 3000 rpm for phase separation (Eppendorf 5810R Multipurpose Centrifuge®). Both top and bottom phases were withdrawn and stored in order to perform the necessary analysis.

### **2.4. Manual binodal curve determination**

The cloud point method (also called titrimetric method) (Kaul, 2000) was used in order to validate the data obtained in the robotic platform. This method determines the binodal curve by calculating the concentration of both phase forming components in the moment when a clear solution becomes turbid due to the addition of one phase solution to the other. The collection of several system points constituted the binodal curve.

### **2.5. HT phase diagram determination**

Through the robotic platform, the determination of the binodal curve was conducted fitting a curve between the region of one-phase systems and two-phase systems. Ninety-six systems containing 50 µL of 1mM methyl violet were formed by the HT platform. The dye was pipetted by MCA 96. In order to construct the binodal curve, it was necessary to identify when each of the random systems was constituted by one or two phases by measuring the difference between the absorbance in the top phase and the bottom phase. In order to measure the content of methyl violet in both



top and bottom phases, 30  $\mu\text{L}$  of each phase were diluted 1:7 in appropriate solution to a final volume of 210  $\mu\text{L}$ , in UV-Star<sup>®</sup> Microplates (Greiner Bio-One, Frickenhausen, Germany). After a mixing step (Eppendorf Thermomixer<sup>®</sup> C) for 1 min at 1000 rpm, the absorbance was measured at 586 nm. When the difference between absorbance of top and bottom phases was below a cut-off value of 0.113 (586 nm), the system was defined as monophasic.

The binodal curve from both manual and robotic measurements were determined by fitting the data points corresponding to one and two-phase systems to an empirical curve developed by Merchuk, (1998), represented below:

$$c_{\text{polymer}} = A \cdot \exp[(B \cdot c_{\text{salt}}^{0.5}) + (C \cdot c_{\text{salt}}^3)] \quad (1)$$

The terms  $c_{\text{polymer}}$  and  $c_{\text{salt}}$  are the polymer and the salt concentrations, respectively, expressed in weight percentage  $A$ ,  $B$  and  $C$  are the fitting parameters obtained by least squares regression. This non-linear regression was performed with Matlab<sup>®</sup> R2018b using the function *lsqcurvefit* (The Mathworks, Natick, ME, USA).

For tie lines determination, the lever arm rule was applied. The composition of top and bottom phases of a specified system (M point) can be inferred by the intersection between the tie line and the binodal curve (Diederich et al., 2013). The lever arm rule correlates the ratio between top phase volume ( $V_{\text{tp}}$ ) and bottom phase volume ( $V_{\text{bp}}$ ) to the distance between the M point and the points in the binodal curve that represents the composition of both top and bottom phases ( $L_{\text{bp}}$  and  $L_{\text{tp}}$ , respectively).

$$\frac{V_{\text{tp}}}{V_{\text{bp}}} = \frac{L_{\text{bp}}}{L_{\text{tp}}} \quad (2)$$

The following equations were used to determine the composition of top and bottom phases, as established by Diederich et al. (2013).

$$c_{\text{PEG}}^{\text{tp}} - f(c_{\text{salt}}^{\text{tp}}) = 0 \quad (3)$$

$$c_{\text{PEG}}^{\text{bp}} - f(c_{\text{salt}}^{\text{bp}}) = 0 \quad (4)$$

$$\frac{(c_{\text{salt}}^{\text{bp}} - c_{\text{salt}}^{\text{M}})^2 + (c_{\text{PEG}}^{\text{M}} - c_{\text{PEG}}^{\text{bp}})^2}{(c_{\text{salt}}^{\text{M}} - c_{\text{salt}}^{\text{tp}})^2 + (c_{\text{PEG}}^{\text{tp}} - c_{\text{PEG}}^{\text{M}})^2} - \left(\frac{V_{\text{tp}}}{V_{\text{bp}}}\right)^2 = 0 \quad (5)$$

$$\frac{c_{\text{PEG}}^{\text{bp}} - c_{\text{PEG}}^{\text{M}}}{c_{\text{salt}}^{\text{bp}} - c_{\text{salt}}^{\text{M}}} - \frac{c_{\text{PEG}}^{\text{M}} - c_{\text{PEG}}^{\text{tp}}}{c_{\text{salt}}^{\text{M}} - c_{\text{salt}}^{\text{tp}}} = 0 \quad (6)$$

Equations (3) and (4) represent the tie line intersections with binodal curve. The points of the binodal curve are represented by  $f(c_{\text{salt}}^{\text{tp}})$  and  $f(c_{\text{salt}}^{\text{bp}})$ , respectively for top and bottom phases. Equation (5) applies the Pythagorean Theorem for two triangles, in which the line of segments  $L_{\text{tp}}$  and  $L_{\text{bp}}$  represent the hypotenuses. Then, the tie line is determined when the slopes of the hypotenuses are equal, as defined in Equation (6). Each tie line was determined using a different M point.

The tie line length (TLL) was calculated according to the following equation:

$$TLL = \sqrt{(c_{\text{PEG}}^{\text{tp}} - c_{\text{PEG}}^{\text{bp}})^2 - (c_{\text{salt}}^{\text{tp}} - c_{\text{salt}}^{\text{bp}})^2} \quad (7)$$

## 2.6. Phase Volume determination

Both binodal curve and tie lines can be determined with the same set of data. In this research, it was found that a salt concentration lower than 2% (w/w) greatly influenced the absorbance of methyl violet, while the polymer (PEG) concentration did not interfere. Thus, for the tie line determination, samples of the top and bottom phases were diluted in a solution of 2% (w/w) salt. Consequently, each salt system requires its own calibration curve of methyl violet.

As the methyl violet partitions in both top and bottom phases for certain system compositions, the determination of phase volumes was based on the mass balance of the dye in the system and the assumption that the volume of the phase is equal to the total volume of the system, as presented in the equations below:

$$C_{MV,stock} \cdot V_{MV} = C_{MV,tp} \cdot V_{tp} + C_{MV,bp} \cdot V_{bp} \quad (8)$$

$$V_{tp} + V_{bp} = 1 \text{ mL}. \quad (9)$$

Concentration of methyl violet in the bottom and top phases ( $C_{MV,bp}$  and  $C_{MV,tp}$ , respectively) were calculated according to the methyl's violet calibration curve. The  $C_{MV,stock}$  and  $V_{MV}$  are the concentration of methyl violet stock solution and the corresponding volume added into the system, respectively.  $V_{tp}$  and  $V_{bp}$  are the volumes of top and bottom phases to be calculated. The non-linear system of equations (Equations 3, 4, 5, 6, 8 and 9) was solved iteratively using *fsolve* operation in Matlab® R2018b (The MathWorks, Natick, ME, USA).

## 2.7. Partitioning of solutes in HT platform

In order to assess how the concentration of the phase forming components and solutes influence the partition of sugar and enzymes in ATPS, different tie line lengths were tested for different concentrations of sugar and enzymes. Solutes partitioning was evaluated separately, since the presence of different concentrations of sugar in the system could affect the accuracy of the enzymatic activity assay, and the sugar-enriched enzymatic cocktail could contribute to an error in the sugar quantification — the glucose concentration in Cellic CTec2 is  $250 \pm 8$  g/L; at the highest protein load experiment (15 FPU/g bagasse),  $2.6 \pm 0.1$  g/L glucose was present in the system. HT quantification of protein and sugar in top and bottom phases was validated by mass balance for the total amount of these solutes in the system.

The glucose concentrations were defined considering the expected conversion capacity of the system and the inhibitory sugar concentration. For a maximum theoretical conversion of biomass, at 10% solid load, the concentration of sugar would be approximately 90 g/L. However, the reaction can be inhibited from a sugar concentration of 27 g/L on. Then, systems containing  $28 \text{ g/L} \pm 0.5$ ,  $29 \text{ g/L} \pm 0.3$ ,  $51 \text{ g/L} \pm 0.5$  and  $61 \text{ g/L} \pm 0.6$  of sugar were performed.

The definition of the enzyme concentration took into consideration reported values of enzyme loads for hydrolysis and the profitability of the process, since the biocatalyst contributes to a substantial part of the operational costs in a biorefinery (Torres, 2016). The enzyme load was calculated based on 5, 10 and 15 FPU/g bagasse, considering a (hypothetical) substrate load of 10% (WIS — water insoluble substrate). Taking into account a working volume of 1 mL, 0.1 g of dry biomass would be expected in each reaction. The volume of enzymatic cocktail to be added to the system was calculated as follows:

$$V_{enz} = \frac{10 \text{ (FPU/g)} \cdot m_{dry \text{ bag}}}{FPase_{cocktail}}, \quad (10)$$

where  $FPase_{cocktail}$  is the total enzymatic activity of the commercial cocktail (146 FPU/mL).

To fulfil the requirements of the liquid handling minimum volume, the stock solution was diluted according to the load of each experiment and to maintain a fixed volume of enzyme preparation of 68  $\mu$ L and sugar preparation of 92  $\mu$ L for all systems.

### 2.8. Analytical methods

The analytical methods for protein quantification, total cellulose activity and sugar quantification are presented below.

#### 2.8.1. Protein quantification

Absorbance at 280 nm and Bradford assay were evaluated for protein quantification. In order to obtain a reliable protein quantification, two main aspects were considered. First, the enzymatic cocktail may not partition equally through the system — especially components other than proteins. In order to evaluate the influence of these contaminants, an ultrafiltration of the enzymatic cocktail was performed using 3.000 MWCO Amicon® Ultra Centrifugal Filters, as described by the supplier. Retentate (target protein solution) and permeate (contaminants) were evaluated through each protein method (absorbance at 280 nm and Bradford assay). Finally,

special attention should be paid to the influence of phase forming components on the absorbance in the wavelength used for each method.

Protein quantification of top and bottom phases was performed using the Coomassie Protein Assay Reagent (Thermo Scientific, USA) (Bradford, 1976). The reaction was performed according to the method provided by the supplier. In this case, 250  $\mu\text{L}$  of Bradford reagent were added, using the MCA arm, to each well of the reaction plate for protein quantification already containing 10  $\mu\text{L}$  of sample, blanks and internal standards.

The phase forming components (and their dilutions) influence the absorbance on Bradford method (González-González et al., 2011). Therefore, the absorbance measurement for each sample was corrected with the corresponding blank presenting the same dilution factor (DF). For the determination of protein concentration, an internal standard (STD) containing a known protein concentration was prepared for each system composition — respecting the same influence of phase forming components for samples and internal standards. Then, sample concentrations were determined by

$$C_{\text{sample}} = \frac{Abs_{\text{sample}}^{\alpha} DF_{\text{sample}}}{Abs_{\text{std}}^{\alpha} DF_{\text{std}}} C_{\text{std}}, \quad (11)$$

where the concentration of the enzyme in the top or bottom phase ( $\alpha$ ) is given by the ratio between the absorbance of the sample ( $Abs_{\text{sample}}^{\alpha}$ ) and the absorbance of the internal standard enzyme solution ( $Abs_{\text{std}}^{\alpha}$ ), both corrected by the respective dilution factors ( $DF$ ), multiplied by the known concentration of the internal standard enzyme solution ( $C_{\text{std}}$ ). Absorbance of both samples and internal standards was corrected by subtracting a blank for each system composition.

### **2.8.2. Filter paper activity (FPase)**

The total cellulase activity in terms of filter paper units (FPU) was measured by reducing in 10 times the scale of the NREL method (Adney and Baker, 2008). The

colour development and sugar quantification were carried out according to the method proposed by Miller (1959).

### ***2.8.3. Sugar quantification***

Sugar concentration in the top and bottom phases of ATPSs was determined using the Megazyme Glucose Reagent assay (Megazyme, Wicklow, Ireland). Samples were diluted in Mili-Q water prior to quantification assay, in order to obtain the measurement in the linearity range of the calibration curve. The reaction, which consisted of 200  $\mu\text{L}$  of the Megazyme Glucose Reagent and 10  $\mu\text{L}$  of sample, was incubated for 10 min at 37 °C and the absorbance read at 505 nm. A calibration curve in the range of 1 - 12 mM glucose was prepared. It was proved that the phase forming components did not influence the quantification method (data not shown). Then, only one blank (composed of water) was enough to complete the set of reaction needed for this quantification protocol. Samples were aspirated and dispensed with the LiHa fixed tips, while Glucose reagent buffer was added to the UV plates containing the diluted samples with MCA 96.

### **2.9. Relative sugar release**

The relative sugar release is the correlation of the enzymatic activity in two different conditions (Moreira et al., 2013). In one condition (control assay), 50  $\mu\text{L}$  of enzymes were incubated at 50 °C, 1300 rpm for 30 min with 100  $\mu\text{L}$  of citrate buffer (50 mM pH 4.8). Simultaneously, the enzymes (50  $\mu\text{L}$ ) were incubated with the phase forming constituents [100  $\mu\text{L}$  salts at 10% (w/w) solution], for the same period of time and temperature. After the incubation time, 7.5 mg of Whatman grade 1 filter paper substrate (GE Healthcare, Chicago, IL) were added to both solutions, and the reaction was carried out at 50 °C, static condition, for 60 min. After diluting the systems with 100  $\mu\text{L}$  of Mili-Q water, the sugar release was measured by Megazyme Glucose Reagent assay.

### 2.10. Enzymatic hydrolysis

The hydrolysis of sugarcane bagasse was conducted for two purposes: identification of the sugar inhibitory concentration and assessment of protein adsorption to sugarcane bagasse. At a scale of 1.5 mL final volume, the hydrolysis was conducted at 10% (w/v) water-insoluble substrate (WIS), pH 4.8 (50 mM citrate buffer), and 0.02% azide monosodic. The reaction was incubated at 50 °C and 1300 rpm (Eppendorf Thermomixer C). The protein load was established at 10 FPU per gram of bagasse (Cellic CTec2 145 FPU/mL). For the sugar inhibition experiments, 10 g/L, 20 g/L, 40 g/L and 60 g/L glucose were added to the reaction media before the hydrolysis. For adsorption experiments, no external sugars were added to the reaction. Sampling was performed at 6, 12, 24 and 48 h for inhibitory sugar experiments and at 3, 6, 24 and 48 h of reaction time for protein adsorption experiments. To stop the enzymatic activity, samples were centrifuged (4000 rpm at 4 °C) for 10 min. Supernatants were collected and analysed for sugar and protein contents, according to conditions described above. For the experiment of sugar inhibitory concentration, samples were boiled at 95 °C for 10 min after being collected, to ensure no remaining enzymatic activity and sugar production.

### 2.11. Data analysis

The TLL experimental data were correlated using Othmer-Tobias (Othmer and Tobias, 1942), which is presented by

$$\left(\frac{1-c_{\text{PEG}}^{\text{tp}}}{c_{\text{PEG}}^{\text{tp}}}\right) = K_{\text{OT}} \left(\frac{1-c_{\text{Salt}}^{\text{bp}}}{c_{\text{Salt}}^{\text{bp}}}\right). \quad (12)$$

The linear dependency of the plots  $\log\left(\frac{1-c_{\text{p,tp}}}{c_{\text{p,tp}}}\right)$  against  $\log\left(\frac{1-c_{\text{s,bp}}}{c_{\text{s,bp}}}\right)$ , and  $\log\left(\frac{c_{\text{w,bp}}}{c_{\text{s,bp}}}\right)$  against  $\log\left(\frac{c_{\text{w,tp}}}{c_{\text{p,tp}}}\right)$  indicates an acceptable consistency of the results.

The standard deviation ( $\sigma$ ) and correlation coefficient ( $r^2$ ) for all correlated data were calculated by the following formulas (Press et al., 2007), respectively:  $\sigma =$

$\sqrt{\sum_{i=1}^N (y_i - f(x_i))^2 / (N - k)}$  and  $r^2 = 1 - \sum_{i=1}^N (y_i - f(x_i))^2 / \sum_{i=1}^N (y_i - \bar{y})^2$ , where  $N$  is the number of point used for the regression, and  $k$  is the number of parameters.

The partition coefficient in a two-phase system can be determined as the ratio of enzyme/sugar concentration in the top phase to that in the bottom phase (Li et al., 2002).

The uncertainties of the measurements calculated by calibration curves were estimated by the formula  $\partial_{meas} = \frac{S_r}{m} \cdot \sqrt{\frac{1}{M} + \frac{1}{N} + \frac{(y_{meas} - \bar{y})^2}{m^2 \cdot SS_x}}$  (Barwick, 2003), where  $S_r$  represents the residual standard deviation of the calibration curve,  $m$  is the slope of the curve,  $M$  is the number of paired calibration points,  $N$  is the number of replicates made on the sample,  $y_{meas}$  is the measured value calculated by the calibration curve,  $\bar{y}$  is the mean of the measured values ( $y$ ) used to estimate the calibration curve and  $SS_x$  is the sum of squares of deviation of the independent values ( $x_i$  data points) from the mean of the  $x_i$  values ( $SS_x = \sum_{i=1}^n (x_i - \bar{x})^2$ ). The errors were propagated accordingly. Measurements presenting the standard deviation within the 95% confidence interval are indicated in the text. In this case, the uncertainty ( $\partial_{meas}$ ) was multiplied by the 2-tailed Student  $t$  value for 95% level of confidence and  $n-2$  degrees of freedom connected to the respective calibration curve.

### 3. Results and Discussion

A strategy to screen and select ATPS for enzymatic reactions, aiming at the partition of product (glucose) and enzyme (protein) to different phases, is presented. This strategy consists of two sequential sections. The first section aims to select phase forming components based on their capability to offer enzymes a suitable environment to release glucose from filter paper. The performance of the enzymes in each phase forming components was compared with their performance when incubated in optimum condition (citrate buffer, 50 mM pH 4.8). The ratio of sugar released under both conditions gives the relative sugar release of the enzymes. This indicator guided the preselection of suitable phase forming components in terms of maintenance of enzymatic activity. Then, the ones which presented a satisfactory



response in this step were selected to be studied in the second section of the described methodology.

Then, in Section 2, we suggest the use of the automated and miniaturized robotic platform developed, which is applied to select biphasic systems that can separate enzymes and sugars unevenly between the phases. Through phase diagrams and partition coefficients of solutes, it is possible to select the most suitable ATPS for our application.

### **3.1. Development of the HT platform**

The developed HT screening platform gives information to determine phase diagrams for different phase forming components (e.g.: polymer molecular weight and salt types) and evaluates the interference of parameters (e.g.: concentration of phase forming components and solutes) in the partition coefficient of the solutes in a short time. Moreover, the scale of each experiment and volume of reactants can be reduced when compared to a manual approach. However, the majority of the techniques regarding the obtainment of binodal curves and tie lines in literature considers a manual approach and is not compatible with HT screening (Bensch et al., 2007). Here, we discuss the methodological differences of published platforms for HT screening of ATPS and the one developed in this work, in terms of equilibrium achievement, two phase system identification and tie lines determination.

#### **3.1.1. Binodal determination**

To determine the binodal curves, points representing mono and biphasic systems in the boarder of the phase transition were used for the regression of parameters to fit to the Merchuk equation (Merchuk et al., 1998). The developed robotic platform determines whether there are one or two phases. For the system PEG/phosphate investigated by Bensch et al. (2007), the addition of methyl violet enabled the identification of phases. The colorful component partitions equally in monophasic systems, or to the top phase when the system is biphasic. In this work, however, it was noted that the hydrophobic marker partitioned unevenly to both phases in some two-phase systems. Then, the identification was dependent on the difference in

concentration of methyl violet in top and bottom phases. Some authors suggest a visual inspection (Zimmermann et al., 2016) or an identification based on the cloud point method (Oelmeier et al., 2011) to determine the two phase systems. Although these approaches save reactants (no dye is needed), the binodal curve and tie lines cannot be determined with the same dataset, and an additional experiment has to be performed to phase volume determination.

By comparing the difference in absorbance, given by the experiment and the visual inspection for 343 systems, a cut-off value of 0.1137 was selected to represent the transition between mono and biphasic systems formed by potassium phosphate and PEG 2000. In this study, a step of 1% (w/w) in the composition of each point was performed (Fig. 1.a). The data generated by the HT method were compared to the results of the manual approach. The HT binodal curve fits in the region within 95% confidence interval of the manual dataset, validating the HT methodology (Fig. 1.b). Moreover, the points obtained by the HT curve differ in 9.9%<sup>1</sup> in relation to the manual values (absolute deviation). Oelmeier et al. (2011) also proved that both liquid handling system and manual approach generated binodal data points for PEG 4000 and PO<sub>4</sub> that fall within the 95% prediction bounds of the fitted curve determined by the combination of both data sets.

---

<sup>1</sup>  $AAD = \frac{1}{K} \sum_{i=1}^K \left( \left( \frac{c_{PEG, manual} - c_{PEG, HTS}}{c_{PEG, manual}} \right)^2 \right)^{0.5}$ , for the independent variable  $C_{salt}$  being 7%, 9%, 11%, 13%, 15%, 17% (w/w).

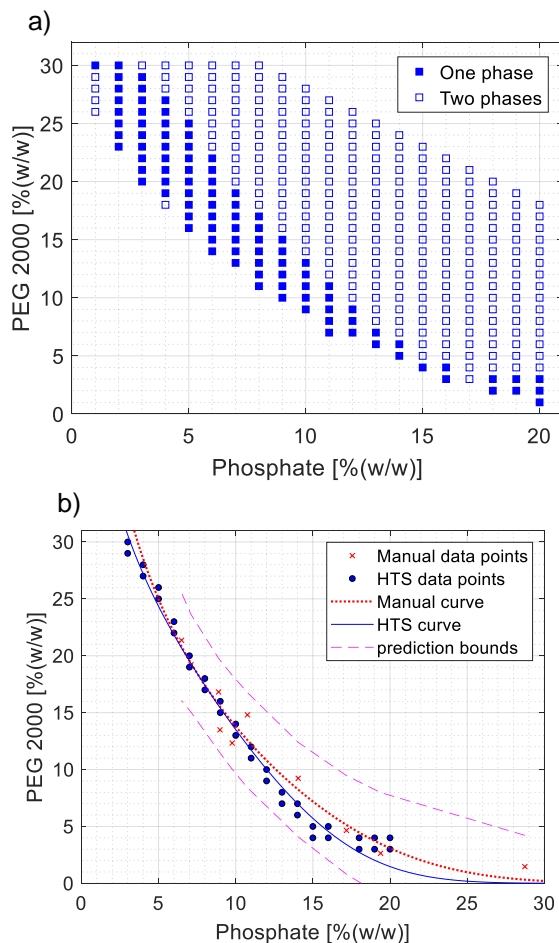


**Fig. 1.** a) Classification of mono and biphasic systems based on the difference in absorbance at 586 nm between top and bottom phases. Analysis of 343 compositions of the phase forming components potassium phosphate and PEG 2000, at 21 °C. b) Comparison between binodal curve determined through HT and manual experiments. Both approaches had the points fit to the Merchuk equation (Merchuk et al., 1998b). Manual curve parameters obtained by least square regression:  $A = 0.8369$ ,  $B = -5.344$ ,  $C = -113.6$ ,  $r^2 = 0.9598$ ,  $\sigma = 0.0157$ . HT curve parameters obtained by least square regression:  $A = 0.6261$ ,  $B = -4.091$ ,  $C = -239.8$ ,  $r^2 = 0.9867$ ,  $\sigma = 0.0106$ .

There are some limitations to distinguish between mono and biphasic systems in highly concentrated systems. For monophasic systems containing high salt concentrations (hydrophilic systems), methyl violet can partition as a separate phase

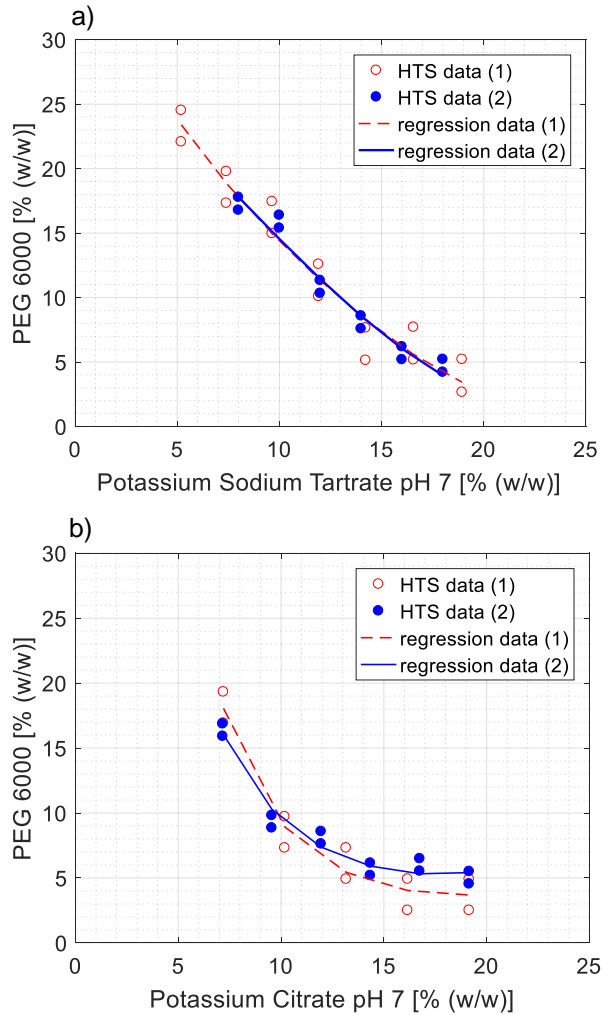
to the walls of the plate. Consequently, the surface of the systems is not homogeneous. Depending on the position of the tips during the withdrawal of the top phase, a deceptive identification of a biphasic system could occur. For systems with high polymer concentrations, the viscosity of the medium could impede the partition of methyl violet, leading to inaccurate results. Moreover, the increase of the molecular weight of the polymer leads to a larger biphasic region above the binodal curve (Iqbal et al., 2016). Therefore, the experimental space indicated in Table 2 was defined according to the molecular weight of the PEG and the effect of it on the binodal curve position.

**Table 2.** Range of salt and polymer concentrations used to determine phase diagrams (at 40 °C) in the HT platform.

PEG (g/mol)	MW	Reliable experimental area	
		Salt [% (w/w)]	Polymer [% (w/w)]
2000		10 - 25	3 - 25
4000		5 - 19	3 - 25
6000		1 - 20	1 - 25

In order to reduce the number of data points used to binodal curve determination (in one plate, 96 systems can be performed), steps of 2.4% (w/w) for both polymer and salt (defined as data 1 in Fig. 2), and 2% (w/w) for salt and 1% (w/w) for polymer (defined as data 2 in Fig. 2) were performed for systems composed by potassium sodium tartrate pH 7 (Fig. 2.a) and potassium citrate pH 7 (Fig. 2.b), both with PEG 6000. The absolute deviation of the binodal curve obtained at 2.4% (w/w) step in relation to the curves obtained within a more narrow step of concentration [2% (w/w) salt and 1% (w/w) PEG] was 1.3%<sup>1</sup> and 14.8%<sup>1</sup> for the systems with potassium sodium tartrate and potassium citrate, respectively. The comparison (in absolute deviation) of the phase diagrams demonstrates that steps up to 2.4% (w/w) in phase components concentration still lead to an accurate binodal curve for screening purposes. Then, depending on the maximum mass concentration of the polymer and salt, defined according to Table 2, steps varying from 1% (w/w) to 2.4% (w/w) can be applied. Variation of phase forming components in steps up to 0.25% (w/w) is

reported in literature, which leads to high precision of the binodal curve (Zimmermann et al., 2016). However, in order to obtain valuable data for the phase diagram determination when using smaller concentration steps, initial guesses have to be accurate, otherwise the experiments might need to be repeated.



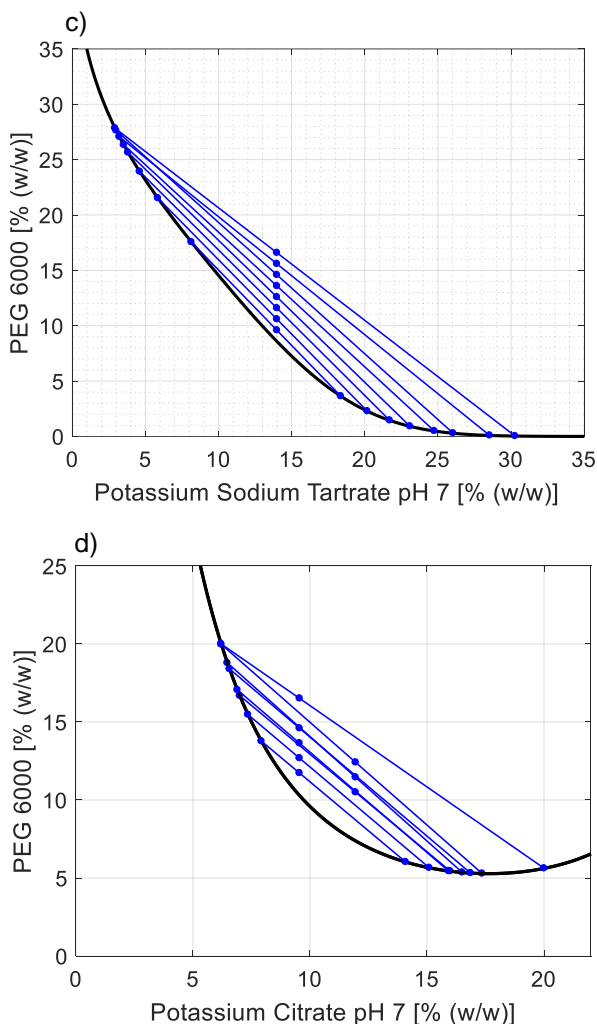


**Fig. 2.** Binodal curves determined for potassium sodium tartrate pH 7 (a) and potassium citrate pH 7 (b), both with PEG 6000 and at 40 °C, with their respective phase diagrams (c) and (d). The binodal curves were determined with two different spaces between points: 2.4% (w/w) for both salt and PEG (data 1); and 2% (w/w) for salt and 1% (w/w) for PEG (data 2). The pair of points representing a mono and a biphasic systems was fit to the Merchuk equation (Merchuk et al., 1998b). The regression parameters are:  $A = 0.5811, B = -3.884, C = -167.4, r^2 = 0.9474, \sigma = 0.0177$  for PEG 6000 and potassium sodium tartrate (data 1);  $A = 0.4784, B = -3.135, C = -199.1, r^2 = 0.9649, \sigma = 0.0104$  for PEG 6000 and potassium sodium tartrate (data 2);  $A = 13.094, B = -16.206, C = 173.752, r^2 = 0.9469, \sigma = 0.0151$  for PEG 6000 and potassium citrate (data 1);  $A = 4.6971, B = -12.8231, C = 163.478, r^2 = 0.9606, \sigma =$

**0.0089** for PEG 6000 and potassium citrate (data 2). For tie lines calculation, M points at 14% (w/w) of salt were used for potassium sodium tartrate, and 9% (w/w) and 12% (w/w) for potassium citrate.

### 3.1.2. Tie lines determination

The tie lines determination method was tested for the systems potassium sodium tartrate pH 7 and potassium citrate pH 7, both with PEG 6000. As the tie line represents a range of polymer-salt composition with common partition coefficient, they should be determined at hydrolysis temperature — 50 °C. However, due to equipment limitations, 40 °C was the highest temperature at which mixing and centrifugation could be operated. After reaching the equilibrium (mixing and phase separation) at 40 °C, the temperature of the system did not influence the partitioning of the solute methyl violet (data not shown).

The lever arm rule requires the composition of one point (M point) per tie line to be determined. By fixing the salt concentration, points presenting different PEG concentrations would lie on different tie lines. In the phase diagram shown in Fig. 2.c, a fixed concentration of salt was used for all M points. The tie lines determined for the system potassium citrate pH 7 and PEG 6000 (Fig. 2.d) took into account two different sets of salt concentration. For both systems, the higher the polymer concentration of the M point, the more unreliable the tie line was. This is indicated by tie lines crossing each other in this region, probably because of the logarithm shape of the binodal curve, leading to a scattered determination of salt concentration in the bottom phase. Then, high polymer concentrated region should be avoided in the phase diagram determination. Moreover, obtaining a suitable tie line to separate protein and sugar at low concentration of components is more interesting at an economic perspective as well.

The Othmer-Tobias (Othmer and Tobias, 1942) correlation indicate the consistency of the determined tie lines. Excluding the last tie line for the system with potassium citrate pH 7, the correlation presented an r-square of 0.97. The same behaviour is observed in the potassium sodium tartrate system: when the last two tie lines were excluded, the r-square increased 16.45%.

The determination of phase volumes neglected the difference of densities in top and bottom phases. However, the density is linearly correlated to the concentration of compounds — and the effect of concentration in density is stronger to salts than to polymers (data not shown). Then, for systems with high mass concentrations of salt and polymer, the difference in phase densities is more pronounced. Not taking into account the influence of phase forming concentration on the density of the phases introduces an error in the volume determination. Diederich et al. (2013) estimated an error of about 1 - 7% in the phase concentrations when neglecting the difference in phase densities in the lever arm rule. We consider this error acceptable for screening purposes.

### **3.1.3. Solute quantification in ATPS**

In order to develop a reliable platform to calculate partition coefficients of solutes, quantifications methods for sugars and enzymes were evaluated. The components of the enzymatic cocktail Cellic CTec2 other than proteins, taken as the permeated of ultrafiltration, represents 27.3% of the absorbance of the cocktail at 280 nm. Since we cannot predict the even partition of these components with the proteins in the ATPS, this method could lead to miscalculation in protein quantification. Contrarily, the permeate fraction does not present signal in Bradford method, being this method selected to quantify proteins. Phase forming components did not interfere with the glucose quantification method. However, the method selected to quantify protein (Bradford) took into account the interference of phase forming components with the reagent.

The accuracy of the Bradford assay can be influenced by the presence of polyethylene glycol. Barbosa et al. (2009) demonstrated that the concentration of the polymer interferes in the absorbance readings of the protein-dye complex. For example, the absorbance of 25 µg/mL protein solution can be up to 80% lower in 40% (w/w) polymer. When diluted in 10% (w/w) polymer, the same protein concentration exhibits a 15% reduction in absorbance at 595 nm ( $A_{595}$ ). According to Bradford (1976), the influence by nonprotein components can be overcome by considering a control with the same solution composition of the samples. However,



high polymer concentrations [ $> 10\%$  (w/w)] decrease the sensitivity of the method. Thus, low protein concentrations could not be detected, even when calibration curves are prepared with the same polymer concentrations (Barbosa et al., 2009). In this research, the Bradford method determines the protein concentration of two times diluted samples of top and bottom phases. Then, even systems containing 20% (w/w) polymer initially would present an appropriate concentration to lead to accurate results. However, proteins were also diluted, possibly implying low sensitivity measurements.

### **3.1.4. Summary of the HT platform**

Dividing the HT screening platform in three steps gives a convenient way to apply this methodology (Fig. 3). In the first step, 96 different compositions of the same polymer-salt system are generated. These systems, classified as mono or biphasic, provide information for binodal curve determination. Moreover, the volumes of top and bottom phases for the biphasic system can be calculated. These data support the determination of tie lines. Two plates can be generated and processed per day, totalizing three days to generate the phase diagrams for 6 polymer-salt systems.

Different tie lines regions and different concentration of the solutes can be explored in the robotic platform. In the second step of the platform, eight different compositions of each polymer-salt combination are assessed in terms of their ability to partition sugar and enzymes. The selection of these system compositions is arbitrary and depends on the goals of the research. In this work, we selected compositions that represent moderate concentration of phase forming components (i. e., systems presenting similar top and bottom phases and close to the binodal curve). The lower the concentration of phase forming components, the lower the viscosity of the system. Less viscous systems are easier to operate, which also increases their accuracy of results. Each deep-well plate can support the study of two polymer-salt combinations, containing eight different composition of phase forming component each. For six polymer-salt combinations, three days are necessary to perform the experiments and analyse the data.

The concentrations of solutes (enzyme and sugar) can vary according to the stage of the enzymatic hydrolysis. End-products of the reaction (sugar) inhibit both the catalytic site of the enzymes and the adsorption of them to the substrate, at high solid concentrations (Kristensen et al., 2009). After 6 hours of reaction,  $76 \pm 4.4\%$  (95% confidence interval) of the protein load was adsorbed to the bagasse. In the end of the reaction (48h), this value increased to  $85 \pm 4.7\%$  (95% confidence interval). Thus, the largest contribution to different concentration of proteins in hydrolysis reaction can be attributed to the enzyme load choice. On the other hand, the proteins would never be 100% adsorbed, since the cocktail presents an amount of non-binding enzymes (Kristensen et al., 2009), and not all proteins measured are enzymes. Regarding the sugars, the maximum glucose concentration was  $43 \pm 2.5$  g/L ( $49 \pm 3\%$  cellulose conversion), achieved after 48 h of reaction without the presence of external inhibitory sugar. After 6h reaction, 62% of the sugar was produced ( $27 \pm 1$  g/L glucose). This concentration can be considered inhibitory and one of the causes that levels off the conversion rate of the reaction. Kristensen et al. (2009) suggested that above a certain glucose concentration (known as glucose level threshold), enzymes are inhibited to a similar extent. However, the presence of additional glucose in the beginning of the reaction promotes a reduction of the initial rate. Consequently, the hydrolysis would take more time to achieve the same conversion as the hydrolysis without the inhibitor at the initial time. In the presence of 60 g/L glucose in the medium, the initial conversion rate is prominently lower.

In order to design a process for enzymatic reactions in ATPS, it is important to take into account the variation of solute concentration in time. In step 3, up to six systems can be assessed regarding the influence of glucose and enzymes concentrations on their own partition coefficient. Some authors assessed the influence of parameters (e.g. pH, NaCl and tie line length) in HT platforms via Design of Experiments (DoE) (Oelmeier et al., 2011). Here, we opted to screen a broader combination of parameters, since these data can be further used for modelling of phase formation and solute partitioning in ATPS. The move to step 3 is selective, since only the systems presenting the most different partition coefficient ratio in step 2 are selected to be further studied. Additionally, step 3 could involve the determination of specific

enzymatic activity, assessing the partition of the different enzymes (cellobiohydrolase, xylanase and  $\beta$ -glucosidase) of the cocktail in the phases. Two days are reserved for step 3, summing up eight days to perform the complete and integrated platform.

As a result of these experiments, the most suitable tie lines (concentration of PEG and salt) can be selected. Even though the systems that lay on the same tie line present similar partition coefficients, these systems can be different in terms of volume phase ratio and total concentration of the components (Hatti-kaul, 2001). As a consequence, the most suitable volume phase ratio can be selected when defining the process and the total concentration of components based on economic issues. Then, not only the partition coefficients of sugar and enzymes were considered to select the systems, but also other characteristics, such as the vulnerability of the system close to the binodal curve or critical point, the accordance of the phase volume ratio with further purification steps and the ease to scale up the process.

## Robotic platform to screen aqueous two-phase systems

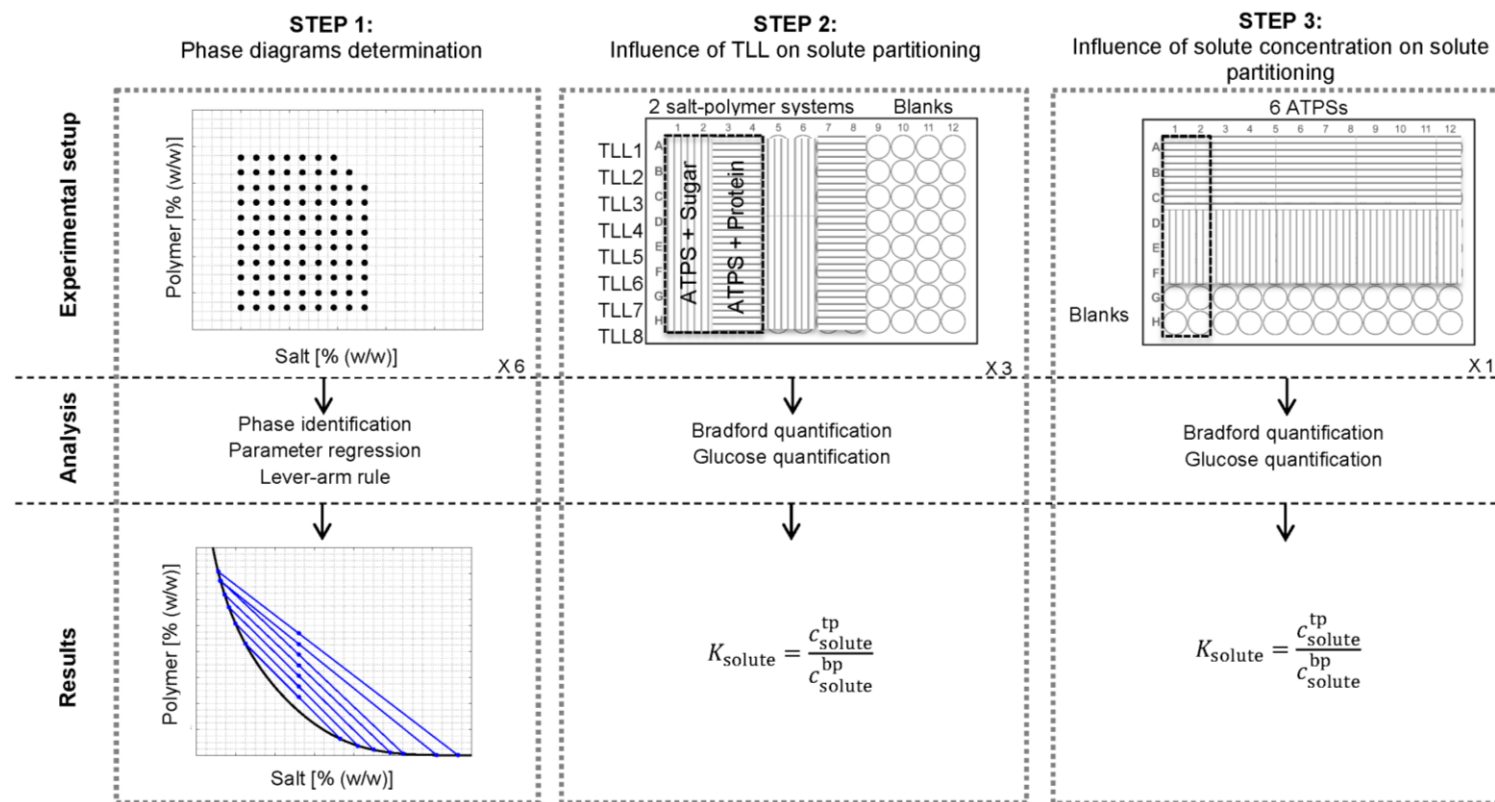


**Fig 3.** Schematic diagram of the robotic platform for ATPS screening. The three steps that compose the platform are represented in terms of experimental setup, analysis and results. In eight days, six polymer-salts can be screened. Step 1 involves the determination of phase diagrams for each polymer-salt system. In step 2, the influence of the phase forming concentration (represented as tie line length) on the partition

coefficient of sugar (horizontal wells) and proteins (vertical wells) is evaluated. The systems that present the most distinct partition coefficient of solutes are selected to step 3. In this stage, up to 6 systems can be assessed regarding the influence of sugar and protein concentration in their partition coefficient. The deep-wells distinguished inside the black rectangles represent the same ATPS (polymer-salt combination and concentration).

### **3.2. Section 1: pre-selection of components for ATPS**

The strategy to select suitable ATPS that can partition sugar and enzymes was applied to three polymer weights and eleven types of salts. The salt types were pre-selected based on their influence over enzymatic activities. In this way, the sugar (from the substrate filter paper) released by enzymes was measured in each phase forming component. The system potassium citrate pH 7 with PEG 6000 presented during the development of the HT platform was evaluated in order to assess the pH influence in the sugar release. The salt solutions potassium citrate pH 5.0 and magnesium sulphate pH 5.0 provided the medium where enzymes could release the highest sugar concentration. They represent around 50% of the sugar released in the optimum conditions (citrate buffer 50 mM).

### **3.3. Section 2: Application of the HT platform**

Six systems comprising three different polymer molecular weights (2000, 4000 and 6000 g/mol) and two types of salts (magnesium sulphate and potassium citrate) were evaluated in the developed HT platform regarding their ability to partition sugar and enzymes.

#### **3.3.1. Determination of phase diagrams (Step 1)**

Binodal curves for each system are shown in Fig. 4. Following the determination of the binodal curves in the HT station, tie lines were calculated. Tie line construction was based on the lever arm rule, which considers the system composition, the empirical binodal curve and the volume ratio between phases.

Polymer of higher molecular weight promotes a shift of the binodal curve towards the origin of the phase diagram, increasing the two-phase region (Fig. 4.a, Fig. 4.b and Fig. 4.c for potassium citrate pH 5; and Fig. 4.d, Fig. 4.e and Fig. 4.f for magnesium sulphate pH 5). As a consequence, low components concentrations are required to form a two phase system composed by high molecular weight polymer. Low concentration of phase forming components is interesting because of costs reduction and ease to recycle back to the process. On the other hand, high molecular

weight polymers are viscous, which can make their handling more difficult and decrease their volume accuracy in the system.

Increasing the pH shifts the binodal curve toward the origin (Fig. 4.c and Fig. 2.d). Due to the four dissociation constants presented by the citric acid, the pH significantly influences the anion species in solution for the systems composed by potassium citrate. At pH 7, almost 100% of the species in solution are trivalent, while at pH 5 the majority of species in solution (approximately 70%) are divalent (Heller et al., 2012). The increase in anion charge leads to a higher polarizability and a more stable ion-dipole salt-PEG interactions. In consequence, less concentration of components is required to form. The significant difference in slope and shape of the binodal curve due to pH change was also observed for the system composed by PEG 1000 and phosphate salt (Diederich et al., 2013). Even though two phase systems can be achieved with lower concentrations of phase forming components at higher pH, the enzymatic reaction aimed to be conducted in ATPS is pH-dependent. Therefore, the enzymatic activity is considered more important than the components (salt-PEG) concentrations.

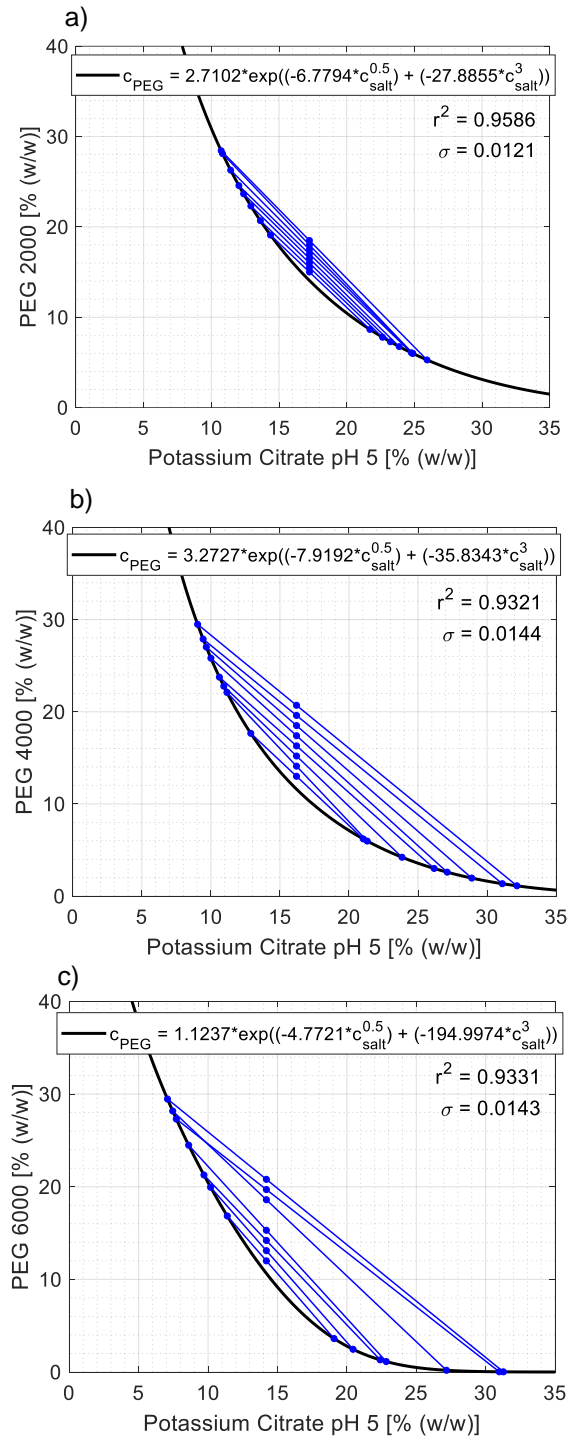
### **3.3.2. Influence of the ATPS composition on solute partitioning (Step 2)**

After the construction of the phase diagrams for each polymer-salt combination, the partitioning of sugar and enzymes in the systems was evaluated. In step 2, the influence of the tie line length (salt-polymer mass concentration) on the partition of solutes was assessed for each polymer-salt combination (Fig. 5). A fixed concentration of glucose and enzymes were added to the systems and top and bottom phases were measured. Mass balances for the total amount of solute in the systems show the accuracy of the measurements. This validation could also be done by comparing the partition coefficient obtained by HT and manual approaches (Oelmeier et al., 2011). However, we considered the mass balance of the solute sufficient to validate our methodology.

Because of the high partition coefficient of enzymes, the systems PEG 2000 – magnesium sulphate and PEG 6000 – potassium citrate presented the most distinct

partition coefficient of solutes. The partition of proteins to the polymer-enriched top phase can be justified by the salting out effect promoted by the ionic strength of the system. In this work, potassium citrate systems promoted a higher salting out effect when compared to the magnesium sulphate system. This is in agreement with the previous finding of (Wiendahl et al., 2009), who reported the precipitation of proteins — as a result of the salting out effect — being more prominent for the citrate than to the sulphate anion. However, these anions were both prepared as sodium salts. If we analyze the Hofmeister series, both salts (potassium citrate and magnesium sulphate) present very similar concentration at the precipitation limit (Kunz et al., 2004). Okur et al. (2017) investigated the molecular level of interaction between proteins and salts. The different types of enzymes in this work make the prediction of the salt effect on proteins according to the Hofmeister series even more ingenious. Then, this leads to the conclusion that another effect is acting as the main driving force to the partition of proteins in these systems. Andrews and Asenjo (2010) mentioned the hydrophobicity as a key factor in determining the partition of proteins in polymer-salt ATPS. The higher the polymer molecular weight, the higher the hydrophobicity of the top phase. This can justify the larger partition of proteins (charged molecules) to the top phase in the system formed by PEG 6000. However, the increase in TLL reduces the free volume available for the protein (Suarez et al., 2018), leading to an exclusion effect of the proteins towards the opposite salt enriched phase. The partition of proteins observed in this work shows an opposite tendency, since the partition coefficient of these molecules increase with the increasing the TLL for the majority of the systems (Fig. 5).





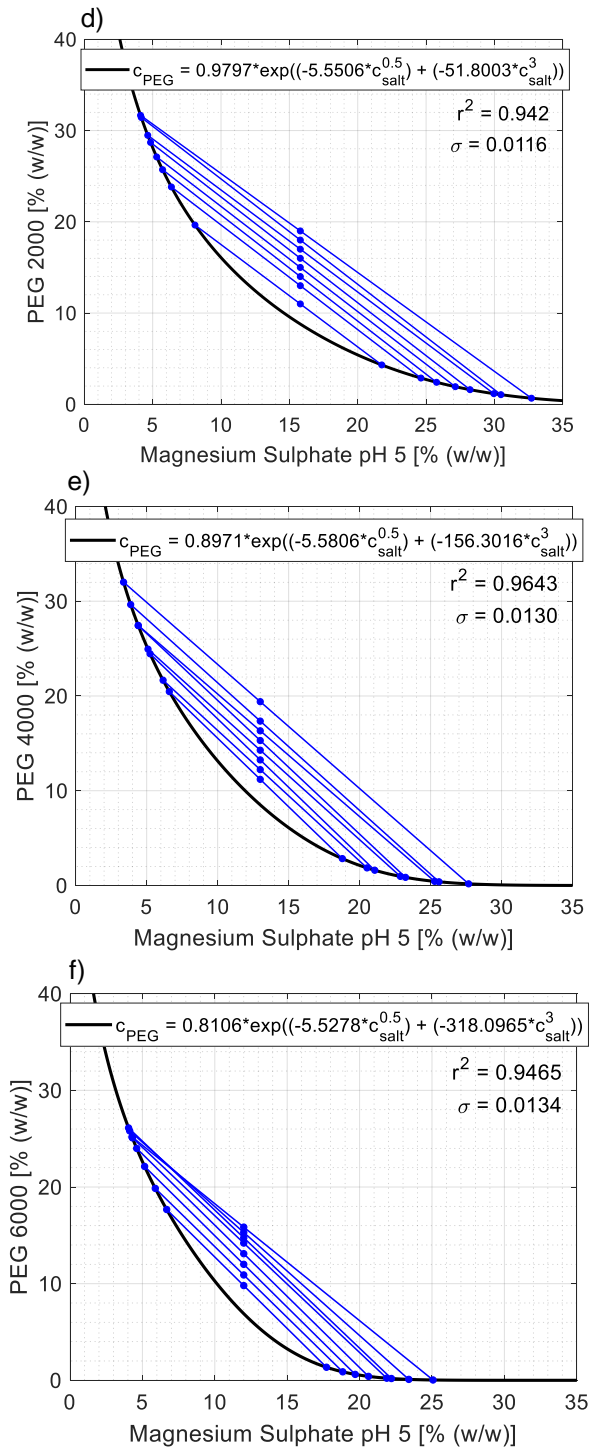


**Fig. 4.** Phase diagrams (binodal curves and tie lines) determined via HT experiments for systems containing two types of salts (potassium citrate pH 5 and magnesium sulphate pH 5) and different molecular weights of PEG (2000, 4000 and 6000 g/mol). The binodal data for all cases showed a good correlation (lowest  $r^2$  was 0.9321), indicating that the experimental data is well described by the empirical equation.

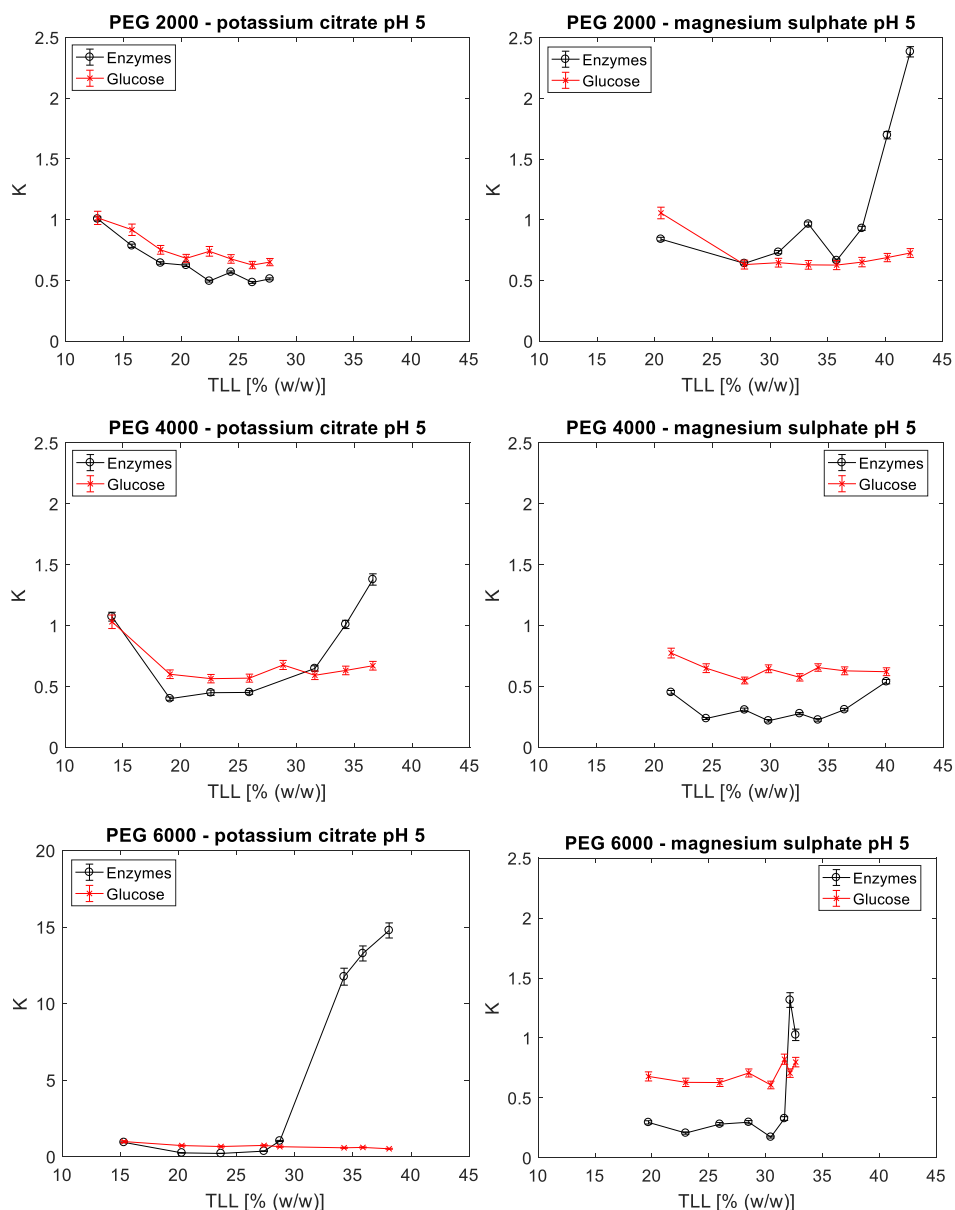


**Fig. 5.** Influence of the system composition on the partitioning of sugar and enzymes. The x-axis was fixed at the same range to facilitate comparison.

### 3.3.3. Influence of solute concentration on solute partitioning (Step 3)

The influence of sugar and enzymes concentrations on their partitioning in the systems was assessed in step 3. Here, only the polymer-salt system and its respective tie lines (6 ATPS in total) that presented the most distinct partition coefficient of solutes in Step 2 were studied. Partition coefficients of sugar and enzymes were determined at 3 different concentrations of these solutes and in 3 different concentrations of the polymer-salt (tie line lengths). The concentration of proteins influenced their partition more significantly for the systems composed by PEG 6000 and potassium citrate. In this line, the partition coefficient tends to decrease when the load of protein increases (Fig. 6.a). This could be explained by the low solubility of protein with increase of its concentration, leading to precipitation to the bottom phase. The systems formed by PEG 2000-magnesium sulphate pH 5 presented partition coefficients of enzymes close to the unity; however, the more concentrated in the system, the higher the partition regardless the load of protein (Fig. 6.b).

Comparing these results with those obtained in Step 2, although they follow similar tendency, the partition coefficient of proteins differs. Considering that the methodology was improved along with the first application of the platform, results of Step 3 should be taken as more reliable (Table 3). Internal standards for Steps 2 and 3 were composed under different strategies. While in Step 2 the internal standard was composed by CellicCTec 10 times diluted, in Step 3 the CelliCTec was diluted 30 or 50 times before being added to compose the internal standard. With the latter approach, we could avoid aggregation of proteins and depletion of the free dye at high protein concentrations during quantification (Barbosa et al., 2009).

**Table 3.** Deviation of the protein mass measured in top and bottom phase in relation to the total mass of protein added in the system (mass balance deviation), for different tie line lengths (TLL). The measured protein concentration was  $0.3 \text{ g/L} \pm 0.03$ ,  $0.6 \text{ g/L} \pm 0.03$  and  $0.9 \text{ g/L} \pm 0.06$ , respectively to the enzymatic loads of 5, 10 and 15 PFU/g bagasse. The values are represented in percentage.

Protein load (FPU/g bagasse)	PEG 6000-potassium citrate pH 5			PEG 2000-magnesium sulphate pH 5		
	TLL 34.2 %	TLL 35.9%	TLL 38.1%	TLL 38.0%	TLL 40.2%	TLL 42.2%
5	$29 \pm 8$	$17 \pm 8$	$15 \pm 8$	$27 \pm 7$	$27 \pm 7$	$29 \pm 8$
10	$41 \pm 5$	$44 \pm 5$	$48 \pm 5$	$27 \pm 4$	$32 \pm 4$	$39 \pm 5$
15	$47 \pm 5$	$46 \pm 5$	$56 \pm 5$	$39 \pm 5$	$35 \pm 5$	$49 \pm 5$

The partition coefficients of sugar are not highly influenced by the concentration of that solute (sugar) in the system (Fig. 6.c and Fig. 6.d). However,  $K_s$  tends to decrease at high concentrations of sugar (60 g/L), for both systems and tie lines assessed. This means that sugar concentrates at the bottom phase when the concentration of this solute in the system is getting close to the saturation concentration. On the other hand, the sum of sugar present in top and bottom phase deviates more from the total mass added when the tie line is higher (Table 4). This could be a consequence of inaccuracy in the determination of volumes when the systems are more concentrated in phase forming components, as mentioned before.

**Table 4.** Deviation of the sugar mass measured in top and bottom phase in relation to the total mass of sugar added in the system (mass balance deviation), for different tie line lengths (TLL). The values are represented in percentage.

Sugar load (g/L)	PEG 6000-potassium citrate pH 5			PEG 2000-magnesium sulphate pH 5		
	TLL 34.2 %	TLL 35.9%	TLL 38.1%	TLL 38.0%	TLL 40.2%	TLL 42.2%
$29 \pm 0.3$	$9 \pm 4$	$6 \pm 4$	$15 \pm 4$	$3 \pm 4$	$2 \pm 4$	$1 \pm 4$
$51 \pm 0.5$	$21 \pm 2$	$37 \pm 3$	$34 \pm 3$	$14 \pm 2$	$16 \pm 2$	$16 \pm 2$
$61 \pm 0.6$	$28 \pm 3$	$34 \pm 3$	$38 \pm 3$	$13 \pm 4$	$7 \pm 2$	$11 \pm 4$

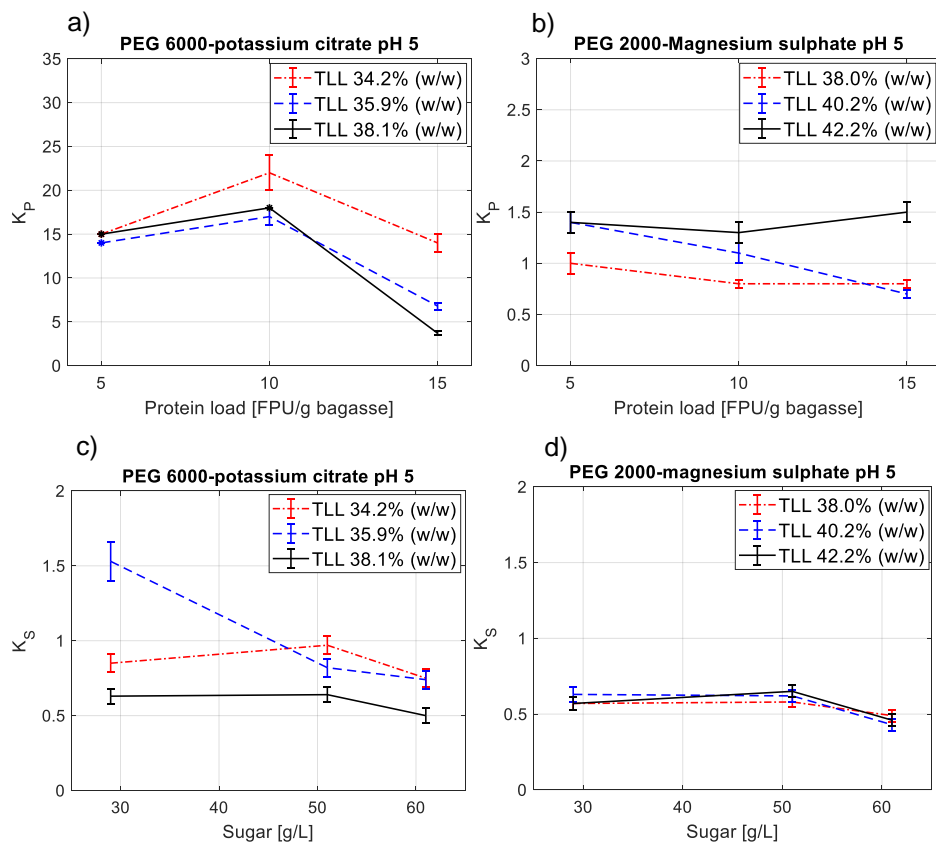


**Fig. 6.** Influence of solute concentration on their partition coefficients in different tie line lengths (TLL). Effect of protein load (5, 10 and 15 FPU/g bagasse) on protein partition coefficient ( $K_p$ ) for ATPS composed by PEG 6000 – potassium citrate pH 5 (a) and PEG 2000 – magnesium sulphate pH 5 (b). Points indicated with asterisk (\*) presented absorbance of bottom phase below the intercept error obtained from the calibration curve. In this case, the maximum detectable concentration of protein in the bottom phase was used to calculate the partition coefficient ( $K_p$ ), which can be the value indicated (\*) or higher. Effect of sugar load (30, 50 and 60 g/L) on sugar partition coefficient ( $K_s$ ) for ATPS composed by PEG 6000 – potassium citrate pH 5 (c) and PEG 2000 – magnesium sulphate pH 5 (d).

Moreover, we could also assume losses of solutes at the interface that are not being quantified in the top and bottom phases, contributing to the larger deviations. Thus, the higher mass balance deviation of certain systems should not be exclusively associated to an inaccurate quantification of the solutes in these systems. For the system composed by PEG 6000-potassium citrate pH5, the mass balance deviations are in general larger, indicating that the loss of solutes at the interface could be more

pronounced in that system. A high salting out effect can also lead to protein precipitation at the interface (Benavides et al., 2011). However, the higher deviation in mass balance occurred when the solutes concentration was increased. This suggests that the higher concentration of solutes is more likely to cause partition to the interface than higher polymer and salt concentrations (higher TLL), probably due to the solubility limit of protein in salts (Wiendahl et al., 2009).

The results obtained in one run of the platform indicate that the ATPS composed by PEG 6000-potassium citrate pH 5 is suitable to the separation of sugar and proteins. Although sugar was almost evenly partitioned to the phases, this feature can be overcome according to the mode of operation of the hydrolysis reaction (e.g. continuously removing of bottom phase or a counter-current system). The high partition coefficient of proteins reveals the potential of this system to separate enzymes. By partitioning enzymes and products to different phases, both reaction and extraction of products can coexist in the same system. Partition of the bagasse to the top phase and maintenance of the enzymatic activity would confirm the application of this system to the enzymatic hydrolysis of cellulose.

#### **4. Conclusion**

The proposed strategy comprehensively screens and selects ATPS to conduct extractive enzymatic reactions. The systems are selected in terms of the phase components that maintain the enzymatic activity and unevenly partition enzymes and sugar to different phases. Associated to the computational solution of equations, the developed robotic platform determines phase diagrams for polymer-salt systems and partition coefficient of solutes under influence of different parameters of interest. Conceptually, when conducted in an extractive mode, the enzymatic reactions that were previously inhibited by products tend to maintain their maximum activities and highly feasible enzymatic processes could be designed using ATPS.

#### **Acknowledgement**

This work was financially supported by the Foundation for Research of State of Sao Paulo, Brazil [grant numbers 2015/20630-4, 2016/04749-4, 2016/06142-0 and

BEPE 2016/21951-1]; and the BE-Basic Foundation, The Netherlands. This research was carried out during a Dual Degree PhD program under agreement between UNICAMP and TU Delft. The authors thank Yi Song for assisting with the TECAN platform and Marcelo Henriques da Silva, for all inputs to the platform development and data analysis.

## References

1. Adney, B., Baker, J., 2008. Measurement of Cellulase Activities Laboratory Analytical Procedure ( LAP ) Issue Date : 08 / 12 / 1996, National Renewable Energy Laboratory (NREL).

Albertsson, P.Å., 1961. Fractionation of particles and macromolecules in aqueous two-phase systems. *Biochem. Pharmacol.* 5, 351–358. [https://doi.org/10.1016/0006-2952\(61\)90028-4](https://doi.org/10.1016/0006-2952(61)90028-4)

Andrews, B.A., Asenjo, J.A., 2010. Theoretical and experimental evaluation of hydrophobicity of proteins to predict their partitioning behavior in aqueous two phase systems: A review. *Sep. Sci. Technol.* 45, 2165–2170. <https://doi.org/10.1080/01496395.2010.507436>

Barbosa, H., Slater, N.K.H., Marcos, J.C., 2009. Protein quantification in the presence of poly(ethylene glycol) and dextran using the Bradford method. *Anal. Biochem.* 395, 108–110. <https://doi.org/10.1016/j.ab.2009.07.045>

Barwick, V., 2003. Preparation of Calibration Curves. A guide to Best Practice.

Baskir, J.N., Hatton, T.A., Suter, U.W., 1989. Protein partitioning in two-phase aqueous polymer systems. *Biotechnol. Bioeng.* 34, 541–558. <https://doi.org/10.1002/bit.260340414>

Benavides, J., Rito-Palomares, M., Asenjo, J.A., 2011. Aqueous Two-Phase Systems, Second Edi. ed, *Comprehensive Biotechnology*. Elsevier B.V. <https://doi.org/10.1016/B978-0-08-088504-9.00124-0>



Bensch, M., Selbach, B., Hubbuch, J., 2007. High throughput screening techniques in downstream processing: Preparation, characterization and optimization of aqueous two-phase systems. *Chem. Eng. Sci.* 62, 2011–2021. <https://doi.org/10.1016/j.ces.2006.12.053>

Bradford, M.M., 1976. A rapid and sensitive method for the quantitation of microgram quantities of protein utilizing the principle of protein-dye binding. *Anal. Biochem.* 72, 248–254. [https://doi.org/10.1016/0003-2697\(76\)90527-3](https://doi.org/10.1016/0003-2697(76)90527-3)

Chundawat, S.P.S., Balan, V., Dale, B.E., 2008. High-throughput microplate technique for enzymatic hydrolysis of lignocellulosic biomass. *Biotechnol. Bioeng.* 99, 1281–1294. <https://doi.org/10.1002/bit.21805>

Decker, S.R., Adney, W.S., Jennings, E., Vinzant, T.B., Himmel, M.E., 2003. Automated Filter Paper Assay for Determination of Cellulase Activity. *Appl. Biochem. Biotechnol.* 105–108, 689–703.

Diederich, P., Amrhein, S., Hammerling, F., Hubbuch, J., 2013. Evaluation of PEG/phosphate aqueous two-phase systems for the purification of the chicken egg white protein avidin by using high-throughput techniques. *Chem. Eng. Sci.* 104, 945–956. <https://doi.org/10.1016/j.ces.2013.10.008>

Ferreira, A.M., Passos, H., Okafuji, A., Tavares, A.P.M., Ohno, H., Freire, M.G., Coutinho, J.A.P., 2018. An integrated process for enzymatic catalysis allowing product recovery and enzyme reuse by applying thermoreversible aqueous biphasic systems. *Green Chem.* 20, 1218–1223. <https://doi.org/10.1039/C7GC03880A>

Freire, M.G., Cláudio, A.F.M., Araújo, J.M.M., Coutinho, J. a. P., Marrucho, I.M., Lopes, J.N.C., Rebelo, L.P.N., 2012. Aqueous biphasic systems: a boost brought about by using ionic liquids. *Chem. Soc. Rev.* 41, 4966. <https://doi.org/10.1039/c2cs35151j>

Goddard, J.P., Reymond, J.L., 2004. Enzyme assays for high-throughput screening. *Curr. Opin. Biotechnol.* 15, 314–322. <https://doi.org/10.1016/j.copbio.2004.06.008>

González-González, M., Mayolo-Deloya, K., Rito-Palomares, M., Winkler, R., 2011. Colorimetric protein quantification in aqueous two-phase systems. *Process Biochem.* 46, 413–417. <https://doi.org/10.1016/j.procbio.2010.08.026>

Hatti-kaul, R., 2001. Aqueous Two-Phase Systems. *Mol. Biotechnol.* 19, 269–177.

Heller, A., Barkleit, A., Foerstendorf, H., Tsushima, S., Heim, K., Bernhard, G., 2012. Curium(III) citrate speciation in biological systems: A europium(III) assisted spectroscopic and quantum chemical study. *Dalt. Trans.* 41, 13969–13983. <https://doi.org/10.1039/c2dt31480k>

Iqbal, M., Tao, Y., Xie, S., Zhu, Y., Chen, D., Wang, X., Huang, L., Peng, D., Sattar, A., Shabbir, M.A.B., Hussain, H.I., Ahmed, S., Yuan, Z., 2016. Aqueous two-phase system (ATPS): an overview and advances in its applications. *Biol. Proced. Online* 18, 18. <https://doi.org/10.1186/s12575-016-0048-8>

Kaul, A., 2000. Chapter 2: The Phase Diagram, in: Hatti-Kaul, R. (Ed.), *Methods in Biotechnology. Aqueous Two-Phase Systems*. pp. 11–21. <https://doi.org/10.1385/1-59259-028-4:11>

Kristensen, J.B., Felby, C., Jørgensen, H., 2009. Yield-determining factors in high-solids enzymatic hydrolysis of lignocellulose. *Biotechnol. Biofuels* 10, 1–10. <https://doi.org/10.1186/1754-6834-2-11>

Kunz, W., Henle, J., Ninham, B.W., 2004. “Zur Lehre von der Wirkung der Salze” (about the science of the effect of salts): Franz Hofmeister’s historical papers. *Curr. Opin. Colloid Interface Sci.* 9, 19–37. <https://doi.org/10.1016/j.cocis.2004.05.005>

Li, M., Kim, J.W., Peebles, T.L., 2002. Amylase partitioning and extractive bioconversion of starch using thermoseparating aqueous two-phase systems. *J. Biotechnol.* 93, 15–26. [https://doi.org/10.1016/S0168-1656\(01\)00382-0](https://doi.org/10.1016/S0168-1656(01)00382-0)

Margeot, A., Hahn-Hagerdal, B., Edlund, M., Slade, R., Monot, F., 2009. New improvements for lignocellulosic ethanol. *Curr. Opin. Biotechnol.* 20, 372–380. <https://doi.org/10.1016/j.copbio.2009.05.009>

Merchuk, J.C., Andrews, B.A., Asenjo, J.A., 1998a. Aqueous two-phase systems for protein separation Studies on phase inversion. *J. Chromatogr. B* 711, 285–293.

Mesa, L., López, N., Cara, C., Castro, E., González, E., Mussatto, S.I., 2016. Techno-economic evaluation of strategies based on two steps organosolv pretreatment and enzymatic hydrolysis of sugarcane bagasse for ethanol production. *Renew. Energy* 86, 270–279. <https://doi.org/10.1016/j.renene.2015.07.105>

Miller, G.L., 1959. Use of Dinitrosalicylic Acid Reagent for Determination of Reducing Sugar. *Anal. Chem.* 31, 426–428.

Modenbach, A.A., Nokes, S.E., 2013. Enzymatic hydrolysis of biomass at high-solids loadings - A review. *Biomass and Bioenergy* 56, 526–544. <https://doi.org/10.1016/j.biombioe.2013.05.031> Review

Moreira, S., Silvério, S.C., Macedo, E.A., Milagres, A.M.F., Teixeira, J.A., Mussatto, S.I., 2013. Recovery of *Peniophora cinerea* laccase using aqueous two-phase systems composed by ethylene oxide / propylene oxide copolymer and potassium phosphate salts. *J. Chromatogr. A* 1321, 14–20. <https://doi.org/10.1016/j.chroma.2013.10.056>

Oelmeier, S.A., Dismer, F., Hubbuch, J., 2011. Application of an aqueous two-phase systems high-throughput screening method to evaluate mAb HCP separation. *Biotechnol. Bioeng.* 108, 69–81. <https://doi.org/10.1002/bit.22900>

Ogawa, J., Shimizu, S., 1999. Microbial enzymes: New industrial applications from traditional screening methods. *Trends Biotechnol.* 17, 13–21. [https://doi.org/10.1016/S0167-7799\(98\)01227-X](https://doi.org/10.1016/S0167-7799(98)01227-X)

Okur, H.I., Hladílková, J., Rembert, K.B., Cho, Y., Heyda, J., Dzubiella, J., Cremer, P.S., Jungwirth, P., 2017. Beyond the Hofmeister Series: Ion-Specific Effects on Proteins and Their Biological Functions. *J. Phys. Chem. B* 121, 1997–2014. <https://doi.org/10.1021/acs.jpcc.6b10797>

Othmer, D.F., Tobias, P.E., 1942. Liquid -Liquid Extraction Data -Toluene and Acetaldehyde Systems. *Ind. Eng. Chem.* 34, 690–692. <https://doi.org/10.1021/ie50390a011>

Phong, W.N., Show, P.L., Chow, Y.H., Ling, T.C., 2018. Recovery of biotechnological products using aqueous two phase systems. *J. Biosci. Bioeng.* xx. <https://doi.org/10.1016/j.jbiosc.2018.03.005>

Pirrung, S.M., Parruca da Cruz, D., Hanke, A.T., Berends, C., Van Beckhoven, R.F.W.C., Eppink, M.H.M., Ottens, M., 2018. Chromatographic parameter determination for complex biological feedstocks. *Biotechnol. Prog.* <https://doi.org/10.1002/btpr.2642>

Press, W., Teukolsky, S., Vetterling, W., Flannery, B., 2007. *Numerical Recipes. The Art of Scientific Computing*, Third Edit. ed. Cambridge University Press.

Selig, M.J., Tucker, M.P., Sykes, R.W., Reichel, K.L., Brunecky, R., Himmel, M.E., Davis, M.F., Decker, S.R., 2010. Lignocellulose recalcitrance screening by integrated high-throughput hydrothermal pretreatment and enzymatic saccharification. *Ind. Biotechnol.* 6, 104–111. <https://doi.org/10.1089/ind.2010.0009>

Suarez, E., Suarez, C.A., Tilaye, T., Eppink, M.H.M., Wij, R.H., Berg, C. Van Den, 2018. Fractionation of proteins and carbohydrates from crude microalgae extracts using an ionic liquid based-aqueous two phase system. *Sep. Purification Technol.* 204, 56–65. <https://doi.org/10.1016/j.seppur.2018.04.043>

Tjerneld, F., Persson, I., Lee, J.M., 1991. Enzymatic cellulose hydrolysis in an attrition bioreactor combined with an aqueous two-phase system. *Biotechnol. Bioeng.* 37, 876–882. <https://doi.org/10.1002/bit.260370912>

Torres, G.B., 2016. *Decision Making at Early Design Stages: Economic Risk Analysis of Add-On Processes to Existing Sugarcane Biorefineries*. University of Campinas.

Van Sonsbeek, H.M., Beeftink, H.H., Tramper, J., 1993. Two-liquid-phase bioreactors. *Enzyme Microb. Technol.* 15, 722–9. [https://doi.org/http://dx.doi.org/10.1016/0141-0229\(93\)90001-I](https://doi.org/http://dx.doi.org/10.1016/0141-0229(93)90001-I)

Wiendahl, M., Olker, C., Husemann, I., Krarup, J., Staby, A., Scholl, S., Hubbuch, U., 2009. A novel method to evaluate protein solubility using a high throughput screening approach. *Chem. Eng. Sci.* 64, 3778–3788. <https://doi.org/10.1016/j.ces.2009.05.029>

Yang, J., Zhang, X., Yong, Q., Yu, S., 2011. Three-stage enzymatic hydrolysis of steam-exploded corn stover at high substrate concentration. *Bioresour. Technol.* 102, 4905–4908. <https://doi.org/10.1016/j.biortech.2010.12.047>

Zimmermann, S., Gretzinger, S., Schwab, M.-L., Scheeder, C., Zimmermann, P.K., Oelmeier, S.A., Gottwald, E., Bogsnes, A., Hansson, M., Staby, A., Hubbuch, J., 2016. High-throughput downstream process development for cell-based products using aqueous two-phase systems. *J. Chromatogr. A* 1464, 1–11. <https://doi.org/10.1016/j.chroma.2016.08.025>



## CHAPTER 3

### A critical assessment of the Flory-Huggins (FH) theory to predict aqueous two-phase behaviour\*

Bianca Consorti Bussamra<sup>1,2</sup>, Devi Sietaram<sup>a</sup>, Peter Verheijen<sup>a</sup>, Solange I. Mussatto<sup>3</sup>, Aline Carvalho da Costa<sup>2</sup>, Luuk van der Wielen<sup>1,4</sup>, Marcel Ottens<sup>1</sup>

<sup>1</sup>Department of Biotechnology, Delft University of Technology. Van der Maasweg 9, 2629HZ. Delft, The Netherlands.

<sup>2</sup>Development of Processes and Products (DDPP), University of Campinas. Av. Albert Einstein, 500. Post Code: 6066. Campinas, Brazil.

<sup>3</sup>Novo Nordisk Foundation Center for Biosustainability, Technical University of Denmark. Kemitorvet, Building 220. 2800, Kongens Lyngby, Denmark.

<sup>4</sup>Bernal Institute, University of Limerick. Castletroy. Limerick, Ireland.

---

\* This Chapter has been published as: **Bussamra, B.C.**, Sietaram, D., Verheijen, P., Mussatto, S.I., da Costa, A.C., van der Wielen, L., Ottens, M., 2021. Separation and Purification Technology 255, 117636.  
<https://doi.org/10.1016/j.seppur.2020.117636>

### **Abstract**

The article brings an analysis on published models used to calculate phase separation in aqueous two-phase systems (ATPS) based on Flory-Huggins (FH) theory, in terms of problem formulation and mathematical solving algorithm. An integrated algorithm is presented, showing different mathematical approaches of using the FH theory. The algorithm involves the estimation of interchange energy, and the calculation of phase compositions. Based on experimental data, the thermodynamic model can provide a useful framework to perform a sensitivity analysis on parameters, in order to understand the influence of salt type, polymer molecular mass, and ionic strength on phase separation. However, this model, restricted to entropic and enthalpic terms, cannot quantitatively describe the data. This occurs mainly because of the strong influence of random experimental errors on the estimation of interchange energy and FH not being an exact description of phase separation in salt based ATPS. After providing a literature overview and mathematical analysis, we bring to the field the application of the FH theory for selecting ATPS and its limitations.

**Keywords:** Flory-Huggins theory, interchange energy estimation, Flory-Huggins interaction parameter, thermodynamic modelling, aqueous two-phase systems, sensitivity analysis.



## 1. Introduction

Aqueous two-phase systems (ATPS) are well-known as downstream processing unit operation to separate valuable compounds from fermentation broth and complex systems [1]. Food industry can rely on this method to separate proteins with the advantages of mild operating conditions, high recovery yield and ease of scaling up [2]. Moreover, this technique can also be applied at the biorenewable energy field, providing solubilisation of the lignocellulosic substrate during the pre-treatment of the biomass [3]. Thermodynamic analysis of ATPS can assist not only to a theoretical understanding of phase separation [4], but also in the prediction of optimal parameters for a specific application [5]. A reliable thermodynamic model can also be applied to repredict phase separation when systems are disturbed due to phase recycle and removal of solutes in a specific application. Consequently, a process design involving ATPS can be highly benefited when a thermodynamic model is integrated after crucial operation units of the process.

Among a wide variety of thermodynamic models [6], Flory-Huggins [7] presents several advantages, such as a clear distinction between entropic and enthalpic effects, and a relatively simple and analytical set of equations. The FH equations [7] were developed for polymer solutions (high molecular weight macromolecules dissolved in low-molecular weight solvents). This theory has been applied broadly to polymer blends and block copolymers [8]. In 1998, Johansson and co-workers [9] introduced a framework based on the FH theory for the prediction of phase separation of ATPS composed of polymer and salt. Among the lattice models, UNIQUAC and UNIFAC have also been used to describe phase behaviour in polymer-salt based ATPS [10].

Because of the charge of the salt ions, the models have been extended to consider the electrostatic interactions between these ions. This long-range contribution is expressed by the Debye-Hückel (DH) and Pitzer-Debye-Hückel (PDH) terms [11] [12]. Apart from the extra term to incorporate the ionic interactions, some models also present ion specific parameters. The electrolyte perturbed chain statistical associating fluid theory (ePC-SAFT) is an example of model which considers the

ionic interaction term, ion specific parameters and the molecular structure of organic anion (e.g. citrate) [13]. The ePC-SAFT model showed quantitatively correct predictions of ATPS composed by polymers and salts [13][14].

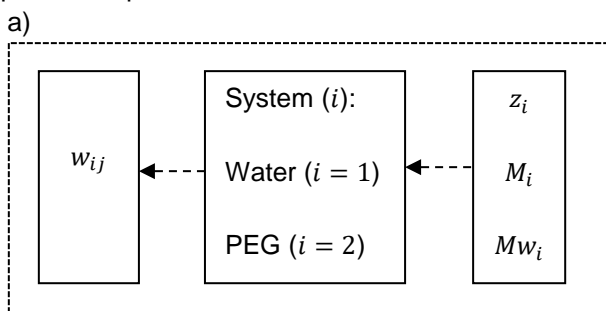
FH model is composed of a combinatorial term (entropic contribution) and a short-range interaction term (enthalpic contribution). Some works [12] have also described the short-range interactions by replacing the enthalpic term of the FH equation (composed by the interchange energy or interaction parameter) for the so called Chen-NRTL. The addition of this enthalpic term to the already defined FH combinatorial contribution (entropic term) and to the PDH long-range interaction contribution improves the fitting of the experimental data, when applied to systems composed by polymer and citrate salts. However, a deep understanding of the influence of the input parameters would benefit the theoretical prediction of phase separation when a FH model composed only by the entropic and the short-range interaction terms are applied. Although there are many techniques to measure the interaction parameter experimentally, they do not correspond exactly to the proper parameters present in the FH theory [4]. In order to avoid this divergence, we propose mathematical ways to estimate the interchange energy using solely the FH theory in a reverse approach. Since the interaction parameters ( $\chi_{ij}$ ) are a direct correlation from the interchange energy ( $w_{ij}$ ),  $\chi_{ij}$  can also be inferred and interpreted based on this approach. Moreover, this work aims to present advances and limitations of existent calculations based on FH theory to predict phase separation in salt-polymer based ATPS. Different problem formulations and numerical methods were developed and evaluated for that purpose. Based on experimental data, two mathematical approaches to regress the interchange energy are presented. The developed framework is divided in two steps (regression of interchange energy and calculation of phase diagram) and provides qualitative prediction and understanding of enthalpic and entropic contributions to phase separation. Based on a useful thermodynamic modelling, the framework could identify trends to guide the screening of ATPS.

## 2. Methods

### 2.1. Research design

The implementation and analysis of FH theory were divided in two steps: step 1, estimation of interchange energy ( $w_{ij}$ ); step 2, calculation of phase diagrams (Figure 1). In step 2, the calculation of volume fractions for each component in top and bottom phases ( $\phi_i^t$  and  $\phi_i^b$ , respectively) through FH theory requires the following input information: interchange energy between the components ( $w_{ij}$ ), degree of polymerization ( $M_i$ ), molecular weight ( $Mw_i$ ), and component charge ( $z_i$ ).

The ATPS studied in this work were formed by polymers and salts. Phase diagrams were determined while varying polymer molecular size, salt type, concentration of these phase forming components (assessed by the tie line length - TLL) and ionic strength (evaluated here in terms of pH and ion charges). Parameters as temperature (T) and pressure (P) were assumed constant. The polymer type was kept as being polyethylene glycol (PEG), varying the molecular weight in 2000 g/mol, 4000 g/mol and 6000 g/mol. The salt types evaluated were sodium phosphate, magnesium sulphate and potassium citrate.



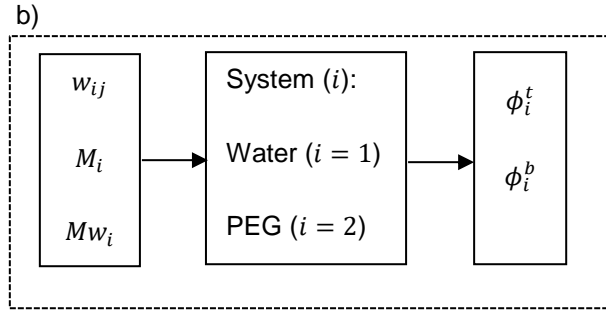


Figure 1: Schematic display of the algorithm applied to calculate interchange energy and phase separation. a) Step 1 of the algorithm - the dashed arrows represent the inverse order of calculation, in which the volume fractions are used to estimate the interchange energy; b) step 2 of the algorithm, used to calculate the phase diagram.

## 2.2. FH framework

The FH equation was derived by Flory [15] and Huggins [16] independently. The FH mean field theory is applied here in order to calculate the volume fraction of components in top and bottom phases. The influence of system variables, such as polymer size or salt type, on phase separation can be directly retrieved from the calculated volume fractions, which provides information to phase diagram construction.

The volume fraction of components is defined by  $\phi_i = \frac{M_i n_i}{N}$ , where  $M_i$  is the degree of polymerisation of component  $i$ ,  $n_i$  the number of molecules of each component and  $N$  is the total number of lattice sites computed as  $N = \sum_{i=1}^m M_i n_i$ , for  $m$  being the number of components in the system. The volume fraction represents the fraction of sites occupied by the components in the total lattice. The concept of lattice models assumes that each site of the lattice is occupied by either a solvent molecule or a polymer segment [17].

The calculation of the optimum volume fractions per component in both top and bottom phases should satisfy the condition that the sum of the Gibbs free energy in both phases is smaller than the Gibbs free energy calculated for the homogeneous system.

The Gibbs free energy of mixing combines an enthalpic ( $\Delta H$ ) and an entropic ( $\Delta S$ ) term and is represented by Equation 1. According to the definition of entropy (Equation 2) and the short range interaction term for enthalpy (Equation 3) [18], the Gibbs free energy of mixing can be rewritten as Equation 4.

$$\Delta G_{mix} = \Delta H_{mix} - T\Delta S_{mix} \quad (1)$$

$$\Delta S_{mix}^c = -NR \sum_{i=1}^m \frac{\phi_i}{M_i} \ln \phi_i \quad (2)$$

$$\Delta H_{mix} = N \sum_{i=1}^{m-1} \sum_{j=i+1}^m \phi_i \phi_j w_{ij} \quad (3)$$

$$\Delta G_{mix} = N \sum_{i=1}^{m-1} \sum_{j=i+1}^m \phi_i \phi_j w_{ij} + NRT \sum_{i=1}^m \frac{\phi_i}{M_i} \ln \phi_i \quad (4)$$

where R is the universal gas constant and has the value of 8.3144 J/K/mol, and T is the temperature.

The FH model is independent on the molecular shape, and because of that the model does not always give an accurate quantitative combinatorial entropy of mixing. The entropy, however, is the dominant term for solutions of molecules of very different size [17].

The pair-wise interchange energy,  $w_{ij}$ , is often replaced with the FH interaction parameter  $\chi_{ij}$ . They are related by  $\chi_{ij} = \frac{w_{ij}}{RT}$  [17]. The dimensionless FH interaction parameter  $\chi_{ij}$  is a measurable quantity. In the FH equation, although  $w_{ij}$  is used,  $\chi_{ij}$  can also be inferred and interpreted from the application of such equations.

### 2.3. Algorithm implementation

In this topic, the problem formulation for each step is presented, in terms of objective functions, constraints and mathematical algorithm. The way of evaluating and comparing the different approaches for interaction parameters determination and phase diagrams calculation are also displayed here.

### 2.3.1. Step 1: Pair-wise interchange energy determination

The interaction parameters were determined through two different mathematical approaches (Table 1). In approach A, it was aimed to obtain a linear expression involving the interchange energy, in which the experimental volume fractions are fitted. Approach B accepts the fact that there might be a difference between experimental and modelled phase compositions. Then, the pair-wise interchange energies are calculated in order to reduce this difference as much as possible. For all the approaches, experimental fractions for each component in top and bottom phases are required.

Table 1: Description of the methods used to determine the interaction parameters (which are derived from the interchange energies), given the compositions of the components in top and bottom phases.

Characteristics	Methods	
	Linear regression, A	Reconciliation, B
Overview	Volume fractions ( $\phi_i^{t/b}$ ) are given experimentally. The interchange energy ( $w_{ij}$ ) are calculated in order to minimize the difference in chemical equilibriums of the components for each phase.	Postulated compositions of the phases are introduced for each experimental point. In the first optimization, the postulated compositions are fit under fixed interchange energy (calculated through linear regression). The second optimization follows by fitting both the postulated compositions and interchange energy.
Objective function	According to the chemical potential equality ( $\mu_i^t = \mu_i^b$ ), and considering that $\mu$ can be expressed as	The objective function searches for the reduction of the sum square of the residues between the

---

	<p> <math>\mu_i^\alpha = C^\alpha w - D^\alpha</math>, for each phase <math>\alpha</math>, the linear solution is written as <math>Cw = D</math>. The matrix <math>C</math> contains the coefficients of <math>w</math>, while the vector <math>D</math> is a function of the experimental volume fractions (<math>\phi_i^{t/b}</math>) and degree of polymerization (<math>M_i</math>).         </p>	<p>           postulated and experimental compositions, as well as interchange energy which satisfy the equilibrium between the phases (<math>\mu_i^t = \mu_i^b</math>), according to Equation 10.         </p>
Mathematical algorithm	<p> <math>w</math> is regressed such as           <math display="block">w = (C^T C)^{-1} C^T D</math> </p>	<p>           Postulated compositions are regressed through minimization of the sum of the squares of the residues between calculated and experimental compositions. <math>w</math> is determined considering the postulated volumes fractions and the chemical equilibrium conditions, though minimization of the difference of chemical potential in the phases for each component.         </p>
Constraints	<p>No constraints are added to this approach.</p>	<p>           The sum fraction is equal to 1 for top and bottom phases. The charge balance constraint is fulfilled in the determination of the interchange energy, once <math>w</math> </p>

---

---

can vary such that charge balance is respected.

---

In the regression of the interchange energy through a linear expression represented by method A, the objective function was written to satisfy the condition that the chemical potential in top ( $\mu_i^t$ ) and bottom ( $\mu_i^b$ ) phases for each component should be equal, according to:

$$\mu_i^t = \mu_i^b \quad (5)$$

Furthermore, the chemical potential consists of the summation of three terms given by:

$$\mu_i = \mu_i^\circ + RT \ln \phi_i + \mu_i^{ex} \quad (6)$$

Where  $\mu_i^\circ$  and  $\mu_i^{ex}$  are the reference equilibrium and excess chemical potential of component  $i$ , respectively, and  $\phi_i$  the volume fraction of component  $i$  with respect to the total of components in that phase. Combining Equation 6 and the constraint imposed in Equation 5, the equilibrium partition coefficient is computed as:

$$\ln K_i^\circ = \frac{1}{RT} ((\mu_i^{ex})^b - (\mu_i^{ex})^t), \quad (7)$$

being  $K_i^\circ = \phi_i^t / \phi_i^b$  the partition coefficient where the component have no charge.

The expression for the equilibrium partition coefficient according to FH is given below:



$$\begin{aligned}
\ln K_i^\circ = M_i & \left( \sum_j^m \left( \frac{\phi_j}{M_j} \right)^t - \sum_j^m \left( \frac{\phi_j}{M_j} \right)^b \right) \\
& - \frac{M_i}{RT} \left( \sum_{j \neq i}^m (\phi_j^t - \phi_j^b) w_{ji} \right. \\
& \left. - \sum_j^{m-1} \sum_{k=j+1}^m (\phi_j^t \phi_k^t - \phi_j^b \phi_k^b) w_{jk} \right)
\end{aligned} \tag{8}$$

where  $m$  is the number of phase forming components and  $M_i$  is the degree of polymerisation of component  $i$ . Also, the relation between the equilibrium partition coefficient ( $\ln K_i^\circ$ ) and the actual partition coefficient ( $K_i$ ), also considering the charge of component  $i$ , is given by:

$$\ln K_i = \ln K_i^\circ + \frac{z_i F \Delta \psi}{RT} \tag{9}$$

The Equations 8 and 9 can be rewritten such that on the left-hand side a linear equation as a function of all interchange energies is obtained and on the right-hand side a constant value composed of the volume fractions and degree of polymerisation (input variables that remain constant during the calculation) is computed ( $constant = f(\phi_i^t, \phi_i^b, M_i, z_i)$ ):

$$\begin{aligned}
& - \frac{M_i}{RT} (\sum_{j \neq i}^m (\phi_j^t - \phi_j^b) w_{ji} - \sum_j^{m-1} \sum_{k=j+1}^m (\phi_j^t \phi_k^t - \phi_j^b \phi_k^b) w_{jk}) = \ln K_i - \frac{z_i F \Delta \psi}{RT} - M_i \left( \sum_j^m \left( \frac{\phi_j}{M_j} \right)^t - \sum_j^m \left( \frac{\phi_j}{M_j} \right)^b \right)
\end{aligned} \tag{10}$$

This regression requires as input a matrix of volume fractions in top and bottom phases, where each column is a component and each row is a data point. Four variables are provided for each phase (volume fractions of water, polymer, anion and cation). However, not all the four variables were measured, even though they are been considered as input data. For each data point, the linear term and the constant

part of the equation (Equation 10) are stored in vectors denominated C and D, respectively. The vector W, containing the interchange energy  $w_{ij}$ , is regressed in order to minimize the residual of the expression  $CW - D$ . This linear regression was performed considering two scenarios for the error: no errors in the chemical potentials (ordinary least square regression) and a constant relative error of 1% on the chemical potential. For the constant relative error, the error model consisted of a weighted variation on the chemical potential, following the equation  $error_{\mu} = 0.01 \frac{\mu_t + \mu_b}{2} \sqrt{2}$ .

An alternative method to estimate the pair-wise interchange energy (Method B, Table 1) consists of setting compositions of the phases as close as possible to the compositions obtained experimentally, by fitting the  $w_{ij}$  according to Equation 10. The initial part of the *reconciliation* method consists on determining appropriated initial guesses for the  $w_{ij}$ . This is performed through the linear regression method considering a constant relative error. Subsequently, given the initial guessed  $w_{ij}$ , the calculated compositions are fit for each experimental point, under the constraint that the chemical potentials are equal in both phases for each component in the system. This constraint provides postulated compositions (and consequently binodal curves) which satisfy the equilibrium condition of the system. The next optimization routine involves the fit of both the compositions and the  $w_{ij}$ . Here, the objective function searches for the reduction of the sum square of the residues between the postulated and experimental volume fractions (difference between the volume fractions over the estimated experimental error), as well as  $w_{ij}$  which satisfy the equilibrium between the phases, according to Equation 10. The input experimental data considers the fractions in weight percentage. When using weight fractions, only two variables are provided for each phase (weight fractions of polymer and salt). These variables are obtained directly from experiments, propagating less errors in their values. In order to consider the weight fractions for the  $w_{ij}$  calculation, the results obtained via volume fractions were used as initial values. The error model for this approach consisted of a weighted variation on the weight fraction, with a minimum being 0.0001, or  $error_{wt} = 0.02 \sqrt{wt(1 - wt)}$ .

In order to evaluate the coherence of both the mathematical algorithm and numerical methods suggested in each of the two approaches used to calculate  $w_{ij}$  (Table 1), volume fractions determined through FH theory were used as input to calculate the  $w_{ij}$ . The volume fractions, used as input to estimate the  $w_{ij}$ , were calculated according to model parameters described in Table 2. The  $w_{ij}$  were applied to the recalculation of volume fractions, according again to the FH theory. The phase diagrams generated through FH theory using reported  $w_{ij}$  (Johansson et al., 1998) and the calculated  $w_{ij}$  were compared. This test was described in Figure 2 a.

Table 2: Model parameter values for polymer-salt ATPS. PEG-phosphate system parameters was retrieved from Johansson et al. (1998) [9].

System	PEG-phosphate
System composition	(1) water, (2) PEG, (3) sodium, (4) phosphate
Interchange energy (J/mol)	$w_{12} = 100$ , $w_{13} = -10000$ , $w_{14} = -30000$ , $w_{23} = -1000$ , $w_{24} = -3000$ , $w_{34} = -50000$
Degree of polymerisation	$M_1 = M_3 = M_4 = 1$ , $M_2 = 100$
Charge	$z_1 = z_2 = 0$ , $z_3 = 1$ , $z_4 = -1.5$
Molecular weight (g/mol)	$Mw_1 = 18$ , $Mw_2 = 6000$ , $Mw_3 = 23$ , $Mw_4 = 94$

Finally, the two approaches to estimate  $w_{ij}$  (Linear regression, A; Reconciliation, B) were compared in terms of reproducibility of the experimental phase diagram (Figure 2 b). The same input compositions experimentally determined were used to calculate the  $w_{ij}$  according to each method (Table 1). The resulting  $w_{ij}$  were applied to the calculation of the phase compositions according to FH theory. In order to obtain the binodal curve, the calculated phase composition data (in weight fraction) was regressed according to the Merchuk equation [19] presented below:

## A critical assessment of the Flory-Huggins (FH) theory

$$c_{polymer} = A \exp[(B c_{salt}^{0.5}) + (C c_{salt}^3)] \quad (11)$$

where  $c_{polymer}$  and  $c_{salt}$  are the polymer and the salt concentrations, respectively, expressed in weight percentage. A, B and C are the fitting parameters obtained by least squares regression. This non-linear regression was performed with the *fmincon* routine in Matlab® R2018b (The Mathworks, Natick, ME, USA).

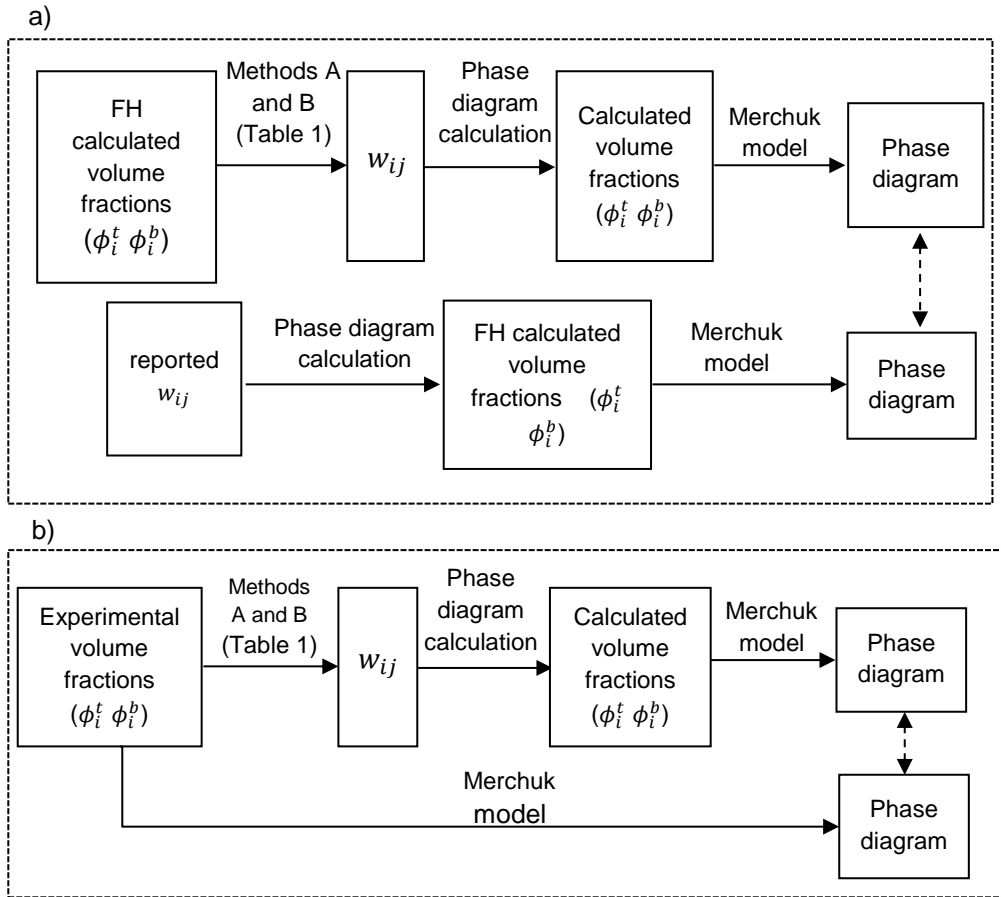


Figure 2: Description of the algorithms to test the mathematical approaches used to determine the pair-wise interchange energies  $w_{ij}$  (a) and the use of experimental data to calculate  $w_{ij}$  and phase diagram according to FH theory (b).

The model parameters for each experimental system are presented in Table 3. The values for the degree of polymerization ( $M$ ) varies for the same polymer molecular weight between Tables 2 and 3. These values were extracted as reported in the cited references. A sensitivity analysis on the  $M$ , performed at this work, brings an indication of the most appropriate value for  $M$ .

Although the thermodynamic model considers four components (water, polymer, cation and anion), the experimental systems present a fifth components, which is the salt not dissociated into ions. In the model, this molecule is being considered under the charge and molecular weight of component four ( $z_4$  and  $Mw_4$ ). The charge ( $z_4$ ) defines the percentage of salt molecule and salt anion in the system, which is connected to the calculation of the molecular weight of this fourth component (Table 3).

Table 3: Model parameter values for polymer-salt ATPS, based on Johansson et al. 2011 [20]. The charge ( $z_4$ ) selection depends on the pH of the system and the speciation of the salts.

System	PEG-sulphate	PEG-citrate
System composition	(1) water, (2) PEG, (3) magnesium, (4) sulphate	(1) water, (2) PEG, (3) potassium, (4) citrate
Degree of polymerisation	$M_1 = M_3 = M_4 = 1$ , $M_2 = 101$ (PEG2000), $M_2 = 202$ (PEG4000), $M_2 = 303$ (PEG6000),	$M_1 = M_3 = M_4 = 1$ , $M_2 = 101$ (PEG2000), $M_2 = 202$ (PEG4000), $M_2 = 303$ (PEG6000),
Charge	$z_1 = z_2 = 0$ , $z_3 = 2$ , $-2 \leq z_4 < 0$	$z_1 = z_2 = 0$ , $z_3 = 1$ , $-3 \leq z_4 < 0$
Molecular weight (g/mol)	$Mw_1 = 18$ , $Mw_2 = 2000$ (PEG2000), $Mw_2 = 4000$ (PEG4000), $Mw_2 = 6000$ (PEG6000), $Mw_3 = 24$ , $Mw_4 = 96 + (1 + \frac{z_4}{z_3})Mw_3$	$Mw_1 = 18$ , $Mw_2 = 2000$ (PEG2000), $Mw_2 = 4000$ (PEG4000), $Mw_2 = 6000$ (PEG6000), $Mw_3 = 39$ , $Mw_4 = 189 + (3 + z_4)Mw_3$

### **2.3.2. Step 2: Phase diagram calculation**

For the estimation of phase diagrams, the compositions of top and bottom phases should be determined, given a certain range of total composition of the system. This calculation was based on Johansson et al. (2011) [20] and implemented in Matlab® R2018b. Other input variables are the interchange energies ( $w_{ij}$ ), the degree of polymerization ( $M_i$ ), the molecular weight ( $Mw_i$ ), and the charge of each component ( $z_i$ ). The optimization routine calculates the number of lattice sites of each component in one of the phases that minimizes the Gibbs energy (Equation 4). The calculation of the phase distribution of each component is restricted to satisfy the chemical equilibrium and the electroneutrality of the system (Equation 5). In this work, we overview this approach, in terms of the thermodynamic basis, and bring improvements in terms of the numerical implementation and structure of the mathematical algorithm.

### **2.4. Monte Carlo sensitivity analysis**

The uncertainty on the  $w_{ij}$  determination, and consequently on the interaction parameters, due to system composition variation was assessed via Monte Carlo sensitivity analysis. The volume fractions of phase forming components (PEG 6000 and sodium phosphate) were calculated through the model input parameters published by Johansson et al. (1998). Weighted errors from 0.01 to 5%, at nine levels, were added to the data, considering the composition of 50 % volume fraction the largest point of error. The errors correspondent to other compositional data ( $\phi_i^\alpha$ ) follow the equation  $error_{\phi_i^\alpha} = 2\sqrt{\phi_i^\alpha(1 - \phi_i^\alpha)}error_{50\% v/v}$ . The  $w_{ij}$  were calculated 4000 and 400 times for each case, through linear regression and reconciliation approach (Table 1), respectively.

## **3. Results and Discussion**

### **3.1. Step 1: FH parameter estimation**

In the FH theory [7], the entropic term assumes an ideal mixture and represents the mixing of dissimilar components. The enthalpic term accounts for the deviation from

ideal mixing due to differences in molecular sizes and energy between the monomeric units and solvent molecules. The key point of the enthalpic part is represented by the interaction energy parameter ( $w_{ij}$ ). This input parameter is influenced by the absolute temperature and pressure, compressibility, degree of polymerization (chain structure), and relative concentrations of phase forming components [7].

The implementation of FH equation considers a set of straightforward input parameters (degree of polymerization, charge and molecular weight of each component), with the exception of the interchange energy ( $w_{ij}$ ) or interaction parameters ( $\chi_{ij}$ ). In order to overcome the extensive experiments to determine these parameters, let alone the fact that they do not correspond exactly to the proper parameter present in the FH theory [4], the FH equation could be used in a reverse way in which interchange energy, and consequently interaction parameters, are determined from experimental data points.

In the first approach to estimate  $w_{ij}$  (Linear Regression, A) given the volume fractions of phase forming components in the top and bottom phases, the equations for the partition coefficient of the phase components were rewritten to a linear format (Equation 10). The problem is solved such as the residue of the difference in chemical potential for each component at top and bottom phases is minimized. However, a consistence variation (at the same time and summing a constant factor) in all the  $w_{ij}$  does not influence the calculated volume fraction of the components in the system. This can be explained thought the solution space of the linear regression. The solution vector  $w_{ij}$  presents a null space ( $N$ ) for the linear problem  $Cw_{ij} = D$ . This means that there is not a single solution for  $w_{ij}$  where the equality  $Cw_{ij} = D$  is satisfied. The null space reflects the ambiguity of the solution and is a cause of interdependence of the equations defined in  $C$ . This interdependence is generated by the constrains of electroneutrality and the fact that the charge of the ions are interconnected.

Alternatively to the Linear Regression approach, the  $w_{ij}$  can be estimated through the ‘Reconciliation’ approach. In this method, postulated volume fractions are introduced for each experimental composition. The objective function searches for the reduction of the sum square of the residues between the postulated and experimental compositions, and the  $w_{ij}$  are determined considering the postulated volume fractions and the chemical equilibrium condition (chemical potential is equal for each phase forming component in both phases).

Both mathematical approaches were validated in terms of estimating coherent results that reproduce the input data. The interaction parameters calculated using both mathematical approaches (Table 1), when applied to phase separation calculation according to FH theory, provided binodal curves nearly equivalent (Figure 3). Moreover, these binodal curves also reproduced the phase compositions used as input data to estimate the  $w_{ij}$  in both approaches. The input data for phase composition was calculated via FH theory for a set of  $w_{ij}$  reported by Johansson et al. (1998).

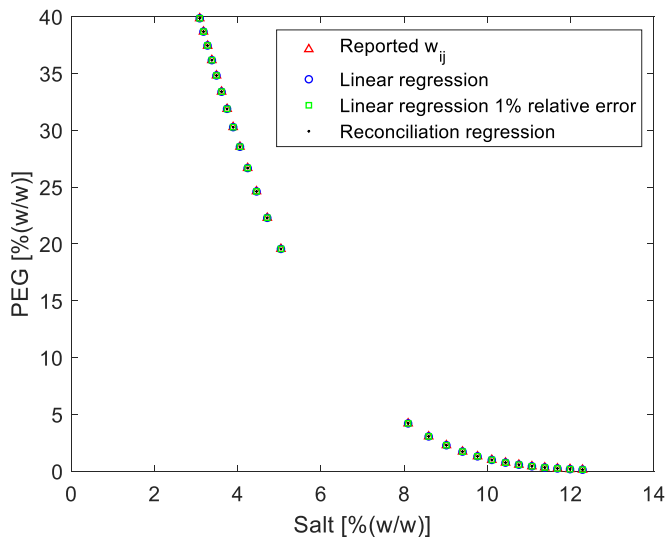


Figure 3: Influence of the mathematical approach to regress the  $w_{ij}$ , given as input the same FH calculated compositions, according to parameters published by Johansson et al. (1998)



[9]. The system is composed by PEG 6000 and sodium phosphate.  $R$  and  $T$  have the values of 8.3144 J/K/mol and 298.12 K, respectively.

For phases to separate, the interaction between polymer segments are more important than the polymer shape, size or excluded volumes [21]. This interaction between phase forming components is presented by the FH interaction parameters. The ambiguity in estimating the interaction parameters, evidenced by the null space, suggests that the volume fraction of the components as the sole source of data in this determination is not enough. In the mathematical approaches compared in Figure 3, all the six  $w_{ij}$  were determined for a system containing four phase forming components.

Because of the charge conservation, the interaction parameters present a fixed relation between each other, for a specific salt (charged molecules of the system) and charge. This relation can be beneficial to determine a set of  $w_{ij}$ , in case a specific one is known or obtained not via the mathematical approaches presented here. However, reducing the number of  $w_{ij}$  to be estimated in order to apply these relations does not improve or alter the results obtained via the linear regression or reconciliation approach. Interaction parameters can also be set to a fixed value in line with physical support. Foroutan and Zarrabi (2008) [11], for instance, fixed the interaction parameter between polymer and salt to zero, while fitted the others according to FH thermodynamic equations and based on experimental values.

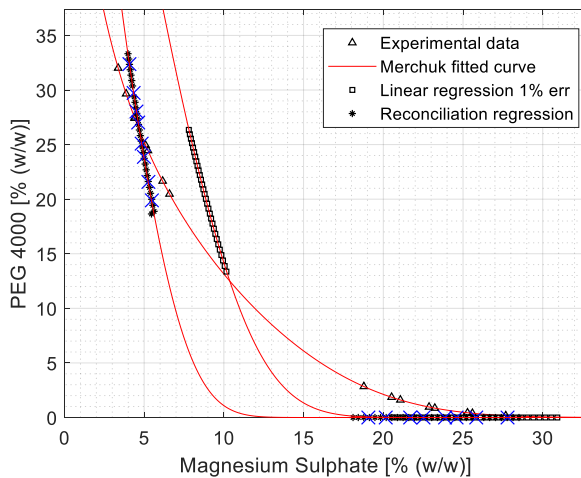
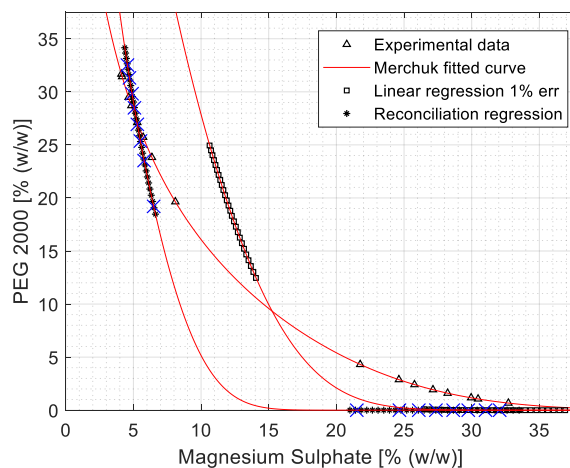
When the methods to estimate the  $w_{ij}$  consider as input experimental data of system compositions, one can expect errors associated to it. The source of these systematic deviations relies on the parameters determination of the binodal curve, according to Merchuk equation, and experimental deviation on the mixing point formulation and on the determination of top and bottom volume ratios through a calibration curve [22]. Moreover, the experimentally calculated top and bottom phase compositions used by this work and published before [22] relies on the extrapolated part of the Merchuk curve, contributing to a certain inaccuracy of the experimental data. Figure 4 shows the phase compositions generated through experimental determination [22] in comparison to compositions calculated by the FH theory. For the later approach,

the  $w_{ij}$  were fitted using the experimental data. In contrast to  $w_{ij}$  fitted using system compositions calculated by FH theory (Figure 3), when the experimental data composition is used instead, the binodal curves are not similar between each other.

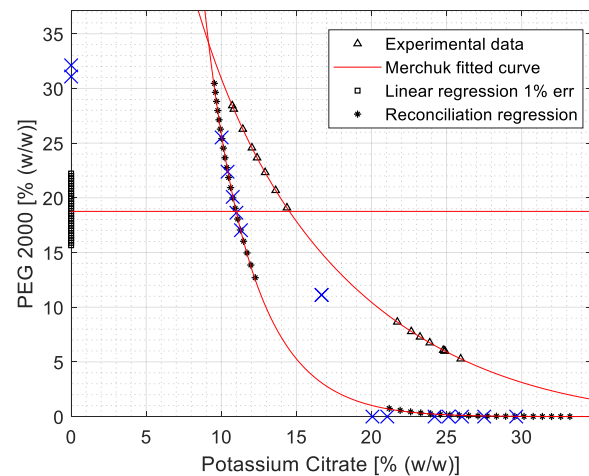
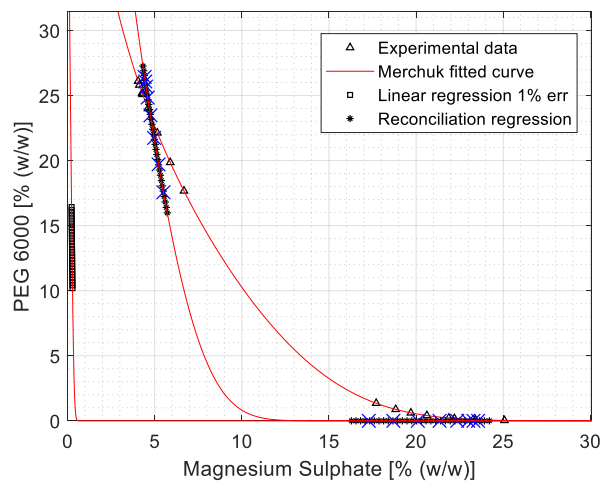
The  $w_{ij}$  estimated by the linear regression could not always generate a binodal curve. The reconciliation approach determines, for each experimental data, a postulated point, being the  $w_{ij}$  fitted in order to reduce the sum square difference between the residues of these two points. The graphs (Figure 4) show these calculated points as blue crosses. The similarity between the experimental and postulated volume fractions does not lead to a set of interaction parameters able to generate similar phase diagrams. For calculating binodal curves via FH model, the optimizer searches for phase compositions that globally minimize the Gibbs energy. For both salt-forming systems studied (potassium citrate and magnesium sulphate) and applying the  $w_{ij}$  estimated by the reconciliation approach, the global minimum output of phase composition differed from the experimental values, for the range of salt and polymer evaluated in the binodal curves. The Gibbs energy surface presents more than two inflection points, leading to false local minima when estimating the interaction parameters [21]. Different sets of estimated  $w_{ij}$  were tried, by randomly varying the initial values of  $w_{ij}$  and/or by applying bigger steps in the optimizer process. However, the calculated binodal curve differs significantly from the experimental one. Based on that, we could infer that the FH model is not an exact description of phase separation in ATPS composed by salt and polymer.

FH model does not present predictive value, being the model only useful for representing the data in a simplified molecular thermodynamic framework [17]. Some physical discrepancies of the FH theory have already been reported, such as loss of the chemical structure of the polymer segment when represented as a sphere; the requirement by the geometry of the lattice site for the conformations of the polymer chain and the solvent to be identical; and the assumption of no volume change upon mixing [21]. Moreover, this theory was developed for polymer solutions, and it is mostly applied to polymer blends, block copolymers [8] and mixture of polymers presenting similar degree of polymerization (chain length) [7]. Regarding

the molecular structure of the ions, the model does not differentiate the organic anion (citrate) from the inorganic sulphate anion. When the non-spherical shape of organic anions is taken into consideration, the thermodynamic model can improve to predict quantitatively polymer/salt ATPS [13].



A critical assessment of the Flory-Huggins (FH) theory



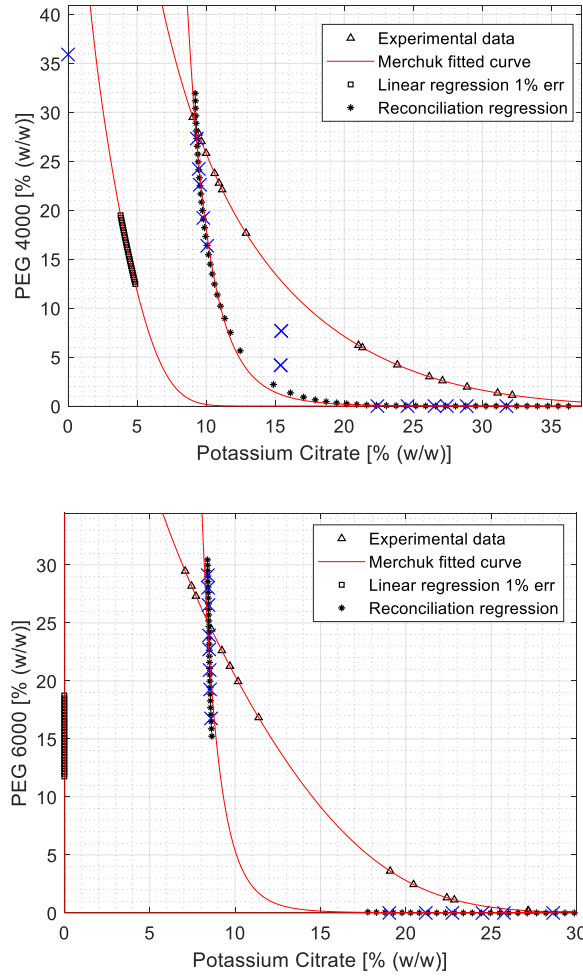


Figure 4: Comparison between experimental and model determined composition of ATPS (represented by binodal curves). The  $w_{ij}$  were calculated using the experimental data. The blue crosses represent the postulated volume fractions calculated by the reconciliation approach.  $z_4 = -1$  for all magnesium sulphate-based systems,  $z_4 = -1.5$  for potassium citrate and PEG 2000 system, and  $z_4 = -0.5$  for potassium citrate and PEG 4000 or PEG 6000 systems.  $R$  and  $T$  have the values of 8.3144 J/K/mol and 313.12 K, respectively.

The measurement errors significantly affect the interaction parameters estimation. Consequently, when experimental data is used to regress the  $w_{ij}$ , the reverse calculation of phase separation differs from the original (experimental) phase

compositions. In order to evaluate how errors in the phase compositions would impact the determination of the  $w_{ij}$ , a Monte Carlo sensitivity analysis was performed on the FH calculated compositions. Given the null space found, the variability was assessed on the  $w_{ij}$  values belonging to a vector perpendicular to the null space. As demonstrated in Figure 3, the use of this data (with no error associated to it) to regress the  $w_{ij}$  provides model-based binodal curves very similar to the original data.

As expected, an increased uncertainty in the data resulted in increasing uncertainty in the  $w_{ij}$ , and consequently in the interaction parameters (Figures 5 and 6). The variability is larger for the reconciliation approach method of estimating these parameters, even though this method (Reconciliation, B) expects error in both weight percentages (salt and polymer), excluding the premise that FH equations should predict experimental compositions. From two experimental observations (weight fractions of salt and polymer) per phase and tie line, the linear regression (method A, Table 1) implies four observations — volume fractions of water, polymer and both ions —, while the reconciliation approach remains exclusively to the two observed data. The variation of the  $w_{ij}$  might also be connected to the composition dependence of this parameter [4], which is represented in this sensitivity analysis by the ‘uncertainty’ in the data.

The linear regression method of estimating the  $w_{ij}$  is sensitive to errors in the data above 1%. As depicted in Figure 5, a large inaccuracy is associated to the determination of  $w_{ij}$ , when an error of 1% or more is applied to the phase composition data. This can be explained by the fact that the non-linearity of the FH theory is evidenced above 1% errors associated to the experimental data, being the linear regression approach only applicable below this threshold. However, different set of interaction parameters can still generate the same binodal curve, as exemplified by the null space case. The influence of the uncertainty in the data should be checked in terms of binodal curve generated, instead of simply the variability on the interaction parameters.

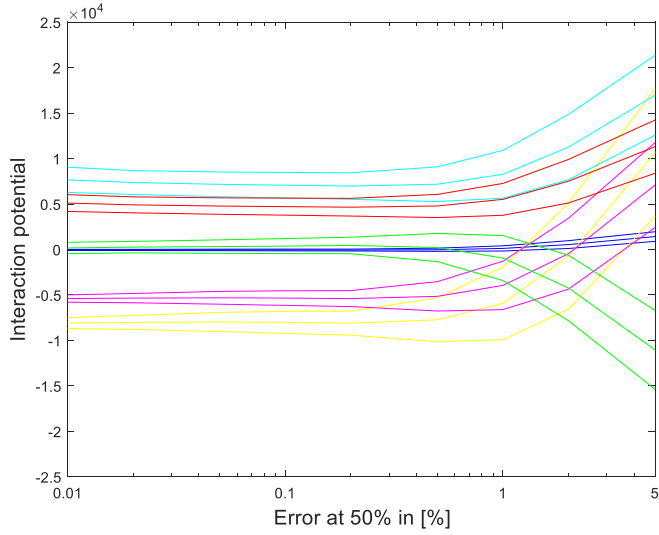


Figure 5: Influence of uncertainty in the data on the estimation of  $w_{ij}$ , according to linear regression method. Errors of 0.01, 0.02, 0.05, 0.1, 0.2, 0.5, 1, 2, and 5% were applied. R and T assume the values of 8.3144 J/K/mol and 298.12 K, respectively. For each  $w_{ij}$ , the mean and the mean  $\pm 1\sigma$  were plotted, according to the legend:  $w_{12} = \text{blue}$ ,  $w_{13} = \text{yellow}$ ,  $w_{14} = \text{magenta}$ ,  $w_{23} = \text{cyan}$ ,  $w_{24} = \text{green}$  and  $w_{34} = \text{red}$ .

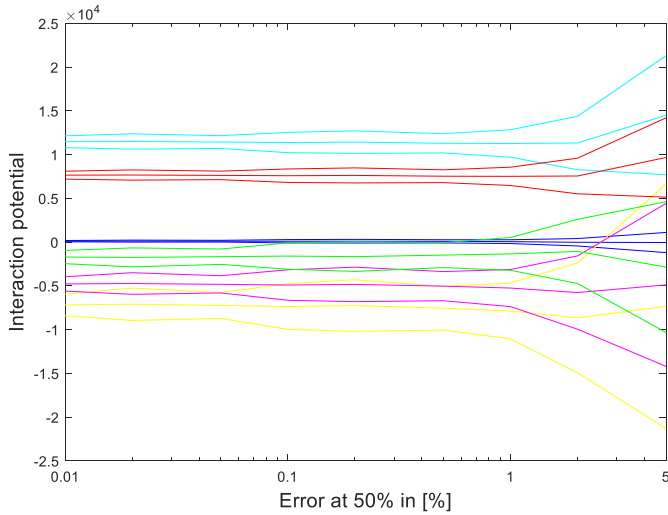


Figure 6: Influence of uncertainty in the data on the estimation of  $w_{ij}$ , according to the reconciliation method. Errors of 0.01, 0.02, 0.05, 0.1, 0.2, 0.5, 1, 2, and 5 % were applied. R and T assume the values of 8.3144 J/K/mol and 298.12 K, respectively. For each  $w_{ij}$ , the mean and the mean  $\pm 1\sigma$  were plotted, according to the legend:  $w_{12} = \text{blue}$ ,  $w_{13} = \text{yellow}$ ,  $w_{14} = \text{magenta}$ ,  $w_{23} = \text{cyan}$ ,  $w_{24} = \text{green}$  and  $w_{34} = \text{red}$ .

### 3.2. Step 2: Determination of phase diagrams

The thermodynamic prediction of phase separation in ATPS composed by polymer and salts, according to the FH theory, was implemented through a mean-field model developed by Johansson et al. (1998) [9]. Within that set of relatively simple and analytical equations, it was intended to qualitatively interpret the general nature of the system and the influence of experimental variables on phase behaviour and partitioning of solutes.

In order to use the set of equations based on FH theory, the interchange energy  $w_{ij}$  or interaction parameter  $\chi_{ij}$  are fundamental and not straight forward obtained. Here, we presented forms of estimating this parameter from experimental data of phase compositions. However, the application of the estimated parameters to the mean-field theory based on FH results in calculated phase separation different to the experimental one (Figure 4). This limitation can be explained by: FH not being an appropriate theory to describe phase separation in ATPS composed by polymer-salt; errors associated to the experimental data used to retrieve the  $w_{ij}$  [22]; reduced set of experimental data exclusively involving the liquid-liquid equilibrium region [23]; not proper numerical implementation of the theory; and poor description of the phase separation when binodal curve is described by Merchuk equation [19]. Moreover, it has been reported the strong dependence of the interaction parameters to the composition of the system [4] [24]. Here, we used a range of experimental data (composed by different phase compositions) to regress one set of  $w_{ij}$  aimed to represent to whole phase separation area. The assumption of interaction parameters being independent on composition has already been assumed by other authors [11], and still a reasonable agreement between modelled and experimental data was observed. Yan and Cao (2014) also estimated the FH interaction parameters by fitting experimental data. The calculation of phase diagrams using the regressed interaction parameters presented a good agreement with the experimental phase diagram. The solution for the Gibbs energy minimization was achieved by assuming a value for the composition of one of the solutes, and retrieving the composition of the other solute via the model equation at system chemical equilibrium [25].



The optimization routine developed and presented by Johansson et al. (2011) [20] to predict phase separation calculates the fraction of each component when the Gibbs free energy is minimized. Considering the chemical equilibrium as a constraint in the problem formulation implies ambiguity, since the derivative of Gibbs energy is the proper chemical potential, and minimizing the Gibbs energy suggests to equalize the chemical potentials. Moreover, the Gibbs energy difference surface is at the optimum very flat, leading to irreproducible results and inefficient search for the global minimum [21]. An alternative to overcome the local minimum is to relieve the restrictions of chemical equilibrium for all the components, except for the water, the uncharged and dominant component of the system [20]. However, this results in volume fractions which do not fulfil the requirement of equal chemical potential between the phases for all the components. It has been already reported that FH model cannot solve simultaneously the chemical potential for all the species of the system [21]. In order to overcome the ambiguity of having such a constraint and the local minimum of the Gibbs energy surface, we suggest the optimization routine to be divided in two steps: first, the fraction of components in a specific phase is determined such that the Gibbs free energy is minimized, followed by a fine tuning of the solutions, where the chemical equilibrium for all the components are solved. Moreover, the single initial guess of phase separation was replaced by a search routine through the whole grid of salt and polymer. Fifty positions (concentrations) of salt, polymer and water were evaluated (resulting in 125000 calculations) in order to obtain the combination which provided the minimum Gibbs energy. This was the initial value used by the optimizer. Apart from the points above, the robustness of the minimization of the Gibbs energy can be affected by scaling issues related to the wide range of compositions and input parameters such as the degree of polymerization and FH interaction parameters [21].

When the salt is considered as an undissociated molecule, the minimization of Gibbs energy fulfils the condition that chemical potentials are in balance for all the components in the system. This approach of connecting the partition of both ions as one molecule between the phases, in order to guarantee charge equilibrium, results in balanced chemical equilibrium, one of the main thermodynamic requirements for

calculating phase separation in two-phase systems. Other studies regarding the modelling of salt-polymer ATPS according to FH theory also supports the consideration of the salt as one molecule for the Gibbs free energy minimization [11]. However, extra terms expressed by the DH and PDH were included in order to consider the electrostatic interaction between the ions [11] [12]. The reference [10] evaluated the influence of the DH term added to both the osmotic virial and UNIQUAC equation for the prediction of phase behaviour in polymer-salt ATPS. For both models, the long-range contribution term improved the quality of fitting the liquid-liquid equilibrium data. In the approach provided here, these electrostatic terms are thought to reduce the ambiguity in determining the interaction parameters, although their contribution were not evaluated at this work.

Both approaches (proposed by Johansson et al 2011 [20] and by this work) of implementing the FH mean-field theory were compared in terms of phase separation for the system PEG 6000 and sodium phosphate, according to input parameters published by Johansson et al. (1998) [9]. The mean of the absolute difference (MAD) between the binodal curves generated by both approaches was 0.71%\* (Figure 7). This analysis measures the deterministic difference between the curves, representing the real distance between the two models.

By analysing the residuals of the calculated data fitted to the Merchuk equation, in Figure 7 b, the deviation of 0.7 % (data not shown) implies the Merchuk is a good approximation of the binodal curve derived from FH calculated data, for this specific system of salt and PEG. Merchuk also provides a good description of the binodal curves for ionic liquid based systems [26]. This empirical equation could also have the exponents adjusted in order to optimize the fitting [26]. Certainly, other experiential equations could be used to correlate the binodal data. Lu et al. [12] compared three different equations to fit experimental data from polymer and

---

\* $MAD = \frac{1}{K} \sum_{i=1}^K |c_{PEG,Johansson} - c_{PEG,Bussamra}|$ , for the independent variable  $C_{salt}$  being 4%, 5%, 6%, 7%, 8%, 9% and 10% (w/w).

potassium salts. In general, the Merchuk-like equation provided the best fit, even though the suitability of the equation seems to be dependent on the constituents of the system.

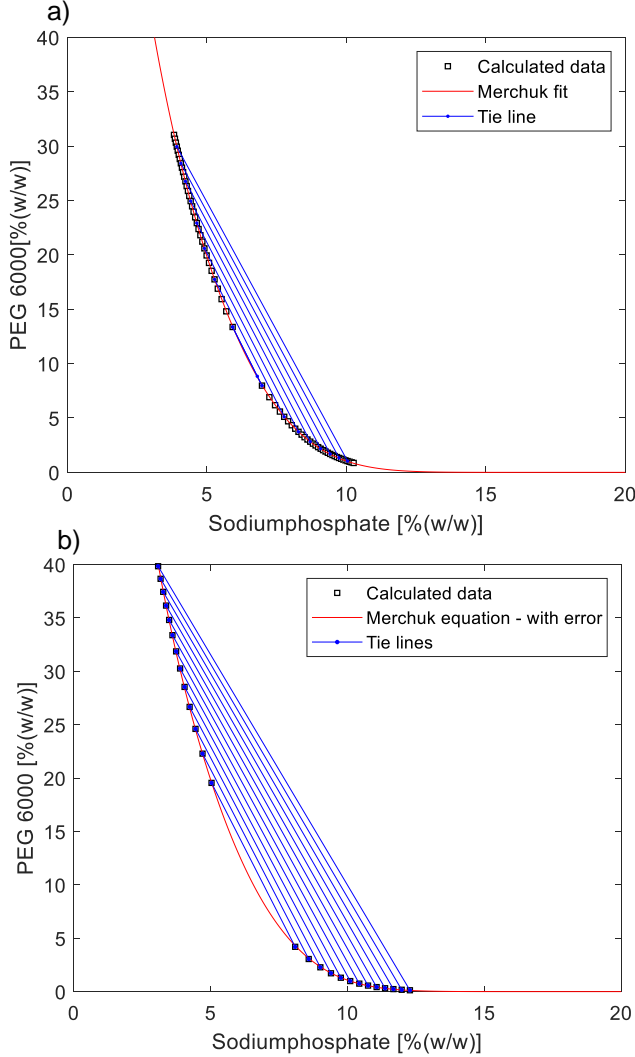


Figure 7: Comparison of binodal curves generated using FH mean-field model and parameters reported by Johansson et al. (1998) [9]. a) Model considering the salt as separated species and not full filling the chemical balance for all the components [20] ( $c_{polymer} = 2.672 \cdot \exp[(-10.3577 \cdot c_{salt}^{0.5}) - (2267.187 \cdot c_{salt}^3)]$ ). b) Model considering the salt as one molecule and providing chemical balance for all the components ( $c_{polymer} = 2.5201 \cdot \exp[(-10.0877 \cdot$

$c_{salt}^{0.5}) - (2262.3493 \cdot c_{salt}^3))$ . R and T assume the values of 8.3144 J/K/mol and 298.12 K, respectively.

However, when the interchange energies ( $w_{ij}$ ) were estimated from experimental data (via the reconciliation method), both approaches to calculate phase separation resulted in binodal curves far apart (Figure 8). The absolute deviation was larger than when the phase separation was calculated using input parameters published by Johansson et al. (1998) [9]. Two likely causes mentioned before of interaction parameters estimated from experimental data do not generate phase separation similar to experimental one are maintained: FH theory does describe properly phase separation of polymer-salt systems, and the errors associated to the experimental data influence the estimation of  $\chi_{ij}$ . When both curves were compared in relation to the experimental binodal curve, Johansson method presented a MAD of 5.1 %<sup>†</sup>, while the method suggested by this work showed a MAD of 4 %<sup>2</sup>. However, these absolute differences do not indicate a preferably curve, since this measurement is influenced by the salt concentration range applied. At low concentration of salt, the calculated concentration of polymer via Merchuk equation varies considerably due to the exponential shape of the binodal curves. Interaction parameters have a great influence over the phase separation calculation, and their choices and estimation procedures should be carefully taken into consideration.

---

<sup>†</sup> $MAD = \frac{1}{K} \sum_{i=1}^k |c_{PEG,model} - c_{PEG,experimental}|$ , for the  $C_{salt}$  range from 4% to 24% (w/w).

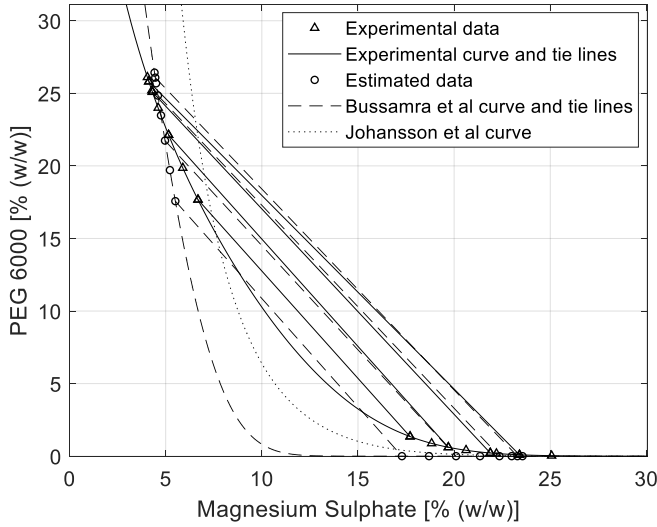


Figure 8: Phase separation calculated via FH theory implemented by Johansson et al. (2011) [20] and by this work. The interchange energies were estimated from the experimental data for the system PEG 6000 and magnesium sulphate. The experimental tie lines and the estimated tie lines (according to the FH model implemented by this work) are also plotted. The binodal curves were fitted according to Merchuk equation.  $R$  and  $T$  have the values of 8.3144 J/K/mol and 313.12 K, respectively.

The interchange energy can be scaled to  $RT$  units, and there is a limited range for the interaction parameters to generate a binodal curve. When the factor  $w_{ij}/RT$  is large, the energy (enthalpic) part is more important for the Gibbs free energy calculation. On the other hand, given a small  $w_{ij}/RT$  factor, the entropic part becomes more important to this calculation. The enthalpy part is a linear term and numerically simpler to be solved. The entropic part involves logarithmic terms and the numerical solution is more complex. The use of scaled interchange energy, or the direct use of the interaction parameter  $\chi_{ij}$ , can also improve the robustness of the Gibbs energy minimization routine [21].

Apart from the interaction potential, the degree of polymerization ( $M_i$ ) and charge of the species ( $z_i$ ) can influence the calculation of phase separation. The later parameter,  $z_i$ , reflects the amount of dissociated ion molecules. The salt dissociation varies according to the pH of the system. In our model, the component 4 (negative

charged species) counts for the anion and the ions present in the salt form. For the system composed by magnesium sulphate salt (figures 9), the charge of component 4 seems to not influence the phase equilibria calculation, neither in the fitting of the model (represented by the blue crosses in figures sub-items b and c). This behaviour was observed for all polymer molecular weights in combination with magnesium sulphate. In contrast to what was pointed out by the magnesium sulphate systems, the potassium citrate systems confirm a clear influence of the ions charge on the phase separation. Moreover, the charge of the anion and the polymer molecular weight seem to be related (Figures 10, 11 and 12). For the experimental data provided and the FH model applied, at higher polymer molecular weights (PEG 4000 and PEG 6000), lower is the solubility of the salt. This is demonstrated by a fitted curve closer to the experimental one when  $z_4 = -0.5$ , in comparison to fitted curves at  $z_4 = -1.5$  or  $z_4 = -3$ . When PEG 2000 is considered, a charge of  $z_4 = -1.5$  represents better the experimental data, implying that more ions are being considered as dissociated in the system. This suggests that the ions influence the estimation of interaction parameters for this system, affecting the calculation of the phase separation according to the speciation of the salt and molecular weight of the polymer.

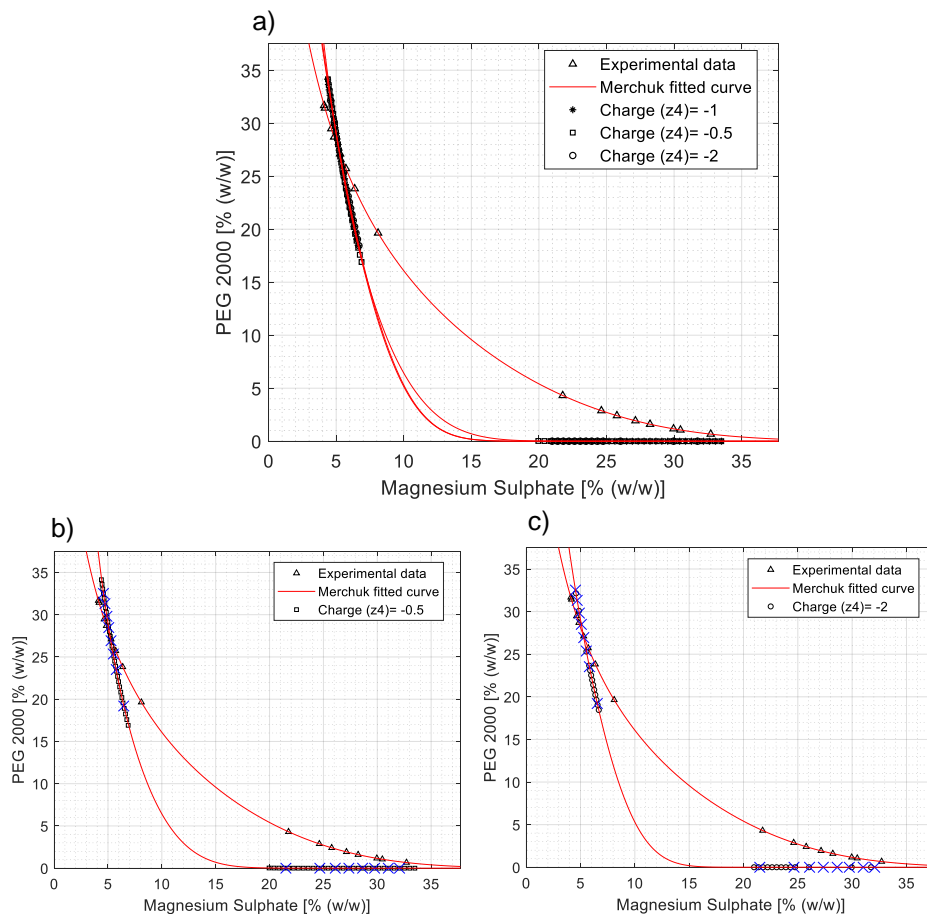


Figure 9: Influence of the charge on the phase separation according to FH theory, for the system composed by Magnesium sulphate and PEG 2000. For each charge selection ( $z_4$ ), the interchange energies were fitted according to the reconciliation approach (Method B, Table 1). The subplots b and c show the fitted points of the model ('postulated' fractions), in blue crosses. R and T have the values of 8.3144 J/K/mol and 313.12 K, respectively.

## A critical assessment of the Flory-Huggins (FH) theory

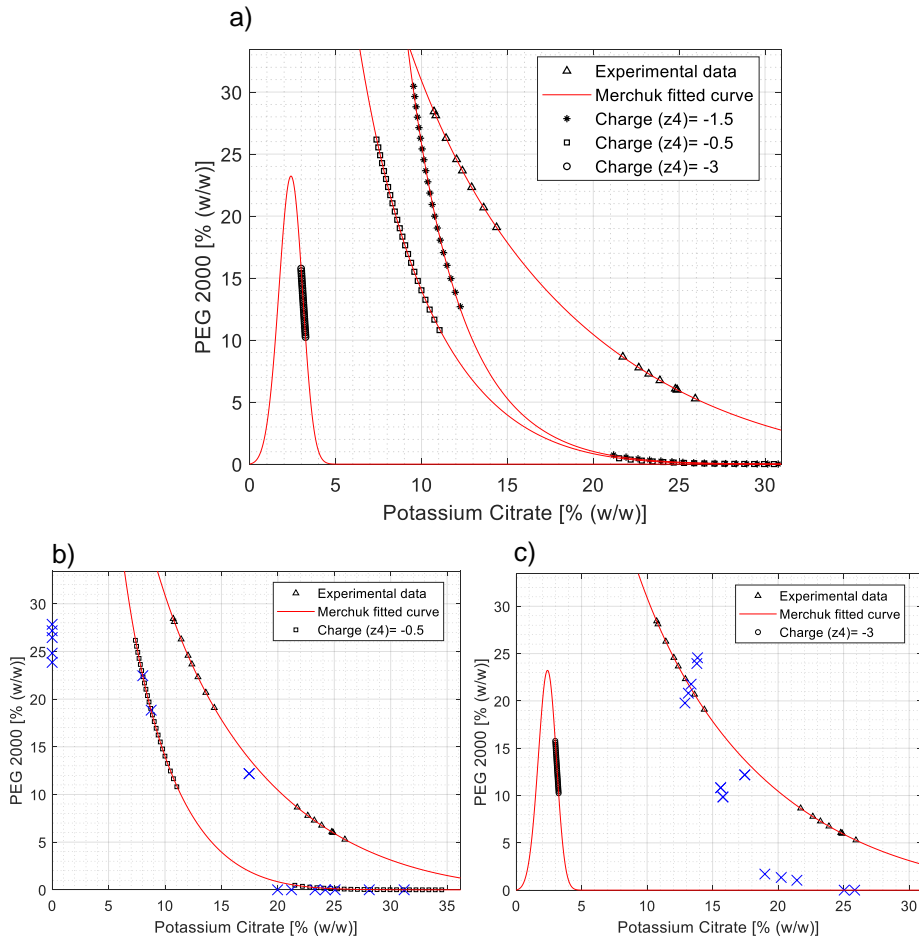


Figure 10: Influence of the charge on the phase separation according to FH theory, for the system composed by Potassium citrate and PEG 2000. For each charge selection ( $z_4$ ), the interchange energies were fitted according to the reconciliation approach (Method B, Table 1). The subplots b and c show the fitted points of the model ('postulated' fractions), in blue crosses. R and T have the values of 8.3144 J/K/mol and 313.12 K, respectively.



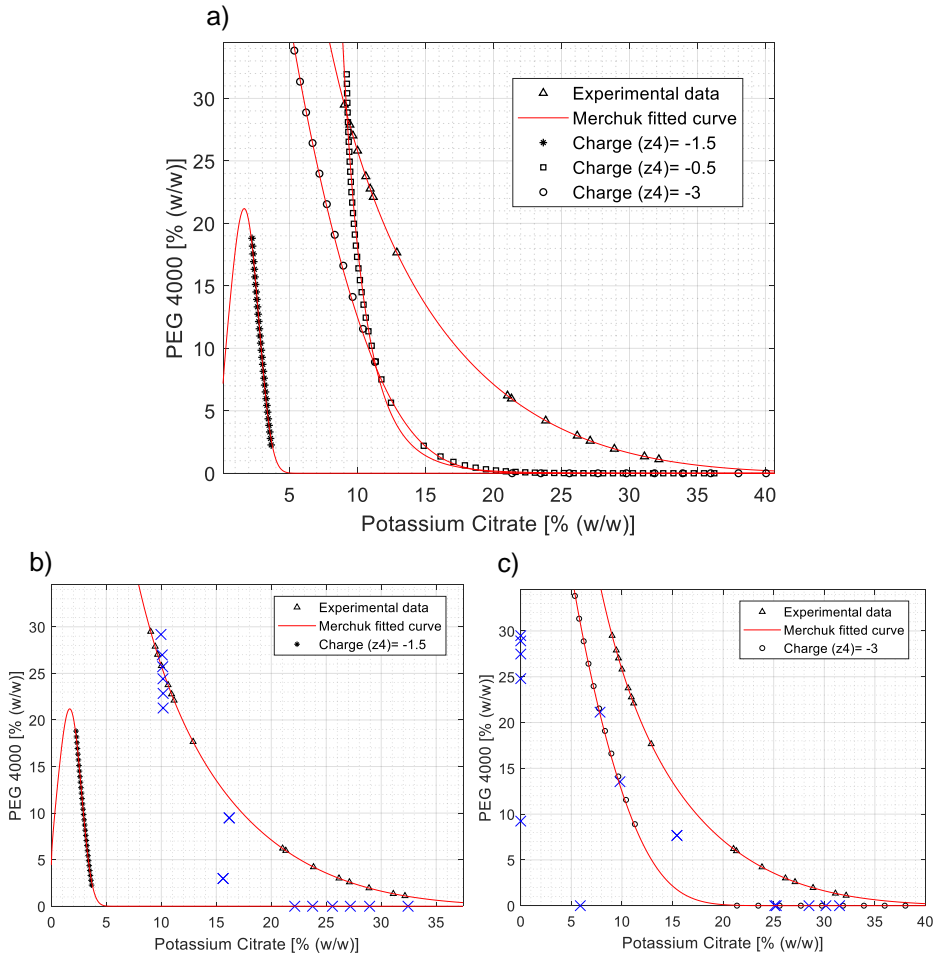


Figure 11: Influence of the charge on the phase separation according to FH theory, for the system composed by Potassium citrate and PEG 4000. For each charge selection ( $z_4$ ), the interchange energies were fitted according to the reconciliation approach (Method B, Table 1). The subplots b and c show the fitted points of the model ('postulated' fractions), in blue crosses. R and T have the values of 8.3144 J/K/mol and 313.12 K, respectively.

## A critical assessment of the Flory-Huggins (FH) theory

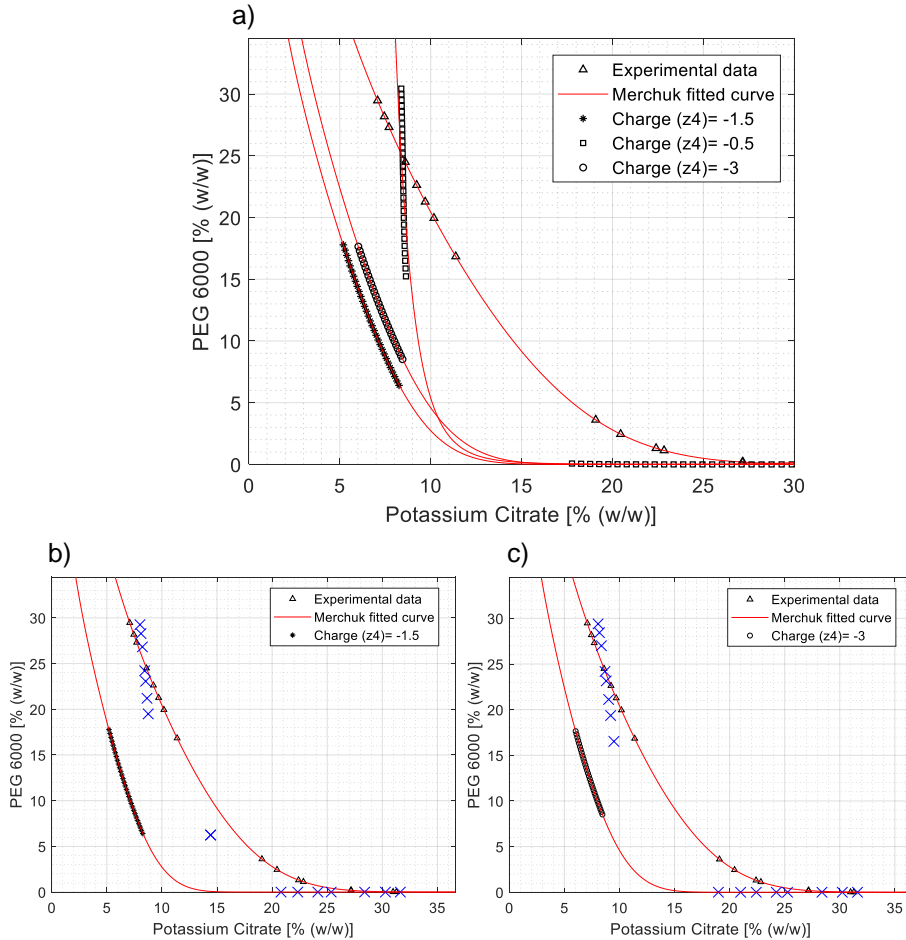


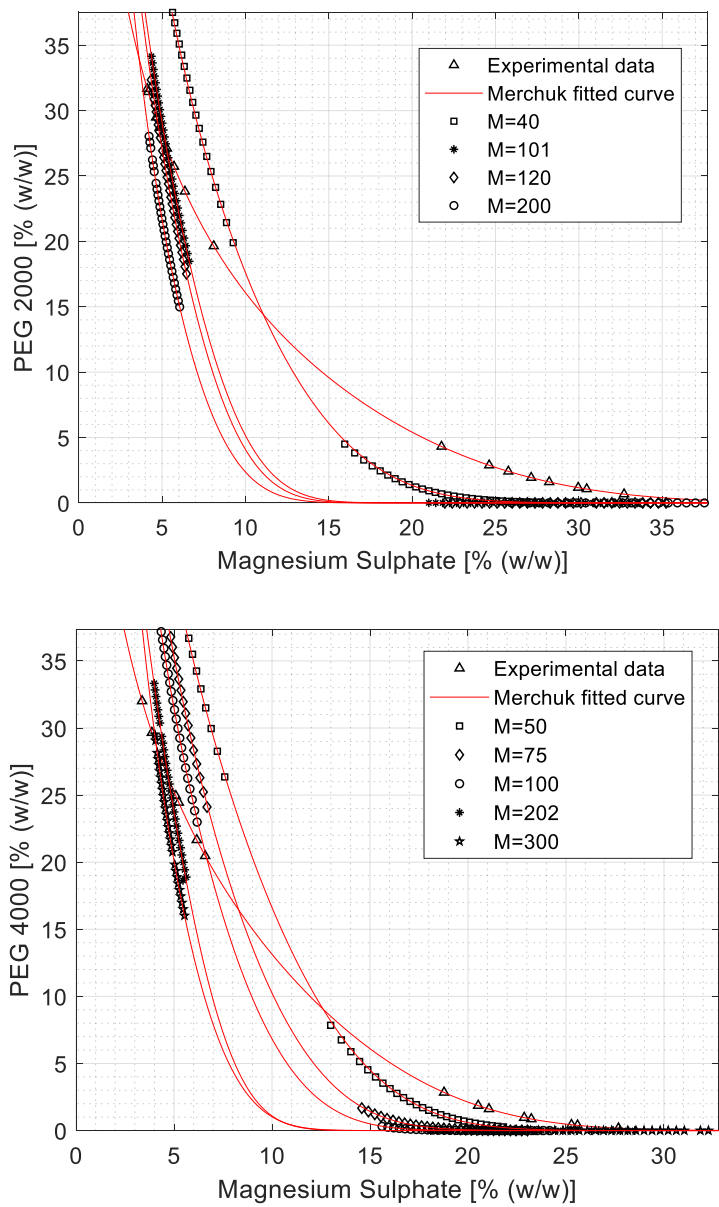
Figure 12: Influence of the charge on the phase separation according to FH theory, for the system composed by Potassium citrate and PEG 6000. For each charge selection ( $z_4$ ), the interchange energies were fitted according to the reconciliation approach (Method B, Table 1). The subplots b and c show the fitted points of the model ('postulated' fractions), in blue crosses. R and T have the values of 8.3144 J/K/mol and 313.12 K, respectively.

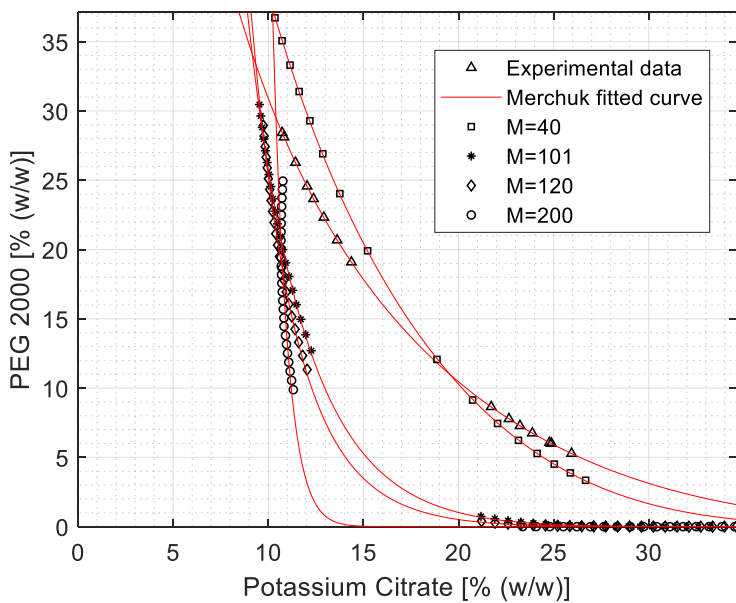
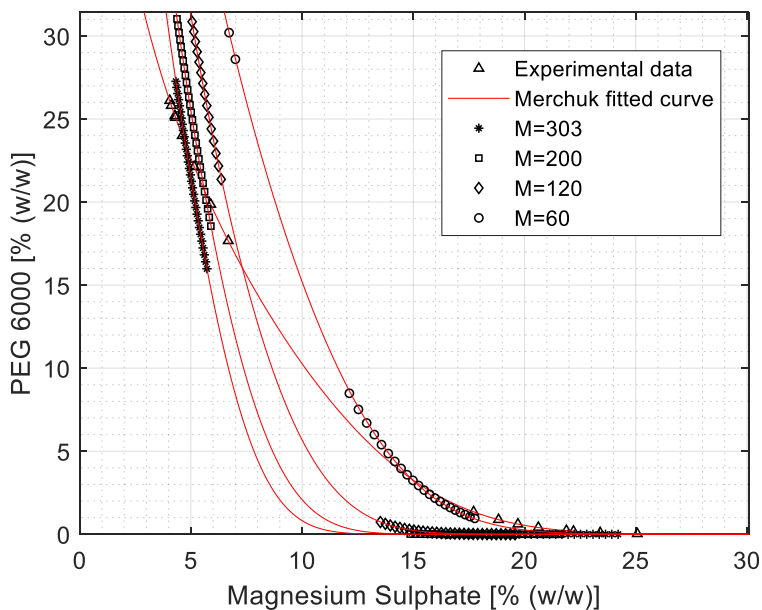
The degree of polymerization is a measure of the molecular size expressed in units of molar volume of water (18 cm<sup>3</sup>/mol). The molar volume of the polymer considers the molecular weight of the molecule, molar volume of every monomer calculated by software material studios and the ratio of monomers [25]. Due to the theoretical assessment of the degree of polymerization, we based our selection on literature indication [20]. Sensitivity analysis showed that the indicated degree of

polymerization should be reduced by approximately 60% (Figure 13). This applies for both salts studied. Applying a group contribution method to defined the molar volume of PEG 4000, its degree of polymerization would be approximately 104 [11]. The correction on the degree of polymerization produced binodal curves based on FH theory closer to the experimental ones. However, the shape of these curves still differs between each other, corroborating the hypothesis that FH model is not a proper quantitative description of phase separation in polymer-based ATPS, being restricted to predict trends (qualitative application).

Even though the FH mean-field theory cannot qualitatively predict the phase behaviour in ATPS, trends can be predicted by evaluating the contribution of the dominant energetics (entropy and enthalpy) to the system. By analysing the Gibbs free energy after mixing, it is possible to estimate whether the system separated to top and bottom phases. In comparison to a monophasic system, a two-phase system presents lower values for the Gibbs free energy (the repulsive intermolecular interaction overcompensates the favourable entropy of mixing). Although the combinatorial entropy  $\Delta S_{mix}$ , defined by Equation 2, predicts only positive values,  $\Delta S_{mix}$  decreases with increasing degree of polymerization. This means that longer molecules favours demixing (aqueous two-phase system formation). This behaviour is demonstrated by the experimental data and calculated curves in Figure 4. Moreover, the model developed here can also predict the same trends when fixing the  $w_{ij}$  and varying the size component of the polymer (represented by the molecular weight and the degree of polymerization) (Figure 14).

A critical assessment of the Flory-Huggins (FH) theory





## A critical assessment of the Flory-Huggins (FH) theory

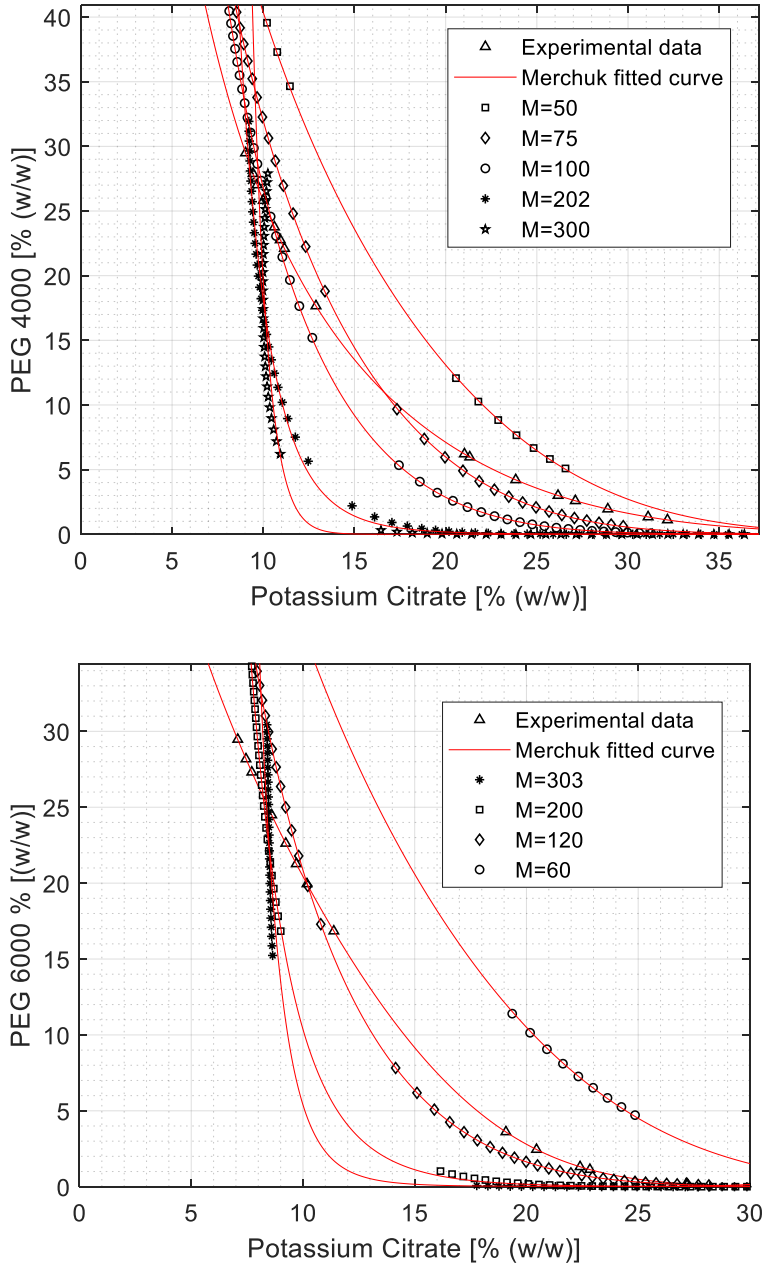


Figure 13: Influence of the degree of polymerization ( $M$ ) on the phase separation according to FH theory, for the systems composed by PEG 2000, 4000 or 6000, in combination with each of the salts magnesium sulphate or potassium citrate. The interchange energies ( $w_{ij}$ ) were fitted considering the  $M$  presented in Table 3 and according to the reconciliation

approach (Method B, Table 1). The simulations were performed by varying exclusively the  $M$  and calculating the phase separation.  $R$  and  $T$  have the values of 8.3144 J/K/mol and 313.12 K, respectively.

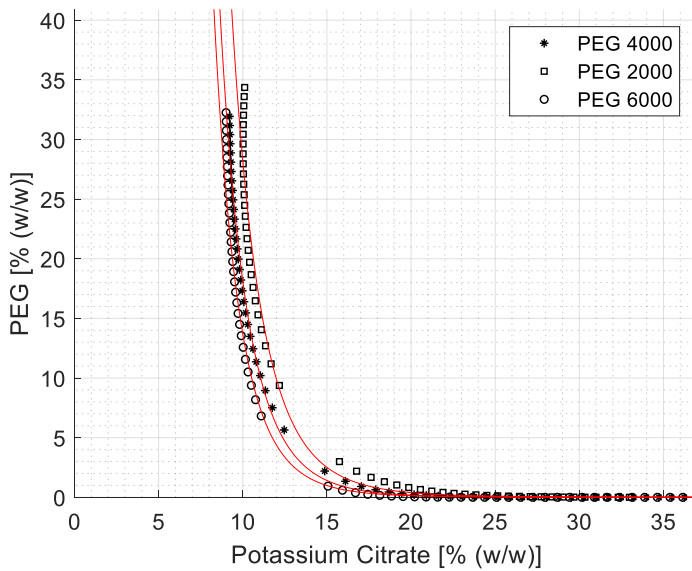
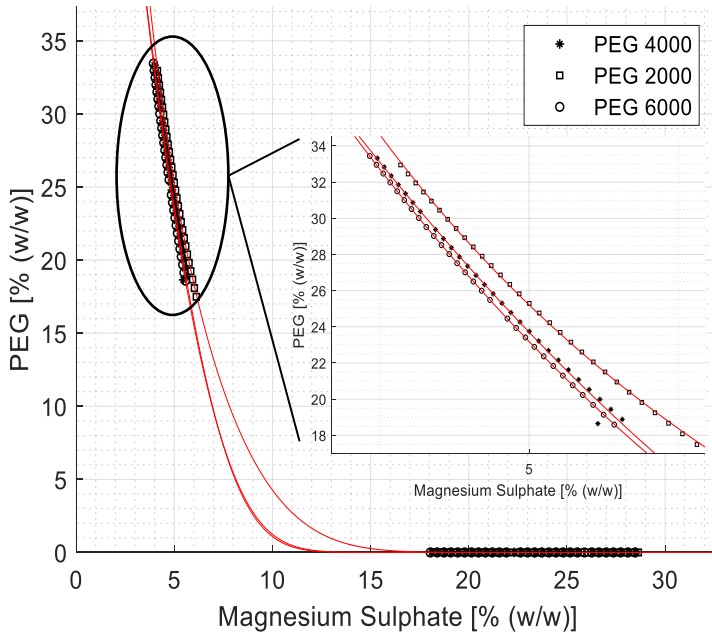


Figure 14: FH model predicts the trend of decrease in monophasic region with increasing the polymer size. The  $w_{ij}$  ( $w_{ij}$ ) were fitted considering the system composed by PEG 4000 and according to the reconciliation approach (Method B, Table 1). The simulations were performed by varying the component size ( $M$  and  $Mw$ ) of the polymer.  $R$  and  $T$  have the values of 8.3144 J/K/mol and 313.12 K, respectively.

The size of the monophasic region of the ATPS is influenced by the hydrophobicity of the anion. An increase in the hydrophobicity of the anion reduces the monophasic region [20]. This trend is observed experimentally, and also by the FH calculated curves. In Figure 15, this is demonstrated for systems composed by both salts and PEG 2000. The same pattern follows for systems containing PEG 4000 and PEG 6000 (data not shown). However, this trend prediction could be bias, once the interaction parameters were regressed considering the experimental data already presenting such a trend. ePC-SAFT can predict ATPS for which no experimental data is given [14]. This capability is mainly assigned to the ion specific parameters. Even though FH applies ion specific interaction parameters, the transferability to other systems were not assessed at this work.

Not only the hydrophobicity of the anion, but also the salting-out power can determine the effectiveness of the ion in forming an aqueous two-phase system. When salts formed by the same cation are compared, the ability to form two phase systems rises with the increase in the valence of the anion [12], because higher valence anions are less hydrated. The salting-out characteristic of the salt is related to the effective volume this component can exclude. However, among the salts analysed here (magnesium sulphate and potassium citrate), the salting-out effect is higher for the sulphate-based salt, even though its valence is lower than the citrate anion. Contrarily to the experimental observation, Sadeghi and Jahani [27] reported a higher effectiveness in salting-out the polymer for the anion citrate than sulphate. In terms of the cation, magnesium showed in our experiment to be more effective than potassium to promote phase separation. This salting-out ability of  $Mg^{2+}$  in comparison to  $K^+$  follows the Hofmeister series and is also observed for ATPS composed by other components than polymer and salts (e.g. ionic liquids and salts)



[26]. This suggests that the cations of these salts also contribute to the phase separation, let alone the anion hydrophobicity mentioned above.

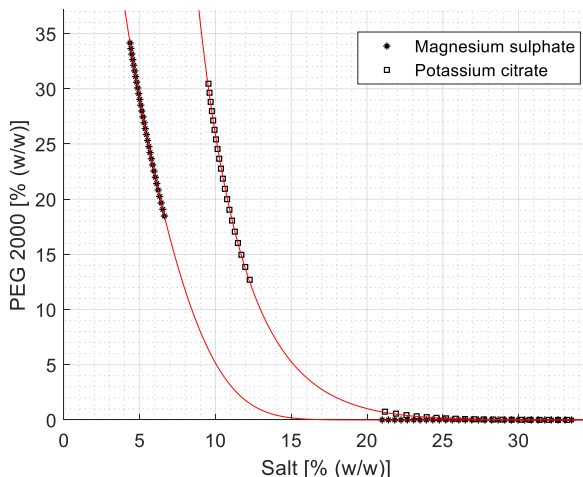


Figure 15: Influence of the salt type on the phase separation. Binodal curves calculated considering the interchange energies ( $w_{ij}$ ) fitted according to the reconciliation approach (Method B, Table 1). R and T have the values of 8.3144 J/K/mol and 313.12 K, respectively.

#### 4. Conclusion

The ATPS formation is susceptible to parameters definition, such as polymer molecular weight and salt type. The mathematical framework suggested by this work, based on the FH thermodynamic model, can be used to perform sensitivity analysis on these parameters, based on predictable trends of phase separation. The algorithm is composed of two steps: estimation of the pair-wise interchange energies and calculation of phase compositions. The thermodynamic modelling of phase separation according to FH theory and applied to polymer-salt ATPS should consider the phase-forming salt as a single (undissociated) molecule in order to satisfy the chemical equilibrium for all the components in the system. Here, we also disclosed a mathematical way of determining the FH interaction parameters based on experimental data. These parameters are not straightforward obtained in literature or by experiments, and this computational approach can boost the application of FH mean-field model to predict phase separation. However, FH interaction parameters

should not be determined purely based on experimental binodal curves, since our results show a non-uniqueness solution. Moreover, the uncertainty in data strongly influences the estimation of the interchange energies. Our analysis on published models and the poor approximation to experimental results obtained by the algorithm sustains the statement that FH model is not an exact description of phase separation in salt based ATPS.

### **Acknowledgement**

This work was supported by the Foundation for Research of State of Sao Paulo, Brazil [grant numbers 2015/20630-4, 2016/04749-4, 2016/06142-0 and BEPE 2016/21951-1]; and the BE-Basic Foundation, The Netherlands. This research was carried out during a Dual Degree PhD program under agreement between UNICAMP and TU Delft.

### **References**

- [1] M. Iqbal, Y. Tao, S. Xie, Y. Zhu, D. Chen, X. Wang, L. Huang, D. Peng, A. Sattar, M.A.B. Shabbir, H.I. Hussain, S. Ahmed, Z. Yuan, Aqueous two-phase system (ATPS): an overview and advances in its applications, *Biol. Proced. Online*. 18 (2016) 18. doi:10.1186/s12575-016-0048-8.
- [2] B.M. Khan, K. Cheong, Y. Liu, ATPS: “Aqueous two-phase system” as the “answer to protein separation” for protein-processing food industry, *Crit. Rev. Food Sci. Nutr.* 59 (2019) 3165–3178. doi:10.1080/10408398.2018.1486283.
- [3] N. Sun, H. Liu, N. Sathitsuksanoh, V. Stavila, M. Sawant, A. Bonito, K. Tran, A. George, K.L. Sale, S. Singh, B. a Simmons, B.M. Holmes, Production and extraction of sugars from switchgrass hydrolyzed in ionic liquids., *Biotechnol. Biofuels*. 6 (2013) 39. doi:10.1186/1754-6834-6-39.
- [4] T.H. Russell, B.J. Edwards, B. Khomami, Characterization of the Flory-Huggins interaction parameter of polymer thermodynamics, *EPL (Europhysics Lett)*. 108 (2014) 66003. doi:10.1209/0295-5075/108/66003.

- [5] M.M. Ahmad, T.M. Przybycien, Towards optimal aqueous two-phase extraction system flowsheets for protein purification, *J. Chem. Technol. Biotechnol.* 88 (2013) 62–71. doi:10.1002/jctb.3858.
- [6] H. Cabezas, Theory of phase formation in aqueous two-phase systems, *J. Chromatogr. B Biomed. Sci. Appl.* 680 (1996) 3–30. doi:10.1016/0378-4347(96)00042-4.
- [7] N.P. Young, N.P. Balsara, Flory–Huggins Equation, in: S. Kobayashi, K. Müllen (Eds.), *Encycl. Polym. Nanomater.*, Springer Berlin Heidelberg, Berlin, Heidelberg, 2014: pp. 1–7. doi:10.1007/978-3-642-36199-9\_79-1.
- [8] D. Kozuch, W. Zhang, S. Milner, Predicting the Flory-Huggins  $\chi$  Parameter for Polymers with Stiffness Mismatch from Molecular Dynamics Simulations, *Polymers (Basel)*. 8 (2016) 241. doi:10.3390/polym8060241.
- [9] H.O. Johansson, G. Karlström, F. Tjerneld, C.A. Haynes, Driving forces for phase separation and partitioning in aqueous two- phase systems, *J. Chromatogr. B Biomed. Appl.* 711 (1998) 3–17. doi:10.1016/S0378-4347(97)00585-9.
- [10] M.T. Zafarani-Moattar, R. Sadeghi, A.A. Hamidi, Liquid-liquid equilibria of an aqueous two-phase system containing polyethylene glycol and sodium citrate: Experiment and correlation, *Fluid Phase Equilib.* 219 (2004) 149–155. doi:10.1016/j.fluid.2004.01.028.
- [11] M. Foroutan, M. Zarrabi, Quaternary (liquid + liquid) equilibria of aqueous two-phase polyethylene glycol, poly-N-vinylcaprolactam, and  $\text{KH}_2\text{PO}_4$ : Experimental and the generalized Flory-Huggins theory, *J. Chem. Thermodyn.* 40 (2008) 935–941. doi:10.1016/j.jct.2008.01.026.
- [12] Y. Lu, T. Hao, Y. Zhou, J. Han, Z. Tan, Y. Yan, Aqueous two-phase systems of polyoxyethylene lauryl ether and potassium gluconate/potassium oxalate/potassium citrate at different temperature-experimental results and modeling of (liquid+liquid) equilibrium data, *J. Chem. Thermodyn.* 71 (2014) 137–147. doi:10.1016/j.jct.2013.12.005.

- [13] T. Reschke, C. Brandebusch, G. Sadowski, Modeling aqueous two-phase systems : III . Polymers and organic salts as ATPS former, *Fluid Phase Equilib.* 387 (2015) 178–189. doi:10.1016/j.fluid.2014.12.011.
- [14] T. Reschke, C. Brandebusch, G. Sadowski, Modeling aqueous two-phase systems: I. Polyethylene glycol and inorganic salts as ATPS former, *Fluid Phase Equilib.* 368 (2014) 91–103. doi:10.1016/j.fluid.2014.02.016.
- [15] P.J. Flory, Thermodynamics of High Polymer Solutions, *J. Chem. Phys.* 10 (1942) 51–61. doi:10.1063/1.1723621.
- [16] M.L. Huggins, Solutions of Long Chain Compounds, *J. Chem. Phys.* 9 (1941) 440–440. doi:10.1063/1.1750930.
- [17] J.M. Prausnitz, R.N. Lichtenthaler, E.G. de Azevedo, *Molecular Thermodynamics of Fluid-Phase Equilibria*, Third Edit, 1986. [http://www.researchgate.net/publication/31750544\\_Molecular\\_Thermodynamics\\_of\\_Fluid-Phase\\_Equilibria\\_\\_J.M.\\_Prausnitz\\_R.N.\\_Lichtenthaler\\_E.\\_Gomes\\_de\\_Azevedo](http://www.researchgate.net/publication/31750544_Molecular_Thermodynamics_of_Fluid-Phase_Equilibria__J.M._Prausnitz_R.N._Lichtenthaler_E._Gomes_de_Azevedo).
- [18] U. Von, *Molecular Thermodynamics of Partitioning in Aqueous Two-Phase Systems*, in: U. von Stockar (Ed.), *Biothermodynamics*, First, 2013.
- [19] J.C. Merchuk, B.A. Andrews, J.A. Asenjo, Aqueous two-phase systems for protein separation Studies on phase inversion, *J. Chromatogr. B.* 711 (1998) 285–293. [http://ac.els-cdn.com/S037843479700594X/1-s2.0-S037843479700594X-main.pdf?\\_tid=eb4d5a4e-5cba-11e7-b31b-00000aacb361&acdnt=1498734534\\_3252589c829f1510402c647b25c7bf59](http://ac.els-cdn.com/S037843479700594X/1-s2.0-S037843479700594X-main.pdf?_tid=eb4d5a4e-5cba-11e7-b31b-00000aacb361&acdnt=1498734534_3252589c829f1510402c647b25c7bf59) (accessed June 29, 2017).
- [20] H.-O. Johansson, E. Feitosa, A.P. Junior, Phase Diagrams of the Aqueous Two-Phase Systems of Poly(ethylene glycol)/Sodium Polyacrylate/Salts, *Polymers (Basel)*. 3 (2011) 587–601. doi:10.3390/polym3010587.

- [21] M.M. Ahmad, S. Hauan, T.M. Przybycien, Flowsheet simulation of aqueous two-phase extraction systems for protein purification, *J. Chem. Technol. Biotechnol.* 85 (2010) 1575–1587. doi:10.1002/jctb.2469.
- [22] B.C. Bussamra, J. Castro Gomes, S. Freitas, S.I. Mussatto, A. Carvalho da Costa, L. van der Wielen, M. Ottens, A robotic platform to screen aqueous two-phase systems for overcoming inhibition in enzymatic reactions, *Bioresour. Technol.* 280 (2019) 37–50. doi:10.1016/j.biortech.2019.01.136.
- [23] M. González-Amado, O. Rodríguez, A. Soto, P. Carbonell-Hermida, M.D.M. Olaya, A. Marcilla, Aqueous Two-Phase Systems: A Correlation Analysis, *Ind. Eng. Chem. Res.* 59 (2020) 6318–6328. doi:10.1021/acs.iecr.9b06078.
- [24] E. Favre, Q.T. Nguyen, R. Clement, J. Neel, Application of Flory-Huggins theory to ternary polymer-solvents equilibria: A case study, *Eur. Polym. J.* 32 (1996) 303–309. doi:10.1016/0014-3057(95)00146-8.
- [25] B. Yan, X. Cao, Phase diagram of novel recycling aqueous two-phase systems composed of two pH-response polymers: Experiment and modeling, *Fluid Phase Equilib.* 364 (2014) 42–47. doi:10.1016/j.fluid.2013.11.037.
- [26] M.G. Freire, A.F.M. Cláudio, J.M.M. Araújo, J. a. P. Coutinho, I.M. Marrucho, J.N.C. Lopes, L.P.N. Rebelo, Aqueous biphasic systems: a boost brought about by using ionic liquids, *Chem. Soc. Rev.* 41 (2012) 4966. doi:10.1039/c2cs35151j.
- [27] R. Sadeghi, F. Jahani, Salting-in and salting-out of water-soluble polymers in aqueous salt solutions, *J. Phys. Chem. B.* 116 (2012) 5234–5241. doi:10.1021/jp300665b.



## CHAPTER 4

### Enzymatic hydrolysis of sugarcane bagasse in aqueous two-phase systems (ATPS): exploration and conceptual process design \*

Bianca Consorti Bussamra<sup>1, 2</sup>, Paulus Meerman<sup>1</sup>, Vidhvath Viswanathan<sup>1</sup>, Solange I. Mussatto<sup>3</sup>, Aline Carvalho da Costa<sup>2</sup>, Luuk van der Wielen<sup>1, 4</sup>, Marcel Ottens<sup>1</sup>

<sup>1</sup>Department of Biotechnology, Delft University of Technology. Van der Maasweg 9, 2629HZ. Delft, The Netherlands.

<sup>2</sup>Development of Processes and Products (DDPP), University of Campinas. Av. Albert Einstein, 500. Post Code: 6066. Campinas, Brazil.

<sup>3</sup>Novo Nordisk Foundation Center for Biosustainability, Technical University of Denmark. Kemitorvet, Building 220. 2800, Kongens Lyngby, Denmark.

<sup>4</sup>Bernal Institute, University of Limerick. Castletroy. Limerick, Ireland.

---

\*This Chapter has been published as: **Bussamra, B.C.**, Meerman, P., Viswanathan, V., Mussatto, S.I., Carvalho da Costa, A., van der Wielen, L., Ottens, M., 2020. *Frontiers in Chemistry* 8, 1–15.  
<https://doi.org/10.3389/fchem.2020.00587>

### **Abstract**

The enzymatic conversion of lignocellulosic material to sugars can provide a carbon source for the production of energy (fuels) and a wide range of renewable products. However, the efficiency of this conversion is impaired due to product (sugar) inhibition. Even though several studies investigate how to overcome this challenge, concepts on the process to conduct the hydrolysis are still scarce in literature. Aqueous two-phase systems (ATPS) can be applied to design an extractive reaction, due to their capacity to partition solutes to different phases in such a system. This work presents strategies on how to conduct extractive enzymatic hydrolysis in ATPS and how to explore the experimental results in order to design a feasible process. While only a limited number of ATPS was explored, the methods and strategies described could easily be applied to any further ATPS to be explored. We studied two promising ATPS, as a subset of a previously high throughput screened large set of ATPS, providing two configurations of processes, having either the reaction in the top phase or in the bottom phase. Enzymatic hydrolysis in these ATPS was performed to evaluate the partitioning of the substrate and the influence of solute partitioning on conversion. Because ATPS are able to partition inhibitors (sugar) between the phases, the conversion rate can be maintained. However, phase forming components should be selected to preserve the enzymatic activity. The experimental results presented here contribute to a feasible ATPS-based conceptual process design for the enzymatic conversion of lignocellulosic material.

**Keywords:** sugarcane bagasse, product inhibition, enzymatic hydrolysis, extractive process, aqueous two-phase systems (ATPS).



## 1. Introduction

The search for alternatives to replace fossil fuels by renewable energy has been seen as a major necessity from now on (Passoth and Sandgren, 2019). In order to reach the requirements established by the Paris Agreement in 2017, net-zero greenhouse gases emission must be achieved by 2050 (Pye et al., 2017). Sun, wind and lignocellulosic residues can be sources of renewable energy (Goldemberg and Teixeira Coelho, 2004). However, different from wind and solar energy, biomass (lignocellulosic residues) can provide a carbon source not only for energy (fuels) production, but also for the production of a wide range of renewable products (Straathof, 2014). Sugarcane bagasse is the most abundant lignocellulosic residue in the Brazilian agriculture. Among the 1.8 billion tonnes of sugarcane processed annually in the world, Brazil is the first producer, holding 41% of the world production. This amount yields approximately 105 million tons of the residue (sugarcane bagasse) per year (UN Food and Agriculture Organization, 2017).

The enzymatic conversion of sugarcane bagasse to obtain monomers of glucose, usually presents a limited efficiency as a consequence of several factors, such as the cellulose crystallinity, product inhibition and enzyme degradation (Gupta et al., 2016). There are several research lines cooperating to improve the utilization of lignocellulose as a raw material to the production of biofuel and chemicals. Pre-treatment of the biomass is necessary to expose the cellulose component to the cellulases. In order to establish a good balance between the decrease of the biomass recalcitrance to enzymatic hydrolysis and disadvantages of each pre-treatment, several types of processes have been investigated: physicochemical, chemical using acids and alkalis, and solvent extraction (Liu et al., 2019). Biological pre-treatments have been proposed as an alternative to chemical ones, mainly because of the reduction of toxic compounds and fermentation inhibitors generation (Sindhu et al., 2016), and improvement in the subsequent enzymatic hydrolysis (Singh et al., 2016; Vaidya and Singh, 2012). The inhibition on cell growth and metabolism, which leads to reduction of product of interest formation in fermentation, can be caused by substances present in the own plant composition, or released during pre-treatment and/or hydrolysis processes. Among many strategies to mitigate this product-

induced inhibition of microbes, studies highlight the use of stabilizing substances and conditions, stream selection and product removal (Cray et al., 2015). In the spectrum of the biocatalysis, the enzyme degradation can be related, for instance, to chemical reaction with lignin (Newman et al., 2013). The development of new biocatalysts, such as accessory enzymes, and use of additives (Vaidya et al., 2014; Donaldson et al., 2014; Fahmy et al., 2019) have been identified as potential fields to promote more efficient and tolerant enzymatic reactions. Moreover, the synergy of fungal enzymes and the design of rational cocktails have provided improved hydrolysis performance (Gupta et al., 2016; Bussamra et al., 2015; Cameron et al., 2015). However, few studies question the conventional process to conduct the enzymatic hydrolysis of cellulose to monomers, e.g. the optimization of reaction conditions, reactor design, enzyme recycling and recovery strategies. The main drawback regarding the enzymatic hydrolysis is the product inhibition of the enzymes (Gupta et al., 2016; Bezerra and Dias, 2005). In other words, the higher the glucose concentration, the least efficient the process is. By addressing this need, a more efficient enzymatic hydrolysis could be performed, reducing the costs of the process, enhancing the yield, and contributing to establish biomass as feedstock for the production of renewables.

In order to overcome the challenge of product inhibition during enzymatic hydrolysis, some solutions have been suggested in literature, including: simultaneous saccharification and fermentation (SSF) (Mohagheghi et al., 1992), development of glucose tolerant enzymes (Cao et al., 2015), partial cellulose hydrolysis (direct use of lignocellulose-derived sugars by the microorganisms) (Chen, 2015) and *in-situ* product removal (Hahn-Hägerdal et al., 1981; Yang et al., 2011). Extractives processes such as SSF indicates a positive effect on cellulose hydrolysis, because the inhibition by ethanol is less harmful to enzymes than the one caused by cellobiose (Bezerra and Dias, 2005). However, ethanol inhibition still exposes a potential problem in the SSF (Wu and Lee, 1997). In order to remove the inhibitor, ATPS can be applied as a strategy to separate the product and the enzymes. ATPS are formed by two immiscible components dissolved in water (Benavides et al., 2011). These components, named as phase forming components (PFC), can be

polymers, salts (Van Sonsbeek et al., 1993), or ionic liquids (Freire et al., 2012). Above a critical concentration of the PFC, the system presents two phases, in which molecules (solutes) can be unevenly partitioned in accordance to the system composition (Baskir et al., 1989).

Even though extractive processes based on *in-situ* product removal have been extensively applied to enzymatic reactions (Ferreira et al., 2018) and/or fermentation (Hahn-Hägerdal et al., 1981); Kulkarni et al., 1999), to the extent of our knowledge, enzymatic hydrolysis in biphasic systems composed by salt-polymer is still rarely reported. This work aims to unlock the potential of a novel and extractive process to conduct the enzymatic hydrolysis of lignocellulosic materials. In this study, we evaluated the efficiency of performing the extractive reaction by ATPS composed by polyethylene glycol and the salts potassium citrate and magnesium sulphate. In the referred systems, glucose and the reactive phase (bagasse and enzymes) can be separated to prevent product (glucose) inhibition. Moreover, we showed how experimental results at lab scale and parameters of the process are interconnected, providing information on technical conditions to further design a new industrial process for lignocellulosic conversion.

## **2. Methods**

### **2.1. Research design**

In this work, the enzymatic hydrolysis of sugarcane bagasse in ATPS was explored and two processes were designed. According to the partitioning of bagasse and solutes in the phases, the reaction and extractive phases can alter. Based on that, two approaches were discussed: hydrolysis occurring in the bottom phase (Figure 1a) and in the top phase (Figure 1b). The process design for each approach was developed according to experimental data and literature evidences. However, the quantitative evaluation of each unit of operation is out of the scope of this work.

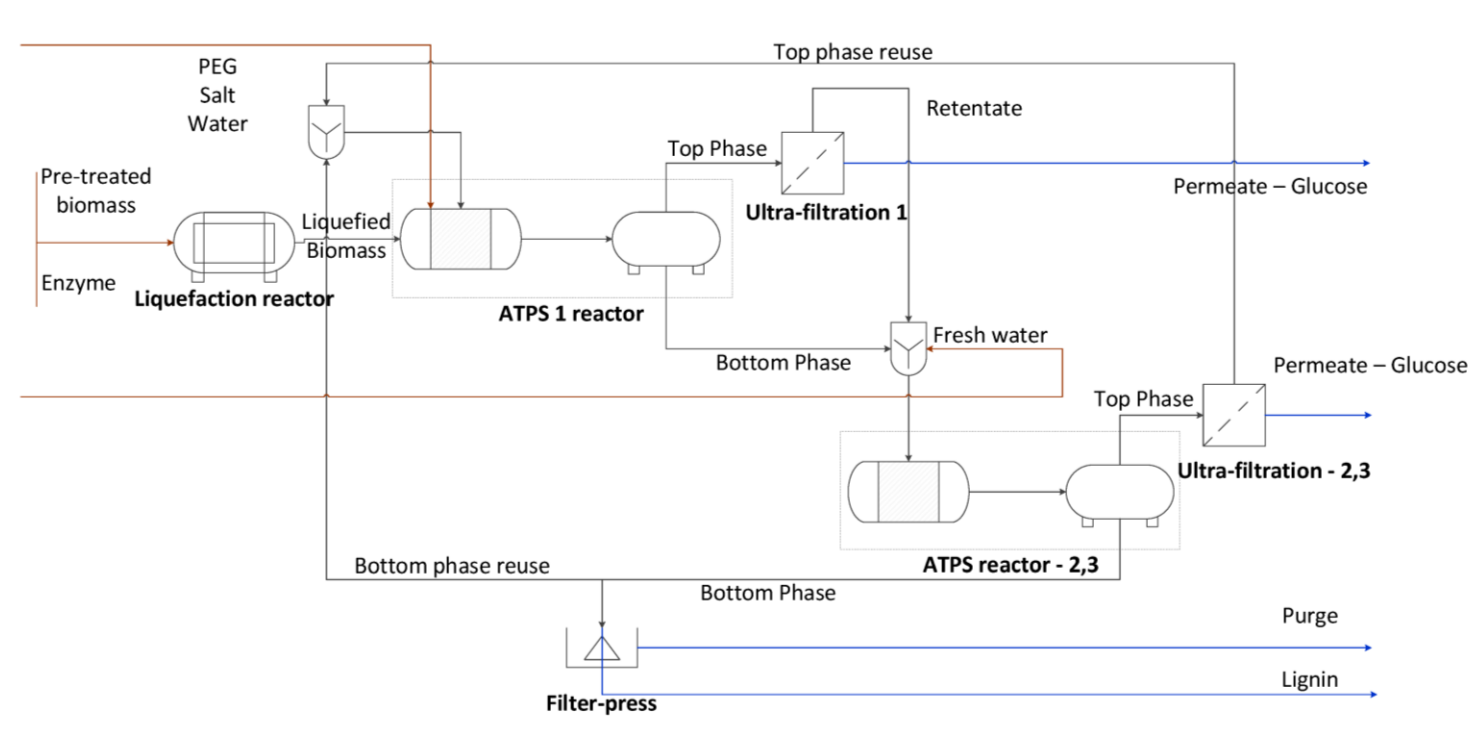
Experimental data provided information for the design of ATPS reactor and ultrafiltration unit operations. The linkage between the experimental results and their usage into the process design is presented in Table 1. The strategy suggested for

## Enzymatic hydrolysis of sugarcane bagasse in ATPS

sugar recovery was based on literature evidences. The findings regarding the behaviour of sugarcane bagasse hydrolysis in ATPS, connected to the potential of system components recycle, yielded insights on how feasible this extractive conversion could be.

The conversion of lignocellulosic biomass into sugars was catalysed by the enzymes presented in the commercial cocktail Cellic CTec 2 (Novozymes, Bagsværd, Denmark). In order to create the extractive environment, ATPS formed by polymer and salts were applied to conduct the reaction. In the explorative investigation of ATPS applied to lignocellulosic conversion, topics such as the adsorption of phase forming components to the bagasse fibres and the influence of enzyme load on the hydrolysis were approached. Sequentially, the potential of recycling the enzymes in a continuous process was evaluated, according to the distribution of specific enzymes among the phases and the adsorption of specific enzymatic activities to the bagasse. To complete the definition of parameters to further design the extractive process, the continuous recovery of sugar (glucose) from the system was theoretically analysed.

a)



## Enzymatic hydrolysis of sugarcane bagasse in ATPS

b)

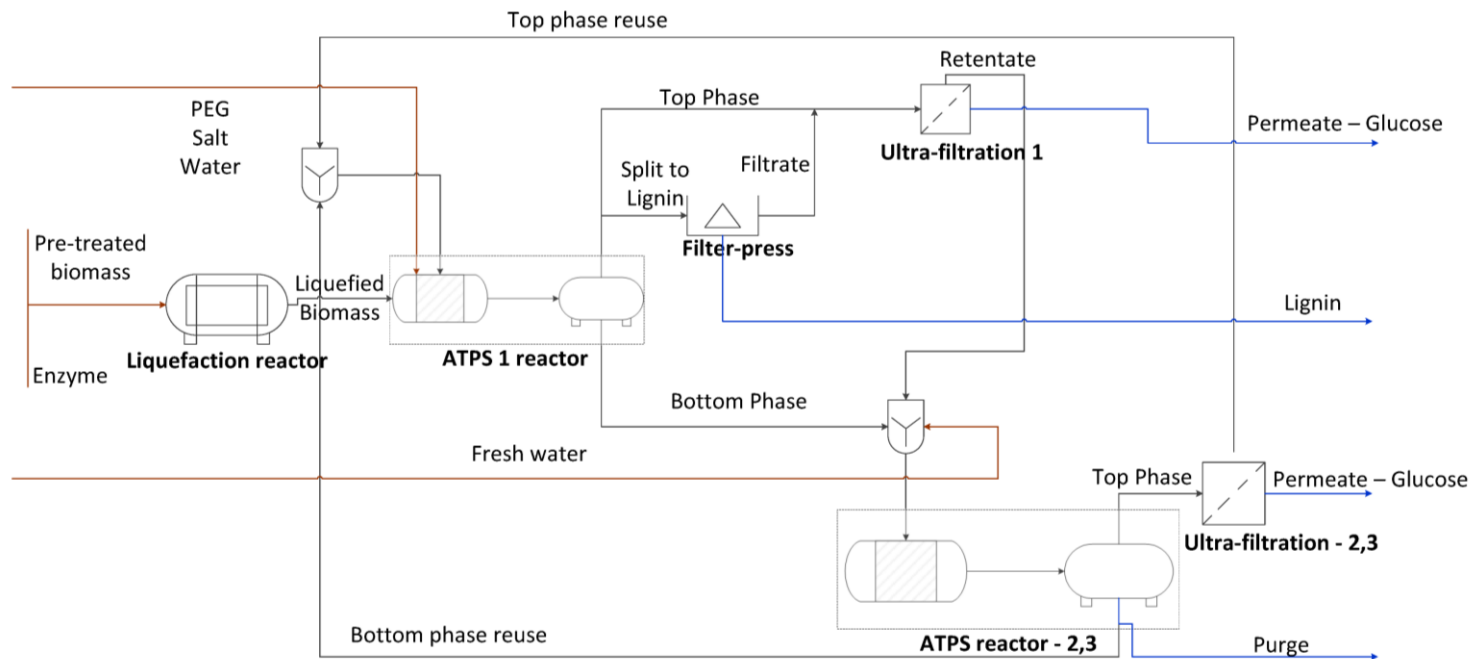


Figure 1 – Conceptual process design for a) hydrolysis in bottom phase (schematic representation of an ATPS process for magnesium sulphate and PEG 6000) or b) hydrolysis in top phase (schematic representation of an ATPS process for potassium citrate and PEG 6000). The numbers represent the how many cycles each unit of operation operates, which can vary for each ATPS and desired efficiency and recovery of the process. Considering an ATPS step with both mixing and separation compartments, two vessels are presented per ATPS unit operation.

Table 1 - Experiments performed to enable a reasonable process design parameters definition.

Experiment	Type of parameter to be defined and the respective unit of operation in the process design
Salt type and polymer molecular weight influence on bagasse partition	ATPS reactor: reaction phase (top or bottom)
Density of PFC before and after their adsorption to bagasse	ATPS reactor: addition mode of PFC to the bagasse
Enzymatic load influence on the concentration of free enzymes (not adsorbed) on conventional hydrolysis (kinetics) and specific enzymatic activities in the supernatant	Ultrafiltration: feasibility to recycle enzymes in terms of available amount of free proteins
TLL (tie line length), salt type and polymer molecular weight influence on the partitioning of proteins and sugars ( $K_s/K_p$ )	ATPS reactor: concentration of PFC in reaction
TLL and time of ATPS hydrolysis (kinetics) influence on sugar release	ATPS reactor: concentration of PFC and residence time of reaction

## Enzymatic hydrolysis of sugarcane bagasse in ATPS

Rate of enzymatic hydrolysis (conventional and ATPS)	ATPS reactor: feed (flow) rate of substrate in order to maintain constant water-insoluble substrate (WIS) in a continuous operation mode and to achieve the desired yield
Binodal curves and tie lines data	ATPS reactor: estimation of outlet concentrations of top and bottom phases given an inlet composition of ATPS
Partitioning of specific enzymatic classes in ATPS (top and bottom)	Ultrafiltration: feasibility to recycle enzymes in terms of enrichment of one specific enzymatic class in continuous operation



## 2.2. Materials

The Brazilian Biorenewables National Laboratory (LNBR) provided the sugarcane bagasse: hydrothermally pre-treated (at 190 °C, 10 min) followed by delignification (at 100 °C, 1 h, and 1% NaOH). Although the presence of lignin does not influence the decrease in conversion with increasing solid loads (Modenbach and Nokes, 2013), this bagasse treatment was selected due to the fact that lignin could interfere in the enzyme performance and, consequently, in the product inhibition study. The bagasse, composed by 79.2%  $\pm$  0.9 cellulose, 2.6%  $\pm$  0.1 hemicellulose, 12.6%  $\pm$  0.3 lignin and 6.2%  $\pm$  0.2 ash (composition determination as defined by Sluiter et al. (2016)), presented a wet basis humidity of 7.6% and was milled at 0.08 mm mesh. The milling process occurred at the speed of 104 rotations per minute (RPM) (Fritsch, Pulverisette 14).

Polyethylene glycol (PEG) with molar mass 2000 g/mol (PEG 2000) and 4000 g/mol (PEG 4000) were purchased from Merck (Darmstad, Germany). PEG 6000 (6000 g/mol) and magnesium sulphate heptahydrate ( $\text{MgSO}_4 \cdot 7\text{H}_2\text{O}$ ) were acquired from J.T. Baker (Fisher, New Jersey, USA). Sodium carbonate ( $\text{Na}_2\text{CO}_3$ ) and 3,5-Dinitrosalicylic acid (DNS), both used for enzymatic activities assays, anhydrous glucose and potassium citrate tribasic monohydrate ( $\text{K}_3\text{C}_6\text{H}_5\text{O}_7 \cdot \text{H}_2\text{O}$ ) were supplied by Sigma Aldrich (Taufkirchen, Germany). The pH was adjusted by adding sodium hydroxide (4 M) or hydrogen chloride, both purchased from Merck. Citrate buffer 50 mM was prepared according to Adney and Baker (2008).

Stock solutions were prepared by dissolving the respective PEG molecular weight or salt in double distilled deionized water (Milli-Q water), in order to obtain the following stock solutions: 38% w/w PEG 2000, 40% w/w PEG 4000, 39% w/w PEG 6000 and 40% w/w magnesium sulphate or potassium citrate solutions.

## 2.3. ATPS formation (equilibrium and separation)

The selection of ATPS composition (salt type and polymer molecular weight) and concentration (tie line length - TLL) were based on data previously published by

Bussamra et al. (2019). The ATPS, respective TLL, experiment to which they were applied and motivation are presented in Table 2.

Table 2 – Connection of the selected ATPS to respective application in experiments.

System	Phase forming components	TLL (%)	Experiment	Motivation
ATPS 1	Potassium citrate and PEG 2000	12.8	Glucose and protein partition	Low TLL, less inhibition of enzymes by PFC. Less viscous system compared to PEG 6000. Lowest TLL reported by Bussamra et al. (2019) for this system composition. Enzymes could be more active compared to ATPS 3.
ATPS 2	Potassium citrate and PEG 6000	15.3	Glucose and protein partition; Hydrolysis kinetics	High $K_{sugar}$ . Enzymes could be more active compared to ATPS 5 (ATPS 4 is less concentrated and less viscous).
ATPS 3	Potassium citrate and PEG 6000	23.7	Glucose and protein partition	High sugar selectivity ( $K_{sugar}/K_{protein}$ ). Lowest TLL to provide high $K_{protein}$ (Bussamra et al., 2019).
ATPS 4	Magnesium sulphate and PEG 2000	20.5	Glucose and protein partition	
ATPS 5	Magnesium sulphate and PEG 6000	30.5	Glucose and protein partition; Hydrolysis kinetics	
ATPS 6	Potassium citrate and PEG 6000	34.2	Liquefaction following hydrolysis	

The ATPS 1 to 5 were evaluated for the partitioning of glucose and proteins, at a fixed concentration of each solute and without the presence of substrate. Because ATPS 6 was not favourable to conduct hydrolysis, the partitioning of solutes was not evaluated at this composition. Systems were formed by addition of the required amount of PEG and salt stock solutions to an aqueous solution of 5 mL total volume. Sugar stock solution (800g/L, prepared in Milli-Q water) was added to a final concentration of 90 g/L in the system. The volume of enzymes (29.5  $\mu$ L) was calculated considering a hypothetical solid load of 10% WIS and an enzyme load of 10 FPU/g bagasse. This amount of enzymatic cocktail corresponded to a protein concentration of approximately 0.92 mg/mL. The systems were incubated for 1h at 50 °C and 250 rpm, in orbital shaker. Phase separation was promoted by centrifugation at 4000 rpm, 40 °C, for 30 min (Eppendorf 5810R Multipurpose Centrifuge®). Top phase was withdrawn using an automatic pipet, while bottom phase via 2 mL syringe coupled with appropriated needle. All systems were prepared in duplicates. The partition coefficient in a two-phase system was determined as the ratio of solute concentration in the top phase to that in the bottom phase (Li et al., 2002).

#### **2.4. Adsorption of phase forming components to sugarcane bagasse**

Predetermined amounts of bagasse (5% WIS) were emerged for 3 h at 250 rpm and 50 °C in four different solutions of phase-forming components (final volume 15 mL): magnesium sulphate (40% w/w), potassium citrate (40%w/w), PEG4000 (40% w/w) and Milli-Q water. Subsequently, the samples were centrifuged at 1300 rpm, 40 °C, for 30 min (Eppendorf 5810R Multipurpose Centrifuge®). The bagasse was separated from the supernatant and the wet basis humidity was determined using a moisture balance (Sartorius Ma35). The density of both the stock solutions of phase forming components and the supernatant liquids were measured using a pycnometer of 5.113 cm<sup>3</sup> (Blaubrand, Germany). The comparison in density of both solutions (stock and supernatant) indicates whether there is a preferential adsorption of phase forming components to sugarcane bagasse in relation to water (for instance, a less concentrated supernatant illustrates a preferential adsorption of the phase forming component to the substrate).

## 2.5. Conventional and ATPS enzymatic hydrolysis

Conventional hydrolysis occurs in the presence of citrate buffer 50 mM, pH 4.8, with 0.02% sodium azide. The conventional hydrolysis kinetics at solid load 10% WIS were performed at enzyme loads 10 FPU/g bagasse, 20 FPU/g bagasse and 40 FPU/g bagasse, at a reaction volume of 30 mL. Samples from conventional hydrolysis were centrifuged at 4000 rpm, 4 °C, for 10 min (Eppendorf 5810R Multipurpose Centrifuge®). Supernatants were collected for both protein and glucose quantifications. Conversion of biomass (x) was calculated according to the following formula, taking into account the amount of soluble sugars in the liquid phase after hydrolysis ( $S_g$ , in glucose equivalent concentration;  $V_H$ , the volume of the solution where the hydrolysis was performed; and the correction factor for hydration 0.9, in order to correct for the water molecule added upon hydrolysis (Selig et al., 2008)), and the initial amount of glucose equivalent in the solid cellulose sample before hydrolysis (W, the weight of dry lignocellulosic sample, and  $F_g$ , the fraction of cellulose in the lignocellulosic sample):

$$x = \left( \frac{S_g \cdot V_H}{W_{dry\ bagasse} \cdot F_g} \right) \cdot 0.9 \cdot 100\% \quad (1)$$

ATPS hydrolysis was conducted at ATPS 2 and 5, as presented in Table 2. The phase forming components (Milli-Q water and salt and PEG stock solutions) were mixed to achieve a volume ratio of 1:1, in a reaction volume of 15 mL according to the respective TLL. The bagasse was added to the system under agitation at a solid load of 10% WIS. Lastly, sodium azide and enzyme were added to a load 0.02% and 20 FPU/g bagasse, respectively. For each time evaluated, a unique system, in duplicate, was prepared, once the withdraw of top and bottom phases requires the discontinuation of the reaction and centrifugation of the system. The centrifugation occurred for 30 min, at 4000 rpm and 40 °C (Eppendorf 5810R Multipurpose Centrifuge®). All hydrolysis reactions were performed at 50 °C and 250 rpm, in orbital shaker.

## 2.6. Liquefaction followed by hydrolysis

For the hydrolysis following the liquefaction, the ATPS were formed by the addition of 9.9 mL of salt (potassium citrate 40% w/w) and 10.1 mL of polymer (PEG 6000 39% w/w) to 6 mL of liquefied bagasse (20% WIS and 10 FPU/g bagasse, for solid load and enzyme load, respectively, in citrate buffer 50 mM pH 4.8, hydrolysed for 24 h). Considering the liquefied bagasse volume being the solvent of the ATPS, the hydrolysis was performed at the TLL 34.2% and volume ratio of 1. However, the ATPS was more concentrated, because part of the liquefied volume was occupied by cellulose, lignin, ash and already released sugars. For comparison with a conventional system, 20 mL of buffer (citrate 50 mM pH 4.8) was added to 6 mL of liquefied bagasse.

## 2.7. Enzymatic activities

An international unit of enzymatic activity is defined as the amount of enzyme required to produce 1  $\mu\text{mol}$  of product per minute. 1mM p-nitrophenyl- $\beta$ -D-glucopyranoside (p-NPG), 1mM p-nitrophenyl- $\beta$ -D-xylopyranoside and 4mM p-nitrophenyl- $\beta$ -D-cellobioside (p-NPC) (Sigma–Aldrich, St. Louis, EUA) were the substrates for the activity determining reaction for  $\beta$ -glucosidase,  $\beta$ -xylosidase and cellobiohydrolase, respectively. After 10 min for  $\beta$ -glucosidase and  $\beta$ -xylosidase, and 30 min for cellobiohydrolase activity measurement, at 50 °C, the reactions (comprised of 80  $\mu\text{L}$  of the substrate and 20  $\mu\text{L}$  of the enzyme) were stopped by addition of 1 mol/L sodium carbonate. Absorbance at 400 nm was used to estimate p-NP concentration release (Bussamra et al., 2015).

The total cellulose activity measured according to the filter paper units (FPU) was performed by reducing the NREL methods (Adney and Baker, 2008) in 10 times. The sugar release was quantified following the methods suggested by Miller (1959).

## 2.8. Sugar and protein quantification

Sugar and protein present in top and bottom phases were measured according to methodology described by Bussamra et al. (2019). Sugar quantification followed the

Megazyme Glucose Reagent assay (Megazyme, Wicklow, Ireland), and no adaptation was needed to ATPS samples. Hydrolysis samples for glucose measurement were boiled for 5 min and 99 °C after collected (Eppendorf Thermomixer® C.), in order to deactivate the enzymes. The protocol used for protein quantification, based on Bradford (1976) method and performed using the Coomassie Protein Assay Reagent (Thermo Scientific, USA), required adaptation for ATPS samples, explained in details in the cited reference (Bussamra et al., 2019). The solute concentrations in g/L were defined per volume of the respective phase being measured.

The uncertainties of the all measurements calculated by calibration curves were estimated according to Barwick (2003), and the errors were propagated accordingly.

### **2.9. SDS-PAGE electrophoresis**

For the analysis of specific enzymes partition in ATPS, the bottom phase of ATPS 2 (Table 2) was evaluated in SDS-PAGE electrophoresis. To prevent interference of salt and PEG in the method, the bottom phase had the phase formation exchanged by Milli-Q water, using a 10.000 MWCO Amicon® Ultra Centrifugal Filters, as described by the supplier. Retentate of this operation (protein enriched) was dissolved in Milli-Q water. Top phase could not be evaluated through this method because the 10.000 MWCO membrane was clotted with the high concentration of PEG 6000 in that phase. The samples were diluted  $\frac{3}{4}$  times in NuPAGE™ LDS Sample Buffer (4X) (ThermoFisher Scientific, USA), and this mixture was heated at 70 °C for 10 min. 12% (w/v) Bis-Tris polyacrylamide gel (NuPAGE™, 1.0 mm, 12-well) (ThermoFisher Scientific, USA) was loaded with 10 µL prepared samples and stained by GelCode™ Blue Safe Protein Stain (ThermoFisher Scientific, USA). Mark12™ Unstained Standard (ThermoFisher Scientific, USA) was used as molecular weight ladder consisting on the following sizes: 200, 116.3, 97.4, 66.3, 55.4, 36.5, 31, 21.5, 14.4, 6, 3.5, 2.5 kDa. The protein concentration of the bottom phase sample preparation was  $0.39 \pm 0.02$  mg/mL. The maximum protein load in the band was 0.5 µg.

### **2.10. Theoretical sequential partitioning of sugar and recovery**

The sequential partitioning of sugar in different stages (continuous process) was modelled based on the mass balance of the components in each stage, and according to the equilibrium dictated by the partition coefficients for sugar and enzyme in the ATPS, and the concentration factor for the ultra-filtration unit. An initial volume ratio of 1 was assumed for equal volume between the top and bottom phases. According to the partition coefficient and volume ratio, the top and bottom phase concentrations and volume ratio were estimated for each stage (cycle).

The concentration factor determined the permeate and retentate concentrations and flow rates. The permeate was assumed to leave the system as glucose, while the retentate was diluted to the original (top) phase volume and recycled back to the ATPS. Thus, in each stage, the concentration of sugar in the retentate was diluted. The calculation was repeated for each stage under the same assumptions. At the simulation presented here, the two different partition coefficients of sugar were assessed (1.5 and 0.71), considering the same concentration factors of 1.5. The result was assessed in terms sugar recoveries after the ultrafiltration unit operation.

## **3. Results**

The evidences from experiments can guide the definition of parameters to design an extractive process to relieve product inhibition. Table 1 contains the defined process design parameters and the correspondent type of experimental data to substantiate the decision-making. The partitioning of components in ATPS depends on the system composition (Benavides et al., 2011), and determines the strategy to recycle system components and recover products. Here, we presented pre-selected ATPS capable to provide different partition coefficients of sugar and enzymes, and how the phase forming components can influence the partitioning of lignocellulosic biomass. The influence of protein load, enzyme adsorption on bagasse and partition of specific enzymatic activities in conventional hydrolysis brought insight on the design of the ultrafiltration unit operation regarding the recycle of enzymes.

### 3.1. Selection of ATPS based on partition coefficients of solutes

The pre-selected systems were previously indicated by Bussamra et al. (2019) as potential ATPS to separate sugar and enzymes. At this work, five systems, described in Table 2, were reproduced to have their partition coefficient measured at higher scale (5 ml). In the design of a process, more important than the partition coefficient itself, is the relation between the partition coefficient of solutes aimed to be separated. The relative partitioning of these solutes represents how efficient is their separation among the phases. In all the systems, the partition coefficients of sugar were higher than for proteins.

The strategy designed to recover the product (sugar) in this process, regardless which phase the bagasse partitions to, suggests the sequential partitioning of sugar to the top phase, and the recovery occurring in that phase. Then, ATPS 2 and ATPS 5 seemed to be the most efficient for that purpose, due to the high selectivity for sugar  $K_{sugar}/K_{protein}$  (Table 3).

Table 3 - Relative partitioning of sugar and protein in 5 different ATPS (systems defined in Table 2).

System	$K_{sugar}$	$K_{sugar}/K_{protein}$
ATPS 1	0.6	1.6
ATPS 2	0.6	2.4
ATPS 3	0.5	2.2
ATPS 4	0.7	1.7
ATPS 5	0.5	5.4

### 3.2. Exploratory investigation of ATPS applied to lignocellulosic hydrolysis

Preliminary investigation on influence of parameters inherent to ATPS (e.g. phase forming components adsorption on the bagasse fibres) is of paramount importance to set up coherent hydrolysis experiments.



The phase forming components influence the bagasse partition in ATPS. After hydrolysis, the systems composed by potassium citrate favoured the lignocellulose partition to the top phase, while systems containing magnesium sulphate triggered the partition to the bottom phase (visual inspection of the systems). Figure 1 presents scenarios where the choice of phase forming components determines whether the reactive phase (phase containing the bagasse) is the top or the bottom phase. The PEG molecular weight was closely related to the partition of the bagasse, being the increase of PEG molecular weight a contributor to increase the partition of bagasse to the top phase. Moreover, bagasse presented a non-selective adsorption of phase forming components. Consequently, the bagasse adsorption of phase forming components does not influence the system composition.

The cellulolytic enzymes adsorb to the substrate and consequently partition according to the substrate-enriched phase in the system (Tjerneld et al., 1985). Due to that, the partition of bagasse in ATPS determines in which phase the reaction occurs, and this is closely related to the selection of operation units in the process design to further recover the product and recycle the phase components. Beyond the fact that enzymes were in very diluted amount in the system, they were mostly adsorbed to the bagasse after 3 h reaction in conventional hydrolysis (Figure 2). For instance, 70% of the proteins adsorbed to the bagasse in the first 3 h for the enzyme load of 20 FPU/g bagasse. Interestingly, protein desorption did not follow the glucose release profile in conventional hydrolysis at 10% WIS, regardless the enzyme load (10, 20 or 40 FPU/ bagasse) (Figure 2).

The two specific activities tested in the commercial cocktail presented similar adsorption to sugarcane bagasse, and this non-selective adsorption did not change according to the enzyme load. Both  $\beta$ -glucosidase and cellobiohydrolase presented less than 5% of enzymatic activity in the supernatant (not adsorbed) after 3 h hydrolysis, except for cellobiohydrolase at enzyme load of 40 FPU/g bagasse, which presented approximately 10% of that activity in the supernatant up to 6 h hydrolysis (Figure 3). We can assume that this reduction of measured enzymatic activity is not only a consequence of protein deactivation, because the non-adsorbed protein also reduced considerably after 3 h reaction (Figure 2).

## Enzymatic hydrolysis of sugarcane bagasse in ATPS

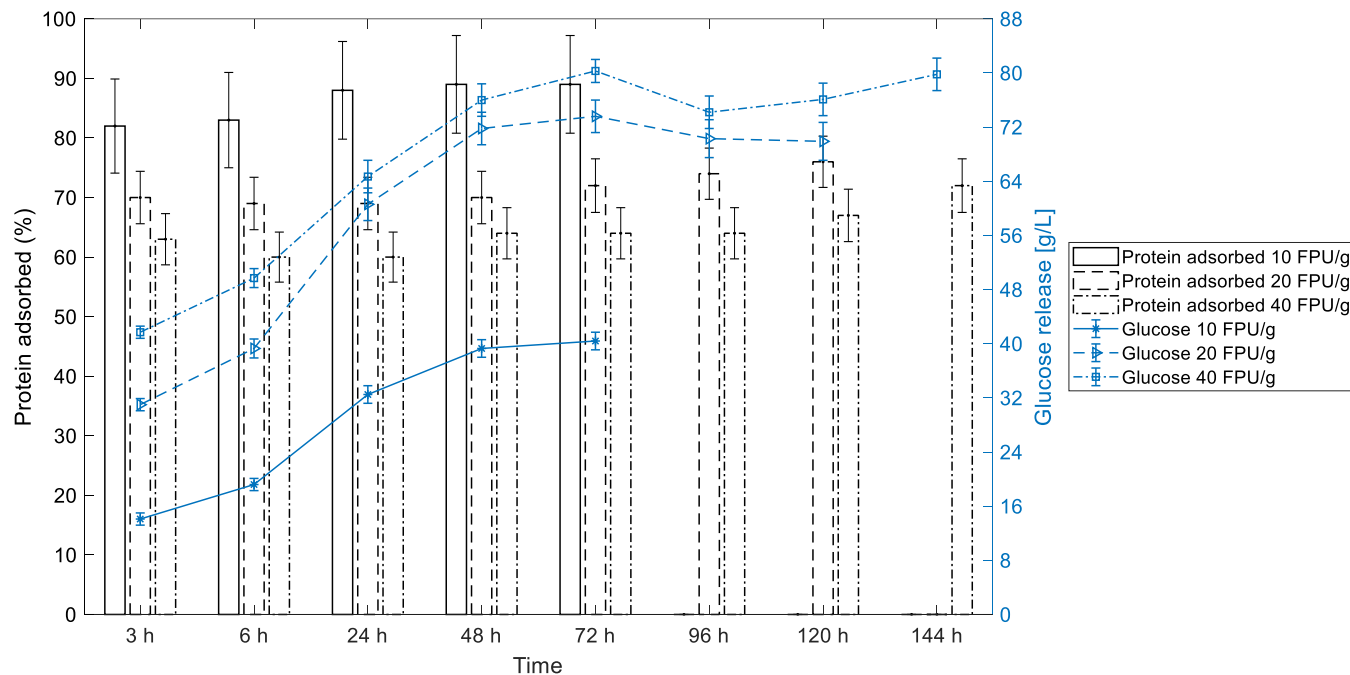


Figure 2 – Protein adsorption/desorption does not follow the glucose release in conventional hydrolysis at 10% WIS (solid load), at different enzyme loads of 10 FPU/g bagasse, 20 FPU/g bagasse, and 40 FPU/g bagasse. The bars represent the protein adsorbed (left y axis), and the curve shows the glucose release (right y axis). The conversion of reaction at each enzyme load achieved  $47\% \pm 1.5$ ,  $79.4\% \pm 3.2$  and  $88.7\% \pm 2.7$ , respectively.

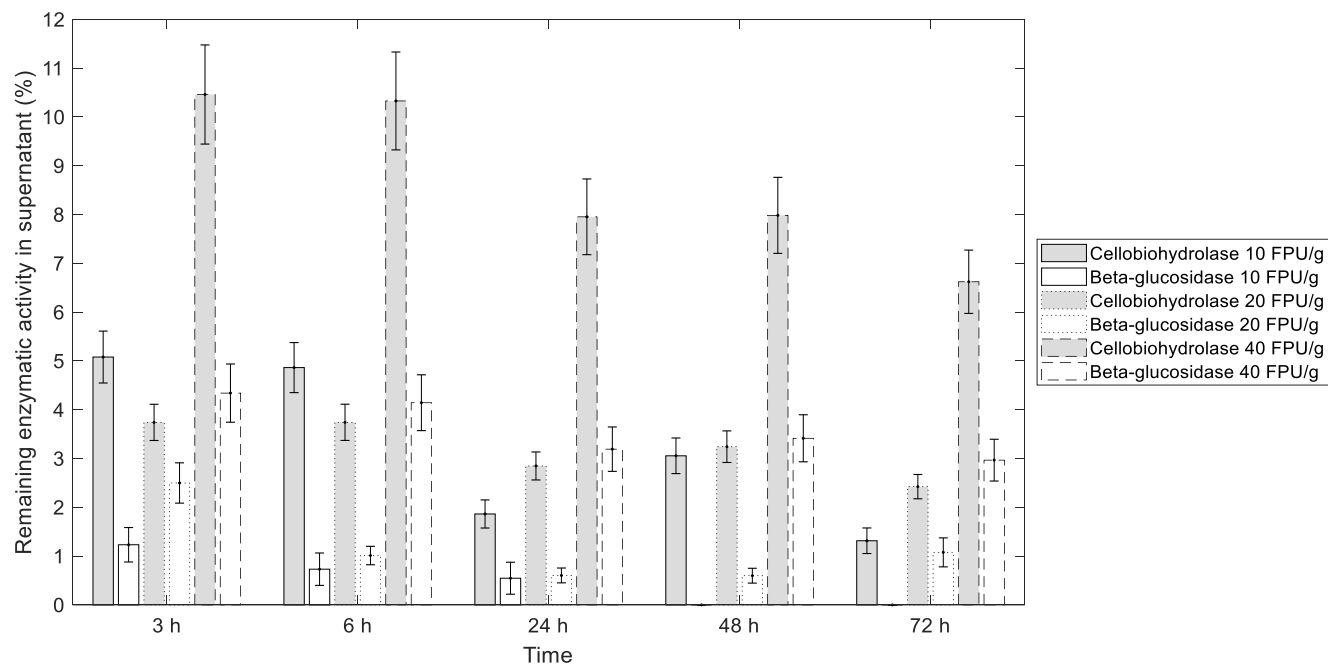


Figure 3 - Selective adsorption of enzymes to the sugarcane bagasse during the conventional hydrolysis reaction at 10% WIS (solid load), at different enzyme loads of 10 FPU/g bagasse, 20 FPU/g bagasse, and 40 FPU/g bagasse. The remaining enzymatic activity corresponds to the percentage of activity quantified in the supernatant in relation to the theoretical activity in case of no enzymatic adsorption. The total theoretical activities of cellobiohydrolase and  $\beta$ -glucosidase are, respectively,  $1.7 \pm 0.2$  and  $3.9 \pm 0.5$  (enzyme load 10 FPU/g bagasse),  $4.1 \pm 0.4$  and  $9.2 \pm 1.2$  (enzyme load 20 FPU/g bagasse), and  $8.3 \pm 0.8$  and  $18.4 \pm 2.4$  (enzyme load 40 FPU/g bagasse).

Considering the protein adsorption and conversion profile of the three enzyme loads evaluated, the one at 20 FPU/g bagasse presented similar protein adsorption (in percentage to the total protein added) in comparison to the higher enzyme load, for the same solid load (10% WIS). This fact indicates that the biomass could still adsorb proteins when the enzyme load increased from 20 to 40 FPU/g. However, the balance between adsorbed (approximately 70%) and free enzymes was achieved and maintained from 20 FPU/g bagasse enzyme load — higher enzyme loads still presents approximately 70% of adsorbed enzymes. On the other hand, the percentage of free cellobiohydrolases increased with the increase of enzyme load (20 to 40 FPU/g bagasse), indicating that there was an excess of this enzyme class in the reaction — cellobiohydrolases are processive enzymes and should be adsorbed to the fibres to provide catalytic function, once they slide along the cellulose chain to the next cleavage site as the product is released (Gupta et al., 2016). Moreover, considering the increase in conversion (approximately 12%) when comparing the enzyme load at 20 FPU/g to 40 FPU/g and the cost of the enzymes, the gain in hydrolysis seems not defensible. Then, the enzyme load of 20 FPU/g bagasse was chosen to conduct the ATPS hydrolysis.

### **3.3. Comparison between conventional and ATPS hydrolysis of lignocellulosic material**

The sugar released in bottom phase of ATPS composed by potassium citrate-PEG 6000 reached the same concentration as the conventional hydrolysis (Figure 4). Because of the uneven partition of sugars in the ATPSs composed by potassium citrate-PEG 6000 (TLL 15.3%) and magnesium sulphate-PEG 6000 (TLL 30.5%), the concentration of sugars during enzymatic hydrolysis contributed to different reaction rates in each phase of the system. For both ATPS studied, the partition coefficient of sugars was smaller than 1 (higher concentration of sugars in bottom phase). For the ATPS hydrolysis, the reaction did not discontinue after 48 h (Figure 4). In conventional hydrolysis, the sugar release ceased after 48 h reaction.

When the system reaction was composed by liquefied substrate (sugarcane bagasse hydrolysed for 24 h at conventional hydrolysis), no extra glucose was released for both conventional and ATPS hydrolysis (Figure 5, a).

## Enzymatic hydrolysis of sugarcane bagasse in ATPS

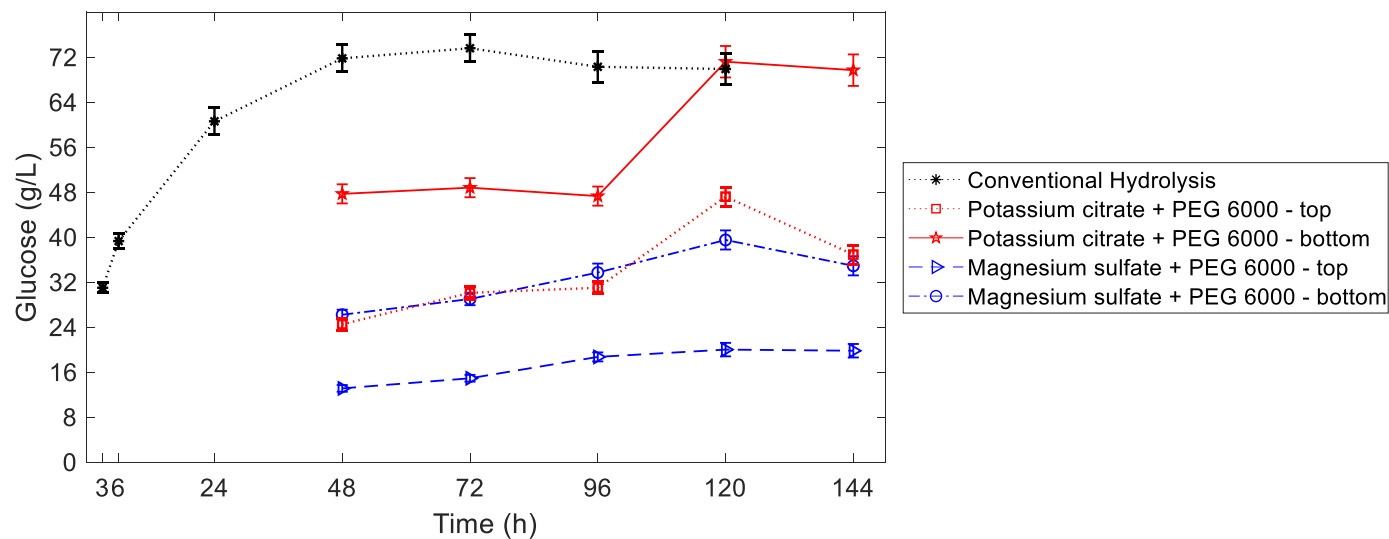


Figure 4 – kinetics of conventional hydrolysis of hydrothermal sugarcane (10% WIS, 20 FPU/g bagasse) bagasse vs ATPS hydrolysis (10% WIS, 20 FPU/g bagasse), without previous liquefaction of the sugarcane bagasse.

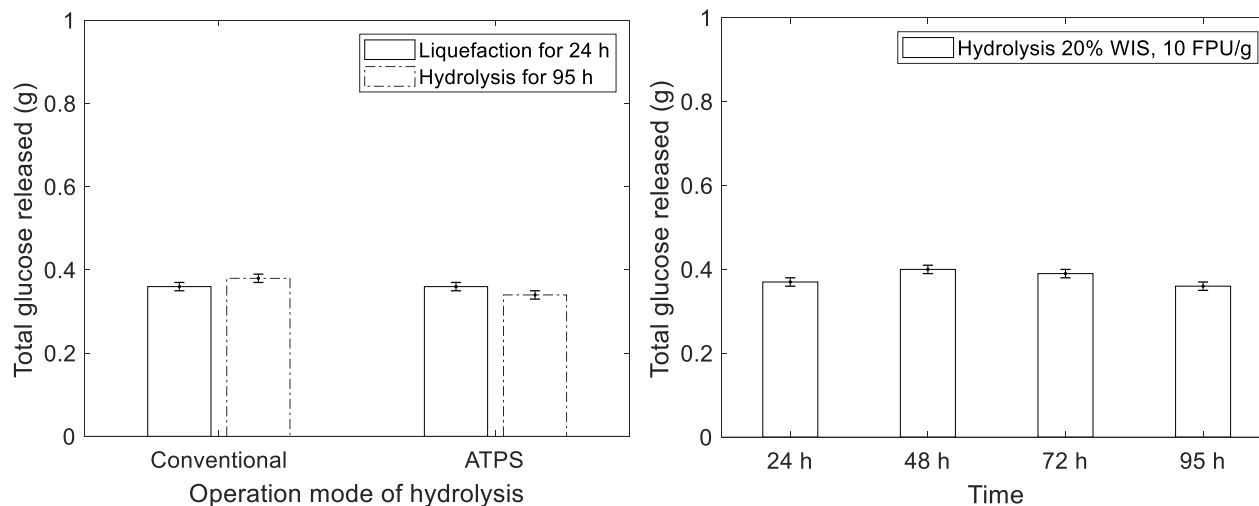


Figure 5 – a) Comparison in sugar release after liquefaction for 24 h (20% WIS solid load and 10 FPU/g bagasse enzyme load) followed by hydrolysis (total reaction of 95 h), for conventional and ATPS operation modes. b) Conventional hydrolysis of sugarcane bagasse (20% WIS solid load and 10 FPU/g bagasse enzyme load) — prolongation of the liquefaction up to 95 h (conversion of  $34.5\% \pm 1$ ). The glucose release was presented in total grams in the reaction, in order to compare systems with different volumes.

### 3.4. Potential of enzyme recycle and sugar recovery in ATPS

Enzymes contribute in a great extent to the costs and to the conversion efficiency of a continuous process of hydrolysis (Torres, 2016). In the process configuration applied to the potassium citrate system (Figure 1, b), in which top phase is the reactive phase, the free enzymes can be recovered in an ultrafiltration step. This operation unit also intends to recycle phase forming components (PEG) and recover the product (sugar). However, the partition of specific enzymes of the cocktail should be even among the phases or the entire cocktail should be one-sided partitioned to avoid the enrichment of the enzymatic cocktail with a specific activity (class of protein) in a continuous process with recycle. The ATPS 2 (potassium citrate and PEG 6000, TLL 15.3%) accomplished these requirements, since all bands of proteins identified in the enzymatic cocktail (lane 2) were also present in the bottom phase (lane 3) (Figure 6).

For both process alternatives, the final product (glucose) is suggested to be recovered from the polymer enriched-phase. The recovery of sugar from salt enriched-phase is rarely reported in literature. On the other hand, the separation of glucose and polymer is widely acquired through ultrafiltration. Even though some systems separate glucose preferably to the bottom phase (salt enriched-phase), the recovery from the top phase is possible through the repartitioning of the sugar-enriched bottom phase to a new sugar-depleted top phase. Evidently, the higher the partition coefficient of glucose in the system, the lower the number of cycles to achieve the desirable concentration of sugar in the end stream of the process. The efficiency of this strategy was assessed theoretically. A recovery of 0.65 kg/kg glucose was achieved through a sequential partition of glucose to the top phase for an ATPS presenting  $K_{sugar}$  of 0.71, after 6 cycles. If the  $K_{sugar}$  increased to 1.5, 0.67 kg/kg recovery would be achieved after 4 cycles (Figure 7).



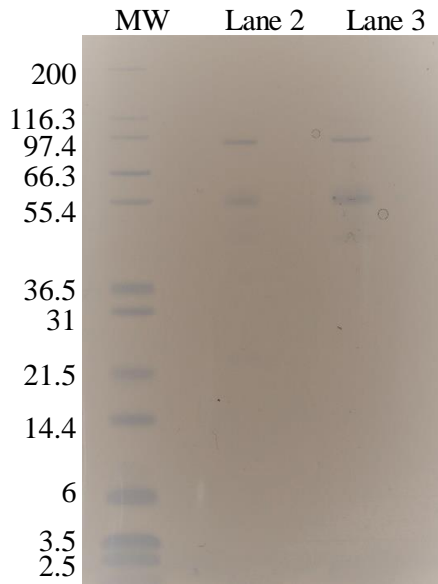


Figure 6 – SDS–PAGE electrophoresis of enzymatic cocktail (lane 2) and bottom phase (lane 3) after partition in the APTS 2 (potassium citrate and PEG 6000, TLL 15.3%). Molecular weights (*MW*), in kDa, in decreasing order (lane 1): 200, 116.3, 97.4, 66.3, 55.4, 36.5, 31, 21.5, 14.4, 6, 3.5, 2.5.

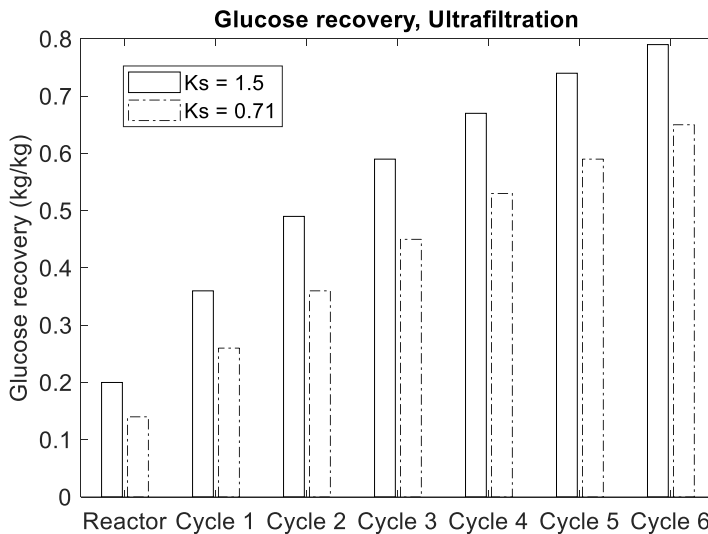


Figure 7 – Sequential APTS formation to recover sugar in the ultrafiltration unit of operation.

#### **4. Discussion**

This section discusses how the experimental results assisted the definition of parameters to a future process design. Moreover, the discussion also indicates the suitability of conducting enzymatic hydrolysis in ATPS.

##### **4.1. ATPS and enzymatic hydrolysis of sugarcane bagasse**

In order to operate lignocellulosic hydrolysis in ATPS, the system formation and equilibrium, influence of viscosity on mixing, and analytical techniques are of paramount importance to a proper reaction conduction and quantification. Even though we showed that the bagasse has non-selective adsorption towards the phase forming components in comparison to water, we suggest the addition of bagasse to the heterogeneous solution under mixing, providing contact to all components at the same time.

During the hydrolysis, the cleavage of specific sites of the polymer chain can affect its hydrophobicity, and consequently its partition in the system. This statement can be supported by the work of Fu et al. (2019), who suggested a method to quantify hydrophobicity based on the partition of natural organic matter on ATPS composed by PEG and potassium citrate. Additionally, during the hydrolysis the density of the substrate decreases, diminishing the gravity force in favour of setting down the substrate components, which might also explain the different bagasse partitioning before and after hydrolysis.

The increase of viscosity due to high solid load can impact the mixing and consequently the efficiency of the reaction (Rosgaard et al., 2007). When operating in ATPS, the concentration of phase forming components, specially the polymer, becomes a great contributor to increase viscosity. Then, the solid load cannot be considered as a unique factor to the mass transfer limitation (set at a maximum of 20% WIS to ATPS hydrolysis by this work). Another limitation of ATPS application relies on the analytical techniques to quantify proteins (Glyk et al., 2015; González-González et al., 2011; Silvério et al., 2012) Some strategies have already been

suggested in literature, using conventional methods of quantification (Bussamra et al., 2019).

Although ATPS seem to maintain the conversion rate due to the inhibitor partition in the system, the ATPS should provide a proper environment to preserve the enzymatic activity. The performance of the enzymes when incubated in the salts potassium citrate (10% w/w pH 5) and magnesium sulphate (10% w/w pH 5) was reduced approximately 50% in relation to the enzymatic activity in optimum conditions (conventional hydrolysis — citrate buffer 50 mM) (Bussamra et al., 2019). Although temperature can be easily controlled to operate in the optimum for the enzymes, pH is an important factor when dealing with ATPS, since the different salts present different properties under pH variation, which can also impact the enzymatic activity. Therefore, an ATPS composed by harmless phase forming components to the enzymes would provide the environment to both preserve the enzymatic activity and overcome product inhibition (through sugar extraction to the opposite phase of the reaction). Alternative phase forming components can provide optimal environment to the catalytic activity, such as ionic liquids (Ferreira et al., 2018).

#### **4.2. Conventional versus ATPS hydrolysis**

Even though the product inhibition was not identified as a cause to decrease cellulose hydrolysis by Bommarius et al. (2008), other authors have refereed to product inhibition as the main factor to decrease the conversion rate at high conversions (Bezerra and Dias, 2005; Xiao et al., 2004). A previous study has identified the advantage to remove inhibitor (sugar) from the reaction in order to maintain the conversion rate (Yang et al., 2011). Here, the stagnation in sugar release after dilution of the 24 h liquefied bagasse indicates that sugar concentration is not the only factor contributing to the product inhibition in enzymatic hydrolysis (Figure 5, b). Considering that 90% of the enzymes were already adsorbed to the fibres at 24 h of reaction at the enzyme load of 10 FPU/g bagasse, the reaction did not stop because of enzyme dilution and consequent inaccessibility to the fibres. Diluting the reaction system without the removal of products kept the inhibitor-to-enzyme ratio constant. Xiao et al. (2004) showed that the decrease of this ratio is

crucial to overcome product inhibition. To a certain extent, the ATPS also decrease this ratio in one of the phase system, partitioning the sugar between the top and bottom. Moreover, the cellulose chain could be inaccessible after 24 h due to the increased proportion of highly-recalcitrant region of the fibres (crystalline cellulose), since amorphous regions are hydrolysed first.

Although the mechanism of cellulase binding on lignocellulosic biomass (substrate-enzyme interaction) is not completely understood, some models can elucidate factors affecting the enzyme rates and activities (Bansal et al., 2009). Cellobiose, released during the cleavage of the bagasse chain during hydrolysis, is a non-competitive inhibitor to cellulases (Bezerra and Dias, 2005). However, some studies classify cellobiose as a secondary inhibitor, once the high glucose concentration (mainly inhibitor) leads to the accumulation of cellobiose. The degree of inhibition caused by glucose is also more pronounced to cellulase mixture than to isolated  $\beta$ -glucosidase (Xiao et al., 2004). The reported nature and degree of glucose inhibition might be a likely cause associated with the decrease in conversion rate after 24 h conventional hydrolysis at solid load of 10% WIS and enzyme load of 10 FPU/g bagasse (Figure 2).

In the potassium citrate-PEG 6000 ATPS hydrolysis, the cellulose conversion increased in 51.5% from 96 h to 120 h, whereas the conventional hydrolysis did not present any sugar release in the same period. However, similar conversion increase (54%) already happened from 6 h to 24 h in conventional hydrolysis. A similar glucan conversion achieved at different times has been demonstrated when the substrate presents change in crystallinity (Gao et al., 2013). The phase forming components could influence the exposure of the amorphous part of the cellulose, as well as reducing the hydrophobicity of the cellulose surfaces, impairing the enzymes binding to the substrate. Moreover, decreasing rates of hydrolysis with high degrees of conversion have been associated to the jamming effect, which is the interference of adjacent enzymes adsorbed on cellulose surface at high protein concentration (Bommarius et al., 2008). Protein degradation could also trigger the discontinuation of the enzymatic conversion (Bansal et al., 2009).

Even though the sugar released in bottom phase during the hydrolysis conducted in ATPS composed by potassium citrate-PEG 6000 (TLL 15.3%) was similar to the sugar released in conventional hydrolysis, some peculiarities of the different approaches can benefit the implementation of the ATPS conversion. In ATPS, the inhibitor is partitioned in the system, and the maintenance of the enzymatic activity after 48 h reaction for ATPS hydrolysis can be an indication that sugar is being removed from the reactive phase. However, the partitioning of sugar and consequently preservation of the reaction rate could also imply a delay in achieving the inhibitory concentration of products in the respective phase.

In both approaches (Figure 1), glucose and protein partition predominantly to the bottom phase. Even though the selectivity for sugars was higher in ATPS 5 (Table 3), the sugar release in that system was lower in comparison to ATPS 2 (Figure 4). This can be explained by the reactive phase (bottom phase, due to bagasse partition) presenting the higher concentration of inhibitor (glucose) among the phases. Moreover, ATPS 2, composed by potassium citrate, could maintain better the optimal catalytic pH than ATPS 5.

The TLL influences directly the hydrolysis performance, once the high concentrated systems can decrease the enzymatic performance and limit the mass transfer of the system. On the other hand, low TLL does not present a satisfactory difference between the partition coefficients of sugar and proteins. To overcome this issue, a liquefaction of the bagasse in buffer (conventional hydrolysis) prior to ATPS formation would promote the adsorption of the enzymes to the bagasse and the conversion at high initial rates. After the ATPS formation, the sugar concentration would partition in the system and the reaction rate would be maintained until the achievement of the inhibitory concentration of products in one of the phases. The mass transfer limitation should be smaller in this mode of operation, once the substrate would be partially hydrolysed when the ATPS are formed. Moreover, the conventional and mild environment used to liquefy the bagasse would prevent the enzymatic activity reduction due to salt contact (present in ATPS) in the beginning of the reaction. Surprisingly, the liquefaction for 24 h followed by hydrolysis did not contribute to the maintenance of the conversion rate (Figure 5). After 24 h

liquefaction (conventional hydrolysis at 20% WIS solid load and 10 FPU/g bagasse enzyme load), the enzymes were already inhibited (Figure 5, b). In order to take advantages of both conventional and ATPS hydrolysis, the liquefaction should provide conversion at high initial rates, and the ATPS formation should enable a high total sugar release due to the partition of product to other phase. Then, a liquefaction of the bagasse for 6 h prior to hydrolysis in ATPS would provide both benefits. Moreover, a higher initial rate could be achieved by increasing the enzyme load to 20 FPU/g bagasse (Figure 2). The liquefaction before the ATPS formation also overcomes the challenge of fitting the volume of bagasse in the volume of the reactive phase, since the substrate will be partially converted and the solid load decreased when biphasic system is formed.

### **4.3. Recycle and recovery of system components**

The strategy designed to recuperate the product (sugar) in this process suggests the sequential partition of sugar to the top phase, and the recovery occurring in that phase (PEG-enriched phase) after ultrafiltration. Theoretically, the permeate stream containing the product also presents soluble lignin and salt — in the same concentration of the salt in top phase. The recovery of sugar could be improved by an ATPS presenting higher partition coefficient of glucose, and by strategies to remove salts in accordance to the application of product stream.

In the system configuration of top phase as reactive phase, the ultrafiltration operation unit also grants the recycle of PEG and enzymes back to the process. However, enzymes do not desorb from bagasse after maximum conversion is achieved in conventional hydrolysis (Figure 2), impairing their recycle to the system reaction as free enzymes. A similar high binding capacity of around 85% of the cellulolytic enzymes has been reported by Gao et al. (2013). This irreversible cellulose binding was observed for hydrolysis involving lignocellulosic substrates, contrarily for amorphous cellulose hydrolysis, in which the substrate favours the desorption after depletion of substrate (Gao et al., 2013). However, due to the extensive solubilisation of cellulose and hemicellulose, the irreversible binding of cellulose is mostly related to the presence of lignin. Moreover, the binding capacity

of the enzymes does not indicate an improved cellulose conversion, since the enzymes can be non-productively bound to the substrate (Gao et al., 2013). The recycle of enzymes from the supernatant has already been demonstrated to succeed at industrial conditions (high solid load and low enzyme dosage) for wheat straw substrate hydrolysis (Haven et al., 2015). This recycling strategy is restricted to the enzymatic stability of the recovered enzymes. Improved conditions for enzyme stability can enhance the potential of recycling free/desorbed enzymes (Haven et al., 2015). In a continuous system, the free enzymes are constantly removed from the reaction. The removal of desorbed/free enzymes does not impact significantly the rate and extent of the hydrolysis (Hu et al., 2018). However, it is important that the recycle occurs after the equilibrium in enzymatic adsorption is achieved.

Considering the reactive phase as the bottom phase, the enzymes are recycled back to the system adsorbed to the unconverted biomass. The recycle of enzymes associated with insoluble solids has already been proven as an effective method to decrease enzyme usage when operating hydrolysis in several rounds (Weiss et al., 2013). The bound enzymes are capable to hydrolyse cellulose from fresh substrate. Moreover, the solid recycle method increases the contact time between catalyst and substrate, and enables unreacted substrate to return to the reaction. Increasing the amount of solid fraction recycled also increases the glucose release. However, the recycle of solids leads to increased lignin in the solid composition and increased total solid concentration, which requires higher tank size and a process able to deal with higher solids concentration and volumes. Then, the process should be balanced in between recycling enzyme activity and increased operating solids concentration. This method of recycling enzymes requires complementation of fresh enzymes at each recycle round, once there are losses of enzymes in the liquid fraction, and non-productive binding to lignin (Weiss et al., 2013).

#### **4.4. Parameter definition to a process design and technical challenges**

Here, we bring an overview of parameter definition when designing the extractive process to relieve product inhibition based on ATPS. Additionally to the process definition provided by the experimental data, we indicate other aspects of the

process design that could be benefited by additional experiments (summarized in Table 4).

Because the phase forming components can influence the partition of the bagasse in the system, polymer and salts can be chosen in order to promote the reactive phase (enriched in substrate and adsorbed enzymes) apart from the glucose-enriched phase. Moreover, the selection of phase forming components and concentration (TLL) should also be based on the capacity of maintaining the enzymatic activity of cellulases. The appropriate choice of components determines the efficiency of the ATPS-based hydrolysis. As presented in Figure 1, the ATPS reactor has a separate vessel for phase separation. At this stage, the bagasse is partially hydrolysed and the process design is not affected by the different partitioning of bagasse observed before and after hydrolysis.

In a continuous process involving ATPS, the recycle of components requires more attention than monophasic systems (conventional hydrolysis), since the recycled stream might not contain the same composition of phase forming components as the initial one (the TLL can alter at each cycle), depending on the recycle, purge and fresh streams of system components. In order to estimate the outlet concentrations of top and bottom phases, given the new inlet composition of the ATPS, phase diagrams previously reported by Bussamra et al. (2019) were used. To automatically predict the new phase compositions partition coefficients, a thermodynamic model should be developed and implemented on the design calculation. Different composition of top phase can affect the repartitioning of sugar. Giving the experimentally determined partition coefficient of this solute in the corresponding system composition, the authentic number of cycles to repartition glucose and achieve the desired sugar recovery can be empirically determined in order to model a reliable recovery operation.

Although the conventional hydrolysis does not indicate a desorption of enzymes after the reaction, PEG has demonstrated to favour enzyme adsorption on the surface of the biomass, preventing the binding to the lignin (Malmsten and Van Alstine, 1996) (Haven and Jørgensen, 2013). This feature of the ATPS could promote the recycle



of enzymes and validate the hydrolysis model proposed by Stickel et al. (2018), in which the concentration of free enzymes increases with the decrease of substrate (glucan). Moreover, the non-selective partition and adsorption of the different enzymatic activities tested suggest a constant recycled cocktail composition. In the dextran-PEG 20000 system reported by Tjerneld et al. (1985), all the cellulolytic enzymes partitioned to the bottom phase, not affecting the continuous process of cellulose conversion in ATPS (Tjerneld et al., 1991). The paradigm that  $\beta$ -glucosidase (from Cellic CTec 2) would not adsorb to the substrate, or adsorb to a minor extent, had already been broken by Haven and Jørgensen (2013). Some preferential adsorption of enzymatic classes has been observed for the cocktail Cellic CTec 3, in which cellobiohydrolase presented a higher binding affinity toward the substrate than endoglucanase (Hu et al., 2018). The preferential adsorption can be connected to the required enzymatic classes to hydrolyse a specific substrate composition. However, the recycle stream of the enzymes is an outcome not only from the ATPS separation reactor, but also from the ultrafiltration operation unit. Based on that, the evaluation of the partition of specific enzymatic classes on retentate and permeate from ultrafiltration should also be considered. Consequently, the recovery efficiency should be assessed in terms of maintenance of enzymatic activity after ultrafiltration (retentate stream), and considering the number of ultrafiltration cycles needed to repartition glucose and obtain the desirable recovery of this product. When assessing the enzymatic activity of the retentate to be recycled to the system, it is also important to regard the theoretical loss of enzymes in the permeate and purge streams (Stickel et al., 2018).

Combining the empirical information reported at this work (Table 1) to literature evidences, a qualitative process was designed to conduct enzymatic hydrolysis in ATPS. Moreover, the kinetic data on conventional and ATPS enzymatic hydrolysis generated here can improve the fundamental understanding of variables regarding the enzymes and substrate. A more detailed and phenomenological understanding of the hydrolysis process can give insights on kinetic models and/or validate existent ones (Bansal et al., 2009). In conclusion, the set of information acquired so far

## Enzymatic hydrolysis of sugarcane bagasse in ATPS

indicates that the ATPS hydrolysis could be reasonable modelled under such considerations.

Table 4 – Information to be retrieved from experiments to provide empirical basis to a reliable definition of parameters to the process design.

Information substantiated by experiments	Type of parameters to be defined in the process design
Partition of specific enzymatic classes after ultrafiltration (retentate and permeate)	Feasibility to recycle enzymes in terms of enrichment of one specific enzymatic class in continuous operation
Enzymatic activity in the ultrafiltration unit (feed and retentate). Model: potassium citrate-based ATPS	Feasibility to recycle enzymes in terms of recovery efficiency (retention coefficient for the process design)
PEG concentration in the ultrafiltration unit (feed and retentate). Model: potassium citrate-based ATPS	Feasibility to recycle PEG (concentration factor for the process design)
Partition of glucose in ATPS (top and bottom) after ultrafiltration, in which retentate composes the next top phase for the repartition of glucose in ATPS	Number of ATPS cycles to repartition glucose and achieve the desired sugar recovery
Thermodynamic model to predict phase separation and partition of solutes in ATPS	Contribution to a reliable calculation of phase composition and partition coefficient of solutes at different TLL (after recycle of PFCs)

## 5. Conclusion

This study demonstrated the suitability of conducting the enzymatic hydrolysis of lignocellulosic materials in aqueous two-phase systems (ATPS). This extractive technique, when applied to enzymatic conversions in the presence of solid substrate, presents peculiarities regarding the enzymatic activity performance and the partition of the substrate in dependence on the system composition. In the ATPS enzymatic hydrolysis, the reactive phase is determined by the substrate enriched-phase, since the majority of the enzymes adsorbs to the fibres. The process design for such application involves a liquefaction of the bagasse prior to the ATPS hydrolysis. Because the proteins does not desorb from the fibres along the hydrolysis, the approach considering the recycle of enzymes when adsorbed to the substrate is more appropriate. Experimental studies on the ultrafiltration unit operation would substantiate the assumptions regarding the feasibility to recover the product and recycle not adsorbed enzymes and phase forming components. Based on the data acquired and literature evidences, this work provides valuable information (technical conditions) to a future quantitative evaluation of the processes.

## Acknowledgement

This work was financially supported by the Foundation for Research of State of Sao Paulo, Brazil [grant numbers 2015/20630-4, 2016/04749-4, 2016/06142-0 and BEPE 2016/21951-1]; and the BE-Basic Foundation, The Netherlands. This research was carried out during a Dual Degree PhD program under agreement between UNICAMP and TU Delft.

## References

- Adney, B., and Baker, J. (2008). Measurement of Cellulase Activities. Laboratory Analytical Procedure ( LAP ) Issue Date : 08 / 12 / 1996.
- Bansal, P., Hall, M., Realff, M. J., Lee, J. H., and Bommarius, A. S. (2009). Modeling cellulase kinetics on lignocellulosic substrates. *Biotechnol. Adv.* 27, 833–848. doi:10.1016/j.biotechadv.2009.06.005.

Barwick, V. (2003). Preparation of Calibration Curves. A guide to Best Practice.

Baskir, J. N., Hatton, T. A., and Suter, U. W. (1989). Protein partitioning in two-phase aqueous polymer systems. *Biotechnol. Bioeng.* 34, 541–558. doi:10.1002/bit.260340414.

Benavides, J., Rito-Palomares, M., and Asenjo, J. A. (2011). *Aqueous Two-Phase Systems*. Second Edi. Elsevier B.V. doi:10.1016/B978-0-08-088504-9.00124-0.

Bezerra, R. M. F., and Dias, A. A. (2005). Enzymatic kinetic of cellulose hydrolysis: Inhibition by ethanol and cellobiose. *Appl. Biochem. Biotechnol.* 126, 49–59. doi:10.1007/s12010-005-0005-5.

Bommarius, A. S., Katona, A., Cheben, S. E., Patel, A. S., Ragauskas, A. J., Knudson, K., et al. (2008). Cellulase kinetics as a function of cellulose pretreatment. *Metab. Eng.* 10, 370–381. doi:10.1016/j.ymben.2008.06.008.

Bradford, M. M. (1976). A rapid and sensitive method for the quantitation of microgram quantities of protein utilizing the principle of protein-dye binding. *Anal. Biochem.* 72, 248–254. doi:10.1016/0003-2697(76)90527-3.

Bussamra, B. C., Castro Gomes, J., Freitas, S., Mussatto, S. I., Carvalho da Costa, A., van der Wielen, L., et al. (2019). A robotic platform to screen aqueous two-phase systems for overcoming inhibition in enzymatic reactions. *Bioresour. Technol.* 280, 37–50. doi:10.1016/j.biortech.2019.01.136.

Bussamra, B. C., Freitas, S., and Costa, A. C. da (2015). Improvement on sugar cane bagasse hydrolysis using enzymatic mixture designed cocktail. *Bioresour. Technol.* 187, 173–181. doi:10.1016/j.biortech.2015.03.117.

Cameron, H., Campion, S. H., Singh, T., and Vaidya, A. A. (2015). Improved saccharification of steam-exploded *Pinus radiata* on supplementing crude extract of *Penicillium* sp. 3 *Biotech* 5, 221–225. doi:10.1007/s13205-014-0212-2.

Cao, L. C., Wang, Z. J., Ren, G. H., Kong, W., Li, L., Xie, W., et al. (2015). Engineering a novel glucose-tolerant  $\beta$ -glucosidase as supplementation to enhance

the hydrolysis of sugarcane bagasse at high glucose concentration. *Biotechnol. Biofuels* 8. doi:10.1186/s13068-015-0383-z.

Chen, R. (2015). A paradigm shift in biomass technology from complete to partial cellulose hydrolysis: Lessons learned from nature. *Bioengineered* 6, 69–72. doi:10.1080/21655979.2014.1004019.

Cray, J. A., Stevenson, A., Ball, P., Bankar, S. B., Eleutherio, E. C. A., Ezeji, T. C., et al. (2015). Chaotropicity: A key factor in product tolerance of biofuel-producing microorganisms. *Curr. Opin. Biotechnol.* 33, 228–259. doi:10.1016/j.copbio.2015.02.010.

Donaldson, L. A., Newman, R. H., and Vaidya, A. (2014). Nanoscale interactions of polyethylene glycol with thermo-mechanically pre-treated *Pinus radiata* biofuel substrate. *Biotechnol. Bioeng.* 111, 719–725. doi:10.1002/bit.25138.

Fahmy, M., Sohel, M. I., Vaidya, A. A., Jack, M. W., and Suckling, I. D. (2019). Does sugar yield drive lignocellulosic sugar cost? Case study for enzymatic hydrolysis of softwood with added polyethylene glycol. *Process Biochem.* 80, 103–111. doi:10.1016/j.procbio.2019.02.004.

Ferreira, A. M., Passos, H., Okafuji, A., Tavares, A. P. M., Ohno, H., Freire, M. G., et al. (2018). An integrated process for enzymatic catalysis allowing product recovery and enzyme reuse by applying thermoreversible aqueous biphasic systems. *Green Chem.* 20, 1218–1223. doi:10.1039/C7GC03880A.

Freire, M. G., Cláudio, A. F. M., Araújo, J. M. M., Coutinho, J. a. P., Marrucho, I. M., Lopes, J. N. C., et al. (2012). Aqueous biphasic systems: a boost brought about by using ionic liquids. *Chem. Soc. Rev.* 41, 4966. doi:10.1039/c2cs35151j.

Fu, H., Liu, K., Alvarez, P. J. J., Yin, D., Qu, X., and Zhu, D. (2019). Chemosphere Quantifying hydrophobicity of natural organic matter using partition coefficients in aqueous two-phase systems. *Chemosphere* 218, 922–929. doi:10.1016/j.chemosphere.2018.11.183.

Gao, D., Chundawat, S. P. S., Sethi, A., Balan, V., Gnanakaran, S., and Dale, B. E. (2013). Increased enzyme binding to substrate is not necessary for more efficient cellulose hydrolysis. *Proc. Natl. Acad. Sci.* 110, 10922–10927. doi:10.1073/pnas.1213426110.

Glyk, A., Heinisch, S. L., Scheper, T., and Beutel, S. (2015). Comparison of colorimetric methods for the quantification of model proteins in aqueous two-phase systems. *Anal. Biochem.* 477, 35–37. doi:10.1016/j.ab.2015.02.007.

Goldemberg, J., and Teixeira Coelho, S. (2004). Renewable energy - Traditional biomass vs. modern biomass. *Energy Policy* 32, 711–714. doi:10.1016/S0301-4215(02)00340-3.

González-González, M., Mayolo-Deloya, K., Rito-Palomares, M., and Winkler, R. (2011). Colorimetric protein quantification in aqueous two-phase systems. *Process Biochem.* 46, 413–417. doi:10.1016/j.procbio.2010.08.026.

Gupta, V. K., Kubicek, C. P., Berrin, J. G., Wilson, D. W., Couturier, M., Berlin, A., et al. (2016). Fungal Enzymes for Bio-Products from Sustainable and Waste Biomass. *Trends Biochem. Sci.* 41, 633–645. doi:10.1016/j.tibs.2016.04.006.

Hahn-Hägerdal, B., Mattiasson, B., and Albertsson, P. Å. (1981). Extractive bioconversion in aqueous two-phase systems. A model study on the conversion of cellulose to ethanol. *Biotechnol. Lett.* 3, 53–58. doi:10.1007/BF00145110.

Haven, M. Ø., and Jørgensen, H. (2013). Adsorption of  $\beta$ -glucosidases in two commercial preparations onto pretreated biomass and lignin. *Biotechnol. Biofuels* 6, 1–14. doi:10.1186/1754-6834-6-165.

Haven, M. Ø., Lindedam, J., Jeppesen, M. D., Elleskov, M., Rodrigues, A. C., Gama, M., et al. (2015). Continuous recycling of enzymes during production of lignocellulosic bioethanol in demonstration scale. *Appl. Energy* 159, 188–195. doi:10.1016/j.apenergy.2015.08.062.

Hu, J., Mok, Y. K., and Saddler, J. N. (2018). Can We Reduce the Cellulase Enzyme Loading Required to Achieve Efficient Lignocellulose Deconstruction by only Using the Initially Absorbed Enzymes? *ACS Sustain. Chem. Eng.* 6, 6233–6239. doi:10.1021/acssuschemeng.8b00004.

Kulkarni, N., Vaidya, A., and Rao, M. (1999). Extractive Cultivation of Recombinant *Escherichia coli* Using Aqueous Two Phase Systems for Production and Separation of Extracellular Xylanase. *Biochem. Biophys. Res. Commun.* 255, 274–278.

Li, M., Kim, J. W., and Peeples, T. L. (2002). Amylase partitioning and extractive bioconversion of starch using thermoseparating aqueous two-phase systems. *J. Biotechnol.* 93, 15–26. doi:10.1016/S0168-1656(01)00382-0.

Liu, C. G., Xiao, Y., Xia, X. X., Zhao, X. Q., Peng, L., Srinophakun, P., et al. (2019). Cellulosic ethanol production: Progress, challenges and strategies for solutions. *Biotechnol. Adv.* 37, 491–504. doi:10.1016/j.biotechadv.2019.03.002.

Malmsten, M., and Van Alstine, J. M. (1996). Adsorption of poly(ethylene glycol) amphiphiles to form coatings which inhibit protein adsorption. *J. Colloid Interface Sci.* 177, 502–512. doi:10.1006/jcis.1996.0064.

Miller, G. L. (1959). Use of Dinitrosalicylic Acid Reagent for Determination of Reducing Sugar. *Anal. Chem.* 31, 426–428.

Modenbach, A. A., and Nokes, S. E. (2013). Enzymatic hydrolysis of biomass at high-solids loadings - A review. *Biomass and Bioenergy* 56, 526–544. doi:10.1016/j.biombioe.2013.05.031 Review.

Mohagheghi, A., Tucker, M., Grohmann, K., and Wyman, C. (1992). High solids simultaneous saccharification and fermentation of pretreated wheat straw to ethanol. *Appl. Biochem. Biotechnol. Part A Enzym. Eng. Biotechnol.* 33, 67–81. doi:10.1007/BF02950778.



Newman, R. H., Vaidya, A. A., and Campion, S. H. (2013). A mathematical model for the inhibitory effects of lignin in enzymatic hydrolysis of lignocellulosics. *Bioresour. Technol.* 130, 757–762. doi:10.1016/j.biortech.2012.12.122.

Passoth, V., and Sandgren, M. (2019). Biofuel production from straw hydrolysates: current achievements and perspectives. *Appl. Microbiol. Biotechnol.* 103, 5105–5116. doi:10.1007/s00253-019-09863-3.

Pye, S., Li, F. G. N., Price, J., and Fais, B. (2017). Achieving net-zero emissions through the reframing of UK national targets in the post-Paris Agreement era. *Nat. Energy* 2, 1–8. doi:10.1038/nenergy.2017.24.

Rosgaard, L., Andric, P., Dam-Johansen, K., Pedersen, S., and Meyer, A. S. (2007). Effects of substrate loading on enzymatic hydrolysis and viscosity of pretreated barley straw. *Appl. Biochem. Biotechnol.* 143, 27–40. doi:10.1007/s12010-007-0028-1.

Selig, M., Weiss, N., and Ji, Y. (2008). Enzymatic Saccharification of Lignocellulosic Biomass. *Natl. Renew. Energy Lab.*, 1–5.

Silvério, S. C., Moreira, S., Milagres, A. M. F., Macedo, E. A., Teixeira, J. A., and Mussatto, S. I. (2012). Interference of some aqueous two-phase system phase-forming components in protein determination by the Bradford method. *Anal. Biochem.* 421, 719–724. doi:10.1016/j.ab.2011.12.020.

Sindhu, R., Binod, P., and Pandey, A. (2016). Biological pretreatment of lignocellulosic biomass - An overview. *Bioresour. Technol.* 199, 76–82. doi:10.1016/j.biortech.2015.08.030.

Singh, T., Vaidya, A. A., Donaldson, L. A., and Singh, A. P. (2016). Improvement in the enzymatic hydrolysis of biofuel substrate by a combined thermochemical and fungal pretreatment. *Wood Sci. Technol.* 50, 1003–1014. doi:10.1007/s00226-016-0838-9.

Sluiter, J. B., Chum, H., Gomes, A. C., Tavares, R. P. A., Azevedo, V., Pimenta, M. T. B., et al. (2016). Evaluation of Brazilian Sugarcane Bagasse Characterization: An Interlaboratory Comparison Study. *J. AOAC Int.* 99, 579–585. doi:10.5740/jaoacint.15-0063.

Stickel, J. J., Adhikari, B., Sievers, D. A., and Pellegrino, J. (2018). Continuous enzymatic hydrolysis of lignocellulosic biomass in a membrane-reactor system. *J. Chem. Technol. Biotechnol.* 93, 2181–2190. doi:10.1002/jctb.5559.

Straathof, A. J. J. (2014). Transformation of biomass into commodity chemicals using enzymes or cells. *Chem. Rev.* 114, 1871–1908. doi:10.1021/cr400309c.

Tjerneld, F., Persson, I., Albertsson, P.-Å., and Hahn-Hägerdal, B. (1985). Enzymatic hydrolysis of cellulose in aqueous two-phase systems. I. partition of cellulases from *Trichoderma reesei*. *Biotechnol. Bioeng.* 27, 1036–1043. doi:10.1002/bit.260270715.

Tjerneld, F., Persson, I., and Lee, J. M. (1991). Enzymatic cellulose hydrolysis in an attrition bioreactor combined with an aqueous two-phase system. *Biotechnol. Bioeng.* 37, 876–882. doi:10.1002/bit.260370912.

Torres, G. B. (2016). Decision Making at Early Design Stages: Economic Risk Analysis of Add-On Processes to Existing Sugarcane Biorefineries. Available at: <http://repositorio.unicamp.br/jspui/handle/REPOSIP/304789>.

UN Food and Agriculture Organization, C. S. D. (FAOSTAT). (2017). Sugarcane production in 2017, Crops/Regions/World/ Production. <http://www.fao.org/faostat/en/#data/QC>. Available at: <http://www.fao.org/faostat/en/#data/QC> [Accessed December 2, 2019].

Vaidya, A. A., Newman, R. H., Campion, S. H., and Suckling, I. D. (2014). Strength of adsorption of polyethylene glycol on pretreated *Pinus radiata* wood and consequences for enzymatic saccharification. *Biomass and Bioenergy* 70, 339–346. doi:10.1016/j.biombioe.2014.08.024.

Vaidya, A., and Singh, T. (2012). Pre-treatment of *Pinus radiata* substrates by basidiomycetes fungi to enhance enzymatic hydrolysis. *Biotechnol. Lett.* 34, 1263–1267. doi:10.1007/s10529-012-0894-7.

Van Sonsbeek, H. M., Beftink, H. H., and Tramper, J. (1993). Two-liquid-phase bioreactors. *Enzyme Microb. Technol.* 15, 722–9. doi:http://dx.doi.org/10.1016/0141-0229(93)90001-I.

Weiss, N., Börjesson, J., Pedersen, L. S., and Meyer, A. S. (2013). Enzymatic lignocellulose hydrolysis: Improved cellulase productivity by insoluble solids recycling. *Biotechnol. Biofuels* 6, 5. doi:10.1186/1754-6834-6-5.

Wu, Z., and Lee, Y. Y. (1997). Inhibition of the enzymatic hydrolysis of cellulose by ethanol. *Biotechnol. Lett.* 19, 977–979. doi:10.1023/A:1018487015129.

Xiao, Z., Zhang, X., Gregg, D. J., and Saddler, J. N. (2004). Effects of sugar inhibition on cellulases and  $\beta$ -glucosidase during enzymatic hydrolysis of softwood substrates. *Appl. Biochem. Biotechnol.* 115, 1115–1126. doi:10.1385/ABAB:115:1-3:1115.

Yang, J., Zhang, X., Yong, Q., and Yu, S. (2011). Three-stage enzymatic hydrolysis of steam-exploded corn stover at high substrate concentration. *Bioresour. Technol.* 102, 4905–4908. doi:10.1016/j.biortech.2010.12.047.



## CHAPTER 5

### **Model-based evaluation and techno-economic analysis of aqueous two-phase systems (ATPS) for enzymatic hydrolysis of sugarcane bagasse \***

Bianca Consorti Bussamra<sup>1,2</sup>, Vidhvath Viswanathan<sup>1</sup>, Solange I. Mussatto<sup>3</sup>, Aline Carvalho da Costa<sup>2</sup>, Luuk van der Wielen<sup>1,4</sup>, Marcel Ottens<sup>1</sup>

<sup>1</sup>Department of Biotechnology, Delft University of Technology. Van der Maasweg 9, 2629HZ. Delft, The Netherlands.

<sup>2</sup>Development of Processes and Products (DDPP), University of Campinas. Av. Albert Einstein, 500. Post Code: 6066. Campinas, Brazil.

<sup>3</sup>Department of Biotechnology and Biomedicine, Technical University of Denmark. Søltofts Plads, Building 223, 2800, Kongens Lyngby, Denmark.

<sup>4</sup>Bernal Institute, University of Limerick. Castletroy. Limerick, Ireland.

---

\* This Chapter will be submitted as: **Bussamra, B.C.**, Viswanathan, V., Mussatto, S.I., Carvalho da Costa, A., van der Wielen, L., Ottens, M., 2012.

### **Abstract**

Enzymatic hydrolysis is a key step in the breakdown of lignocellulosic materials, allowing access to the individual components (sugar monomers). However, enzymatic hydrolysis is inhibited by cellobiose (a reaction intermediate) and glucose (the final product) during the breakdown of cellulose. This drawback disables the effective use of high solid loads in lignocellulosic processes, since it would boost the need for more enzymes, and thereby elevate costs. A strategy to overcome the product inhibition is the execution of the hydrolysis while the products are being separated from the reaction. In this study, the extractive enzymatic hydrolysis of sugarcane bagasse based on aqueous two-phase systems (ATPS) was modelled by integrating hydrolysis and ATPS models. The developed integrated model enables the analysis of the ATPS hydrolysis (for batch and continuous mode) in terms of recycle of components and identification of the major influencers of the process, both technically and economically. In this conceptual design of extractive enzymatic hydrolysis, one of the major bottlenecks identified was the partitioning of glucose to both phases. To recover the product, the model counted with a multi cycle-batch to sequentially recover sugar from the bottom phase, by replacing the polymer-enriched phase (top phase). At each cycle, glucose could be separated by ultrafiltration from the top phase, while polymer was recycled back to the process to the next separation stage. The recovery and reuse of the phase forming components was imperative for economic feasibility.

**Keywords:** aqueous two-phase systems (ATPS), process design, extractive hydrolysis, process modelling, techno-economic analysis.

## 1. Introduction

In the search for alternatives of conventional oil and gas-based processes, the use of lignocellulosic materials has emerged as one of the potential feedstocks [1]. Lignocellulosic materials are primarily composed of cellulose, hemicellulose and lignin [2]. Glucose is an important product of the sugarcane bagasse valorisation chain as it is a precursor to a variety of other products [3]. When the lignocellulosic feedstock is used as a source of glucose, an entirely new supply chain is established. On the other hand, lignocellulosic material can also serve as an energy source.

Enzymatic hydrolysis is a key step in the breakdown of lignocellulosic material, where cellulose and hemicellulose are converted to glucose and other sugar monomers. While enzymatic hydrolysis is highly specific and requires mild reaction conditions, it suffers from the disadvantage of high cost and product inhibition [4]. The high cost of this unit operation is associated to the amount of catalyst, the hydrolysis yield, the recycle of enzymes, and the capital and operating costs associated with long hydrolysis time [5]. Regarding the product inhibition, different process configurations appear as an alternative to avoid high concentrations of sugars (cellobiose and glucose) in the reaction.

This work integrates aqueous two-phase system (ATPS) for enzymatic hydrolysis of sugarcane bagasse, via conceptual process design. When applied to enzymatic hydrolysis, the ATPS is expected to overcome the product inhibition caused by glucose on cellulase enzymes. Composed of two aqueous phases (PEG and salt), the ATPS could selectively separate the enzymes and sugars. The removal of the product from the reacting system is the best alternative to reduce product inhibition [6]. The continuous glucose removal can be acquired through bioreactor design, applying separate reactors for the reaction, or via membrane reactor [6]. The integration of the bioconversion with downstream processing steps has also been proved as a concept able to operate in continuous mode. Integrating ATPS to ultrafiltration unit operation creates a temporarily immobilized system with *in situ* product removal [7]. However, the evaluation of the ATPS process alternative to the enzymatic hydrolysis has not yet been performed at a conceptual design basis.

To compete with the conventional processes, the technical and economic feasibility are paramount. Here, the valorisation of the sugarcane bagasse chain considers the pre-treatment, enzymatic hydrolysis, and sugar recovery, focusing on the enzymatic hydrolysis unit operation. The model developed to provide a theoretical assessment of the ATPS for enzymatic hydrolysis combines an enzymatic hydrolysis model [8] and an empirical model describing the partitioning of solutes in ATPS [9]. For the enzymatic hydrolysis, the base case model assumes hydrolysis in a conventional (monophasic) system. The ATPS model integrates the reaction with a separation unit, which is developed as a multi-cycle batch process for the recovery of sugars. Apart from the conversion, other aspects of the process concerning the recyclability and reuse of system components are also evaluated. Experimental results were used to validate the models and fit model parameters.

The integrated model evaluated the performance for both batch and continuous systems. The concentration of both enzyme and glucose impacted the reaction kinetics. On comparing the operating costs for all scenarios, the conventional system for enzymatic hydrolysis succeeds because of the reduced processing equipment and costs associated with phase forming components.

## **2. Methods**

### **2.1. Research design**

The base scenario of this process involves the pre-treatment of the lignocellulosic material, the enzymatic hydrolysis in ATPS, and the recovery of glucose. The detailed design focused on the enzymatic hydrolysis. The designed case characterized by the ATPS hydrolysis was compared to the base case defined as conventional hydrolysis. Hydrothermal pre-treatment was considered for this design. The sugarcane hydrolysis in ATPS was conceptually assessed through the implementation of a model composed by two parts: hydrolysis and ATPS multi-batch separation. The integrated model was comprised of liquefaction of the biomass, hydrolysis reactor and separator, and ultrafiltration units. The choice for the downstream process to recover the sugar was assessed through a qualitative



analysis of four options of unit operations. The ATPSs were composed by potassium citrate or magnesium sulphate with polyethylene glycol (PEG). Depending on the salt used, the enzymes tend to partition to the bottom phase (magnesium sulphate) or to the top phase (potassium citrate) [10].

## **2.2. Selection of the sugar recovery unit operation**

Four downstream processing unit operations to recover the product after hydrolysis were assessed. The purification methods were evaluated according to nine qualitative parameters: process conditions (suitability of the process regarding temperature, pressure, harsh chemical environments); utility requirement (need of utilities, e.g. steam, electricity requirements, cooling/chilled water requirement); solvent recovery (the possibility to recover the solvents, otherwise there is a high impact on the waste production); product recovery (yield of the process); operating cost (the choice of raw material, mainly utilities and consumables); investment cost (process method and equipment, maturity of the technology, automation, scale of operation, number of equipment); technical feasibility (technology provider in lab/pilot scale, maturity of the technology); environment impact (amount of waste produced, waste treatment methods, impact of the chemicals/utilities used); product purity (purity of the final obtained product, the need and level of further polishing).

The characteristics of each purification method classified them in a grade scale of -1, 0 or +1, for each parameter. The selected unit operation was integrated to ATPS hydrolysis process design.

## **2.3. Base case definition**

The base case model is represented by the kinetics of conventional hydrolysis. Three reactors in series were designed to hydrolyse the biomass, operating as such that the purge of the previous reactor is the feed of the next one. The model description of the conventional hydrolysis is also used for the hydrolysis in ATPS in order to describe the biomass conversion prior to phase separation. Then, the process designs for the pre-treatment and enzymatic hydrolysis apply for both the base case and the ATPS hydrolysis.

### **2.3.1. Pre-treatment design**

The hydrothermal pre-treatment implemented at this work was designed by Inbicon [11] to the IBUS process. It presents commercial feasibility, high solids operability and high process recoveries. The choice for the hydrothermal pre-treatment concerned, apart from the environmentally benefits of the methods and the high content of cellulose in the fibres, the recovery of lignin and hemicellulose.

In the IBUS process, the dry matter content (bagasse) entering the process is assumed to be at 50% solid content, in a flow rate of 140 ton/h. A preliminary soaking reactor operates at 80 °C for 20 minutes. This process uses recycled water containing acetic acid released from the pre-treatment, reducing the pH of the biomass containing slurry and diluting it to 15% water insoluble solids (WIS)[12]. In the next step, the biomass is heated at 190 °C by introducing water at high pressure and temperature in liquid state. At this stage, the solids are increased to 35% WIS [12]. During the pre-treatment, the biomass (at 190 °C and 15 atm) is hydrolysed to breakdown the structural components and allow the access to the cellulose. The hydrothermal reactor operates in continuous counter-current mode. The liquid fraction (hydrolysate) containing 5% WIS moves to a multi-effect evaporation system to concentrate the hydrolysate. The steam used for the evaporation is obtained during the depressurisation of biomass and liquid fractions after pre-treatment. The obtained condensate after evaporation (containing acetic acid) is recycled back to the soaking reactor. A purge stream is introduced to prevent the accumulation of the degradation products. Finally, the pre-treated biomass (20% WIS) is cooled and depressurized to proceed to the enzymatic hydrolysis step, which is performed at 50 °C. The transfer between reactors was done using particle pumps.

### **2.3.2. Enzymatic hydrolysis design**

The incoming stream from the hydrothermal pre-treatment is a fibrous slurry containing mainly cellulose and lignin. The flow rates, in order to keep the WIS % constant, are represented in Table 1. In reactor 1, the NREL reported flow rate [8] was scaled up to the flows of this study. For. reactors 2 and 3, the flow rates were

modified such as the WIS (w/w %) was constant throughout. Although no extra enzymes were added, 50% of the enzyme load of the previous reactor was considered to recycle back to the system. The enzyme load corresponds to 20 mg/g glucan. The residence time is defined by the volume divided by the purge flow.

The dry mass fraction of enzymatic hydrolysis determines the final concentration of the product [6]. NREL reports enzymatic hydrolysis on 20% WIS [13]. The IBUS process performs enzymatic hydrolysis at 25% solids. Here, the design focussed on 20% solids. The composition of the biomass is represented in Table 2.

Table 1: Flow ratios for the hydrolysis reactors in the base case.

	Reactor 1	Reactor 2	Reactor 3
Feed (ton/h)	266.6	85.3	45.19
Enzyme input (ton/h)	28.4	-	-
Hydrolysate (ton/h)	209.7	40.12	10.3
Purge (ton/h)	85.3	45.19	34.89
Volume (m <sup>3</sup> )	2660	2660	2660
Residence time (h)	31	5	76

Table 2: Biomass composition and properties used in the hydrolysis experiments and hydrolysis model reported by Stickel et al. (2017) [8]. The simulations reproduced from Stickel et al. (2017) [8] were performed with different bagasse compositions, named Lot 1 and Lot 2. The former represents a washed pre-treated biomass with reduced amount of soluble sugars in comparison to Lot 2.

	Experimental	Lot 1 [8]	Lot 2 [8]
Mass fraction total solids of slurry	-	0.301	0.389
Mass fraction insoluble solids of slurry	-	0.173	0.201
Lignin fraction of solids	0.12	0.30	0.27
Polysaccharide fraction of solids	0.79 (cellulose); 0.02 (hemicellulose)	0.64	0.65
Ash fraction of solids	0.06	0.04	0.02

Density of liquid (g/mL)	-	1.08	1.08
Soluble sugar concentration (g/L)	-	139	182

Note: the polysaccharide fraction of solids does not include xylan.

After the establishment of the batch process simulation, the model was extended for the continuous process. In the continuous process, there is an initial start-up batch phase, followed by a continuous phase. The start-up batch phase is defined by the residence time of that phase. In the continuous model, the feed rate is balanced with the rate of hydrolysis, to be able to maintain constant WIS [8]. A direct scale-up of the parameters was performed for the design flow rate at this work (20% WIS). The values considered for the scale up were the flow ratios and the feed/reactor mass ratio.

#### 2.4. Enzymatic hydrolysis

The experimental hydrolysis was performed at pH 4.8 (citrate buffer 50mM), with 0.02% sodium azide. The conventional hydrolysis kinetics at solid load 10% WIS (hydrothermal pre-treated bagasse, Table 2) was performed at enzyme loads of 10, 20, and 40 FPU/g bagasse at a reaction volume of 30mL. The enzymatic cocktail, available as Cellic CTec 2 (Novozymes, Bagsværd, Denmark), presented  $77.6 \pm 2.2$  mg/mL protein content, and activity of 169.5 FPU/mL (being FPU, filter paper activity [14]). The results of these experiments were published by Bussamra et al., 2020 [10].

#### 2.5. Hydrolysis model

The enzymatic reaction was described by a Michaelis-Menten kinetic model, based on product competitive-inhibition [8]. This model has been applied and studied for the continuous hydrolysis [8], and can be integrated with an ATPS model. The model allows for comparison with experimental data, since it takes into consideration known parameters: concentration of glucan, glucose and enzymes. Even though other models could satisfactorily represent the reaction [15], unknown parameters would be needed, such as the individual enzyme concentrations.

The implemented model aims at giving an initial estimation on the influence of glucose on the reaction kinetics in a continuous process. The overall scheme of the process modelled at this stage is shown in Figure 1. The input streams of the process are the feed containing pre-treated biomass (F1), and the buffered enzyme stream (F2). The final product is obtained in the purified sugar stream (F3) after a solid-liquid separation. A purge stream (F4) removes the accumulated lignin to keep the reactor solid content constant. The mass flow rates were expressed in kg/h. The mass balances were performed for glucan (G), insoluble lignin (L), glucose (g), xylose (x), soluble lignin (sl), enzyme (e) and reaction mass (mT, in kg). The concentration terms are expressed in mass fractions, *fi*.

The basic equations used for the hydrolysis model are described below [8].

$$\frac{dm_T}{dt} = F_1 + F_2 - F_3 - F_4 \quad (1)$$

$$\frac{df_L}{dt} = \frac{F_1}{m_T} f_{L1} - \frac{F_4}{m_T} f_{L4} + R_L - \frac{f_L}{m_T} \frac{dm_T}{dt} \quad (2)$$

$$\frac{df_G}{dt} = \frac{F_1}{m_T} f_{G1} - \frac{F_4}{m_T} f_{G4} + R_G - \frac{f_G}{m_T} \frac{dm_T}{dt} \quad (3)$$

$$\frac{df_e}{dt} = \frac{F_2}{m_T} f_{e2} - \frac{F_3}{m_T} f_{e3} - \frac{F_4}{m_T} f_{e4} - \frac{f_e}{m_T} \frac{dm_T}{dt} \quad (4)$$

$$\frac{df_{sl}}{dt} = \frac{F_1}{m_T} f_{sl1} - \frac{F_3}{m_T} f_{sl3} - \frac{F_4}{m_T} f_{sl4} + R_{sl} - \frac{f_{sl}}{m_T} \frac{dm_T}{dt} \quad (5)$$

$$\frac{df_g}{dt} = \frac{F_1}{m_T} f_{g1} - \frac{F_3}{m_T} f_{g3} - \frac{F_4}{m_T} f_{g4} + R_g - \frac{f_g}{m_T} \frac{dm_T}{dt} \quad (6)$$

$$\frac{df_x}{dt} = \frac{F_1}{m_T} f_{x1} - \frac{F_3}{m_T} f_{x3} - \frac{F_4}{m_T} f_{x4} - R_x - \frac{f_x}{m_T} \frac{dm_T}{dt} \quad (7)$$

For the batch model, the flows in Equations 1 to 7 were set to zero. Since the volume was constant throughout, the term  $\frac{dm_T}{dt}$  was set to 0.

The reaction rate for glucan conversion to glucose is given by

$$\tilde{r} = k_{cat} \tilde{c}_{eA} \quad (8)$$

where  $k_{cat}$  is the enzyme disassociation constant (1/h), and  $\tilde{c}_{eA}$  (mol/m<sup>3</sup> slurry) is the concentration of enzymes absorbed in biomass, defined by

$$\tilde{c}_{eA} = \frac{\tilde{c}_G \tilde{c}_e}{\tilde{c}_G + \epsilon_l k_m [1 + (c_g + c_x)/k_I]}, \quad (9)$$

where  $c_g$  and  $c_x$  are the molar concentrations (mol/ m<sup>3</sup> slurry) of glucose and xylose, respectively, and  $k_m$  and  $k_I$  are the Michaelis-Menten constant and inhibition constant, respectively.

The concentrations in slurry basis (lignin and glucan) are presented with the tilde, while those without the tilde are in liquid basis. All concentrations are expressed in kmol/m<sup>3</sup>, unless otherwise mentioned. The  $\epsilon_l$  parameter relates the liquid and slurry volumes, as follows

$$\epsilon_l = \frac{\rho_T}{\rho_l} f_l \quad (10)$$

where  $\rho_T$  and  $\rho_l$  are the slurry and liquid densities, respectively.  $f_l$  is the liquid fraction ( $1 - f_{is}$ ), where  $f_{is}$  is the fraction of insoluble solids (*glucan + lignin*).

$$\rho_T = \left( \frac{f_{is}}{\rho_{is}} + \frac{f_l}{\rho_l} \right)^{-1} \quad (11)$$

The liquid and slurry concentrations can then be related by the following relations:

$$\tilde{c}_i = \epsilon_l c_i \quad (12)$$

$$c_i = \frac{\rho_T}{\epsilon_l \cdot MW_i} f_i \quad (13)$$

Finally, the reaction rate equations, in mass fraction concentration units (kg/kg.h) are given by:

$$R_G = - \frac{MW_G}{\rho_T} \tilde{r} \quad (14)$$

$$R_g = \frac{MW_g}{\rho_T} \tilde{r} \quad (15)$$

$$R_L = R_G k_L \frac{MW_L}{MW_G} \quad (16)$$

$$R_{sl} = -R_L \quad (17)$$

The lignin solubilisation rate  $R_L$  is presented as a factor of the glucan solubilisation rate (Equation 16). In order to maintain the lignin profile constant in the continuous process simulation, the  $R_L$  was normalized by multiplying it by the term  $\frac{MW_L}{MW_G} \cdot k_L$  assumed the value of 0.6.

The parameters of the batch model were regressed using the experimental data published [8]. These points were extracted using a Matlab built code available online called 'grabit' [16]. The values of the fit parameters are shown in Table 3.

Table 3: Rate model fitting parameters [8].

Parameter	Value
$k_m$	0.046 mol/L
$k_I$	0.033 mol/L
$k_{cat}$	4200 (1/h)

Even though Table 2 shows the total soluble sugar concentration, Equation 9 of the model requires the initial concentration of xylose and glucose. These concentrations were defined based on results from McMillan et al. (2011), where the concentration of xylose and glucose are 89.9 and 29.3 g/l respectively [17], while the total soluble sugar concentration is 139 g/L. The concentration of xylose and glucose were then normalised to the concentrations of Lot 2 (117.71 g/l and 38.36 g/l, xylose and glucose respectively). The enzyme molecular weight was defined at 65 kDa (65000 g/mol), which is the molecular weight of the cellobiohydrolases. The molecular weight of glucan, glucose, xylose and lignin were set at 162, 180, 150 and 122 g/mol, respectively.

## 2.6. ATPS model

The ATPS selectively partitions the molecules to a preferential phase. The binodal curves and empirical relationships were obtained from Bussamra et al. (2019) [18]. For a given system and inlet concentration, the equilibrium data (outlet concentrations) were estimated. The ATPS model [9] was initially implemented for a single batch process, and later extended to a single multi-cycle batch process followed by a continuous model. All values and parameters were estimated from Patel et al. (2018) [9] and Mistry et al. (1966) [19], unless mentioned otherwise.

The equilibrium concentrations are calculated as follows:

$$\frac{dm_i}{dt} = F_1x_{1,i} + F_2x_{2,i} - F_3x_{3,i} - F_4x_{4,i} \quad (18)$$

$$x_{3,i} = x_{top,i} \quad (19)$$

$$x_{2,i} = x_{bottom,i} \quad (20)$$

$$K_i = \frac{C_{top,i}}{C_{bottom,i}} \quad (21)$$

$$M_{O,i} = M_{top,i} + M_{bottom,i} \quad (22)$$

$$x_{top,i} \times \sum M_{top,i} = M_{top,i} \quad (23)$$

where  $F_i$  and  $x_i$  are the flow (kg/s) and mass fraction (%), respectively, and  $i$  represents the components.  $M_i$  means the total (kg), and  $C_i$  the concentration of solute (g/L)  $i$ .

For the binodal data and tie-line determination, empirical correlations were used as reported by Mistry et al. (1996) [19]:

$$\ln(PEG) = A + BX^3 + C\sqrt{X} \quad (24)$$

$$A = A_0 + A_1N + A_2\sqrt{N} \quad (25)$$

$$B = B_0 + B_1\sqrt{N} \quad (26)$$

$$C = C_0 + C_1N + C_2N\sqrt{N} \quad (27)$$



Where  $N$  is the concentration of sodium chloride.

Inlet composition and flow rates can be used to estimate the average concentration of the phase forming components  $\overline{P_{i,j}}$ , according to the following formula:

$$\overline{P_{i,j}} = \frac{\sum_{in} F_i P_i}{\sum_{in} F_i} \quad (28)$$

The tie-lines can be determined through an empirical model considering the slope ( $D_1$ ) and intercept ( $D_2$ ), as follows:

$$PEG = D_1 \cdot Salt + D_2 \quad (29)$$

With the model equations, the system was first analysed for a multi-cycle batch process (sequential reactor). The multicycle process consists of a filling step, mixing and settling (not modelled), draining the bottom phase and refilling the batch with fresh salt. For this analysis, the bagasse was assumed to partition to the bottom phase. The remaining unconverted biomass and lignin stream were separated from the aqueous salt phase containing enzymes via solid-liquid separation. The enzymes were recycled back to the system. In the ultrafiltration modelling, the retention factor for PEG and sugar were defined as 1 and 0, respectively. The phase compositions, binodal curve and tie-lines were estimated only once (after filling), rather than after each point in the simulation.

In this design, the slope of the ATPS (magnesium sulphate + PEG 6000) was based on experimental data [18]. Knowing the slope (-1.53) and the average concentration on inlet stream, the intercept could be determined. It was assumed that the tie lines were parallel to each other (equal slope). Even though the design begins with the assumption of using a single tie line, the phase composition quickly changes, when assuming the addition of fresh phase forming compound. Here, the phase composition was assumed constant for each cycle. Consequently, the partition coefficient was assumed to be a single absolute value, not deriving from the polynomial equations.

The theoretical purity of the sugars and enzymes (solutes defined as  $i$  and  $j$ ) was calculated according to Equation 32 [20], where  $P_{i,\alpha}$  is the purity of a solute specified as  $i$  in the respective phase  $\alpha$  (recovery phase). This calculation only considers the sugar and protein fractions and hence the purity is relative to only these two components.

$$P_{i,\alpha} = \frac{100Y_{i,\alpha}C_i}{Y_{i,\alpha}C_i + (100 - Y_{j,\alpha \neq 1})C_j} \quad (30)$$

$C_i$  represents the concentration of the solute  $i$ . The yield  $Y$  is defined for top and bottom phases as follows:

$$Y_{top,i} = \frac{100}{1 + \left(\frac{1}{R} \frac{1}{K_i}\right)} \quad (31)$$

$$Y_{bottom,i} = \frac{100}{1 + (RK_i)} \quad (32)$$

where  $R$  is the phase volume ratio defined by the volume of top phase divided by the volume of bottom phase, and  $K_i$  is the partition coefficient of the solute  $i$ .

## 2.7. Process design: integrated model

The hydrolysis and ATPS formation are integrated as an extractive reaction (Figure 1). Even though they are combined in the process, they are designed and treated as individual tasks. The systems formed by PEG and a salt (potassium citrate or magnesium sulphate) were selected based on a previous study [18]. The selection was based mainly on the partition coefficients of the solutes.

The hydrolysate from the conventional hydrolysis reactor is processed in the ATPS reactor, where sugars and enzymes partition according to their partition coefficients. The product (glucose) enriched phase (top or bottom) depends on the phase forming component being applied. Here, for both configurations the glucose was assumed to be recovered in the top phase. The sugars from the top phase are separated from PEG in an ultrafiltration operation.

In the batch process configuration, ATPS can sequentially repartition sugars from the bottom phase to top phase by providing fresh PEG to the system. In this case, the concentrated PEG from the ultrafiltration top phase outlet can be recycled and reused. The PEG obtained in the retentate of the ultrafiltration operation is reintroduced in a next ATP reactor (ATPS 2) along with the bottom phase of ATPS 1. At this stage, if salt concentration in the bottom phase exceeded 30% WIS, the retentate was diluted with a water stream. It is assumed that the ATPS is performed at hydrolysis temperature to maintain enzymatic activity. The reaction rate is calculated in a single phase (reaction phase), considering the compositions of the respective phase and partitioning of the substrate (bagasse) and enzymes totally to that phase.

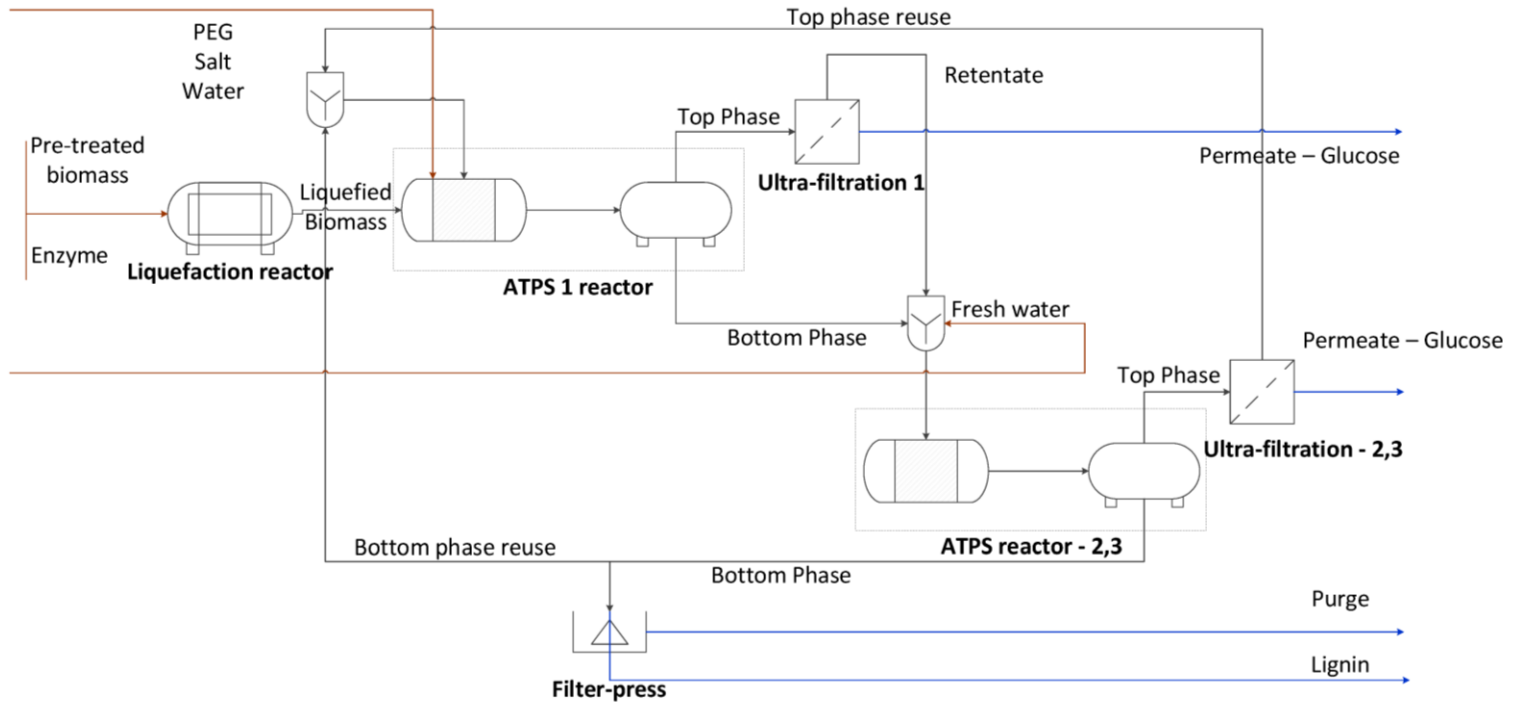


Figure 1: Schematic representation of the integrated model, considering the sequential separation of glucose from bottom phase to top phase.

Table 4: Assumptions considered for the liquefaction and batch ATPS hydrolysis reactors, and configuration for the ultrafiltration and filter press units.

Liquefaction (L) and ATPS hydrolysis (H)		Ultrafiltration and filter press	
Temperature	50 °C	Insolubles retention coefficient	1
Initial solids loading (L)	35% WIS [11]	Solubles retention coefficient	0
Enzyme load (L)	10 mg/g glucan	Salt retention coefficient	0
Protein concentration (L)	74.6 g/L	PEG retention coefficient	1
Residence time (L)	6 h [11]	Enzyme retention coefficient	0.5
Glucan conversion (L)	32% [11]	Concentration factor	1.5
Hemicellulose conversion (L)	49%	ATPS 3 bottom phase split to reactor	0.6
Initial solids loading (H)	15% WIS	Insolubles recovery in filter press	99.5%
Enzyme load after liquefaction (H)	14.6 mg/g glucan	Solubles in filtrate of filter press	93.5%
Glucan conversion (H)	90%	Cake dry mass of filter press	60-65%
Settler residence time (H)	5 h		

The configuration of the processes for both magnesium sulphate and potassium citrate based systems are represented elsewhere [10]. The first step in the enzymatic hydrolysis is the liquefaction reactor, which is performed in a rotating drum reactor at high solid loads. The high solids feed (35% WIS) is mixed with enzymes in the drum reactor which uses the principle of gravity mixing and thus enables mixing at high solids [11]. The parameters of the liquefaction reactor are presented in Table4.

At the batch reactor, the liquefied fraction (hydrolysate from the liquefaction reactor) is mixed with the phase forming components such that the final solids are 15% WIS. The process is assumed to proceed up to 90% conversion of the initial glucan in the reactor. Only glucan hydrolysis was considered — xylan and oligomers remain unconverted (Table 4).

Before the top phase is processed in the ultrafiltration unit, the hydrolysis broth separates to top and bottom phases in a settler. For the recycle of PEG, a concentration factor of 1.5 is assumed at the ultrafiltration unit. The cycles, consisting of ATPS formation, phase separation and recovery/recycle of products, occurs for three times. The ultrafiltration set-up is shown in Table4.

The partition coefficients for sugars and proteins were obtained from Bussamra et al., 2019 [18]. For the magnesium sulphate based system, glucan and lignin were assumed to partition to the bottom phase ( $k = 0.001$ ). Glucose and xylose were assumed to have the same partition coefficient, as that for soluble lignin ( $k = 0.71$ ). Enzymes had their partition coefficients at  $k = 0.21$ . For the potassium citrate case, the bagasse is assumed to partition to the top phase along with the enzymes ( $k = 1.5$ , for both proteins and insoluble solids). The partition coefficient for sugar was taken as  $k = 0.6$ . The top phase from the ATPS reactor is split to two fractions, one to lignin separation and the other to the ultrafiltration (fraction of ATPS top phase split to lignin is equal to 0.6). Lignin separation reduces the solids fraction processed before the first ultrafiltration and the choking of the membrane. The lignin was separated in a filter-press as a cake, while the filtrate was combined with the top phase fraction and processed in the ultrafiltration unit. Table5 summarized the characteristics of both magnesium sulphate and potassium citrate-based systems.

A sensitivity analysis on the partition coefficient of sugars and retention coefficient of enzymes was performed in order to evaluate their influence on the hydrolysis performance. The influence of the partition coefficient of sugar was assessed for the magnesium sulphate based system, and the retention coefficient for the potassium citrate-based system.

Table 5: Process configurations for the extractive hydrolysis in both magnesium sulphate and potassium citrate based ATPS.

<b>Magnesium sulphate</b>	<b>Potassium citrate</b>
Glucan and enzyme partition to bottom phase	Glucan and enzyme partition to top phase
Reaction occurs in bottom phase	Reaction occurs in top phase
Glucose partitions to top/bottom phase ( $k = 1.5$ or $k = 0.71$ )	Glucose partitions to bottom phase ( $k = 0.6$ )
Lignin separation after glucose repartitioning	Lignin separation before first ultrafiltration
Enzyme recycling from bottom phase (High recovery)	Enzyme recycling from top phase (50% or 90% enzyme retention)

For the simulation of the continuous process, all assumptions from the batch process configuration remained the same, unless mentioned otherwise. The recycled stream of the batch process was used as a starting point to estimate the recycle stream composition of the continuous system, which was determined for every time point until steady state was achieved. The enzyme load was set at 20 mg/g glucan (in order to compare with the base model).

The inlet flow streams for the continuous reactor were the liquefied biomass from the liquefaction reactor and the recycle stream containing the phase forming components. Two outlet streams were considered, one which was processed in the ultrafiltration unit and the purge stream to maintain the reactor solids content constant. The purge stream also acts as phase forming components for the succeeding ATPS reactor.

## 2.8. Economic margin of the design case and economic evaluation of the integrated case.

For the economic feasibility achievement, an intern rate return (IRR) higher than 5% was stipulated, and 330 operating days were taken as representation of the sugarcane harvest period in Brazil. All reactor equipment were assumed to be 304 SS [21]. For the liquefaction reactor, a maximum reactor volume of 250 kgallons was assumed [3]. The batch hydrolysis reactors have been scaled to the maximum reactor size available for processing, 1 M gallons [21] [22]. For the settler unit, a maximum size of 500 kgallons was assumed. Ultra-filtration units were sized based on the permeate flow at an average flux of 67 kg/m<sup>2</sup>/hr [22]. For the lignin press, a maximum membrane area of 170 m<sup>2</sup> was used to determine number of equipment [22]. The pumps were sized according to the required flow rates.

The ATPS configuration (reaction occurring in top or bottom phase) was economically evaluated for a batch process. The capital investment was estimated based on the equipment size for both potassium citrate and magnesium sulphate systems. The equipment comprised of three ATPS units (ATPS 1, ATPS 2, ATPS 3), three ultrafiltration units (UF 1, UF 2, UF 3) and a filter press. The purchase costs [21] [22] were scaled based on the plant cost index [21].

$$Purchase\ cost = base\ cost \frac{purchase\ year\ index}{base\ year\ index} \quad (33)$$

$$New\ cost = base\ cost \left( \frac{new\ size}{base\ size} \right)^n \quad (34)$$

The total capital investment costs considered the equipment purchase and installation costs. The calculation basis of each subcategory of the capital investment costs is presented in Table 6.

Table 6: Calculation basis of the total capital investment and operating costs in terms of installed cost (ISC), total direct cost (TDC), fixed capital investment (FCI) or total manufacturing cost (TMC).



Capital investment cost	Factor
Warehouse	4% of ISC
Site Development	9% of ISC
Additional Piping	4.5% of ISC
Prorateable Expenses	10% of TDC
Field Expenses	10% of TDC
Home Office & Construction Fee	20% of TDC
Project Contingency	10% of TDC
Other Costs (Start-Up. Permits. etc.)	10% of TDC
Land	2% of FCI
Working capital	5% of FCI
Maintenance and repairs	3.5% of FCI
Operating supplies	1.25% of FCI
Operating labour	15 % of TMC

The operating costs of the process includes the costs of the raw materials, operating labour, utilities, and equipment related maintenance costs. Enzymes were assumed at € 517/ton and costs were estimated for an enzyme load of 10 mg/g glucan for all scenarios. Utilities were considered as a factor of 0.25 to the raw materials cost assumed for the conventional system [23]. To take into account the additional equipment and associated utility costs for the ATPS hydrolysis system, the utilities cost from the conventional system is multiplied by a factor of 1.5. The other costs were calculated as a factor of the fixed capital investment (FCI) or total manufacturing cost (TMC) [23], as shown in Table 6.

For the sensitivity analysis, the parameters enzyme, sugarcane bagasse and potassium citrate costs varied with  $\pm 10\%$  and  $\pm 25\%$ . The potassium citrate cost was also evaluated at the level - 50%. Their impact was analysed on the operating costs.

For the economic evaluation of the continuous process, the base model was extended with a micro filtration unit for sugar separation and an ultrafiltration unit for enzyme recovery, according to the model designed by NREL [22]. The operating

costs for the continuous system were estimated based on the mass balances for the individual systems. The utility costs for the microfiltration and ultrafiltration of the base case assumed a factor of 0.30 in relation to the raw material costs, and was considered to be the same for the ATPS process.

### 3. Results and Discussion

#### 3.1. Sugar recovery strategy

The sugar recovery after hydrolysis contributes to the techno and economic feasibility of the process. The purification method depends, however, on the application of the sugars produced. Here, simulated moving bed (SMB) chromatography, fixed bed batch ion exchange (IEX) chromatography, evaporation and ultrafiltration were evaluated. SMB has been used for the separation of glucose from other mono-sugars and process impurities [24] [25]. Also, IEX has been used to isolate the mono sugars at different purities [26] [27]. Evaporation has been used for concentrating sugar streams from the enzymatic hydrolysate [13]. Literature reports the use of ultrafiltration to separate the sugars at a cut off molecular weight membrane of 50 kDa [4]. By the qualitative analysis on the individual methods (Table 7Table ), ultrafiltration was selected as the unit operation to recover sugar in the ATPS hydrolysis design presented here. From Table 7, it can be seen that SMB, IEX and ultrafiltration have similar outcomes, with no specific weighing factors on the metrics. While SMB and IEX are advantageous in terms of final product purity, the high cost and complexity are disadvantages. The drawback of ultrafiltration in terms of final product purity relies on its inability to separate the individual sugars. However, the presence of monomers of sugar with five and six carbons can still be interesting for a biorefinery context [28].

Table 7: Qualitative analysis on a three-point scale basis (-1, 0, +1) of the downstream method to recover sugars after the hydrolysis of sugarcane bagasse.

Metrics	SMB	IEX	Evaporation	Ultrafiltration
Process condition	+1	+1	-1	+1

Utility requirement	0	0	-1	0
Solvent & recovery	+1	+1	+1	+1
Product recovery	+1	+1	-1	0
Operating cost	0	0	-1	0
Investment cost	-1	-1	0	+1
Feasibility	0	0	+1	+1
Environment impact	0	0	-1	0
Product purity	+1	+1	-1	-1
Total evaluation	+3	+3	-4	+3

### 3.2. Enzymatic hydrolysis model

The model implemented at this work was sufficient similar to the results published by Stickel et al., 2018 [8] (data not shown), and our implementation could be extended for the continuous model. A direct scale-up of the parameters was performed for our design flow rate, assuming 20% WIS (Figure 2). The steady state concentration of glucose for this system is around 100 g/L. These set of values were used for the process modelling and as the basis for comparison.

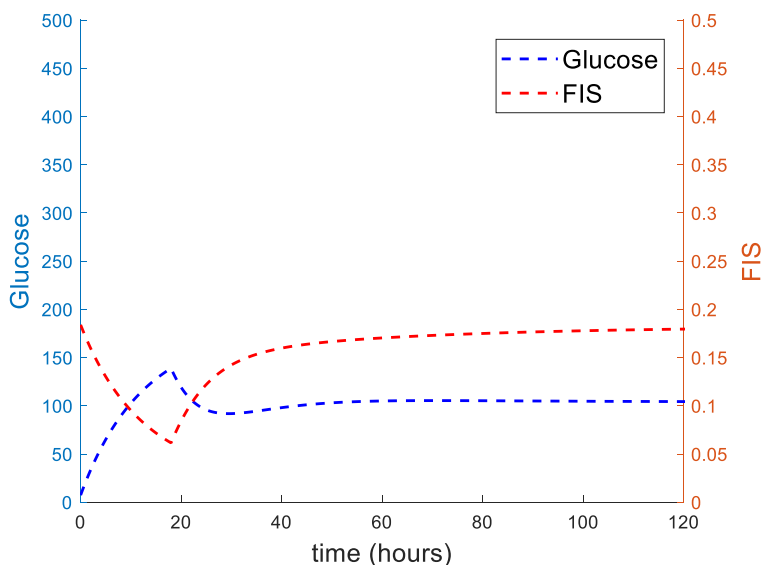


Figure 2: Concentration profile of glucose (g/L) and insoluble solids (FIS %) for the ATPS hydrolysis design in continuous mode.

Even though the presence of inhibitors such as sugar and acetic acid impacts the completion of conversion and fit of the reaction model to the experimental data [8], here we show that the enzyme load also affects the model fit. The activity of the enzymes used in the NREL model [8] is not known. For the experimental hydrolysis, the enzymatic activity (FPU/mL) impacts the amount of calculated enzymes (in mg) as an input to the model. The enzyme load of 20 FPU/g bagasse (approximately 8.8 mg protein/g bagasse) presented the best fit to the hydrolysis model (Figure 3).

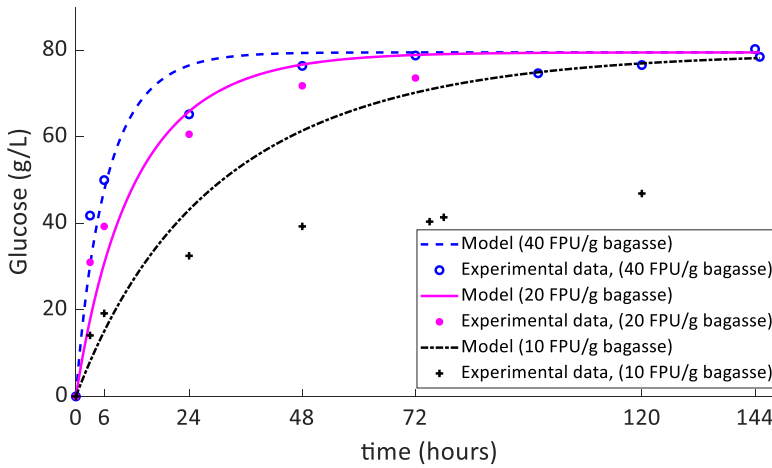


Figure 3: Batch-mode enzymatic hydrolysis of hydrothermal pre-treated bagasse (10% WIS) under three different loads of enzymes (10, 20 and 40 FPU/g bagasse) and the fitting to the hydrolysis model.

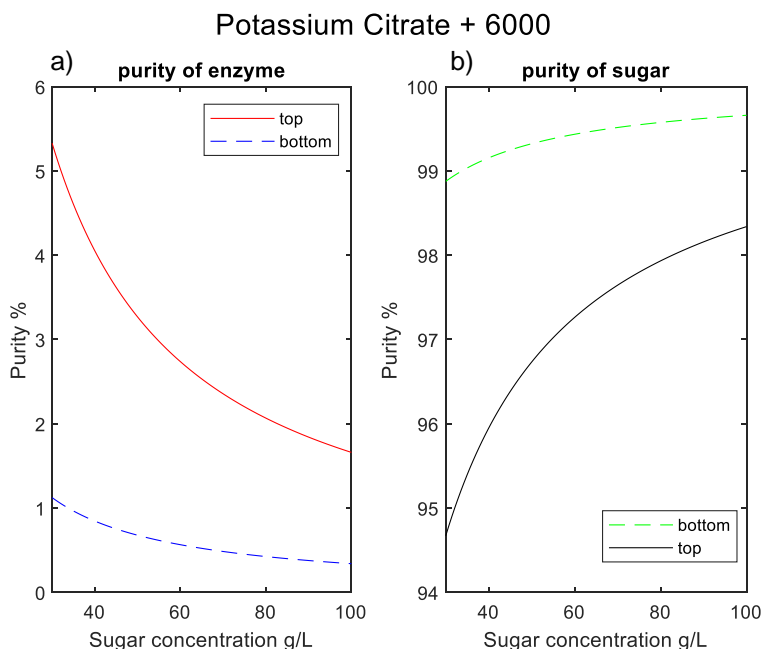
The pumping of the slurry substrate is a logistical challenge when operating the continuous enzymatic hydrolysis of lignocellulosic biomass [8]. The liquefaction unit operation reduces the solid load in ATPS reactor and offer a better integration of the recycled phase forming components. While solid loads up to 30% have been reported [29], experimental results were available for 10% solid loads, being this the solid load of the simulations presented at this work.

### 3.3. ATPS model

The ATPS model implemented here was compared to the literature case published by Patel et al. [9], showing similar results (data not shown). The contact of the bottom phase with a concentrated retentate stream allows the achievement of new equilibrium and a consecutive partition of glucose [10]. The volume ratio of the new composition also plays a role in the glucose repartitioning. The higher concentration of PEG in the retentate causes an increase in the phase ratio and a shift to a higher tie-line in comparison to the previous equilibrium. The model developed through empirical correlations can predict these compositions. However, only absolute values of partition coefficients have been used by our models. The impact of dilutions

(via make-up streams) and change in volume ratios during the process were not considered. For each purification cycle, a certain fraction of enzymes can possibly be recovered in the ultrafiltration along with the PEG in the retentate and thus improving the enzyme reusability. Continuous separation of glucose in ATPS through ultrafiltration has also been reported [7], for a molecular weight cut-off of the membrane at 10 kDa.

Even though an uneven partition coefficient of the solutes is desired to an extractive process based on ATPS, the disparity in the amount of the solutes influences mostly the separation. In an enzymatic hydrolysis of biomass, sugars are more abundant than enzymes. In this scenario, although sugar presented similar partition between the phases [18], the purities of these solute are considerably higher than that of the enzymes (Figure 4). Then, the selective partitioning of enzymes does not influence on the purity of this solute for neither phases.



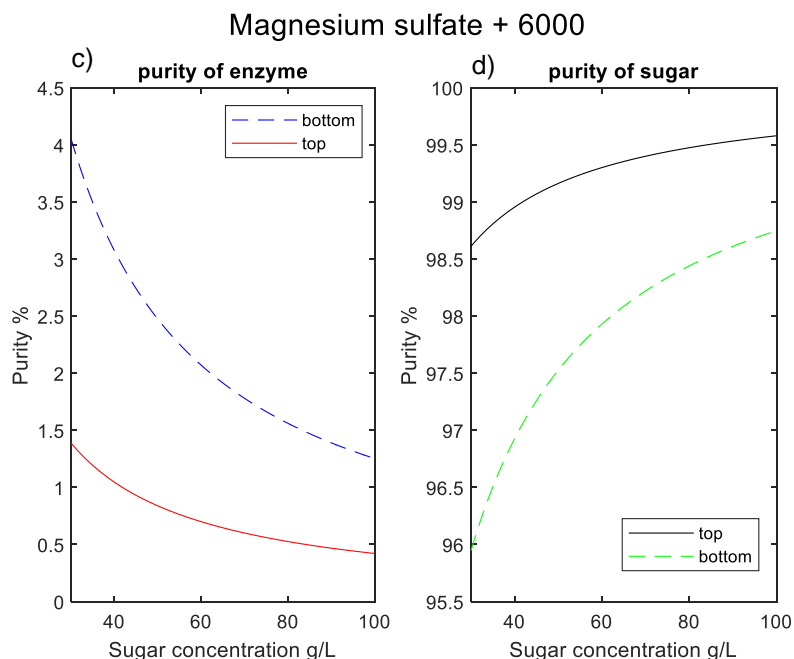


Figure 4: Purity of enzymes and sugar in both top and bottom phases, at different concentrations of sugar (30 to 100 g/L) and constant load of enzymes (0.9 g/L, which represents the protein concentration in a hydrolysis system at 20% WIS, loaded at 10 FPU/g bagasse). a) and b) represents the ATPS composed by potassium citrate and PEG 6000 (TLL 34.2%,  $k_s = 0.6$ ,  $k_e = 12$ ); c) and d) represents the ATPS composed by magnesium sulphate and PEG 6000 (TLL 34.2%,  $k_s = 0.6$ ,  $k_e = 0.2$ ). Partition coefficient data were retrieved from [30].

### 3.4. Process design

According to the model-based analysis for the batch process, ATPS hydrolysis performed better than the conventional hydrolysis (base case) after 15 h reaction (Table 8), even though the glucose (inhibitor) concentration in the reaction phase (bottom phase for the magnesium sulphate system) was higher when operating in ATPS. The overall mass balance for the batch process for both salt-based ATPS are presented as Supplementary Material. The reaction rate is a function of adsorbed enzymes, concentration of glucan and sugar monomers. Consequently, the relative

concentration of glucan and adsorbed enzymes are higher when compared to the conventional system, contributing to superior reaction rate.

Table 8: Simulated hydrolysis performance for conventional and magnesium sulphate based ATPS.

	Conventional	ATPS		
		$k_s = 0.71$	$k_s = 1$	$k_s = 1.5$
Conversion after 15 h reaction (%)	68.3	74.6	77.8	82.3
Glucose concentration (% w/w)	13.2	-	-	-
Glucose top phase (% w/w)	-	11.4	14.6	18.8
Glucose bottom phase (% w/w)	-	16.1	14.6	12.5

The integrated ATPS reactor and separator allows the simultaneous hydrolysis and ATPS formation, leading to a continuous separation of glucose from the reaction phase. However, systems presenting high sugar concentrations can achieve the inhibitory concentration in the reaction phase due to the partition coefficient close to the unit for the ATPS formed by the salts potassium citrate or magnesium sulphate and the polymer [18] .

The phase forming components reduce the activities of the enzymes by approximately 50% [18]. In order to mimic this scenario, a simulation was performed such that the enzyme concentration was reduced by half (Figure 5 and Table 9).



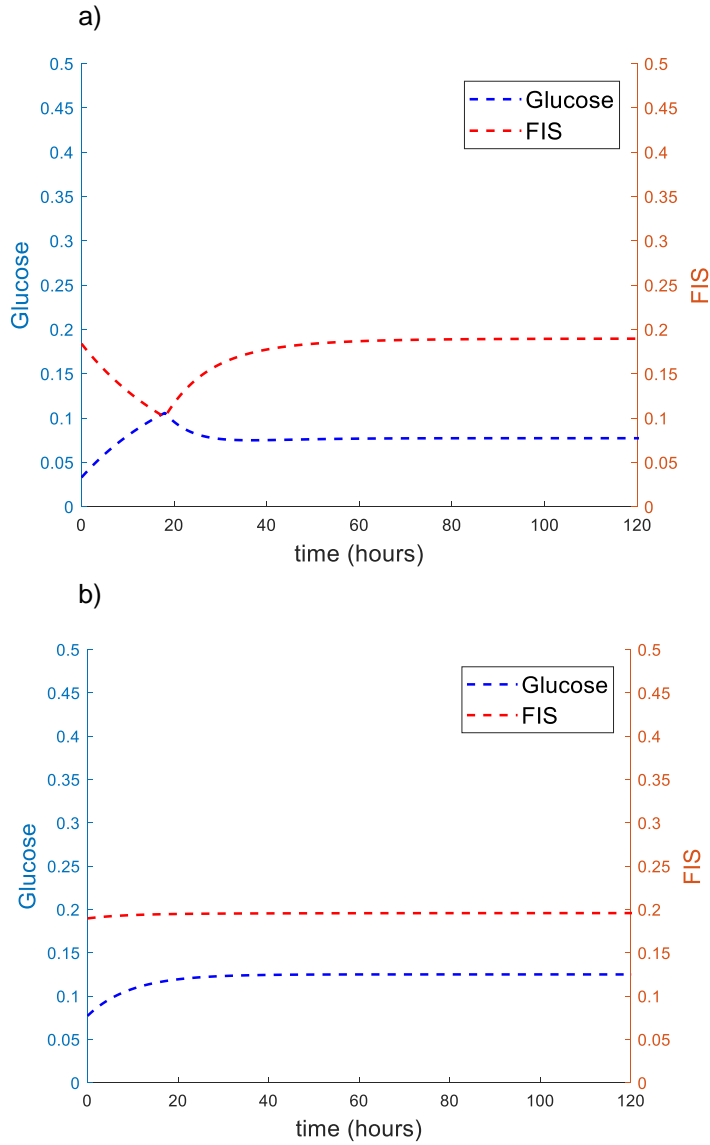


Figure 5: Simulated reaction profile and solids (FIS) assuming reduction of 50% on enzyme concentration, to mimic enzymatic activity in ATPS. Two reactors were considered in this simulation, a) and b), respectively.

Table 9: Reactor operating parameters assuming reduction of 50% on enzyme concentration. Two reactors were considered in this simulation. A cumulative yield of 53.24% was achieved.

	Reactors used in the simulation	
	1	2
Feed F1 (ton/h)	266.6	159.96
Enzymes F2 (ton/h)	28.4	-
To ATPS F3 (ton/h)	135.04	60
Purge F4 (ton/h)	159.96	99.96
Residence time (h)	17	16
Yield $\left( Glucan_{initial} / Glucan_{final} \right)$	0.45	0.50

Additionally, a further simulation was performed to mimic the lower glucose release in the reacting phase caused by the influence of phase forming components on the enzymatic activity. At each time point, the sugar concentration was reduced by half (Figure 6 a). The reduction in glucose concentration promotes a decrease in the steady content of solids, indicating a higher reaction rate when less product is present in the reacting phase.

In order to compare the effect of reducing only the sugar concentration, an extra simulation was performed (Figure 6 b) for which enzyme content was not reduced, and the flow rate was maintained the same for visualizing the differences. The reduction of the insoluble solids and increase of the glucose released at the steady state for the preserved enzymatic activity scenario evidence the importance of selecting suitable phase forming components for the ATPS hydrolysis.

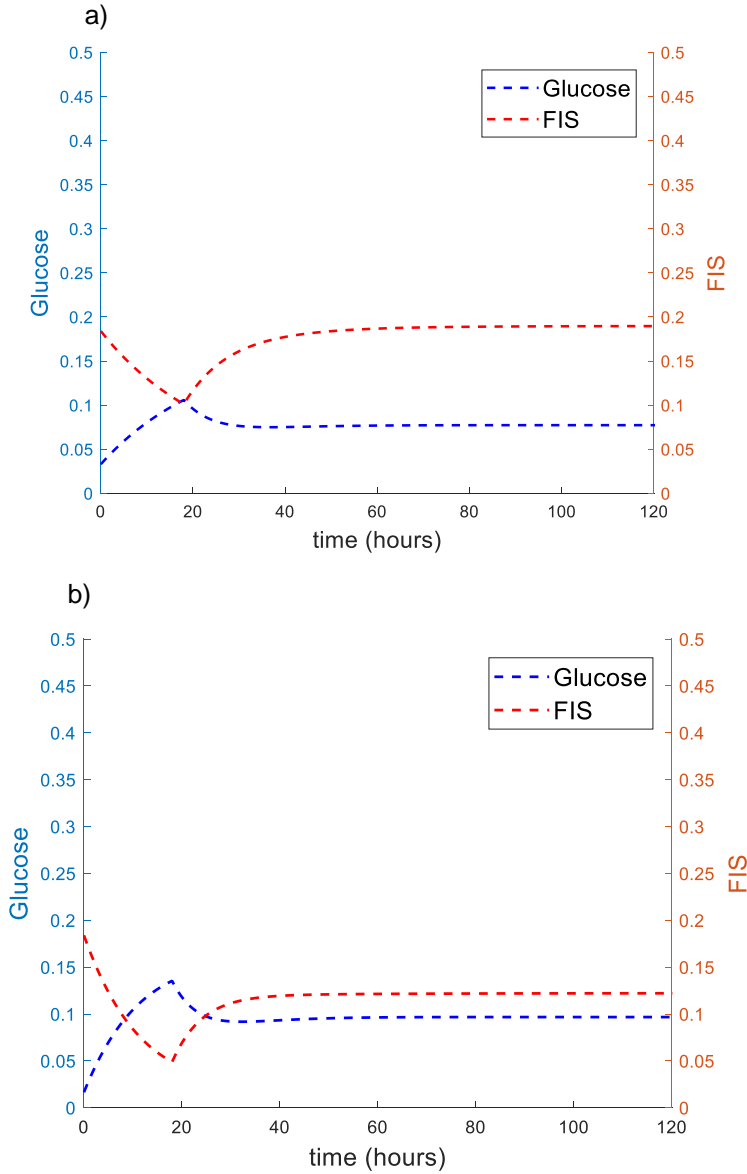


Figure 6: Simulated reaction profile (glucose release and solids, FIS) assuming 50% reduction on glucose concentration due to enzyme activity reduction. A hypothetical ATPS presenting  $k_s = 1$  was considered. a) enzyme concentration is reduced by half; b) enzyme concentration is not sensitized. The flow rates were kept the same for comparison reasons.

The extractive hydrolysis can be evaluated in terms of glucose recovery in the ultrafiltration unit (permeate stream). With the multiple ATPS and ultrafiltration units, it is assumed that in each cycle, glucose partitions from the bottom phase to the top phase, enhancing the recovery (Table 10). The sugar yield increases at each cycle. However, the glucose concentration decreases at the respective cycle, since the system is diluted. Even though the partition coefficients for sugar are smaller than 1 for both salt-based systems, the high concentration of glucose in the bottom phase allows considerable recovery of the product in each cycle.

Table 10: Permeate stream composition and glucose recovery for each ultrafiltration unit operation, for both salt-based system.

	<b>Magnesium sulphate</b>			<b>Potassium citrate</b>		
	UF1	UF2	UF3	UF1	UF2	UF3
<b>Glucose (ton/batch)</b>	11.36	10.34	7.76	12.59	10.03	8.85
<b>Mass fraction (w/w)</b>	0.16	0.13	0.14	0.17	0.14	0.13
<b>Cumulative Glucose recovery (kg/kg)</b>	29	56	76	33	58	81

The glucose recovery is calculated based on the glucan concentration before liquefaction.

Since on both configurations (magnesium sulphate or potassium citrate-based ATPS) the reaction is allowed to proceed up to 90% conversion, the recycle of enzymes to the system determines the efficiency of the hydrolysis. The recycle of adsorbed enzymes in the bagasse fibres is more efficient than the system configuration in which enzymes are considered to be in the supernatant (desorbed enzymes) [10]. This is a consequence not only of the low availability of desorbed enzymes, but also because of the retention coefficient (50%) of the desorbed proteins in the ultrafiltration unit. With a higher enzyme retention coefficient (90%), the increase in the enzyme load reduces the reaction time from 24 h to 11 h for the potassium citrate system. For the magnesium sulphate-based system (reaction in the bottom phase), in which the enzymes are desorbed to the unconverted biomass, the reaction time is lower (21 h), when the design considers the recycle of the

proteins. When no recycle of enzymes is considered, the potassium citrate-based system overcomes in terms of time to achieve 90% conversion (Table 11).

Table 11: Effect of enzyme recycle in the ATPS hydrolysis ( $k_s = 0.71$ ) and comparison to the conventional hydrolysis.

	Magnesium sulphate	Potassium citrate
Enzyme loading after recycle (mg/g glucan)	33.33	25.71
Reaction time after recycle (h)	21	24
Reaction time without recycle (h)	29	26
Reaction time for conventional hydrolysis (h)	39	

In the continuous simulation of the extractive reaction, the conversion is a function of the residence time and kinetics. The residence time is dependent on the reactor volume and purge flow rate. The final reactor volume were set at 3000 m<sup>3</sup> — literature reports a maximum reactor volume of 3600 m<sup>3</sup> [22]. In order to increase the residence time (and consequently the conversion), either the reactor volume should be increased or the purge flow should be decreased. However, for the process designed for the reaction to occur in the bottom phase, the purge flow rate composes the bottom phase for the succeeding ATPS reactor. Consequently, the purge rate impacts the composition and volume ratios of the following ATPS. The concentration of the purge stream is also limited by the solubility of the phase forming components. Apart from the unfeasible concentrations due to the low flow rate in purge streams, high system concentrations could also influence the mixing and mass transfer and, consequently, the conversion. The optimization of the composition at each stage of the reaction would also depend on the concentration factor of the ultrafiltration unit and make up streams for phase forming components and/or water.

The partition coefficient of sugar strongly influences the glucose recovery not only for the batch process, but also for the continuous ATPS process (Table 12). The search for ATPS which present partition coefficient of sugars higher than unit increases the conversion and sugar recover efficiency. The continuous conventional

hydrolysis simulated a conversion of 76.7%, with a feed to purge ratio of 3.5. The feed to purge ratio of the magnesium sulphate-based system was set at 2, due to the composition limitation. For the process designed for the reaction to occur in the top phase (potassium citrate-based system), the purge stream is considered as the top phase stream (where the conversion is calculated). Logically, the higher retention coefficient of enzymes enables higher conversions (Table 13). To improve the conversion at continuous ATPS hydrolysis, the number of hydrolysis reactors could be increased. Increasing the number of ATPS hydrolysis reactors would also increase the complexity of downstream operations due to the number of equipment. In the current scenario, the ATPS hydrolysis reactor (ATPS 1) is followed by three additional ultrafiltration units (UF1, UF2, UF3) and two ATPS units (ATPS2, ATPS3). The addition of an extra hydrolysis reactor would possibly require additional downstream equipment and/or complicate the recycling procedure. Alternatively, ATPS 2 and ATPS 3 could be considered as hydrolysis reactors instead of exclusively as separation units. This would increase the residence time in ATPS 2 and ATPS 3 reactors and thereby the glucan utilisation.

Table 12: Glucose recovery for the ATPS continuous hydrolysis at the magnesium sulphate-based ATPS. The residence time and purge flow were simulated at 16 h and 180 ton/h, respectively.

	Partition coefficients for sugar ( $k_s$ )					
	$k_s = 0.71$			$k_s = 1.5$		
	UF 1	UF 2	UF 3	UF 1	UF 2	UF 3
Ultrafiltration (UF) units						
Mass fraction glucose (% w/w)	0.15	0.15	0.14	0.20	0.19	0.17
Glucose recovery (initial glucan, % w/w)	24	44	60	33	58	77
Enzyme load (feed + recycle stream, mg/g)	53.3			57.5		
Conversion at steady state (%)	44.4			60.5		

Table 13: Glucose recovery for the ATPS continuous hydrolysis at the potassium citrate-based ATPS, considering a feed to purge ratio of 2.38. The residence time was 18.1 h.

	Retention coefficient of enzymes ( $R_e$ )					
	$R_e = 0.5$			$R_e = 0.9$		
	UF 1	UF 2	UF 3	UF 1	UF 2	UF 3
Ultrafiltration (UF) units						
Mass fraction glucose (% w/w)	0.14	0.13	0.13	0.14	0.13	0.13
Glucose recovery (initial glucan, % w/w)	19	36	51	20	38	53
Enzyme load (feed + recycle stream, mg/g)	48.1			122		
Conversion at steady state (%)	73.7			88.4		

### 3.5. Techno-economic analysis

The techno-economic analysis contributes to the determination of feasibility limits of the ATPS enzymatic hydrolysis. For the batch mode operation, the ATPS hydrolysis process is more expensive than the conventional hydrolysis process, both on total capital investment (Table 14) and operating costs (Table 15). The major reasons are the number of equipment used for the processing and the cost of additional phase forming components. An alternative to reduce the operating costs would be to add a unit operation to recover the salts from the purge stream for recycle. However, this strategy would further increase the capital investment cost.

Table 14: Total capital investment breakdown for the batch process (in euros, €).

	ATPS hydrolysis	Conventional hydrolysis
Purchase cost	20.3E+6	11.9E+6
Installed cost	34.0E+6	19.5E+6
Warehouse	1.4E+6	780.9E+3
Site Development	3.1E+6	1.8E+6
Additional Piping	1.5E+6	878.5E+3
Total Direct Costs (TDC)	40.0E+6	22.9E+6
Prorateable Expenses	4.0E+6	4.0E+6
Field Expenses	4.0E+6	4.0E+6
Home Office & Construction Fee	8.0E+6	8.0E+6
Project Contingency	4.0E+6	4.0E+6
Other Costs (Start-Up. Permits. etc.)	4.0E+6	4.0E+6
Total Indirect Costs	24.0E+6	24.0E+6
Fixed Capital Investment (FCI)	63.9E+6	46.9E+6
Land	1.3E+6	938.3E+3



Working Capital	3.2E+6	2.3E+6
Total Capital Investment (TCI)	68.4E+6	50.2E+6

With respect to the equipment costs, even though the conventional process requires three reactors for hydrolysis, the final product is directly the hydrolysate and no further downstream is required other than the filter press. For the ATPS process, the number of enzymatic hydrolysis reactors was estimated at three (for  $k_s = 1.5$ ) or five (for  $k_s = 0.7$ ). The distribution of the individual equipment to the total purchase cost is shown in Figure 7. The cost of each equipment is presented in the Supplementary Material.

The major difference in the process between the conventional and ATPS processes is the assumption of enzyme recycle for the later. Consequently, a higher retention coefficient of enzymes leads to a decrease in the installed cost — for  $R_2 = 0.5$ , installed cost was 32.6E+6, while for  $R_2 = 0.9$ , installed cost was 31.6E+6. The total capital investment costs for the scenarios considering for  $k_s = 1.5$  for magnesium sulphate system, and  $R_e = 0.5$  and  $R_e = 0.9$  for the potassium citrate system are, respectively, 65.5E+6, 65.5E+6 and 62.6E+6.

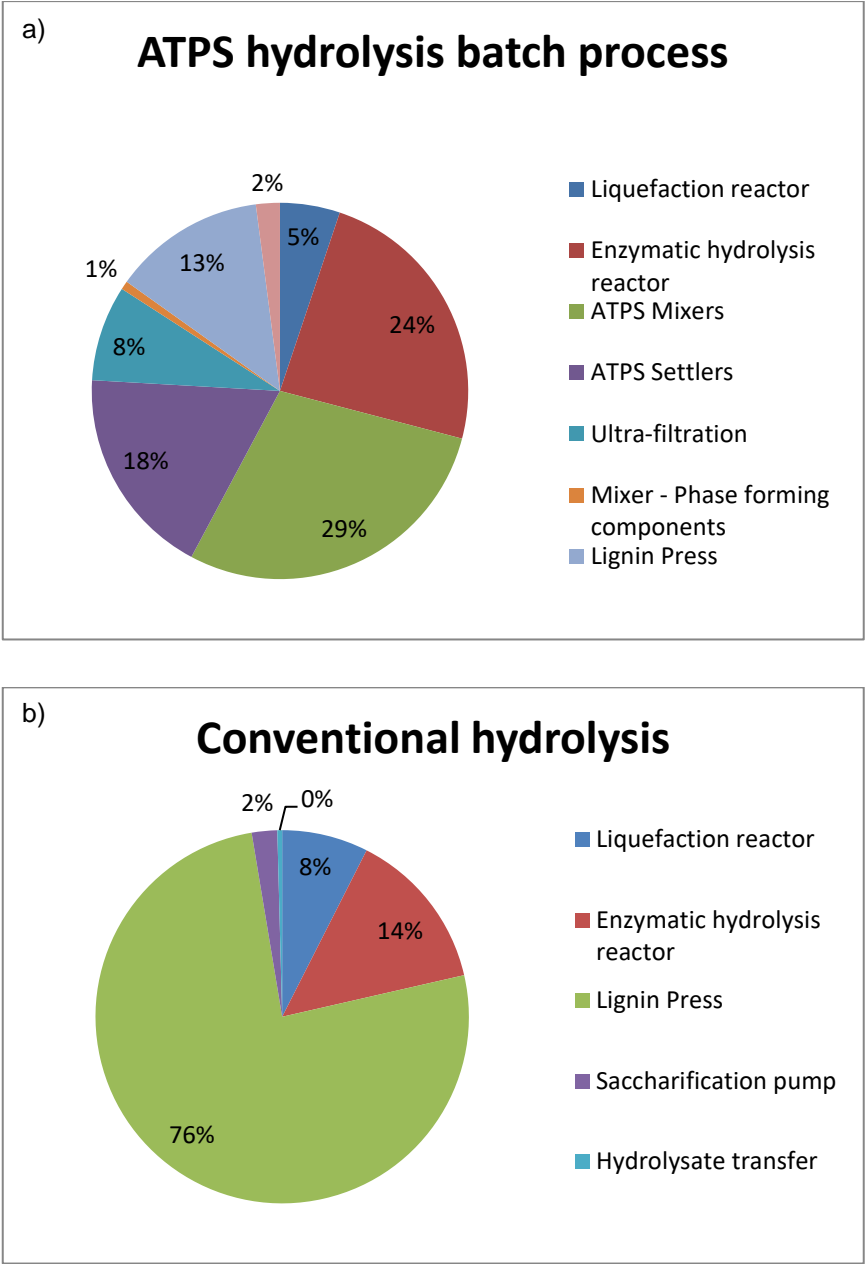


Figure 7: Equipment cost distribution for a) ATPS hydrolysis process and b) conventional hydrolysis process, when operating in batch.

The major operating costs of the process are associated to the raw materials (Table 15). Among them, enzymes and sugarcane bagasse are the main contributors (Supplementary Material). Even though sugarcane is typically processed in the pre-treatment, the cost of untreated bagasse was assumed. The same cost of bagasse was assumed for the conventional hydrolysis process for the sake of comparison.

The relative difference in operating costs of the magnesium sulphate system to the conventional system is 17%, while that of potassium citrate is 57%. The reason for the difference between ATPS is the cost of magnesium sulphate and potassium citrate, which differs by a factor of 10. The difference between the ATPS system and the conventional system are the costs associated with phase forming components make up stream, membrane replacement and wastewater treatment. The main contributors to the operating costs were sensitized to evaluate their impact on the economics of the proposed technology (Table 16).

Table 15: Summary of operating costs for ATPS and conventional hydrolysis operated in batch.

Operating costs (€)	Magnesium sulphate		Potassium citrate		Conventional
	$k_s = 0.71$	$k_s = 1.5$	$R_e = 0.5$	$R_e = 0.9$	
<b>Raw Materials</b>	46.0E+6	46.0E+6	69.1E+6	69.1E+6	43.4E+6
<b>Utilities</b>	16.3E+6	16.3E+6	16.3E+6	16.3E+6	10.9E+6
<b>Maintenance and repairs</b>	2.2E+6	2.1E+6	2.1E+6	2.0E+6	1.6E+6
<b>Operating supplies</b>	798.8E+3	765.0E+3	765.0E+3	2.0E+6	586.4E+3
<b>Operating labour</b>	2.4E+6	2.4E+6	2.4E+6	2.4E+6	2.0E+6
<b>Wastewater treatment</b>	5.0E+3	4.8E+3	4.1E+3	4.1E+3	
<b>Consumables (membrane)</b>	644.3E+3	644.3E+3	644.3E+3	644.3E+3	

<b>Total OPEX</b>	68.4+6	68.2E+6	91.3E+6	92.5E+6	58.5E+6
-------------------	--------	---------	---------	---------	---------

Table 16: Sensitivity analysis on the parameters (enzyme, bagasse, and potassium citrate) and their influence on the operational costs.

Scenario/case	Parameter sensitized	Operating costs (10 <sup>6</sup> €/year)					
		+	+	Base	- 10	- 25	- 50
		25%	10%		%	%	%
Magnesium sulphate based ATPS ( $k_s = 0.71$ )	Enzyme	73.1	70.3	68.4	65.8	63.6	-
	Bagasse	74.5	70.8	68.4	65.9	62.3	-
Potassium citrate based ATPS ( $R_e = 0.5$ )	Enzyme	96.1	93.2	91.3	90.6	86.5	-
	Bagasse	97.4	93.7	91.3	88.9	85.2	-
	Potassium citrate	-	-	91.3	89	86.7	80.9

In terms of product throughput, the glucose concentration in the final stream is similar for the ATPS (15 w/w %,  $k_s = 0.71$ ) and the conventional hydrolysis (13 w/w %). For the magnesium sulphate system considering the higher partitioning of sugar ( $k_s = 1.5$ ), the final product stream concentration is 17% w/w % and would benefit in terms of product price. Otherwise, since this is a slight difference in product concentration, the ATPS process would not contribute positively to the final glucose selling price, turning the ATPS batch process economically unfeasible.

The total capital investment for the continuous process is summarized in Table 17. The major contributor for the equipment costs are the membrane units (Supplementary Material). This also considerably increases the cost contribution of the base case when compared to the batch process. A breakdown of the individual equipment cost to the total purchase cost is shown in Figure 8.

Table 17: Total capital investment breakdown for the continuous process (in euros, €).

	ATPS hydrolysis (€)	Conventional hydrolysis (€)
Purchase cost	17.5E+6	12.3E+6
Installed cost	30.4E+6	22.1E+6
Warehouse	1.2E+6	884.6E+3
Site Development	2.7E+6	2.0E+6
Additional Piping	1.4E+6	995.2E+3
Total Direct Costs (TDC)	35.7E+6	26.0E+6
Prorateable Expenses	3.6E+6	3.2E+6
Field Expenses	3.6E+6	3.2E+6
Home Office & Construction Fee	7.1E+6	6.4E+6
Project Contingency	3.6E+6	3.2E+6
Other Costs (Start-Up. Permits. etc.)	3.6E+6	3.2E+6
Total Indirect Costs	21.4E+6	19.1E+6
Fixed Capital Investment (FCI)	57.1E+6	45.1E+6
Land	1.1E+6	901.5E+3
Working Capital	2.9E+6	2.3E+6
Total Capital Investment (TCI)	61.1E+6	48.2E+6

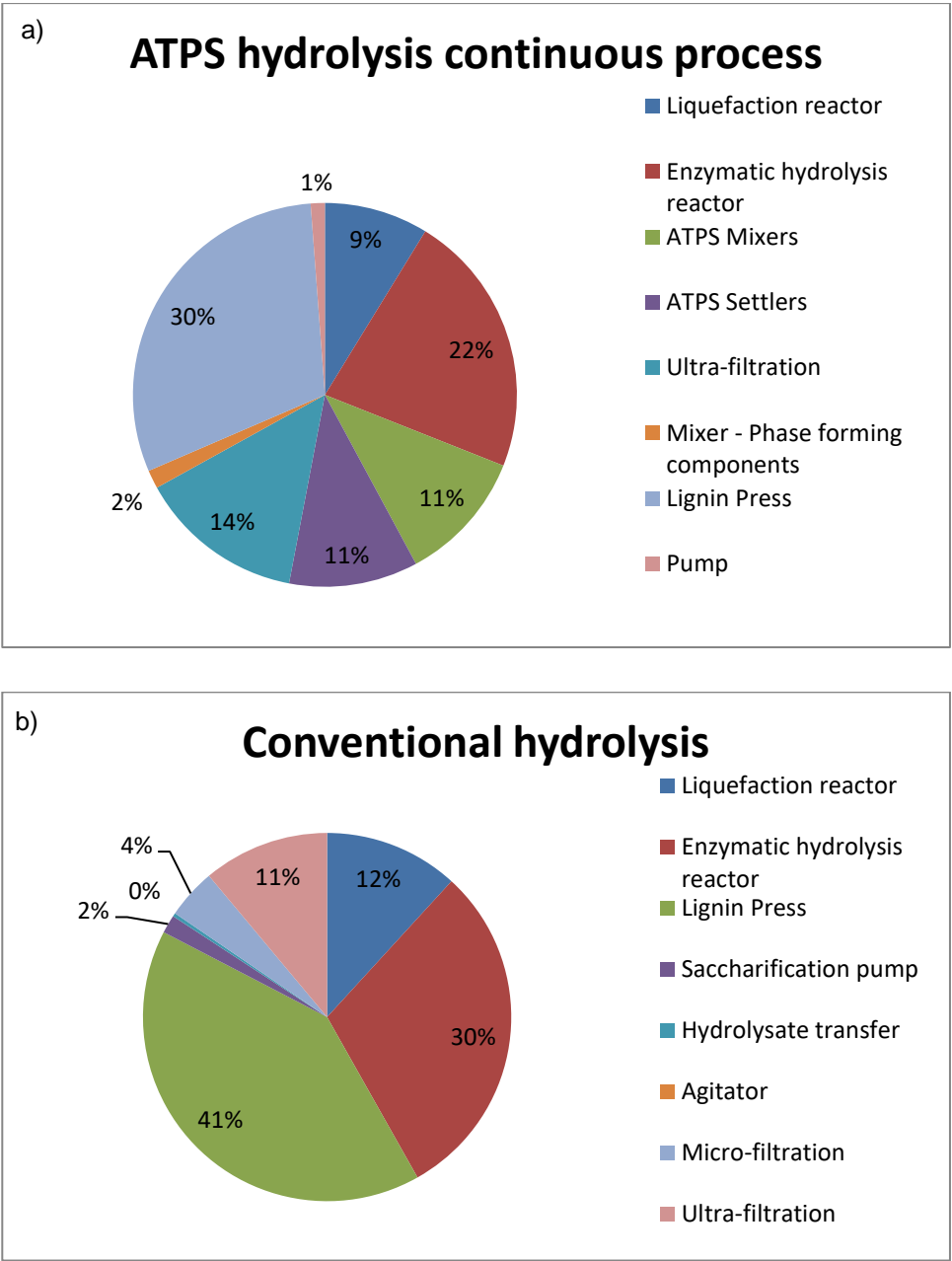


Figure 8: Equipment cost distribution for a) ATPS hydrolysis process and b) conventional hydrolysis process, when operating in continuous.

The operating costs for the continuous process are summarized in Table 18. Similar to the results from the batch process, the impact of the phase forming compounds (potassium citrate) is negative on the process economics. The higher productivity in continuous process increases the make-up stream consumption. For the magnesium sulphate case, even though the costs are comparable to the base case, the reactor conversions are not in the same order because of the limitations posed on the purge flow rate.

Table 18: Summary of operating costs for ATPS and conventional hydrolysis operated in continuous.

Operating costs (€)	Magnesium sulphate		Potassium citrate		Conventional
	$k_s = 0.71$	$k_s = 1.5$	$R_e = 0.5$	$R_e = 0.9$	
<b>Raw Materials</b>	69.1E+6	69.0E+6	348.2E+6	336.8E+6	43.4E+6
<b>Utilities</b>	13.0E+6	13.0E+6	13.0E+6	13.0E+6	13.0E+6
<b>Maintenance and repairs</b>	2.2E+6	2.1E+6	2.1E+6	2.0E+6	1.3E+6
<b>Operating supplies</b>	798.8E+3	765.0E+3	765.0E+3	2.0E+6	479.0E+3
<b>Operating labour</b>	2.4E+6	2.4E+6	2.4E+6	2.4E+6	2.0E+6
<b>Wastewater treatment</b>	5.0E+3	4.8E+3	4.1E+3	4.1E+3	
<b>Consumables (membrane)</b>	644.3E+3	644.3E+3	644.3E+3	644.3E+3	506.1E+3
<b>Total OPEX</b>	88.2E+6	87.9E+6	367.2E+6	356.9E+6	60.8E+6

In terms of process design, the recovery and reuse of phase forming component and enzymes are of paramount importance for the economic feasibility of the process. The enzyme recycle via ultrafiltration was conceptually supported by this work. Consequently, a higher enzyme load would be justified to improve the kinetics.

However, it is yet to be determined how the enzymes perform after recycling with the phase forming components. The ultrafiltration is mainly applied to separate the glucose from PEG. A unit operation that could separate the glucose from the bottom phase in the potassium citrate based ATPS could improve the process economics. For the continuous implementation of aqueous two phase systems, other type of equipment present as an alternative to the mixer-settlers, such as the column contactors [31]. Following this approach, tubular reactors could be applied to solute extraction based on ATPS. Because of their large and adjustable length/diameter ratio, the settling time could be reduced and no external equipment for phase separation is needed [32]. The operation of the enzymatic hydrolysis in tubular reactors would be advantageous when compared to batch process in terms of less accumulation at the system interface, efficient mass transfer of solutes between the two phases and less manipulation of samples (and consequent loss of sample) between the steps [32]. Counter-current extraction could also be an alternative to improve the separation of molecules in ATPS. A counter-current device can be set up through a series of tubular extractors into a multi-stage arrangement. Within this configuration, mixing and settling occur in the same vessel and can be potentially applied as a continuous multi-step ATPS. However, for the application in the extraction of invertase from spent yeast, no improvement was observed when compared to the batch process [33]. On the other hand, several parameters can be adjusted to maximize the resolution in counter-current. The application of counter-current chromatography for separation based on ATPS has been demonstrated and proven to purify enzymes in one-step [34].

The validation of the equipment choice could rely on parameters such as the efficient recovery of biomolecules, the (feasible) operational models for process optimization, the possibility of phase recirculation, large scale operation, control and automation. Although the incomplete characterization of mixer-settler units restrains a practical design platform implementation of this equipment, mixer-settler units have an inherent assembling easiness compared with column contactors and they are suitable for individual stage (mix, coalescence, and separation) optimization [31].



## Conclusion

The extractive hydrolysis based on aqueous two-phase system (ATPS) was modelled by integrating two models previously published in literature. From the analysis of the hydrolysis model, the glucan concentration played an important role on the reaction kinetics, since it determines the concentration of enzymes adsorbed. The main undesirable events concerning the reaction and separation in ATPS are the low enzyme activity, low selectivity of the systems to sugars and enzymes, and slow separation kinetics. When the hydrolysis is analysed integrated with the separation of glucose via ATPS, the partition coefficient of this product can determine an ATPS reaction kinetics faster than in conventional system. For the batch system, the ATPS modelled reaction achieved 90% conversion within 11 to 24 h, in contrast to 40 h in the conventional system. For the continuous system, the purge stream is strongly connected to the efficiency of the process, once it determines the residence time of the reaction and the technical feasibility of the consecutive separation unit, in terms of system concentration. In conventional hydrolysis, however, the purge stream could be set at lower levels, achieving higher conversions.

In economic aspects, the cost of phase forming components is the main contributor to the operating costs, and the main obstacle to ATPS process replace conventional hydrolysis of sugarcane bagasse. Batch and continuous ATPS modes of operation yielded higher CAPEX and OPEX compared to the conventional process. The development of novel (and cheaper) phase forming components, and new apparatus in order to improve ATPS operation, are possible directions to bring ATPS into an industrial reality. Alternative unit operation to recover sugar from the salt-enriched phase could also improve the ATPS process performance. In the current set-up, the downstream unit operation to recover sugar and recycle the components compose the majority of the equipment costs. The feasibility of the ATPS hydrolysis could be enhanced by systems with higher selectivity for sugars, better maintenance of enzymatic activity and efficient recycle of enzymes and phase forming components.

## References

1. Jørgensen H, Kristensen JB, Felby C. Enzymatic conversion of lignocellulose into fermentable sugars: challenges and opportunities. *Biofuels, Bioprod Biorefining* [Internet]. 2007;1:119–34. Available from: <http://doi.wiley.com/10.1002/bbb.4>
2. McCann MC, Carpita NC. Designing the deconstruction of plant cell walls. *Curr Opin Plant Biol* [Internet]. 2008;11:314–20. Available from: <https://linkinghub.elsevier.com/retrieve/pii/S136952660800071X>
3. Davis RE, Grundl NJ, Tao L, Biddy MJ, Tan EC, Beckham GT, et al. Process Design and Economics for the Conversion of Lignocellulosic Biomass to Hydrocarbon Fuels and Coproducts: 2018 Biochemical Design Case Update; Biochemical Deconstruction and Conversion of Biomass to Fuels and Products via Integrated Biorefinery Path [Internet]. Golden, CO (United States); 2018 Nov. Available from: <http://www.osti.gov/servlets/purl/1483234/>
4. Jørgensen H, Kristensen JB, Felby C. Enzymatic conversion of lignocellulose into fermentable sugars: challenges and opportunities. *Biofuels, Bioprod Biorefining*. 2007;1:119–34.
5. Fahmy M, Sohel MI, Vaidya AA, Jack MW, Suckling ID. Does sugar yield drive lignocellulosic sugar cost? Case study for enzymatic hydrolysis of softwood with added polyethylene glycol. *Process Biochem* [Internet]. Elsevier; 2019;80:103–11. Available from: <https://doi.org/10.1016/j.procbio.2019.02.004>
6. Andrić P, Meyer AS, Jensen P a., Dam-Johansen K. Reactor design for minimizing product inhibition during enzymatic lignocellulose hydrolysis: I. Significance and mechanism of cellobiose and glucose inhibition on cellulolytic enzymes. *Biotechnol Adv* [Internet]. 2010;28:308–24. Available from: <https://linkinghub.elsevier.com/retrieve/pii/S0734975010000054>
7. Larsson M, Arasaratnam V, Mattiasson B. Integration of bioconversion and downstream processing: Starch hydrolysis in an aqueous two-phase system. *Biotechnol Bioeng*. 1989;33:758–66.

8. Stickel JJ, Adhikari B, Sievers DA, Pellegrino J. Continuous enzymatic hydrolysis of lignocellulosic biomass in a membrane-reactor system. *J Chem Technol Biotechnol* [Internet]. 2018;93:2181–90. Available from: <http://www.ncbi.nlm.nih.gov/pubmed/25197847><http://doi.wiley.com/10.1002/jctb.5559>
9. Patel N, Bracewell DG, Sorensen E. Dynamic modelling of aqueous two-phase systems to quantify the impact of bioprocess design, operation and variability. *Food Bioprod Process* [Internet]. Institution of Chemical Engineers; 2018;107:10–24. Available from: <http://dx.doi.org/10.1016/j.fbp.2017.10.005>
10. Bussamra BC, Meerman P, Viswanathan V, Mussatto SI, Carvalho da Costa A, van der Wielen L, et al. Enzymatic Hydrolysis of Sugarcane Bagasse in Aqueous Two-Phase Systems (ATPS): Exploration and Conceptual Process Design. *Front Chem* [Internet]. 2020;8:1–15. Available from: <https://www.frontiersin.org/article/10.3389/fchem.2020.00587/full>
11. Larsen J, Haven MØ, Thirup L. Inbicon makes lignocellulosic ethanol a commercial reality. *Biomass and Bioenergy* [Internet]. Elsevier Ltd; 2012;46:36–45. Available from: <http://dx.doi.org/10.1016/j.biombioe.2012.03.033>
12. Christensen BH, Gerlach LH. Method and apparatus for conversion of cellulosic material to ethanol. United States Patent; 2012.
13. Humbird D, Davis R, Tao L, Kinchin C, Hsu D, Aden A, et al. Process Design and Economics for Biochemical Conversion of Lignocellulosic Biomass to Ethanol: Dilute-Acid Pretreatment and Enzymatic Hydrolysis of Corn Stover [Internet]. Golden, CO (United States); 2011 Mar. Available from: <http://www.osti.gov/servlets/purl/1013269/>
14. Adney B, Baker J. Measurement of Cellulase Activities. Laboratory Analytical Procedure ( LAP ) Issue Date : 08 / 12 / 1996. Natl. Renew. Energy Lab. 2008.
15. Kadam KL, Rydholm EC, McMillan JD. Development and Validation of a Kinetic Model for Enzymatic Saccharification of Lignocellulosic Biomass. *Biotechnol Prog*

[Internet]. 2004;20:698–705. Available from: <http://doi.wiley.com/10.1021/bp034316x>

16. Grabit [Internet]. MathWorks. Available from: <https://nl.mathworks.com/matlabcentral/fileexchange/7173-grabit>

17. McMillan JD, Jennings EW, Mohagheghi A, Zuccarello M. Comparative performance of precommercial cellulases hydrolyzing pretreated corn stover. *Biotechnol Biofuels* [Internet]. 2011;4:29. Available from: <http://biotechnologyforbiofuels.biomedcentral.com/articles/10.1186/1754-6834-4-29>

18. Bussamra BC, Castro Gomes J, Freitas S, Mussatto SI, Carvalho da Costa A, van der Wielen L, et al. A robotic platform to screen aqueous two-phase systems for overcoming inhibition in enzymatic reactions. *Bioresour Technol* [Internet]. Elsevier; 2019;280:37–50. Available from: <https://doi.org/10.1016/j.biortech.2019.01.136>

19. Mistry SL, Kaul A, Merchuk JC, Asenjo JA. Mathematical modelling and computer simulation of aqueous two-phase continuous protein extraction. *J Chromatogr A* [Internet]. 1996;741:151–63. Available from: <http://www.sciencedirect.com/science/article/pii/0021967396001793>

20. Jyh-Ping C. Partitioning and separation of  $\alpha$ -lactalbumin and  $\beta$ -lactoglobulin in PEG/potassium phosphate aqueous two-phase systems. *J Ferment Bioeng* [Internet]. 1992;73:140–7. Available from: <https://linkinghub.elsevier.com/retrieve/pii/0922338X9290579J>

21. Humbird D, Davis R, Tao L, Kinchin C, Hsu D, Aden A, et al. *Process Design and Economics for Biochemical Conversion of Lignocellulosic Biomass to Ethanol: Dilute-Acid Pretreatment and Enzymatic Hydrolysis of Corn Stover*. Golden, CO (United States); 2011 Mar.

22. Davis RE, Grundl NJ, Tao L, Biddy MJ, Tan EC, Beckham GT, et al. *Process Design and Economics for the Conversion of Lignocellulosic Biomass to Hydrocarbon Fuels and Coproducts: 2018 Biochemical Design Case Update*;

Biochemical Deconstruction and Conversion of Biomass to Fuels and Products via Integrated Biorefinery Path. Golden, CO (United States); 2018 Nov.

23. Jyh-Ping C. Partitioning and separation of  $\alpha$ -lactalbumin and  $\beta$ -lactoglobulin in PEG/potassium phosphate aqueous two-phase systems. *J Ferment Bioeng.* 1992;73:140–7.

24. Wooley R, Ma Z, Wang NHL. A nine-zone simulating moving bed for the recovery of glucose and xylose from biomass hydrolyzate. *Ind Eng Chem Res.* 1998;37:3699–709.

25. Kanchanalai P, Realf MJ, Kawajiri Y. Solid-phase reactive chromatographic separation system: Optimization-based design and its potential application to biomass saccharification via acid hydrolysis. *Ind Eng Chem Res.* 2014;53:15946–61.

26. Chen K, Hao S, Lyu H, Luo G, Zhang S, Chen J. Ion exchange separation for recovery of monosaccharides, organic acids and phenolic compounds from hydrolysates of lignocellulosic biomass. *Sep Purif Technol* [Internet]. Elsevier B.V.; 2017;172:100–6. Available from: <http://dx.doi.org/10.1016/j.seppur.2016.08.004>

27. Chen K, Luo G, Lei Z, Zhang Z, Zhang S, Chen J. Chromatographic separation of glucose, xylose and arabinose from lignocellulosic hydrolysates using cation exchange resin. *Sep Purif Technol* [Internet]. Elsevier; 2018;195:288–94. Available from: <https://doi.org/10.1016/j.seppur.2017.12.030>

28. Liu S, Lu H, Hu R, Shupe A, Lin L, Liang B. A sustainable woody biomass biorefinery. *Biotechnol Adv* [Internet]. 2012 [cited 2015 Aug 18];30:785–810. Available from: <http://www.sciencedirect.com/science/article/pii/S0734975012000262>

29. Di Risio S, Hu CS, Saville BA, Liao D, Lortie J. Large-scale, high-solids enzymatic hydrolysis of steam-exploded poplar. *Biofuels, Bioprod Biorefining* [Internet]. 2011;5:609–20. Available from: <http://doi.wiley.com/10.1002/bbb.323>

30. Bussamra BC, Gomes JC, Freitas S, Mussatto SI, da Costa AC, van der Wielen L, et al. A robotic platform to screen aqueous two-phase systems for overcoming inhibition in enzymatic reactions. *Bioresour Technol.* 2019;280.
31. Espitia-Saloma E, Vázquez-Villegas P, Aguilar O, Rito-Palomares M. Continuous aqueous two-phase systems devices for the recovery of biological products. *Food Bioprod Process* [Internet]. Institution of Chemical Engineers; 2014;92:101–12. Available from: <http://dx.doi.org/10.1016/j.fbp.2013.05.006>
32. Vázquez-Villegas P, Aguilar O, Rito-Palomares M. Study of biomolecules partition coefficients on a novel continuous separator using polymer-salt aqueous two-phase systems. *Sep Purif Technol* [Internet]. 2011;78:69–75. Available from: <https://linkinghub.elsevier.com/retrieve/pii/S1383586611000578>
33. Vázquez-Villegas P, Aguilar O, Rito-Palomares M. Continuous enzyme aqueous two-phase extraction using a novel tubular mixer-settler in multi-step counter-current arrangement. *Sep Purif Technol* [Internet]. 2015;141:263–8. Available from: <https://linkinghub.elsevier.com/retrieve/pii/S1383586614007400>
34. Magri ML, Cabrera RB, Miranda M V., Fernández-Lahore HM, Cascone O. Performance of an aqueous two-phase-based countercurrent chromatographic system for horseradish peroxidase purification. *J Sep Sci* [Internet]. 2003;26:1701–6. Available from: <http://doi.wiley.com/10.1002/jssc.200301532>

## CHAPTER 6

### Conclusion and outlook

In order to apply aqueous two-phase systems (ATPS) as an extractive reaction system in enzymatic hydrolysis of sugarcane bagasse, a screening methodology, thermodynamic model of ATPS formation and a conceptual process design were developed. There was no significant improvement of the enzymatic hydrolysis of sugarcane bagasse using ATPS. The influence of phase forming components on the enzymatic activity and the low selectivity of sugars were the main obstacle for the extractive hydrolysis in ATPS. However, in this work we disclosed how to operate hydrolysis in ATPS, setting directions for future research in this field.

The high throughput platform used to screen ATPS — using miniaturizing volumes in an automatized way — may boost ATPS' application on innovative industrial processes and commercial products. Fundamental background knowledge was obtained during the development of a thermodynamic model to predict phase separation in ATPS. A critical review of literature and intensive application of the Flory-Huggins (FH) theory to our data led us to the conclusion that the well-recognized FH theory cannot correctly describe phase formation in salt-polymer ATPS. Moreover, the development of an integrated process design to mathematically simulate the ATPS hydrolysis showed the current economical unfeasibility of the proposed extractive process, when compared to the well-established conventional process. This hurdle to the industrial implementation of ATPS can also open opportunities to novel research in the field, focusing on removing the encountered limitations of the technology. The process design used mathematical prediction of the hydrolysis profile (glucose release and solid content) to explore the influence of variation of enzyme and sugar loads, and recycle of enzymes.

The investigation of phase forming components, operational conditions and partition of target molecules led to ATPS systems that currently cannot be applied in an industrial setting for the production of 2G bioethanol. The high throughput

## Conclusion and outlook

platform developed in this work has the potential to exhaustively screen systems to design effective ATPS for a target application involving the partition of sugars and proteins in polymer-salt systems. The tailored (and simple) approach to quantify proteins taking into account the interference of phase forming components with the analytics promotes a fast (and reliable) screening of APTS. Via the robotic platform, phase diagrams can be determined and the partition coefficient of the solutes under the influence of parameters of interest can be assessed. However, the temperature of the experiments was limited to the temperature range of the centrifuge used in this work (maximum of 40 °C). Another limitation of the developed robotic platform lies in the translation of the calculated masses to volumes during the systems formation. The variation of top and bottom phase densities of each system, plus the non-conservation of volume upon mixing, can impact the phase diagram determination. For a screening purpose, the suggested approximations on these factors were sufficient to indicate potentials ATPS for our target application.

The fundamental study in thermodynamic modelling of ATPS presented in this thesis provides insights on parameters governing the phase formation. Through models, the influence of the parameters can be assessed diminishing experimental efforts. The specific application of the Flory-Huggins theory to polymer-salt based systems disclosed important advances to a proper application of the theory and determination of the Flory-Huggins interaction parameters. Developing this work required a critical view on the assumptions when selecting a thermodynamic model to describe a system, and a comprehensive evaluation of mathematical approaches to solve a given problem. The deviation of the experiments compared to the Flory-Huggins model suggests that another thermodynamic framework might have to be applied to our ATPS to achieve better predictions. Finally, the thorough evaluation of the Flory-Huggins theory applied to salt based ATPS indicated that literature should always be critically reviewed, instead of taken for granted.

Operating ATPS in an industrial scale is not yet a reality, although the exhaustive lab-scale research performed on the topic. Modelling the ATPS process is a step forward to identify the bottlenecks and insight to advance on this technology. Dynamic modelling and process design are important tools and a starting point to



scale-up a technology before its implementation in pilot and/or industrial scale. In this work, the conceptual process design of ATPS applied to the enzymatic conversion of lignocellulosic biomass was developed. Through the conceptual process design, we could assess the implementation of ATPS for enzymatic hydrolysis in biorefineries and advantages towards the conventional/well-established process. The main bottleneck identified concerns the operation with phase forming components and the biocompatibility of the process. Polymers and salts are not present in other upstream processes prior to the ATPS formation, requiring extra attention to integrate with other unit operations of the process. Because of the high cost associated with these phase forming components, polymers and salts should be efficiently recycled in the process. Even though the design considered the recycle, its efficiency has to be experimentally confirmed. Another particularity of solvents recycling in ATPS process is the reproducibility in composition of the original stage. This feature was addressed in this work, by delimiting purge streams flows and considering back up streams for system dilution. Through predictive models, phase separation and partition of solutes can be determined. Unfortunately, we could not apply a thermodynamic model to accurately predict phase separation and partition of the solutes due to the uncertainties concerning the FH model considered previously. Considering the biocompatibility, the main undesirable events are the low enzyme activity in salts, low selectivity of the systems to sugars and enzymes, and slow separation kinetics.

When the components of the reaction are employed as phase forming compounds, the bagasse in high amounts or even the carbohydrates (sugar) solution can compose one of the phases. This approach reduces the number of extrinsic chemicals composing the two-phase systems. Consequently, operational costs would also be reduced, the recycle needs diminished and the biocompatibility improved. However, the lignocellulosic material is not water soluble, which prevents it from being a phase forming component to ATPS. Regarding the released sugar, biphasic systems can be formed in the presence of polymers under high concentration of sugars in both phases. Because the necessary concentration of

## Conclusion and outlook

sugar is higher than the inhibitory concentration for the enzyme, this approach becomes unfeasible.

In the continuous processing, the ATPS reactor consisted of two compartments for mixing and separation of the phases. Automated mixed settler units would improve the performance of the reaction. Considering that a large part of the capital costs are associated with the equipment, efforts in material science and equipment design to develop cheaper and versatile apparatus would improve the process design and boost their implementation at the industrial scale.

# SUPPLEMENTARY MATERIAL

## Chapter 2

### *Formation of Aqueous Two-Phase systems (ATPSs)*

After the formation of the systems according to the worklists (volumes definition) and liquid classes (pipetting definitions), top and bottom phases were withdrawn in a strategic way to avoid contamination with the other phase. The former was sampled from the liquid surface using the liquid level detection of the liquid handling station. The latter was taken from the bottom of the deep well plate. Even when systems were prepared manually, the withdrawn of top and bottom phase was performed at the robotic platform, which counts with constant parameters to pipet the samples. In the script, an intermediate step to avoid contamination with the other phase was included. After aspiration of the top phase, the tips were immersed and retracted for 5 times in a trough filled with water and ethanol in order to remove droplets outside the tips. The risk of bottom phase contamination with top phase was reduced by discarding the first and last third parts of the sampled volume. Then, 20  $\mu\text{L}$  were first discarded in the same intermediate trough used to clean the tips outside, acting as conditioning volume — first aliquot used to create similar conditions as the subsequent aliquots in order to increase precision, accuracy and eliminate eventual contaminants. For the phase diagram determination, the last 30  $\mu\text{L}$  (excess volume) were discarded in the wash station of the platform. In the solute partitioning experiments, 150  $\mu\text{L}$  of top and bottom phase were withdrawn and reserved for further quantitative analysis, being 20  $\mu\text{L}$  extra aspirated from bottom phase as conditioning volume.

**Table S1.** Definitions of aspiration and dispense parameters applied to each procedure performed at the robotic platform.

Application	Aspiration							Dispense				
	speed ( $\mu\text{L/s}$ )	Delay (ms)	System trailing airgap ( $\mu\text{L}$ )	Leading airgap ( $\mu\text{L}$ )	Trailing airgap ( $\mu\text{L}$ )	Aspiration position	Retract speed (mm/s)	speed ( $\mu\text{L/s}$ )	Delay (ms)	Breakoff speed ( $\mu\text{L/s}$ )	Aspiration position	Retract speed (mm/s)
Sample handling to dilution procedure and withdrawal of top phase from the systems	10	1000	20	5	5	Liquid level with tracking	20	20	1000	15	z-max without tracking	5
Sample handling to quantification reactions (UV plate preparation)	10	1000	20	10	0	z-max without tracking	10	20	1000	15	z-max without tracking	10
Water handling to dilution of samples with fixed tips and water handling	150	200	20	10	10	Liquid level +2 mm with tracking	10	400	0	200	z-dispense	50

to compose the systems												
Calibration curves												
samples handling and enzyme pipetting to compose the internal standards	15	1000	10	10	5	Liquid level +1 mm with tracking	5	20	0	15	Liquid level +1 mm without tracking	5
PEG handling to compose the systems <sup>1</sup>	10	1000	20	15	10	Liquid level +2 mm with tracking	5	15	1000	50	z-max with tracking	10
PEG handling to compose the systems <sup>2</sup>	15	1000	10	10	5	Liquid level +2 mm with tracking	10	20	0	15	Liquid level without tracking	15
Enzyme addition to the system for the partitioning study	15	1000	20	10	5	Liquid level +1 mm with tracking	5	20	0	15	Liquid level +1 mm without tracking	5
Sugar addition to the system for the partitioning study	100	200	20	10	5	Liquid level +2 mm with tracking	10	200	0	150	z-dispense	50

## Supplementary material

Withdrawal of bottom phase from the systems to storage	15	1000	20	10	0	z-max without tracking	15	30	1000	20	z-max –2 mm without tracking	5
Withdrawal of bottom phase from the systems to phase diagram determination	15	1000	20	10	10	z-max without tracking	10	15	1000	100	z-max without tracking	5
Methyl violet addition to the systems – MCA	15	1000	15	15	5	z-max without tracking	10	15	1000	150	z-max –5 mm with tracking	5
2% salt solution addition to dilution of systems – MCA	50	500	20	10	5	z-max without tracking	5	350	200	300	z-dispense	42

<sup>1</sup> For volumes lower than 200  $\mu\text{L}$ , the dispense speed was set at 20  $\mu\text{L/s}$  and the breakoff speed, at 15  $\mu\text{L/s}$ .

<sup>2</sup> For volumes lower than 15  $\mu\text{L}$ , the retract speed after dispense was set at 20  $\mu\text{L/s}$  and the breakoff speed, at 100  $\mu\text{L/s}$ .

MCA: Multi-channel Arm.

***Internal standards***

For protein quantification, each system composition (tie-line length) evaluated presents its own internal standard. The internal standard was composed of the same phase forming concentration than the system to be quantified, plus a known concentration of protein. In Step 2, two internal standards were performed: 100  $\mu\text{L}$  system blank (top or bottom phase) and 10  $\mu\text{L}$  CellicCTec 10 times diluted (known concentration); and 150  $\mu\text{L}$  system blank (top or bottom phase) and 10  $\mu\text{L}$  CellicCTec 10 times diluted, performed in duplicates. These internal standards were diluted two times before analysis. The protein calculated in the sample was the average between the concentrations calculated using these two different internal standards. In Step 3 of the platform, the samples that were quantified without dilution had their internal standard composed by 50  $\mu\text{L}$  of the system blank (top or bottom phase) and 10  $\mu\text{L}$  CellicCTec 50 times diluted. The internal standards applied in the quantification of the two times diluted samples were composed by 50  $\mu\text{L}$  of the system blank (top or bottom phase), 40  $\mu\text{L}$  of water and 10  $\mu\text{L}$  CellicCTec 30 times diluted. Both samples and internal standards have to present the same dilution/composition of phase forming components in order to neglect their influence in the Bradford analysis. The blanks should be performed with the same dilution of the sample to be quantified.

**Table S2.** Coefficients for Othmer-Tobias and Bancroft equations ( $n_i$  and  $k_i$ ), correlation coefficients ( $r^2$ ) and standard deviation of the correlated data ( $\sigma$ ) for the eight polymer-salt system combinations studied.

System	Othmer-Tobias			
	$n_1$	$k_1$	$r^2$	$\sigma$
<b>PEG 2000</b>				
Potassium citrate pH 5	2.355	0.2088	0.9364	0.0509
Magnesium sulphate pH 5	1.1743	0.8632	0.9594	0.0467
<b>PEG 4000</b>				
Potassium citrate pH 5	0.9132	1.2085	0.875	0.0813
Magnesium sulphate pH 5	1.1845	0.6865	0.9398	0.0542
<b>PEG 6000</b>				
Potassium citrate pH 5	0.946	1.201	0.866	0.1071
Magnesium sulphate pH 5	1.0967	0.7831	0.7885	0.0897
Potassium citrate pH 7*	1.7873	0.2492	0.9709	0.0283
Potassium sodium tartrate pH 7**	1.2466	0.6811	0.93405	0.0618

\*The last tie line was not considered in the Othmer-Tobias correlation.

\*\* The last two tie lines were not considered in the Othmer-Tobias correlation.



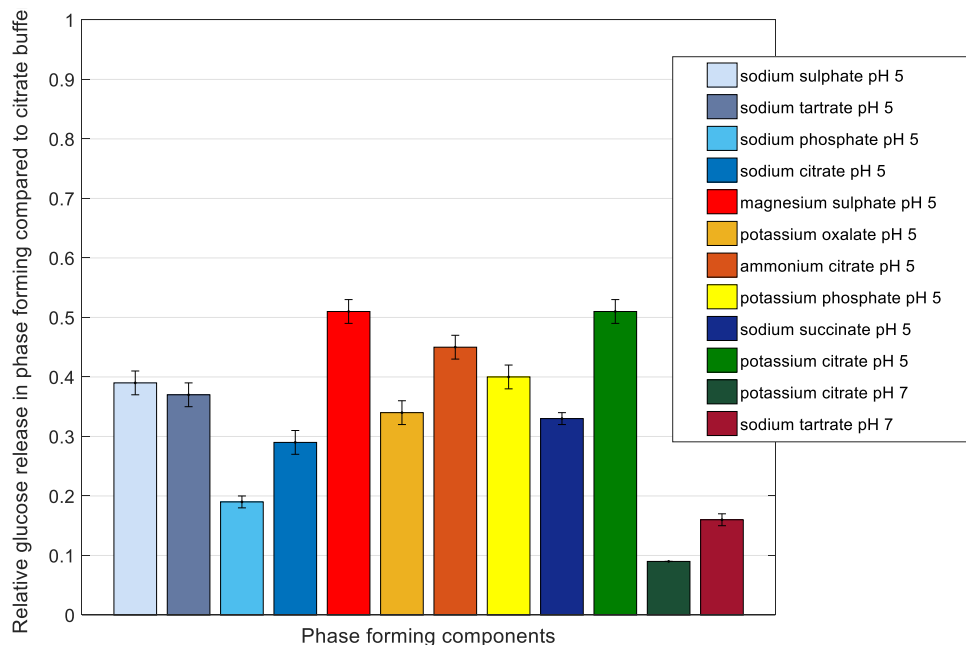


**Fig. S1.** Capability of enzymes (Cellic CTec2) to release glucose from filter paper when incubated in different phase forming components. Absolute amount of glucose in each of the phase forming components were divided by the glucose produced when enzymes were incubated in optimum condition (citrate buffer pH 4.8). Error bars indicate the standard deviation derived from the calibration curve plus appropriated error propagation. The enzymes were diluted 200 times.

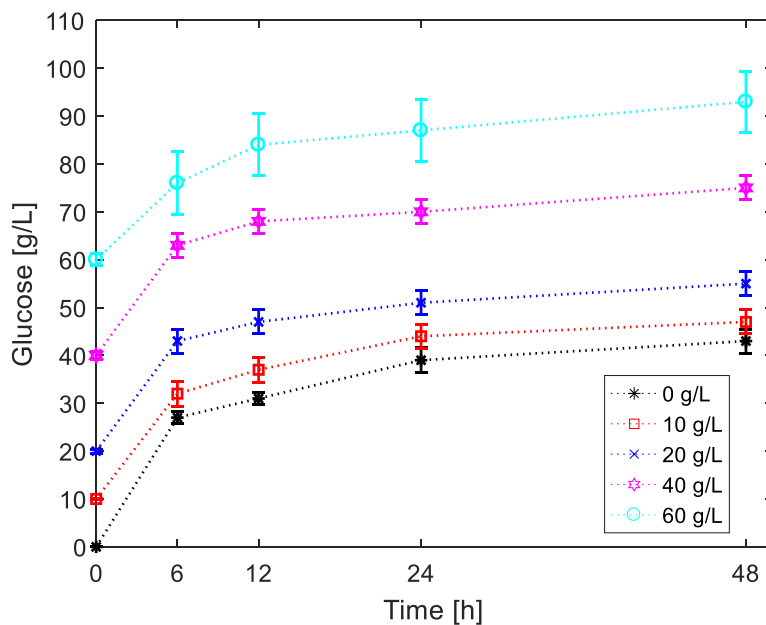


**Fig. S2.** Conventional hydrolysis of hydrothermal sugarcane bagasse at 10% WIS (solid content) and 10 FPU/g bagasse (enzyme load), under different loads of additional glucose to the reactions. Cellulose conversion at 0 g/L, 10 g/L, 20 g/L, 40 g/L and 60 g/L, are  $49 \pm 3 \%$ ,  $42 \pm 3 \%$ ,  $39 \pm 3 \%$ ,  $40 \pm 3 \%$ ,  $37 \pm 7 \%$ , respectively.

**Table S3.** Composition of M points used to determined tie lines and respective volumes and component concentrations of top and bottom phases. The systems are indicated in the left side of the table. The TLL represented in bond were selected to be screened at Step 3 of the high-throughput platform.

	Total composition			Top phase		Bottom phase			
	TLL [%]	PEG [% (w/w)]	Salt [% (w/w)]	PEG [% (w/w)]	Salt [% (w/w)]	Vol. [μL]	PEG [% (w/w)]	Salt [% (w/w)]	Vol. [μL]
PEG 6000 and Potassium sodium tartrate pH 7	17.3	9.6	14.0	17.5	8.2	427.5	3.6	18.4	572.5
	24.0	10.6	14.0	21.5	5.9	431.4	2.3	20.2	568.6
	28.2	11.6	14.0	23.9	4.6	451.0	1.4	21.7	549.0
	31.4	12.6	14.0	25.6	3.8	471.9	0.9	23.1	528.1
	33.4	13.6	14.0	26.3	3.5	506.7	0.5	24.8	493.3
	35.8	14.6	14.0	27.6	3.0	522.8	0.3	26.0	477.2
	37.0	15.6	14.0	27.1	3.2	574.4	0.1	28.5	425.6
	39.0	16.6	14.0	27.8	2.9	595.2	0.0	30.3	404.8
PEG 6000 and potassium citrate pH 7	9.9	11.7	9.6	13.8	7.9	736.1	6.0	14.1	263.9
	12.5	12.7	9.6	15.5	7.4	715.7	5.7	15.1	284.3
	14.4	10.5	12.0	16.7	7.0	705.7	5.4	16.0	294.3
	14.7	13.6	9.6	17.1	6.9	709.5	5.4	15.9	290.5
	16.6	14.6	9.6	18.4	6.6	757.1	5.3	16.9	242.9
	16.8	11.5	12.0	18.8	6.5	449.8	5.4	16.5	550.2
	18.4	12.4	12.0	20.0	6.2	454.0	5.3	17.4	546.0
	19.9	16.5	9.6	20.0	6.2	485.0	5.6	20.0	515.0

Supplementary material

PEG 2000 and potassium citrate pH 5	12.8	15.0	17.3	19.1	14.4	608.1	8.6	21.7	391.9
	15.7	15.5	17.3	20.7	13.6	598.3	7.8	22.6	401.7
	18.2	16.0	17.3	22.3	12.9	579.8	7.3	23.2	420.2
	20.4	16.5	17.3	23.7	12.4	576.6	6.8	23.9	423.4
	22.5	17.0	17.3	24.6	12.0	590.7	6.1	24.8	409.3
	24.3	17.5	17.3	26.3	11.4	567.1	6.0	24.9	432.9
	26.2	18.0	17.3	28.1	10.8	542.8	6.0	24.9	457.2
	27.7	18.5	17.3	28.4	10.7	571.1	5.3	25.9	428.9
PEG 2000 and Mg sulphate pH 5	20.5	11.0	15.8	19.6	8.1	436.2	4.3	21.8	563.8
	27.8	13.0	15.8	23.8	6.4	483.4	2.9	24.6	516.6
	30.7	14.0	15.8	25.7	5.7	497.2	2.4	25.8	502.8
	33.3	15.0	15.8	27.1	5.3	519.0	1.9	27.1	481.0
	35.8	16.0	15.8	28.7	4.8	531.3	1.6	28.2	468.7
	<b>38.0</b>	<b>17.0</b>	<b>15.8</b>	<b>29.5</b>	<b>4.6</b>	<b>559.2</b>	<b>1.2</b>	<b>30.0</b>	<b>440.8</b>
	<b>40.2</b>	<b>18.0</b>	<b>15.8</b>	<b>31.4</b>	<b>4.2</b>	<b>557.8</b>	<b>1.1</b>	<b>30.5</b>	<b>442.2</b>
	<b>42.2</b>	<b>19.0</b>	<b>15.8</b>	<b>31.7</b>	<b>4.1</b>	<b>591.3</b>	<b>0.7</b>	<b>32.7</b>	<b>408.7</b>
PEG 4000 and potassium citrate pH 5	14.1	13.0	16.2	17.7	12.9	593.3	6.2	21.0	406.7
	19.1	14.1	16.2	22.1	11.2	503.9	6.0	21.3	496.1
	22.6	15.2	16.2	22.8	10.9	591.9	4.2	23.8	408.1
	25.9	16.3	16.2	23.8	10.6	640.8	3.0	26.2	359.2
	28.8	17.4	16.2	25.8	10.0	637.6	2.6	27.1	362.4
	31.6	18.5	16.2	27.0	9.7	660.1	2.0	28.9	339.9
	34.3	19.6	16.2	27.9	9.4	687.8	1.3	31.1	312.2

	36.6	20.7	16.2	29.5	9.0	690.2	1.1	32.2	309.8
PEG 4000 and Mg sulphate pH 5	21.4	11.2	13	20.5	6.6	474.4	2.8	18.8	525.6
	24.5	12.2	13	21.7	6.2	523.6	1.9	20.5	476.4
	27.8	13.3	13	24.5	5.2	509.6	1.6	21.1	490.4
	29.9	14.3	13	24.9	5.1	555.2	1.0	22.9	444.8
	32.6	15.3	13	27.4	4.4	543.6	0.9	23.2	456.4
	34.1	16.3	13	27.4	4.4	588.2	0.4	25.3	411.8
	36.4	17.4	13	29.6	3.9	579.7	0.4	25.6	420.3
	40.1	19.4	13	32.0	3.4	603.8	0.2	27.7	396.2
PEG 6000 and potassium citrate pH 5	15.3	12.0	14.2	16.8	11.4	634.0	3.6	19.1	366.0
	20.3	13.1	14.2	19.9	10.2	608.5	2.5	20.4	391.5
	23.7	14.2	14.2	21.3	9.7	645.9	1.3	22.4	354.1
	27.4	15.3	14.2	24.5	8.6	606.7	1.1	22.8	393.3
	28.7	16.4	14.2	22.6	9.2	722.6	0.2	27.2	277.4
	<b>34.2</b>	<b>18.6</b>	<b>14.2</b>	<b>28.2</b>	<b>7.5</b>	<b>657.9</b>	<b>0.2</b>	<b>27.2</b>	<b>342.1</b>
	<b>35.9</b>	<b>19.7</b>	<b>14.2</b>	<b>27.3</b>	<b>7.7</b>	<b>721.2</b>	<b>0.0</b>	<b>31.0</b>	<b>278.8</b>
	<b>38.1</b>	<b>20.8</b>	<b>14.2</b>	<b>29.5</b>	<b>7.1</b>	<b>705.6</b>	<b>0.0</b>	<b>31.3</b>	<b>294.4</b>
PEG 6000 and Mg sulphate pH 5	19.7	9.8	12.0	17.7	6.7	517.7	1.35	17.7	482.3
	23.0	10.9	12.0	19.9	5.9	528.0	0.88	18.8	472.0
	26.0	12.0	12.0	22.1	5.2	529.3	0.61	19.7	470.7
	28.5	13.1	12.0	24.0	4.6	538.1	0.41	20.6	461.9
	30.5	14.2	12.0	25.1	4.3	562.1	0.22	21.9	437.9
	31.6	14.8	12.0	26.1	4.0	561.8	0.18	22.2	438.2

## Supplementary material

32.1	15.3	12.0	25.8	4.1	591.3	0.09	23.4	408.7
32.6	15.9	12.0	25.2	4.3	628.7	0.03	25.1	371.3

## Chapter 5

Table S4: Total mass balance for the magnesium sulfate based ATPS.

	Inlet			Outlet			In-Out	
	Biomass	PFC	Water (Dilution)	Enzymes	Permeate	Lignin	Purge	
<b>Ton/batch</b>	153,58	30,00	71,73	4,66	205,69	16,31	37,97	0,00
<b>Glucan</b>	34,94					0,88	0,01	34,05
<b>Xylan</b>								
<b>Glucose</b>	2,06				29,44	0,03	10,43	-37,83
<b>Lignin</b>	14,51					8,40	0,08	6,03
<b>sollignin</b>					4,45	0,00	1,58	-6,03
<b>Xylose</b>	6,30				4,65	0,00	1,65	0,00
<b>Ash</b>	1,08					1,06	0,01	0,00
<b>Extractives</b>	3,23				0,01	3,19	0,03	0,00
<b>Enzyme (protein)</b>				0,35	0,11	0,00	0,24	0,00
<b>Water</b>	91,46	7,83	71,73	4,31	158,65	2,70	10,20	3,78
<b>PEG</b>		0,02				0,00	0,02	0,00
<b>Salt</b>		22,15			8,39	0,03	13,73	0,00

Table S5: Total mass balance for the potassium citrate based ATPS.

	In			Out			In-Out	
	Biomass	PFC	Water (Dilution)	Enzymes	Permeate	Lignin	Purge	
<b>Tons/batch</b>	153,58	30,00	87,96	4,66	214,72	31,99	29,48	0,00
<b>Glucan</b>	34,94					1,34	0,01	33,59
<b>Xylan</b>								
<b>Glucose</b>	2,06				31,47	1,53	6,38	-37,32
<b>Lignin</b>	14,51					8,55	0,06	5,91
<b>sollignin</b>					4,72	0,23	0,96	-5,91
<b>Xylose</b>	6,30				5,03	0,25	1,02	0,00
<b>Ash</b>	1,08					1,07	0,01	0,00
<b>Extractives</b>	3,23				0,83	2,39	0,01	0,00
<b>Enzyme (protein)</b>				0,35	0,27	0,08	0,00	0,00
<b>Water</b>	91,46	-1.39	87,96	4,31	151,75	13,51	13,35	3,73
<b>PEG</b>		2,11				2,01	0,11	0,00
<b>Salt</b>		29,28			20,66	1,04	7,58	0,00

## Supplementary material

Table S6: Summary of equipment cost for the batch process.

	Description	Material	Number of Units	Cost	Basis	New Purchase cost	Total Purchase Cost	Installation factor	Installation cost
ATPS hydrolysis									
Liquefaction reactor	250000 gallons	304 SS	2	480,0E+3	2009	521,9E+3	1,0E+6	2,5	2,6E+6
Enzymatic hydrolysis reactor	1MM gallons	304 SS	5	844,0E+3	2009	917,7E+3	4,9E+6	1,5	7,3E+6
ATPS Mixers	1MM gallons	304 SS	6	844,0E+3	2009	917,7E+3	5,8E+6	1,5	8,7E+6
ATPS Settlers	500000 gallons	304 SS	8	422,0E+3	2009	458,9E+3	3,7E+6	1,5	5,5E+6
Ultra-filtration	Membrane area		3	1,3E+6	2011	1,2E+6	1,7E+6	2,5	4,2E+6
Mixer - Phase forming components	100000 gallons	304 SS	1	84,4E+3	2009	91,8E+3	148,9E+3	1,7	253,1E+3
Lignin Press	170 m2	316 SS	1	2,6E+6	2010	2,7E+6	2,7E+6	1,7	4,5E+6
Saccharification pump	340 GPM 150ft	316 SS	3	47,2E+3	2009	51,3E+3	154,0E+3	2,3	354,1E+3
Hydrolysate transfer	2152 gpm, 171 ft	316 SS	1	26,8E+3	2009	29,1E+3	29,1E+3	2,3	67,0E+3
Misc pump	2152 gpm, 171 ft	316 SS	8	26,8E+3	2009	29,1E+3	233,1E+3	2,3	536,2E+3
Agitator				52,5E+3	2009	57,1E+3			
Total							20,3E+6		34,0E+6
Conventional hydrolysis									
Liquefaction reactor	250000 gallons	304 SS	1	480,0E+3	2009	521,9E+3	521,9E+3	2,5	1,3E+6



Supplementary material

Enzymatic hydrolysis reactor	1MM gallons	304 SS	6	844,0E+3	2009	917,7E+3	5,8E+6	1,5	8,8E+6
Lignin Press	170 m2	316 SS	2	2,6E+6	2010	2,7E+6	5,3E+6	1,7	9,0E+6
Saccharification pump	340 GPM 150ft	316 SS	3	47,2E+3	2009	51,3E+3	154,0E+3	2,3	354,1E+3
Hydrolysate transfer	2152 gpm, 171 ft	316 SS	1	26,8E+3	2009	29,1E+3	29,1E+3	2,3	67,0E+3
Agitator				52,5E+3	2009	57,1E+3			
Total							11,9E+6		19,5E+6

Table S7: Summary of raw material costs for magnesium sulfate-based ATPS process.

		Partition coefficient of sugar considered in the process					
		$k_s = 0.71$			$k_s = 1.5$		
	Price (Euro/ton)	Input to process (ton/h)	Annual consumption	Total cost	Input to Process (ton/h)	Annual consumption	Total cost
<b>Pre-treated sugarcane bagasse</b>	€ 20,00	€ 153,58	1,2E+6	€ 24,3E+6	€ 153,58	1,2E+6	24,3E+6
<b>Enzymes</b>	€ 517,00	€ 4,66	36,9E+3	€ 19,1E+6	€ 4,66	36,9E+3	19,1E+6
<b>PEG</b>	€ 1.500,00	€ 0,02	15,8E+0	€ 23,8E+3	€ 0,01	7,9E+0	11,9E+3
<b>Magnesium sulfate</b>	€ 150,00	€ 21,95	17,4E+3	€ 2,6E+6	€ 21,95	17,4E+3	2,6E+6
<b>Total</b>				€ 46,0E+6			46,0E+6

Table S8: Summary of raw material costs for potassium citrate-based ATPS process.

Retention coefficient of enzyme in the process: $R_e = 0.5$				
	Price (Euro/ton)	Input to process (ton/h)	Annual consumption	Total cost
<b>Pre-treated sugarcane bagasse</b>	€ 20,00	€ 153,58	1,2E+6	€ 24,3E+6
<b>Enzymes</b>	€ 517,00	€ 4,66	36,9E+3	€ 19,1E+6
<b>PEG</b>	€ 1.500,00	€ 2,11	1,7E+3	€ 2,5E+6
<b>Potassium citrate</b>	€ 1000,00	€ 29,28	23,2E+3	€ 23,2E+6
<b>Total</b>				€ 69,1E+6

Table S9: Summary of equipment cost for the continuous process.

	Description	Material	Number of Units	Cost	Basis	New Purchase cost	Total Purchase Cost	Installation factor	Installation cost
ATPS hydrolysis									
Liquefaction reactor	250000 gallons	304 SS	2	480,0E+3	2009	521,9E+3	1,0E+6	2,5	2,6E+6
Enzymatic hydrolysis reactor	1MM gallons	304 SS	2	2,0E+6	2009	2,2E+6	4,4E+6	1,5	6,6E+6
ATPS Mixers	1MM gallons	304 SS	1	2,0E+6	2009	2,2E+6	2,2E+6	1,5	3,3E+6
ATPS Settlers	500000 gallons	304 SS	2	991,7E+3	2009	1,1E+6	2,2E+6	1,5	3,2E+6
Ultra-filtration	Membrane area		1	1,3E+6	2011	1,2E+6	1,7E+6	2,5	4,2E+6
Mixer - Phase forming components	100000 gallons	304 SS	1	198,3E+3	2009	215,7E+3	272,8E+3	1,7	463,7E+3
Lignin Press	170 m2	316 SS	2	2,6E+6	2010	2,7E+6	5,3E+6	1,7	9,0E+6
Saccharification pump	340 GPM 150ft	316 SS	3	47,2E+3	2009	51,3E+3	154,0E+3	2,3	354,1E+3
Hydrolysate transfer	2152 gpm, 171 ft	316 SS	1	26,8E+3	2009	29,1E+3	29,1E+3	2,3	67,0E+3
Misc pump	2152 gpm, 171 ft	316 SS	8	26,8E+3	2009	29,1E+3	233,1E+3	2,3	536,2E+3
Agitator				52,5E+3	2009	57,1E+3			
Total							17,5E+6		30,4E+6
Conventional hydrolysis									
Liquefaction reactor	250000 gallons	304 SS	2	480,0E+3	2009	521,9E+3	1,0E+6	2,5	2,6E+6
Enzymatic hydrolysis reactor	1MM gallons	304 SS	2	2,0E+6	2009	2,2E+6	4,4E+6	1,5	6,6E+6

## Supplementary material

Lignin Press	170 m2	316 SS	2	2,6E+6	2010	2,7E+6	5,3E+6	1,7	9,0E+6
Saccharification pump	340 GPM 150ft	316 SS	3	47,2E+3	2009	51,3E+3	154,0E+3	2,3	354,1E+3
Hydrolysate transfer	2152 gpm, 171 ft	316 SS	1	26,8E+3	2009	29,1E+3	29,1E+3	2,3	67,0E+3
Agitator				52,5E+3	2009	57,1E+3			
Micro-filtration	100 kg/m2/h		1	400183,90 8	2011	387,7E+3	387,7E+3	2,5	969,4E+3
Ultra-filtration	67 kg/m2/h		1	1012229,8 85	2011	980,8E+3	980,8E+3	2,5	2,5E+6
Total							12,3E+6		22,1E+6

# ACKNOWLEDGEMENT

The Dual Degree PhD brought to me new approaches and perspectives professionally, but mostly personally. It is impossible to thank those who only contributed professionally to the accomplishment of this thesis, because every single step work-related, also changed me as a person.

Looking back, thank you the originators of the main idea of this PhD to overcome product inhibition by two phase systems: my supervisor at UNICAMP Aline Carvalho da Costa. She shared this idea with her husband Martin Aznar (*in memoriam*), who would contribute with the thermodynamic prediction of the system. When I started my PhD, Aline shared this idea with me. I felt so honour to be able to perform this project. Thank you Aline for trusting me the development of such special project for you and for our field.

Luuk, without you this project would not be possible. Our first contact was in a course during my master degree at UNICAMP, Brazil. I was impressed by your carefulness with us, from the language barrier until the technical content, and that you could share all your knowledge with the Brazilian students. When I started my PhD, I didn't hesitate to contact you to suggest a collaboration. We started developing the project together and planning my trip to The Netherlands. Every meeting with you inspired me to do a better job and motivated me to pursue the scientific career. Thank you for the greatest opportunity of my life.

Marcel, since my first day at TU Delft until the accomplishment of this PhD thesis, you inspired me to growth professionally and personally. You taught me how to be a scientist. I admire how you conducted the supervision of this project. Thank you for the freedom to explore the research topics, for the guidance to keep me focused, for so many opportunities to go to conferences/courses and for trusting me with my students.

Solange, thank you for supervising this PhD project with so much attention to the details. I have learnt a lot from you, at each challenging part of the project and each

submission on our papers. Thank you for receiving me in Denmark. You definitely are an inspiration for all woman in science.

Sindelia, if I am where I am today, it is because of you. My first scientific project was supervised by you, and you showed science to me in an graceful and joyful way. You open the doors for me in Campinas, which also brought me where I am today. Thank you for being my daily inspiration.

Peter, the intention when I contacted you was to contribute with the mathematical implementation and solution of a thermodynamic model. After 1 year working together, the results were much more than a scientific paper together: you became my friend. When I considered to pursue the academia career, I was inspired by you. Thank you for donating your time, knowledge and patience.

Thank you to my students. I have learnt from you as much as you contributed to this project. Joana, my first Master student, who showed me a passion for supervising students. Thank you, Joana, for joining this project. Paulus, thank you for all the experimental work and enthusiasm for learning. Devi, you could not surprise me more. You turned the most challenging part of my project achievable, because of your intelligence and creative mind-set. Vidhvath, you performed the process design of this project with mastery. Thank you for every brainstorming session and for your resilience to deliver an exceptional work.

Thank you BPE group for having me. I was supposed to join the group for 1 year. 3 years passed with extension after extension, and the group has always cheered with me in every victory and supported me in each failure. Monica and Vick, you were the first ones that I met in my very first day at TU Delft. Thank you guys for always being supportive and friendly. Marcelo, you have one of the quality that I admire the most in people: you are willing to help others – thank you for sharing so much with me, all the support and care with my project and all the fun we had in the lab. Previous BPE PhDs Carlos, Susanna, Silvia (what a lottery to go to New York together, and also win the lottery to our first Broadway experience together!), Debby, Miao, Joana, Rita, Chema and Joan. Thank you all for our trips together, celebrations and daily life

during the PhD. To Mariana, Marina, Tiago, Roxana, Daphne, Oriol, Marijn and Lars I wish you lots of success and joy during the PhD journey. Thank you all BPE members Adrie, Ludo, Max, Stef and Kawieta (since before we meet each other in person, you take care so much of me, dankjewel, Kawieta).

My paranymphs, Monica and Song. To be in a different country and start a new life is much more pleasant when we have friends and supporters. Thank you for being my friends inside and outside university. Monica, every day, every moment, you were available to help and share. You were the best conference partner - how much fun we had in Copenhagen, Orlando and Guarujá! Song, it was such a pleasure to operate the robot (Frederico) with you! I will never forget our trip to Switzerland, the amazing sunset we have seen and that in pizzeria there they do not allow to warm up the salami.

To the dual degree PhDs students, together we made our Brazilian family in Delft to explore all features of The Netherlands and remember our home country and culture in the difficult times. I am honour to have met each of you guys! Renato was the first and the example. Wesley, Ana Maria, Andreia, Elisa, Felipe and Carla, you were always there to help, to support and to celebrate – thank you. Meissa, thank you for bringing so much taste do delft with your amazing cooking skills. Lucas, you were one of my best companies in Delft. Thank you for all walks on Sundays afternoon in Delft, pictures, ice creams, apple pie and for our amazing Christmas trip to Chamonix in 2017! Rafael, our friendship was one of the best things of this whole experience in Delft. I will keep it short: we lapidated the friendship stone with all support, trips and fun together during the last 4 years. Tiago, your unique point of view to see the world and your family conquered my heart.

To all friends that I have met in The Netherlands during my PhD, and could bring color and joyful to the greatest experience of my life, in special Kanaalweg group and Delft crew: Ben, Jiun, Ulric, Elie, Rishab, Mehmet, Giacomo, Lisa, Lucy, Joe, Fabi, Mark, Nati, Guillermo, Alberto, Marilia, Tim, Angelo, Mattia and Paolo. For every name written here there is a particular story that I keep always with me. Also, thank you to the Brazilian girls with who I share my life with: Ana (Gêmea), Larissa,

Thaís, Tati, Iza, Grazi, Cássia, Amanda, Julia and Ariane. Thank you to the Catholic community, in special Father Eli, who always received me with open arms and guided me through difficult times.

Alessandra, my talented cousin, thank you for expressing your art and creativity in the cover of such a special book. It represents a lot to me.

Mãe, você entende minhas apresentações mesmo em inglês, aprendeu sobre ATPS, hidrólise do bagaço e Flory-Huggins para me acompanhar em todas as aventuras dessa jornada. Pai, seus ouvidos atentos e palavras sábias me guiaram por esse caminho que hoje nos enche de alegria. Renan, irmão é a palavra mais completa para te descrever. Você é meu irmão em todos os sentidos e facetas do significado desta palavra. Ah, e você foi uma das maiores felicidades durante meu doutorado com sua vinda surpresa para Holanda no verão de 2017. Eu nunca vou me esquecer da melhor surpresa da minha vida! Meus avós, nós aprendemos juntos como podemos estar presentes na vida um do outro mesmo estando longe. Conto os dias para a próxima ida ao Brasil para ver vocês curtindo o bisneto Ennio.

Ennio, meu filho. Você foi o maior incentivo para que esse trabalho se concluísse. Teije, thank you for sharing with me the greatest adventure of my life: raising and taking care of our little miracle. It has been a tough journey to combine our responsibilities with the accomplishment of this thesis. Thank you for the incentive to make this possible.



# PUBLICATION RECORD

## Full Articles

1. **Bussamra, B.C.**, Sietaram, D., Verheijen, P., Mussatto, S.I., da Costa, A.C., van der Wielen, L., Ottens, M., 2021. A critical assessment of the Flory-Huggins (FH) theory to predict aqueous two-phase behaviour. *Sep. Purif. Technol.* 255, 117636. <https://doi.org/10.1016/j.seppur.2020.117636>
2. **Bussamra, B.C.**, Meerman, P., Viswanathan, V., Mussatto, S.I., Carvalho da Costa, A., van der Wielen, L., Ottens, M., 2020. *Enzymatic Hydrolysis of Sugarcane Bagasse in Aqueous Two-Phase Systems (ATPS): Exploration and Conceptual Process Design*. *Front. Chem.* 8, 1–15. <https://doi.org/10.3389/fchem.2020.00587>
3. **Bussamra, B.C.**, Castro Gomes, J., Freitas, S., Mussatto, S.I., Carvalho da Costa, A., van der Wielen, L., Ottens, M., 2019. *A robotic platform to screen aqueous two-phase systems for overcoming inhibition in enzymatic reactions*. *Bioresour. Technol.* 280, 37–50. <https://doi.org/10.1016/j.biortech.2019.01.136>
4. **Bussamra, B.C.**, Freitas, S., Costa, A.C. da, 2015. *Improvement on sugar cane bagasse hydrolysis using enzymatic mixture designed cocktail*. *Bioresour. Technol.* 173–181. <https://doi.org/10.1016/j.biortech.2015.03.117>
5. Delabona, P. da S., Silva, M.R., Paixão, D.A.A., Lima, D.J., Rodrigues, G.N., Lee, M. do S., Souza, M.G. da S., **Bussamra, B.C.**, Santos, A.S., Pradella, J.G. da C., 2019. *A novel Scytalidium species: understand the cellulolytic system for biomass saccharification*. *Brazilian J. Chem. Eng.* 36, 85–97. <https://doi.org/10.1590/0104-6632.20190361s20170495>
6. (In preparation)<sup>1</sup> **Bussamra, B.C.**, Viswanathan, V., Mussatto, S.I., Carvalho da Costa, A., van der Wielen, L., Ottens, M. Model-based evaluation and techno-economic analysis of aqueous two-phase systems (ATPS) for enzymatic hydrolysis of sugarcane bagasse

---

<sup>1</sup> The article under preparation consists of the Chapter 5 of this PhD thesis.

## Presentations in events

1. Oral and poster presentation at the **Biopartitioning and Purification Conference**, 2019. *Aqueous two-Phase Systems Applied to Enzymatic Reactions: Screening Methodology, Thermodynamic Modelling and Process Design*. Guarujá, Brazil. Award for the Best Poster Presentation.
2. Poster presentation at **American Chemical Society Meeting**, 2019. Aqueous two-phase systems (ATPS) as a tool to overcome product inhibition in lignocellulosic conversions. Orlando, FL.
3. Oral presentation at **Biotechnology Symposium**, 2018. *Guide to Supervision*. TU Delft, The Netherlands.
4. Oral presentation at **ABC<sup>2</sup> — Anything but Conventional Chromatography**, 2017. From Bench-scale to High Throughput Platform: Phase Diagram Determination and Solute Partition Analysis in Aqueous Two Phases Systems. Lisbon, Portugal.
5. Poster presentation at **Biopartitioning and Purification**, 2017. *Aqueous Two-Phase Systems for Extractive Enzymatic Hydrolysis of Biomass*. Copenhagen, Denmark.
6. Honorable mention due to the scientific quality and oral presentation towards specialized jury at the **V Meeting of the Green Chemistry Brazilian School**, 2015. *Improvement of the enzymatic cocktail for enzymatic hydrolysis of the sugarcane bagasse*. CNPEM/LNBR, Campinas, Brazil.

## ABOUT THE AUTHOR

Bianca Consorti Bussamra was born in 24 July 1989 in Tietê, Brazil. With 18 years old, she started her studies in Biotechnology Engineering at Sao Paulo State University, in Assis, Brazil. The five years of graduation was experienced with two internships abroad, scientific awards, participation in events and in the junior company formed by the undergraduate students. In 2010, Bianca was selected as one of the 20 undergraduate students from Latin America to develop a research project in the XIX Summer Scholarship Program, Brazilian Center for Research in Energy and Materials. In the same year, Bianca presented her scientific initiation work on the nineteenth “Jornada de Jóvenes Investigadores”, Universities Association of Montevideo, in Paraguay, and her work was awarded as the best oral presentation in the field of Renewable Energy.

In 2011, she went to Poland to undertake an internship in an consulting company in Biotechnology (BioTech Consulting). In 2012, Bianca spent one semester at Technical University of Madrid, UPM (Madrid, Spain), and followed an internship at the Centre for Plant Biotechnology and Genomics, CBGP/ UPM - INIA, in the field of plant hormonal regulatory networks. In the same year, Bianca moved to Campinas to start her Master’s degree in Chemical Engineering at University of Campinas (UNICAMP). The experimental part was performed in cooperation with the Brazilian Biorenewables National Laboratory, LNBR (Campinas, Brazil), involving fermentation, protein purification and design of experiments. Apart from the technical skills, the Master’s degree offered the opportunity to Bianca to develop her scientific writing and publish her first scientific article in a peer-review journal.

After completing the Master’s degree, Bianca joined the Research and Innovation department at Solvay Group as a trainee, in Paulinia, Brazil. She left the private sector to start her Dual Degree PhD in Biotechnology at Delft University of Technology, TU Delft (The Netherlands), and in Chemical Engineering at University of Campinas, UNICAMP (Brazil). During her PhD, Bianca focused on the development of sustainable bioprocesses, aimed at an efficient conversion of renewable feedstock into sugars. She has also been involved with the development of thermodynamic models, process design and techno economic analysis.





Delft University of Technology  
University of Campinas